LABORATORY OF NEUTRON PHYSICS OF THE JOINT INSTITUTE FOR NUCLEAR RESEARCH

The Joint Institute for Nuclear Research (JINR) is the international centre for experimental and theoretical research in the field of elementary particle physics, nuclear and neutron physics, condensed matter research and some other related topics.

The Convention establishing JINR was signed on 26 March 1956 by the Plenipotentiaries of the Governments of the Member States, and the Charter regulating the activities of the Institute was adopted on 23 September the same year.

The research policy of JINR is handled by the Scientific Council which is convened twice annually.

The structure of JINR is determined by its specialization and by the principle of governing it internationally. Current scientific and financial affairs of the Institute's Laboratories, common services as well as the work of several specialized departments are guided by the Institute Directorate.

Among the JINR common services there are: library, publishing department, experimental physics facilities division, medical service, etc.

The Laboratory of Neutron Physics is one of seven JINR Laboratories. It was established in 1956, soon after the foundation of JINR. In 1960 the idea of Prof. D.I.Blokhintsev (11.01.1908-24.01.1979) was successfully realized: a principally new source of neutrons was put into operation. The creation of a pulsed reactor has actually initiated a new direction in the development of research neutron sources.

An extended scientific program was carried out on this new source under the leadership of the Laboratory director Prof. I.M.Frank (23.10.1908-22.06.1990) and his deputy Prof. F.L.Shapiro (06.04.1915-30.01.1973).

Academician, 1958 Nobel Prize Winner for Physics, Prof. I.M.Frank was at the head of this large international body for over 30 years. During these years a whole family of unique pulsed neutron sources for nuclear physics and condensed matter research were being designed, constructed and operated. In 1983 the new high flux pulsed reactor IBR-2 was put into operation at the Laboratory.

Today the scientific activity of the Laboratory is connected with two fields of physics: subatomic physics and condensed matter physics. The former includes investigations of the neutron as elementary particle and the study of compound nuclear states in the reactions induced by slow neutrons. The latter comprises the study of the mechanisms of superconductivity, the investigation of other urgent problems of the physics of solids, surfaces, liquids and of molecular biology. Besides, works are being carried out on the use of nuclear physics methods for applied research.

Laboratory Organigram

Directorate:
Director:
V.L.Aksenov
Deputy Directors:
I.Natkaniec
Yu.P.Popov
Scientific Secretary:
A.V.Belushkin

Reactors and Technical Departments
Head: V.D.Ananiev

- Reactor Safety Physics
  Head: E.P.Shabalin
- **IBR-2**
  Head: A.V.Vinogradov
- IBR-30+LUE-40
  Head: S.A.Kvasnikov
- Mechanical Maintenance
  Head: A.A.Belyakov
- **Electrical Engineering**
  Head: V.P.Popov
- Design Office
  Head: B.I.Voronov
- **Construction**
  Head: A.N.Kuznetsov

Scientific Departments

- Nuclear Physics
  Head: W.I.Furman
  - Physics of Neutron
  - Nuclear Reactions
  - Nuclear Data
  - Polarized Neutrons and Nuclei
- Condensed Matter
  Head: Yu.M.Ostanevich
  - Neutron Diffraction
  - Small Angle Scattering
  - Inelastic Scattering
  - Polarized Neutrons
- **Low Temperature Physics**
  Head: B.V.Vasiliev
- Radiation Research & Neutron Activation Analysis
  Head: V.M.Nazarov
- Applied Research
  Head: V.I.Luschikov
  - Elemental Analysis
  - X-ray Diffraction
  - High-T_c Superconductivity
- Electronics&Computing
  Head: V.G.Tishin
  - Automation & Data Acquisition
  - Computer Networks
  - Scientific Computing

Administration Services
Head: S.V.Kozenkov

- Secretariat
- Personnel
- Finance & Purchasing
- Translation Office
- Graphics & Painting
- Photography

DIRECTOR'S REPORT

This report covers the activities of the Laboratory of Neutron Physics in the year from 1 October 1990 to 1 October 1991 in connection with the fact that the neutron sources at LNP traditionally operate for physical experiment from mid-October to mid-June next year and have a scheduled shutdown for improvement and maintenance from June to October.

The past year was a difficult year for the Laboratory. Nevertheless, on the whole, it was a successfull and reassuring year.

Neutron Sources

The pulsed reactor of periodic operation IBR-2 still remains the most high flux pulsed neutron source in the world. Both in 1990 and 1991 the reactor worked faultlessly. It has run 2570 hrs in 10 cycles for physical experiment. Pulsed reactors of periodic operation produce high neutron fluxes and are, at the same time, very economic. So the active core of the IBR-2 is designed for about 20 years of continuous operation in the present regime. In a shorter period of 5 years the moving reflector must be replaced, having worked out its radiation resource. Next time it is to be replaced in 1993. In 1991 work went on manufacturing the moving reflector of a new design to allow reduction of the neutron pulse width by a factor of 2.

The main task of the 1991 year program for upgrading the IBR-2 was to manufacture a solid methane cold moderator. After testing it will be installed to bring a tenfold increase in cold neutron flux. As the result, on three channels (No. 4,5,6) the cold neutron flux will be 10 times higher than that from the ISIS, for example. The present state of things allows one to think that in autumn 1992 the moderator will be installed on the IBR-2 reactor.

The IBR-30 booster with the linear electron accelerator LUE-40 as the injector serves mainly nuclear physics experiments. In the reported year its running time amounted to 2240 hours in 9 cycles. In prospect the booster will be replaced by the new High Resolution Neutron Source (HRNS) that would generate up to 2×10^{15}n/sec with a pulse width of up to 0.5 μsec. In 1991 the Laboratory in cooperation with the Institute of Nuclear Physics of the Academy of Sciences of Russia (Novosibirsk) and NICIET (Moscow) were carrying out design work on the linear electron accelerator and the target.

Research Program

The Laboratory's three main areas of research are fundamental and nuclear physics, condensed matter physics and applied research (use of nuclear physics facilities and methods for analysis of industrially produced materials, development of manufacturing technologies of new HTSC materials and design and construction of advanced physical instruments). Scientists and engineers of the Electronics and Computing Department take active part in development of the spectrometers suit of the Laboratory. They are also responsible for upgrading and operation of the Laboratory's Computing network. The main scientific results obtained by scientists of the Laboratory are reviewed per areas. Here are just some of them.

Theoretical investigations went in close connection with main experimental programs. Measurement of the neutron lifetime using ultracold neutrons (discovered in 1968 by a team of LNP scientists led by late Prof. F.L.Shapiro) is presently the most perspective direction of research. A theoretical study of interaction processes of UCN's with trap's walls has shown that uncertainly in τ value could reach 6 sec due to gravity corrections. High temperature superconductivity remains one of the intriguing problems of the physics of condensed matter. Calculations made in the past year evidenced in a most convincing manner in favour of the correspondence between the Superconducting Glass Model and the behaviour of oxide superconductors in external magnetic fields at temperatures higher than $\sim$0.7 T_c.

An original method for measuring the neutron lifetime proposed at LNP has yielded the most precise for today value of $\tau_{1/2}$=888.4 sec. This result was obtained in joint measurements carried out by LNP and PINP scientists at the reactor in Gatchina. Further advance in precision is limited by UCN flux density (10 n/cm^3). In 1991 a project formed to build a new facility on the high flux reactor of aperiodic operation at the Institute of Experimental Physics (Arzamas), earlier used for industrial purposes only, to enable production of UCN's with a density of 5×10^5 n/cm^3 (note, for comparison, that ILL, Grenoble, avails of 10^2 n/cm^3).

A number of new results were obtained in a study of compound states of nuclei. Observation of γ-cascades following thermal neutron capture of Gadolinium-157 evidenced for possibility of single particle transitions between 4S and 3P neutron shells at the energy of 2 to 3 MeV. It is impossible to observe these effects with the other nuclear spectroscopy methods. The joint efforts of theorists and experimentalists have successfully promoted investigation of fission processes.

A systematic study of the structure of yttrium high temperature superconductors on copper substitution has yielded a curious result: the substitution site (in a plane or a chain) is not of so a crucial importance as it was believed before. The important role play purely structural properties (e.g. the bond length) that need to be further investigated.

The neutron diffractometer for real time measurements DN-2 and the texture diffractometer NSVR open vast possibilities for applied neutron diffractometry.

To promissing results, though requiring further analysis, belong the results of SANS investigations of micellar systems. The SANS method gives the possibility, offered by no other method, of extracting new information on the physical chemistry of solutions.

The time-of-flight spectrometer on polarized neutrons provides for an efficient way of studying properties of surfaces. This spectrometer operates in two modes: polarized neutrons reflection from and transmission through a sample. The transmission mode appeared extremely informative also in the study of the dynamics and electromagnetic properties of HTSC's.

The past year saw the startup of the new inverted geometry spectrometer NERA-PR for inelastic neutron scattering studies with a higher resolution than it was provided before by the KDSOG-M spectrometer of analogous design. The new spectrometer allowed refinement of the data on phonon spectra of yttrium high temperature superconductors. This method of inverted geometry comes out to be highly efficient in studying magnetic excitations in f-electron systems.

In the field of applied research there should be especially emphasized the efforts of the scientists of the Low Temperature Physics Division in investigating the problem of building SQUID's from HTSC materials.

An extended front of investigations were carried out by the neutron activation analysis method. For them a specialized air-operated system REGATA for sample transportation was installed on the IBR-2. The time of transportation of a sample after irradiation to a detector is 12 sec. The Van-de-Graaf machine serves element analysis experiments with single charge ions of H, He, C, N, O accelerated to energies from 0.7 to 6 MeV.

In 1991 work continued on modernization of existing and construction of new spectrometers. The attention of the Lab's directorate concentrated mainly on the construction of two diffractometers on channel 5: the High Resolution Fourier Diffractometer and the Powder Diffractometer for Time Resolved Studies. Their construction is planned to be completed and first experiments started in spring 1992.

Construction of the HRFD is a conceptually important task. Mastering Fourier-analysis technique would give reduction of the neutron pulse width down to 7 μsec and a resolving power of $\Delta d/d=5\times10^{-4}$ at the high time-averaged flux on the sample of $10^7 n/cm^2 sec$. New possibilities will open and to real-time experiments: resolution of up to 300 μsec and the averaged flux of $5\times10^7 n/cm^2 sec$.

The reconstruction of the POLYANA spectrometer for experiments with polarized neutrons and nuclei has been accomplished this year. On it experiments will continue on the study of enhanced parity violation effects in resonances discovered by the L.B.Pikelner's group in 1982.

Scientists of the Laboratory reported on the results of their studies at many an international conferences and meetings. Some of them were hosted by the Laboratory and some were organized with its participation. The largest was the VI International School on Neutron Physics, one in a series of regular meetings hosted by the Laboratory every four years since 1969. The important result of these Schools is extending international cooperation. So at the VI School it was decided to organize two workshops on the scattering of neutrons in condensed matters, one in USA and the other in France.

Training Center

At the beginning of the 1991 year the Dubna branch of the Moscow State University that started work in 1961 on the initiative of Prof. D.I.Blokhintsev, the first Director of the JINR, has been reorganized into the Training Center at the JINR. To two earlier courses of training, in the physics of elementary particles and in the physics of nucleus, there added two more, in nuclear methods as applied to condensed matter research and in radiation biology. The founders of the Training Center are the JINR, the Moscow State University and the Moscow Engineering Physical Institute. Students of these and other high schools live and study in Dubna during their two senior years to have specialized knowledge and training for work on modern nuclear reactors and accelerators. This specialized training is especially important for future investigators of condensed matters. The Training Centre is open to students from any country and not only from the JINR Member States.

Personnel

During the past year there were some changes in the organization of the Laboratory, including the formation of two new research divisions - the Low Temperature Physics Sector (head B.V.Vasiliev) and the Radiation Research and Neutron Activation Analysis Sector (head V.M.Nazarov).

In June 1991 the Scientific Council of the JINR has appointed by election Prof. Yu.P.Popov and Dr.I.Natkaniec to serve their second three-year terms as Deputy-Directors of LNP. Dr.I.Natkaniec supervises work of the Condensed Matter Physics Department and the Electronics and Computing Department. Prof. Yu.P.Popov directs work of the Nuclear Physics Department, Applied Research Department and the Radiation Research and Activation Analysis Sector. Dr. V.G.Tishin was appointed to head the Electronics and Computing Department.

The number of staff decreased by 30 peoples mainly due to reduced number of scientists from the JINR Member States (except for those from the hosting State of the JINR) to amount to the total of 580 peoples on 1 October 1991.

On 15 July 1991 the JINR and BMFT have signed agreement on scientific cooperation and participation of Germany in scientific research in Dubna.

This year the Laboratory of Neutron Physics had a heavy loss. Dr. V.N.Efimov, the leading scientist of the Nuclear Physics Division who was with the Laboratory for over 30 long years died in September 1991. Dr. V.N.Efimov was a noted theorist who made a valuable contribution to the theory of few-nucleon systems. His name is written in the history of the Laboratory for ever.

V.L.Aksenov

NEUTRON SOURCES

The IBR-2 Pulsed Reactor

In the period from 1 October 1990 to 1 October 1991 the IBR-2 has operated for 2569 hours (10 cycles) to feed the physical experiments staged on 11 beam-lines.

The IBR-2 performance in the reported period is detailed in Table 1.

Beginning from October 1987 the IBR-2 operates with the new moving reflector, MR-2 (PO-2),in place of the first moving reflector, MR-1 (PO-1), having run 13211 hours since the reactor startup. The MR-2 design service time is 18000 hours. Its operating age by 1 October 1991 amounted to 12166 hours. The maximum fluence the MR-2 blade is built to sustain is 6.7×10^{25} n/m^2. By 1 October 1991 it was 4.38×10^{25} n/m^2.

The annual program of measurements on the IBR-2 reactivity power effect has been successfully performed. The details are reported in the following sections.

Table 1 The characteristics of the IBR-2 reactor operation in the reported period

1.	Average thermal power	2 MW
2.	Peak power in pulse	1500 MW
3.	Half width of fast neutron pulse	215 μsec
4	Thermal neutron flux density from surface	
	- of flat moderator,	
	time averaged,	5×10^{12} n/(cm^{2}sec)
	same at burst maximum	4×10^{15}n/(cm^{2}sec)
	- of grooved moderator,	
	at burst maximum	10^{16}n/(cm^{2}sec)
5.	Pulse repetition rate	5 p.p.s.

IBR-2 Investigations. Main results

These regular investigations have the aim of providing experimental confirmation of the stable and safe operation of the reactor. The collected data are used to estimate reliability of the whole reactor and of its components.

Monitoring and diagnostics of the reactor

Actually, the parameters of the reactor are stable on average. At the same time the extent of reactor noise varies during operation and it can be taken as the indirect parameter of the current reactor state control. In the IBR-2 reactor this control is executed by two tightly bound systems, one for monitoring and the second for diagnostics of the reactor state.

Noises are being measured and the data collected during every reactor cycle to yield main statistical characteristics of power pulses, reactivity and moving reflector fluctuations. The

Fig.1.1. The clustering time diagram (the step-like diagram) and power fluctuations during the reactor performance with the MR-2 moving reflector.

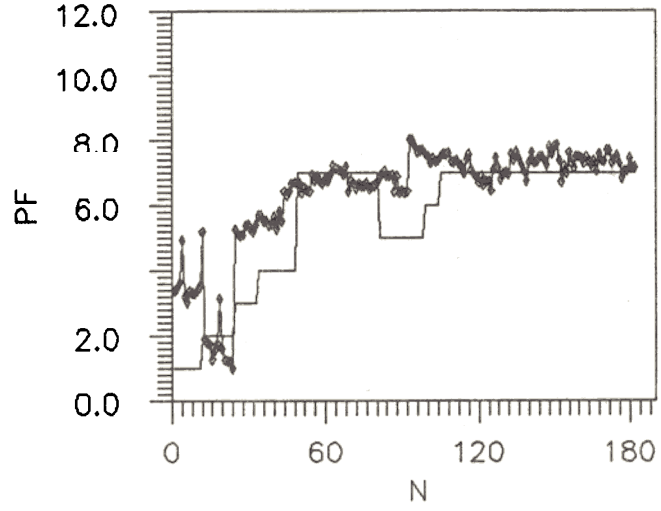

noise spectrum analysis by the pattern recognition method helps to reveal anomalous spectral structures. During the reported 1991 year the IBR-2 operated in the same stable regime as in 1990. Changes in reactor noise extent are illustrated in Fig.1.1 through power fluctuation standard deviations (SD) and cluster time characteristics. The noise extent transition seen at the outlet of this curve reflects vibration instability of the MR-2 in the initial period of operation. Then the curve shows stabilization and further perfect operation of the reflector.

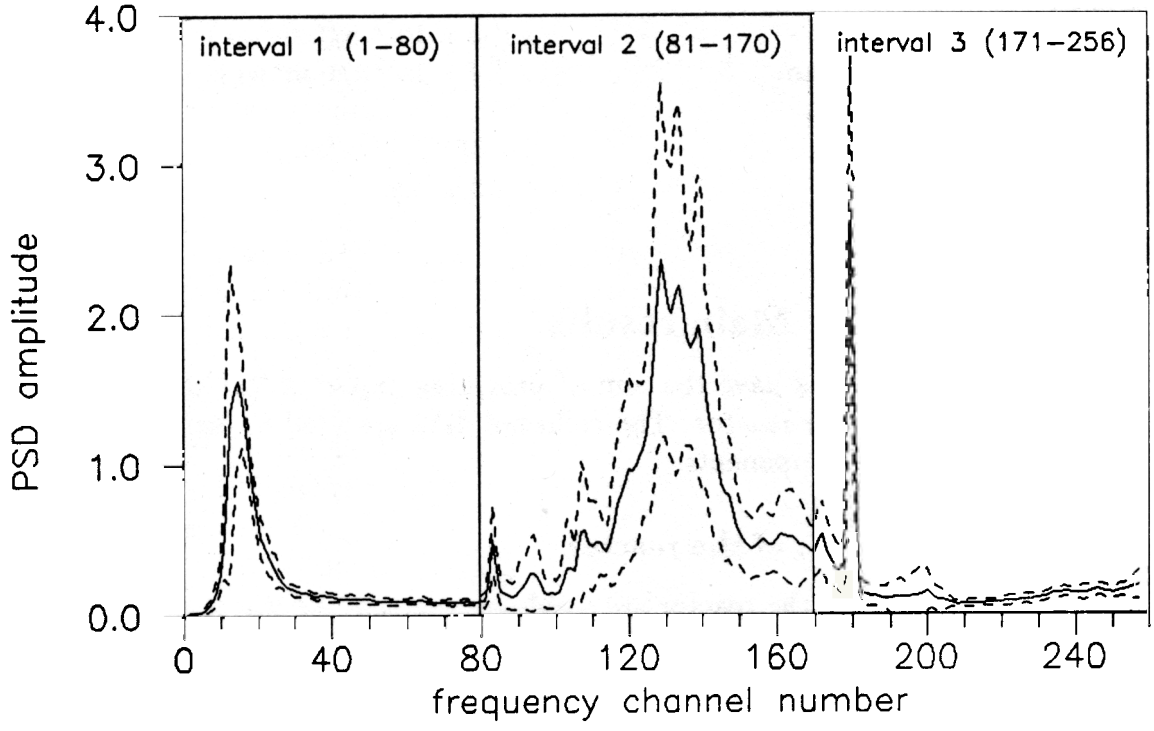

Fig.1.2. The average power spectral density representing the 7th (see Fig.1.1) cluster center (solid line) with ± standard deviations (dashed lines) in every frequency channel. The splitting of the full frequency interval into three is shown.

Another characteristic of the noise extent is the averaged spectrum, the "cluster 7" center shown in Fig.1.2 by the solid line. The dashed lines represent standard deviations in each of the frequency windows. The total frequency interval is divided into three, low, medium and high frequency, windows. These windows can be processed separately to extract detailed information about changes in reactor performance. For example, thus obtained information evidences, that the statistical characteristics of the new power fluctuation source, first observed in 1989, did not change in the reported period (the frequency from 1 to 1.5 Hz in the window ([80, 170], Fig.1.2). This source appears at an average power of 0.9 MW and its intensity grows by 1.2% (in SD units) with the increase of power to 2 MW. Its connection has been established with the vibrations of the moving reflector, MR, or to be more exact, with the vibrations of its mounting hardware and helium jacket.

Additionally, a narrow region ([175-185] window in Fig.1.2) with the peak, which reflects the moving reflector behaviour, was analysed. This peak is responsible for the appearance of two subclusters (the reactor substates). A cyclic transition from one to the other is observed with the time of occupation of each substate being no shorter than a complete two-week cycle. This observation can be explained by the fact that the vibrations of the moving reflector depend on its startup conditions. The reactivity variation corresponding to this transition is on the level of only $6 \times 10^{-7}\Delta$ K/K and thus influences neither the operation characteristics nor safety of the reactor.

The "noise pattern" of the IBR-2 operation in the reported period gives evidence of stability of the fluctuations due to reactor and modulator hardware and shows no tendency towards their aggravation or degradation. The noise component due to the cooling system remains unchanged too.

In the reported period measurements on the sensitivity of the diagnostics' system have been undertaken. This diagnostics system based on the pattern recognition method has been shown to be capable of extracting anomalous fluctuations on the level of about $10^{-7}\Delta$ K/K.

Operations

The annual measurement of the dynamical characteristics of the IBR-2 reactor was performed during the scheduled reactor cycle in May, 1991. The mean reactor power was 2 MW, the sodium circulation flow rate 90 m^3/h. The prompt power was modulated with reactivity adjustment rod (AR). The swing of AR displacements was 9 steps (it is about 15 mm). This swing corresponds to about 10% power relative variation. The period of reactivity variation was 0.2 sec, which is 160 times as much as the reactor pulsation period. A specially developed computer treatment has shown that the dynamical parameters of the IBR-2 reactor remained unchanged in the reported period. The stability threshold at a flow rate of 90 m^3/h was estimated to have its earlier value of 8 MW, at a flow rate of 65 m^3/h this estimate is about 2 MW.

IBR-2 Development

The PC-based Control and Monitoring System (PCCMS)

Work has continued to improve the IBR-2 control and monitoring system in a search for higher reliability of control of the reactor state and the state of the maintenance equipment. At the same time the system has been under constant development to increase its information

capability on the basis of recent achievements in the field. In 1990 the KFKI (Budapest, Hungary) has advanced a Detailed Plan for the creation of an automated control and monitoring system for the IBR-2 reactor. Soviet experts have approved the Plan and the contract has been signed in June 1990, between the JINR and the firm "Metripleks" for the supply of the first assignment, the IBR-2 technological parameters control system equipment. The delivery of the system components has been accomplished by May 1991 and assembly work has started. There was started test operation of the system in parallel with the existing equipment in the end of 1991. This will help the staff to get adapted to the system and develop new, more convenient programs for the data acquisition and treatment. The whole PCCMS complex comprises, besides the equipment for the technological parameters control, also the equipment of the reactor state control system and electronics to execute necessary logic operations of reactor monitoring and shielding (Fig.1.3).

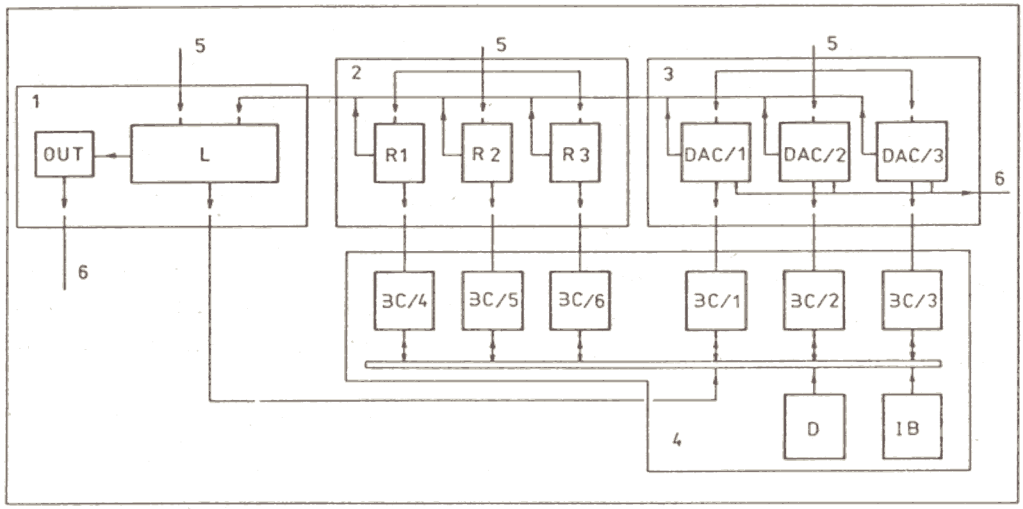

Fig.1.3. Schematical structure of the PCCMS complex of the IBR-2 reactor. 1. Emergency and monitoring signal system. 2. Reactor parameters control system. 3. Technological parameters control system. 4. Information and diagnostics system. 5. Input signals. 6. Output monitoring signals.

The moving reflector, MR-2PM

Work has continued to build the new moving reflector MR-2PM, in which the combination of the heterogeneous structure of nickel rotors with the opposite motion of the main and auxilliary reflector would be realized. In the reported period a considerable number of the new machine components have been manufactured and much attention given to strength control of the rotors.

Solid methane cold moderator

Work on the creation of a solid methane cold moderator (SMCM) for three IBR-2 beamlines (No.4,5,6) is now nearing completion. The schematical view of the moderator is shown in Fig.1.4. The neutron moderation medium is solid methane at 20 K cooled with gaseous helium

Fig.1.4. The schematical view of the solid methane cold moderator.

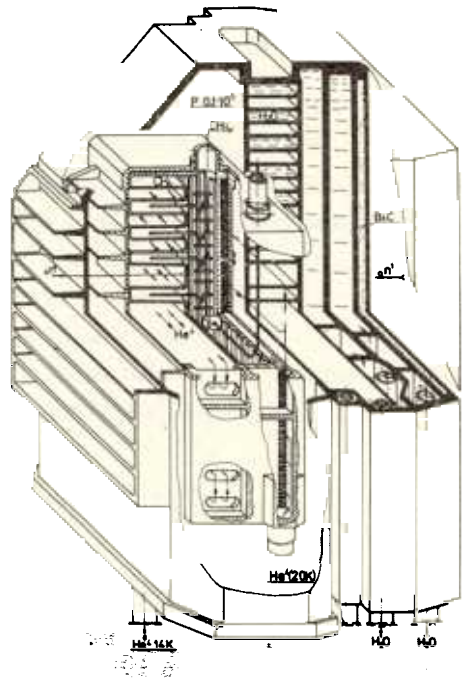

at 10-15 K. The expected effect is a tenfold rise of the cold neutron flux in the direction of the three above indicated beam-lines. In the reported period the design work has been completed, the methane-helium chamber, the main component of the moderator, manufactured and vacuum tested. Strain measurements of the chamber were also performed in a wide temperature range up to the working temperature of 20 K. A test rig for the moderator has been commissioned to conduct cold testing of the moderator. The preparatory work for this test is now under way. The new liquid helium production machine was adjusted and started supply of the laboratory physicists with liquid helium.

An instrument to measure solid methane swelling under reactor radiation has been developed. The instrument has guages to help measurement of temperatures and volumes of small methane boxes with flexible walls. This instrument is to be installed near the IBR-2 water moderator by the fall of 1991 and irradiated during two or three scheduled cycles to develop perfect conditions of solid methane cold moderator performance.

Table 2: Characteristics of potential alternatives to the IBR-2

Version	Mean power, MW	Thermal neutron flux, relative, n/sec	Thermal neutron pulse μsec	Background power, %
IBR-2	2	1	300	6
IBR-2,modified				
-PuO_2 fuel	4	1.3	110	6
-U fuel	4	0.8	125	20
-Np fuel	2	0.5	80	1.3–3
IBR-3, new concept of reactor design,				
-U fuel	4	1.3	115	3–4
-Np fuel	0.4	0.06	30–50	1.3–3
LANSCE, ISIS	–	0.01	30	~ 1

Comparative characteristics of potential alternatives to the current IBR-2 reactor

There are plans to start construction of a modified version of the IBR-2 reactor on termination of the first fuel cycle of the PuO_2 core in 1995–1996. Some alternatives were discussed during the year, including those, which offer replacement of plutonium with some other fissile material. The conclusion was made that some of them could ensure shorter pulses (to 50 μsec), some lower background power (2-3%), but none could bring simultaneous improvement of the three main parameters of the neutron source: the flux, the pulse duration, the background power (see Table 2). Preference was given to PuO_2 as the fuel, as it helps to keep high the thermal and cold neutron flux, the most advantageous parameter of the IBR-2 reactor, which is now about 100 times as much as that from the spallation neutron sources.

The Booster IBR-30 + LUE-40

The IBR-30 + LUE-40 has resumed operation on 21 June 1990 after the shutdown for maintenance and machine development. The user running time actually achieved in the reported period was 2243.6 hours (9 cycles). Detailed information on the IBR-30 + LUE-40 operations is given in Table 3. In 1991 the Design Department staff of the LNP have developed a new tantalum target for the IBR-30. The realization of this design would allow more effective use of photoneutrons in the core and uniform distribution of heat release over the fuel elements around the target channel. Schematical views of the now operating tungsten target and of the new tantalum target are given in Figs. 1.5 and 1.6. The new target has been manufactured and is under test now.

Table 3: The parameters of the IBR-30 booster

Electron energy	32 MeV
Electron pulse duration	1.6 μsec
Frequency	100 sec^{-1}
Current in pulse	0.4 A
Average current	64 μA
Average electron beam power	2 kW
Target material	tungsten
Multiplication	200
Neutron pulse duration	4.2 μsec
Mean thermal power	10 kW
Average intensity	3.6×10^{14}n/sec

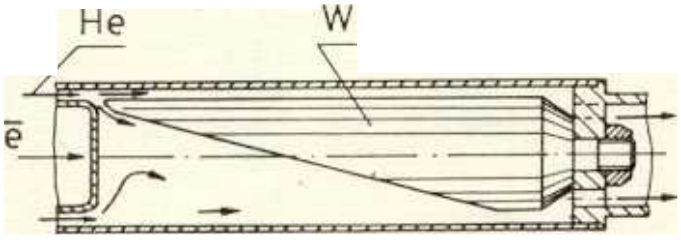

Fig.1.5. The now operational tungsten target

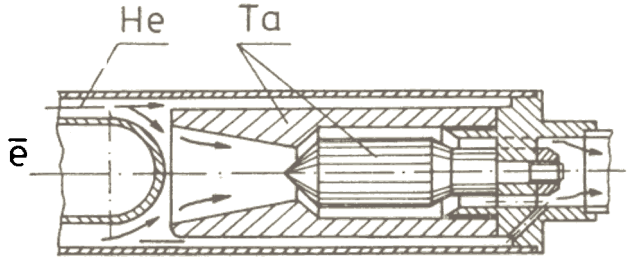

Fig.1.6. The proposed new tantalum target

The High Resolution Neutron Source (HRNS) (A Project)

The high resolution neutron source (HRNS) is proposed to replace the now operating U-Pu booster, IBR-30. It would be a subcritical, highly enriched uranium target on the basis of a powerful linac LUE-100. This source would produce up to 2×10^{15}n/sec with a pulse duration below 1 μsec and a pulse repetition rate up to 200 Hz to serve the nuclear physics experiments by the time-of-flight method. The quality of the source is expected to exceed that of the current IBR-30 booster by two orders of magnitude. Design studies go in two directions, one for the construction of the new LUE-100 electron accelerator and the second for the fabrication of the uranium target.

The Electron Accelerator LUE-100

A conceptual study has been undertaken for the building of the electron accelerator with the parameters: beam power 10 kW, electron energy 150 MeV, electron pulse duration 0.3 μsec, pulse repetition rate 200 Hz. The possibility to actually achieve these parameters has been proved, the construction cost estimated, the development engineering organizations and manufacturer provisionally outlined.

The Multiplying Target Station

Conceptual studies have been undertaken for the construction of the uranium multiplying target to yield ten versions including neutronics and thermohydraulics aspects of construction. The account of this work has been released and the choice made on its basis. Plans and specifications have been drawn of the HRNS with the electron accelerator to 150 MeV and the beam power of 10 kW. The 90%-enriched uranium-molibdenium alloy will be taken as the fissile material. The conversion media are to be natural uranium and mercury. The core will be cooled with a compulsory air flow and the converter by means of the natural convection of mercury. The operational value of the multiplication factor has the upper limit of 0.98. In the stationary mode of the booster the core produces the power of 20 kW, the intensity of 0.9×10^{15}n/sec, the fast pulse duration of 0.45 μsec and the delayed neutrons background of 10%. The target construction allows the reactivity modulation with the help of the four-blade neutron reflector, which rotates at 50 cycles per second. In this mode the power yield would be 50 kW at the maximum value of 0.98 for multiplication factor, the neutron beam intensity 2×10^{15}n/sec at 200 Hz pulse repetition rate, the pulse duration 0.9 μsec, the time averaged delayed neutrons background 11.8%. Plans and specifications include neutronics and thermohydraulics analysis of the core and converter design, the construction details of fuel elements and their assemblies in the core; the principal scheme of the uranium-mercury convertor together with the water-mercury cooling scheme; the construction of the neutron reflectors, moderators and shielding.

Schematical layout of IBR-2 experimental facilities

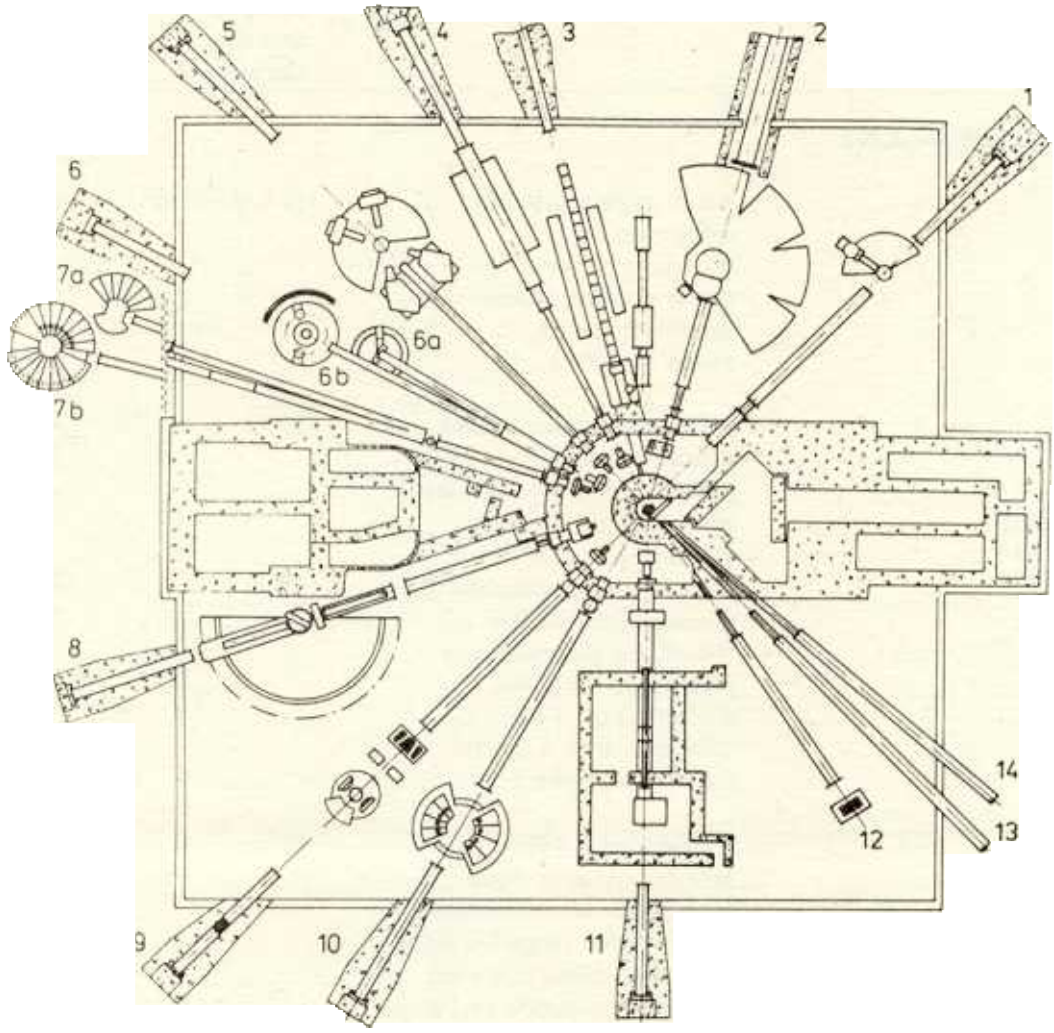

Beam line	Spectrometer
1	Diffractometer on ideal crystals **"DIFRAN"**
2	Direct geometry spectrometer **"DIN-2"**
3	Ultracold neutrons channel **"UCN"**
4	Small angle scattering diffractometer **"MURN"**
5	High resolution Fourier diffractometer and powder diffractometer for time-resolved studies **"DN-5"**
6A	Single crystal diffractometer **"DN-2"**
6B	Single crystal diffractometer with pulsed magnetic field **"SNIM"**
7A	Texture diffractometer **"NSVR"**
7B	High resolution inverted geometry spectrometer **"NERA"**
8	Polarized neutron spectrometer **"SPN"**
9	Neutron reflectometer (project) **"REFLEX"**
10	Inverted geometry spectrometer **"KDSOG"**
11, 12	Test beams

Neutron Spectrometers at IBR-2 Reactor

Spectrometer	Beam No.	Applications	Thermal neutron flux on the sample	Resolution range
DIFFRACTOMETERS				
"MURN"	4	Small angle scattering diffractometer. Structure of inhomogeneous systems, macromolecules, alloys, range 10–1000Å.	$(0.6\text{–}3.7)\times10^7$	$0.007\leq Q\leq 0.7$Å $\Delta Q/Q=0.04\text{–}0.18$
"DN–5" (project to be put into operation in 1992)	5	a)High resolution Fourier diffractometer for powders (HRFD). "Ab initio" studies of low symmetry structures.	10^7	$\lambda=0.9\text{–}12$Å $\Delta d/d=5\times10^{-4}$Å at d=2Å
		b)Powder diffractometer for time-resolved studies. Transition phenomena in solids with temporal resolution ca. 1 sec (300 μsec with a special detector assembly).	5×10^7	$\lambda=0.9\text{–}12$Å $\Delta\lambda=0.04$Å
"DN-2"	6A	Single crystal diffractometer. Atomic structures,phase transitions,etc. Temperature range 5–1000K. Real time diffraction with temporal resolution ca.1 min.	10^7	$\lambda=1.2\text{–}20$Å $\Delta\lambda=0.05$Å $\Delta d/d=0.01$, for $\Theta=80°$, d=2Å $\Delta d/d=0.1$, for $\Theta=10°$, d=60Å
"SNIM"	6B	Single crystal diffractometer. The pulsed (1ms) magnetic field on the sample is up to H=25T. Magnetic structures and phase transitions.	4×10^6	$\lambda=0.8\text{–}20$Å $\Delta\lambda=0.04$Å
"NSVR"	7A	Texture diffractometer. Texture analysis of metals, minerals and ceramics. Short range order studies in glasses and liquids.	10^6	$\lambda=0.8\text{–}7.6$Å $\Delta\lambda=0.015$Å

INELASTIC SCATTERING SPECTROMETERS

"DIN-2"	2	Direct geometry spectrometer, a reactor-phased chopper with curved slits, a sample area up to 200 cm^2. Atomic dynamics of metals, alloys and liquids.	2.5×10^5	δE=0.5–120meV $\Delta E_o/E_o$=4–10%
"NERA"	7B	High resolution inverted geometry spectrometer. Stochastic motion of atoms and molecules. Atomic and magnetic dynamics, phase transitions.	4.6×10^6	δE=0–500meV ΔE/E=2–6% (inelastic) ΔE=40–600μeV (quasielastic)
"KDSOG"	10	Inverted geometry spectrometer. A sample of up to 200cm^2 in area, 5–500K, 0–4kbar. Atomic and magnetic dynamics.	6.6×10^6	δE=1–300meV ΔE/E=5–14%

SPECIAL SPECTROMETERS

"DIFRAN"	1	Diffractometer on ideal crystals Neutron interferometry, coherent lengths.	1.9×10^6	λ=0.2–4Å $\Delta\lambda$=0.04Å
"UCN"	3	Investigations with ultracold neutrons of the surface properties of magnetic and non-magnetic materials.	400 n/s	Range λ=700–2500Å
"SPN"	8	Polarized neutrons spectrometer (p$\geq$94%). Magnetic field on a sample is up to 6000 Oe. Study of surface phenomena, internal fields and inhomogeneities in magnetic and superconducting materials.	2.5×10^5	$\Delta\lambda$=0.03Å λ=0.8–10Å
"REFLEX" (project)	9	Neutron reflectometer. Surface and interfacial phenomena studies by polarized and unpolarized neutron specular reflection	2.5×10^5	λ=0.5–15Å $\Theta_{grazing}=(2\text{–}12)\times10^{-3}$rad $\Delta\Theta=2\times10^{-4}$rad

Notes: 1) The average over time neutron flux (n/cm^2 /sec) (column 4) was measured by activation of a golden foil, which replaced the sample.

2) Accepted notations: λ is the neutron wavelength; Q is the scattering vector length ($\mathbf{Q}=\mathbf{k}-\mathbf{k}_o$); Δ - the resolution of spectrometer over the corresponding parameter; E_o and E the energy of the neutron before and after scattering, respectively; δE is the neutron energy change per scattering event.

Schematical layout of IBR-30+LUE-40 experimental facilities

Beam line	Spectrometer
1	Study of (n,α) and (n,p) reactions (**"PARKS"**)
1A	Study of two-quanta decay of compound states (**"CASCADE"**)
2	Medium resolution diffractometer **"DN-3"**
3	Study of sub-barrier fission (**"DRENIS"**)
3	Measurements of nuclear physics constants

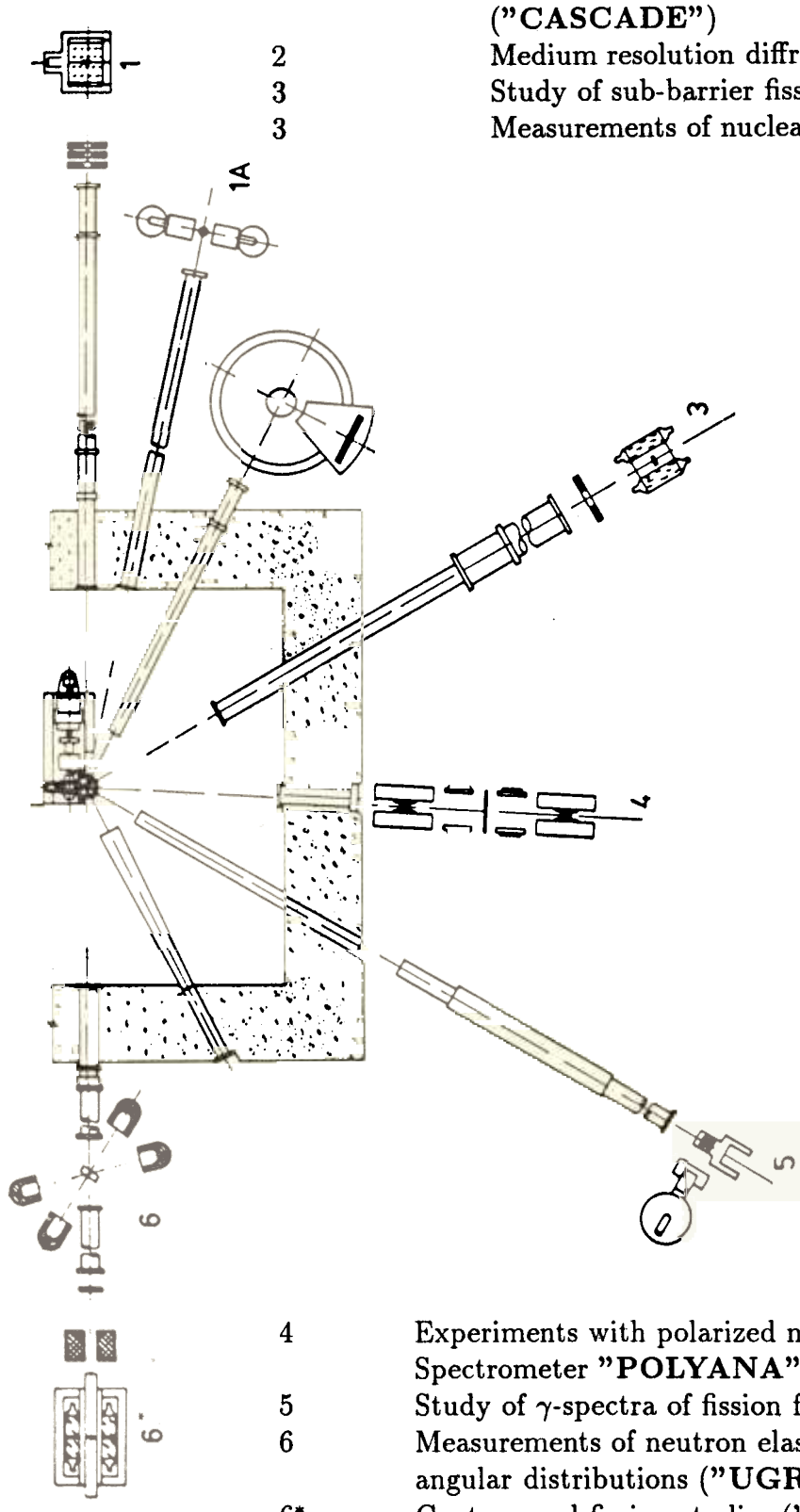

4	Experiments with polarized neutrons and nuclei Spectrometer **"POLYANA"**
5	Study of γ-spectra of fission fragments (**"DELRENE"**)
6	Measurements of neutron elastic scattering angular distributions (**"UGRA"**)
6*	Capture and fission studies (**"ROMASHKA"**)

Neutron Spectrometers at IBR-30+LUE-40 Booster

Spectrometer	Beam No.	Flight path, m	Exploratory range
Spectrometers for Nuclear Physics			
Study of (n,α)- and (n,p)-channels of decay on stable and radioactive nuclear targets (**"PARKS"**)	1	30–85	1–10^4 eV
Study of two-quanta decay of compound states (**"CASCADE"**)	1A	20	0.02–0.2 eV
Measurements of nuclear physics constants	3	120	1–10^4 eV
Study of sub-barrier fission (**"DRENIS"**)	3	60	1–100 keV
Experiments with polarized neutrons and nuclei (**"POLYANA"**)	4	60	0.1–10^4 eV
Study of γ-spectra of fission fragments (**"DELRENE"**)	5	60	0.1–100 eV
Measurements of neutron elastic scattering angular distributions (**"UGRA"**)	6	250	0.1–400 keV
Measurements of γ-multiplicity in the capture and fission processes (**"Romashka"**)	6*	500	0.1–100 keV
Spectrometers for Condensed Matter Research			
"DN-3" Medium resolution diffractometer. Structure of single crystals and powders in extreme conditions (pressure, temperature)	2	flux on the sample 8×10^5 n/cm^2/s	λ=0.2–6Å Δd/d=0.008 at d=1Å

NUCLEAR PHYSICS

INVESTIGATION OF FAST NEUTRON-INDUCED REACTIONS FOLLOWED BY CHARGED PARTICLES EMISSION

Yu.M.Gledenov, G.Khuukhenkhuu, S.S.Parzhitsky,
Yu.P.Popov, P.V.Sedyshev, M.V.Sedysheva
Laboratory of Neutron Physics, JINR, Dubna
Bao Shanglian, Cao Wentian, Tang Guoyou
Peking University, Peking, China
Fan Guoying, Zhou Hongyu
Normal University, Peking, China
Chen Zemin, Qi Huiquan
Tsinhua University, Peking, China

Energy spectra of emitted charged particles from neutron-induced reacions were mainly measured either at low neutron energies ($E_n \leq 100$ keV) or at high neutron energies ($E_n \geq 10$ MeV). A systematic study of these reactions in the intermediate energy range was practically not carried out apart from some data obtained by means of the activation analysis method. At the same time the use of neutrons with energies in a few MeV range allows one to not only obtain averaged over a wide energy range parameters of the compound nucleus but to trace how decay characteristics change with increasing excitation energy to the region of giant multipole resonances. At that, the possibility appears to investigate the contribution and the role of different nuclear reaction mechanisms.

In June 1990 measurements started of charged particles spectra from the $^{6}Li(n, \alpha)^{3}H$ and $^{10}B(n, \alpha)^{7}Li$ reactions on D-D neutrons with the purpose to study (n, p) and (n, α) reactions in the energy range of a few MeV. The measurements were carried out on beams of high-intensity neutron generators of the Chinese Joint Centre of Nuclear Research (Peking) using a flat electrode and two-section ionization chamber with two grids, which made a good showing in our experiments on slow neutrons. The results of the first and subsequent measurements have shown that the two-grid ionization chamber can be used for the charged particle spectrometry from neutron induced nuclear reactions in the energy range of a few MeV.

In the Laboratory of Neutron Physics, JINR, there is being manufactured the new high-luminosity ionization chamber specially dedicated for the work on a beam from a neutron generator. At the end of the 1991 year we are planning to begin measurements with this new chamber.

STUDY OF P-PARITY NONCONSERVATION IN THE $^{6}Li(n, \alpha)^{4}Li$ REACTION INDUCED BY POLARIZED NEUTRONS

J.Andrzejewski, A.D.Antonov, Yu.M.Gledenov,
M.P.Mitrikov, Yu.P.Popov
Laboratory of Neutron Physics, JINR, Dubna
V.A.Vesna, I.S.Okunev, B.G.Peskov, E.V.Shulgina
Petersburg Nuclear Physics Institute, Gatchina, USSR

P-odd asymmetry of the type $W \sim 1 + \alpha_{pN}(\vec{\sigma}_n \cdot \vec{k}_t)$ was measured in the geometry $\vec{\sigma}_{n\uparrow\uparrow}\vec{k}_{n\uparrow\uparrow}\vec{k}_t$, where σ is the neutron spin, $\vec{k}_t$, $\vec{k}_n$ the unity vectors of triton emission and neutron incidence directions. In the last years much attention was being paid to the experiments on and theoretical interpretation of parity nonconservation effects in few-nucleon systems of the type nd → tγ, pp → pp, np → dγ, $^{18}F^{*} \rightarrow {}^{18}F + \gamma$, etc.[1-4]. The aim was to extract contributions of charged and neutral weak currents and to evaluate weak interaction constants, f_π, $h^{\Delta T}_{\rho,\omega}$. By measuring P-odd asymmetry of the polarized thermal neutron capture reaction $^{6}Li(n, \alpha)^{3}H$ having a strong capture cross section one may achieve a higher accuracy in P-odd effects determination. The experimental value of the P-odd asymmetry coefficient

$$\alpha_{pN}^{exp} = -(6.44 \pm 5.50)\times 10^{-8}$$

was determined[5] by subtraction of the result for the main reaction. The obtained value for the P-odd asymmetry coefficient improves significantly the accuracy of preceeding measurements[6], $\alpha_{pN} = (0.7 \pm 8.0)\times 10^{-7}$, and is essentially smaller than the theoretical estimate[7] made by taking into account the well refined cluster structure of ^{6}Li and ^{7}Li.

V.M.Dubovik, V.Zenkin. Ann.Phys., v.172 (1986) 100.
2 E.G.Adelberger. Ann.Rev.Sci., v.35 (1985) 501.
3. M.Kaiser, G.Meisser. NPA, 499 (1989) 699.
4. B.Despllanques et al. Ann.Phys., v.124 (1980) 449.
5. V.A.Vesna et al. JETP Lett., v.52 (1990) 660 (in Russian)
6 V.A.Vesna et al. JETP Lett., v.38 (1983) 26 (in Russian).
7 M.M.Nesterov, I.S.Okunev. JETP Lett., v.48 (1988) 573 (in Russian).

ON THE STUDY OF (n, p) AND (n,α) REACTIONS ON STABLE AND RADIOACTIVE NUCLEI

J.Andrzejewski, Yu.M.Gledenov, Yu.P.Popov, V.I.Salatsky,
P.V.Sedyshev
Laboratory of Neutron Physics, JINR, Dubna
G.V.Zamyslov, A.I.Kislitsky, G.V.Ljubansky,
V.A.Pshenichnyi, N.P.Fedoseev
Institute for Nuclear Research, Kiev,Ukraine

Within the framework of the program for the study of nuclear reactions followed by emission of charged particles thermal neutron cross-sections for the $^{36}Ar(n, \alpha)^{33}S$ and $^{50}V(n, p)^{50}Ti$ reactions and a cross-section for the $^{7}Be(n,p)^{7}Li$ reaction at an energy of 24.5 keV were measured. The experiments were carried out at the reactor of the Institute for Nuclear Research of the Ukranian Academy of Sciences using the ionization chamber filled with a natural argon mixture containing 0.337% ^{30}Ar, and the system for the registration of two-dimensional spectra capable of measuring amplitude spectra from the chamber's collector in a given amplitude window of signals from the target. These spectra for the vanadium target are shown in the Figure. The peak at 2 MeV results from the registration of the sum energy of an alpha-particle and the recoil nucleus ^{33}S from the $^{36}Ar(n,\alpha)^{33}S$ reaction, a step at 1.8 MeV corresponds to the registration of only alpha-particles from this reaction and the peak at 2.9 MeV is due to protons from the $^{50}V(n,p)^{50}Ti$ reaction.

The value we have obtained for the cross-section of the (n, α) reaction on ^{36}Ar induced by thermal neutrons was equal to (6.3±0.6) mb, which is somewhat higher than the value of (5.5±0.1) mb reported earlier in ref.[1]. The value of the cross-section of the (n, p) reaction on ^{50}V induced by thermal neutrons was obtained in our measurements to be equal to (277±42) μb, that is, noticeably different from the value of (400±20) μb given in[2]. This difference is possibly due to the difficulty of identification in work[2] of the proton peak from the reaction under measurement in the region of an overlap with the right hand edge of the large triton peak from the reaction on lithium admixture. This difficulty was eliminated in our measurements by using the selection mode.

The $^{7}Be(n, p)^{7}Li$ reaction at the neutron energy E_n=24.5 keV was investigated on the filtered neutron beam from the reactor. The cross-section of this

reaction was determined by two methods. The first method used the comparison with the cross-section of the $^{6}Li(n, \alpha)^{3}H$ reaction measured under the same conditions. The second method employed as a reference the cross-section of the $^{7}Be(n,p)^{7}Li$ reaction on thermal neutrons from[3]. The weighed average of two methods gives for the cross-section of the $^{7}Be(n,p)^{7}Li$ reaction at 24.5 keV a value of (18±4) b. The cross-section estimate for the studied reaction we have obtained by extrapolation of the data of work[3] to neutron energies below 13 keV to be equal to 18 barns. The cross-section value deduced from the data on the $^{7}Li(n, p)^{7}Be$ reaction in ref.[3] for the same neutron energies by using the detailed balance principle was equal to 20 barns. Thus the cross-section values we have obtained for the $^{7}Be(n, p)^{7}Li$ reaction at the energy E_n = 24.5 keV are in agreement with evaluations by different methods.

At the present time we continue investigation of (n, p) and (n, α) reactions on radioactive nuclei (^{36}Cl, ^{49}V, ^{56}Co and ^{58}Co) in the neutron energy range up to 10 keV on 30 m and 85 m flight paths of the IBR-30 booster.

1 Mughabghab S.F. et al. Neutron Cross Sections, Academic Press, N.Y. (1981), v.1, part A, p.18-1.

2. D'hondt P. et al. Nuclear Data for Science and Technology. Proc. Int. Conf., Antwerp., 1982, p.147.

3. Koehler P.E. et al. Phys.Rev. C (1988) v.37, p.917.

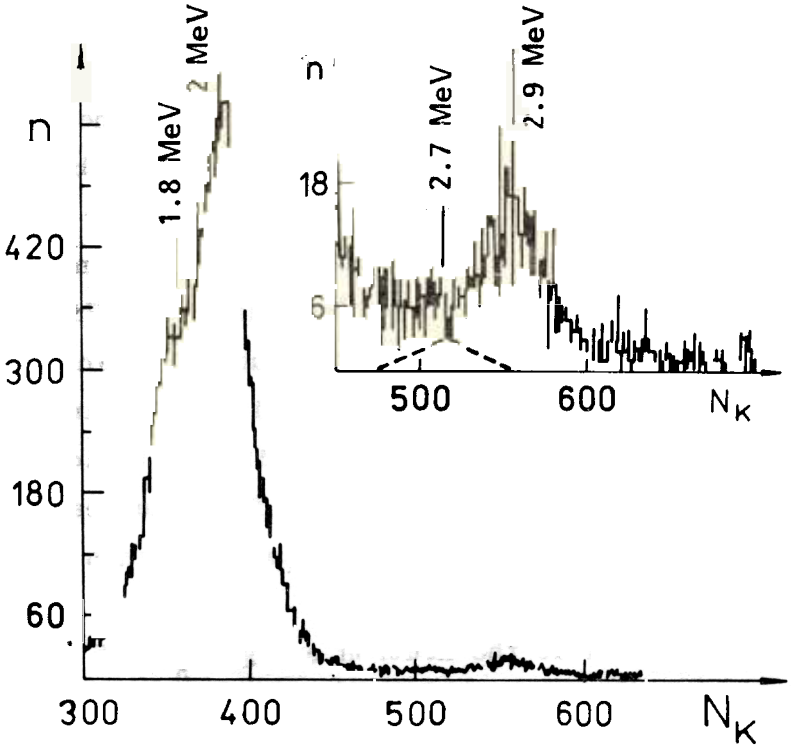

EFFICIENCY CALIBRATION OF THE LITHIUM GLASS NEUTRON DETECTOR

Yu.M.Gledenov, P.V.Sedyshev

Laboratory of Neutron Physics, JINR, Dubna

Bao Shanglian, Cao Wentian

Peking University, Peking, China

On neutron beams of the IBR-30 booster there was measured the efficiency of the neutron detector NE912 (lithium glass with a ^{6}Li isotope content of 99.63 percent, thickness 9.55 mm and diameter 45.5 mm) in the neutron energy range from 100 eV to 150 keV. In order to estimate the contribution of gamma-radiation background there was used the detector NE913 (^{7}Li enrichment to 99.99 percent) having the same dimensions as the scintillation detector under study. Time-of-flight spectra measured with lithium glasses were compared with analogous spectra from the two-section ionization chamber where the target was a thin in comparison with scintillators layer of ^{6}LiF (260x2 $\mu g/cm^2$).

The measurements were performed on a 85-meter flight path. The analysis of obtained results shows that efficiency calibration of the detector NE912 is possible in the neutron energy range from 100 eV to 150 keV on the 500-meter flight path with a statistical accuracy less than 2% for 20 days of IBR-30 running time. By moving to a 250-m flight path one reduces the measuring time to 3 days. However, in this case the energy uncertainty increases considerably (for example at E_n = 100 keV it is above 10%).

CASCADE

CASCADE GAMMA-DECAY OF COMPOUND STATES OF HEAVY NUCLEI

V.A.Khitrov, Yu.P.Popov, A.M.Sukhovoj
Laboratory of Neutron Physics, JINR, Dubna

The procedure to investigate two step γ-cascades is under development[1]. In[2] there is suggested the new method for constructing complex (above 300 transitions and 100 levels) decay-schemes of compound-states of heavy nuclei. The method avails of both spectroscopic information on single γ-transitions (energy, intensity) and the data on cascades of transitions (presence of two successive order transitions, cascade intensity). This method allows one to establish highly reliable decay schemes of complex nuclei up to the excitation energy of 3÷4 MeV. At that transition and level multiplets are unambigously identified and transitions placed by accident are removed effectively from the decay scheme. An increasing number of observed states in ^{181}Hf (Fig.1) and ^{187}W (Fig.2) are compared with predictions of different level density models.

By means of an algorithm[3] for the decomposition of cascade intensity distributions into components connected with the registration of primary and secondary transitions there is obtained a lower (but near to real) estimate of the radiative strength function (RSF) of primary transitions with energies above E_1 = 0.5 MeV both for ^{137}Ba (points in Fig.3) and for ^{181}Hf (Fig.4)[4÷6].

The main conclusions:

a) the RSF's are described more precisely by the model of the giant electrical dipole resonance with the width, Γ_G, depending on the nucleus temperature and γ-quanta energy (lower curves) than by the analogous dependence at Γ_G=const (upper curves);

b) to describe the resulting dependence of RSF's one must take into account single-particle transitions between 4S and 3P neutron shells which contribution is large enough.

1. S.T.Boneva et al. Particles and Nucleus, v.22 (1991), p.479-511.
2. S.T.Boneva et al. Izv.Akad.Nauk SSSR, ser.fiz., v.55 (1991), p.841-849.

3. S.T.Boneva et al. Z.Phys.A - Hadrons and Nuclei, A338 (1991), p.319-323.
4. A.M.Sukhovoj. In: Nuclear Spectroscopy and Structure of Atomic Nuclei. Abstracts of 41st Meeting, Leningrad, "Nauka", 1991, p.78.
5. V.A.Bondarenko et al. Ibid., p.77.
6. V.A.Bondarenko et al. Ibid., p.112.

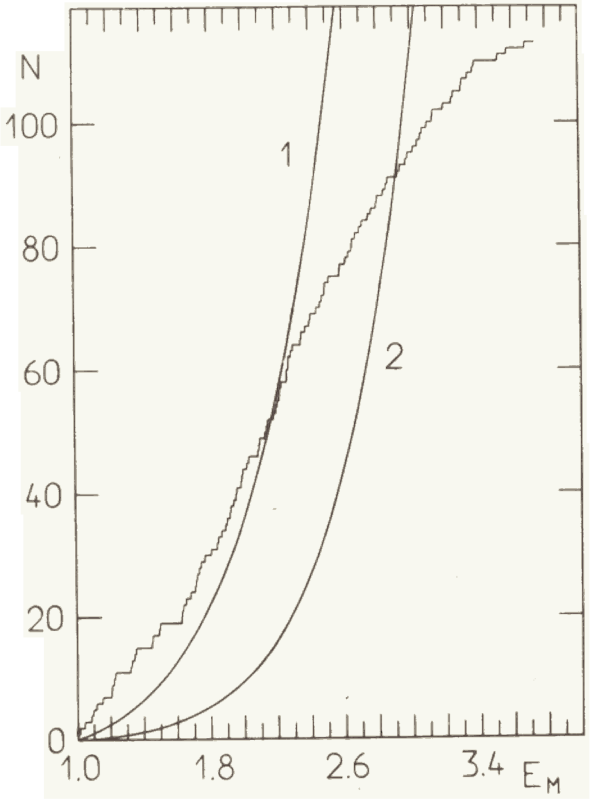

Fig.1. An increasing number, N, of levels with I = 1/2 and 3/2 observed experimentally and predicted by different models for ^{181}Hf.

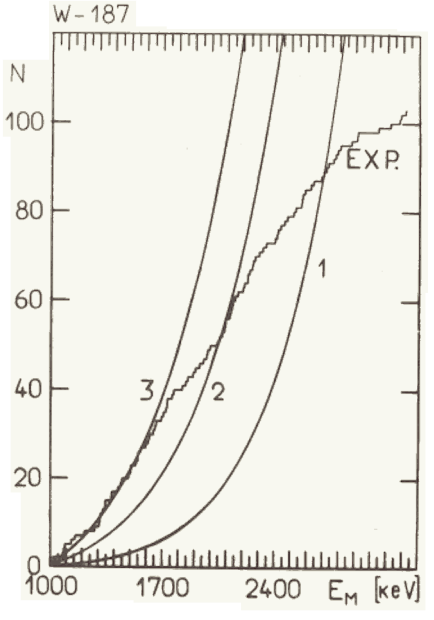

Fig.2. The same for ^{187}W.

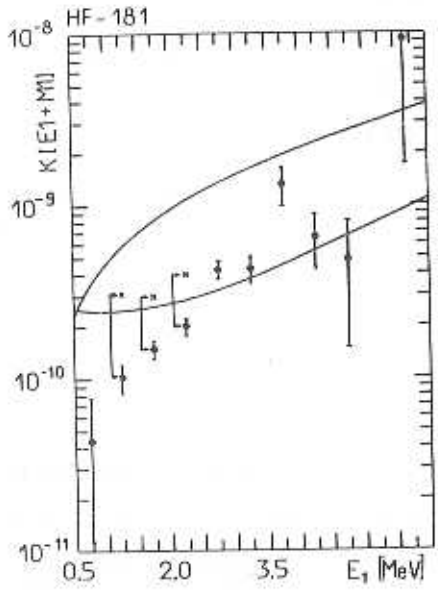

Fig. 3. The radiative strength function of primary transitions in ^{181}Hf. Points - lower estimate, crosses - upper estimate.

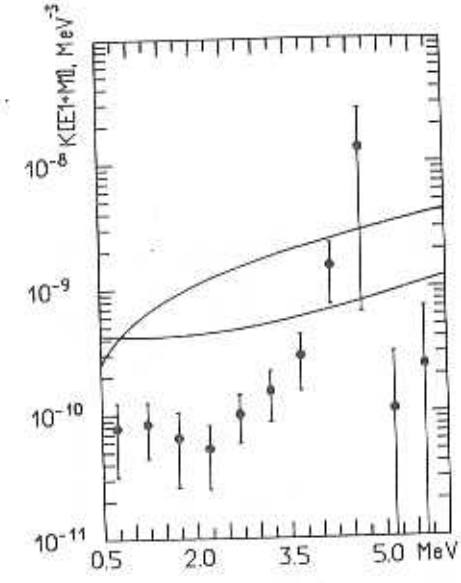

Fig. 4. The same for ^{137}Ba.

RESULTS OF NEUTRON LIFETIME MEASUREMENT WITH GRAVITATIONAL UCN TRAP

V.P.Alfimenkov, V.I.Luschikov, V.N.Shvetsov, A.V.Strelkov
Laboratory of Neutron Physics, JINR, Dubna
V.P.Gudkov, A.G.Kharitonov, V.V.Nesvizhevsky, A.P.Serebrov,
S.O.Sumbaev, R.R.Taldaev, V.E.Varlamov, A.V.Vasilyev
Petersburg Nuclear Physics Institute, Gatchina, USSR

Precise measurements of the neutron lifetime and β-decay asymmetry provide additional information for the check of the Standard Model of electroweak interactions and a search for possible deviations.

In the reported experiment the neutron lifetime has been measured with ultra-cold neutrons (UCN), confined in a gravitational trap.

The reported experiment had the aim to decrease UCN storage losses and measure directly the decay exponent. For that substances with a small capture cross section (Be, O_2) were used to cover trap walls and the measurements were performed at low temperatures (15 K). To estimate neutron losses correctly spectral measurements of stored neutrons were made. The measured probability of UCN losses accounted for 3% neutron β-decay probability.

The UCN storage time in a trap (τ_{st}) is determined by the free neutron lifetime (τ_n) and the time of neutron losses due to their interactions with walls (τ_{los})

$$\tau_{st}^{-1} = \tau_n^{-1} + \tau_{los}^{-1} \qquad (1)$$

The probability of UCN losses is proportional to the loss factor η and is the function of the UCN energy (E), the shape and dimensions of the trap (R) and the critical energy of the trap walls material (E_{lim})

$$\tau_{st}^{-1} = \tau_n^{-1} + \eta * \gamma(E, R, E_{lim}) \qquad (2)$$

In eq. (2) τ_{st}^{-1} is the linear function of the argument γ, which is calculated for the given E, R, E_{lim}. The neutron lifetime τ_n^{-1} can be obtained by extrapolation to zero argument γ.

The results of measurements are shown in the Figure as the linear function $\tau_{st}^{-1}(\gamma)$. Besides the measurements with oxygen traps, the measurements with

beryllium traps were performed to demonstrate the conditions for UCN storage before oxygen freezing.

The results on the neutron lifetime, obtained in our experiment are: τ_n = 885.0±7.7 s for the traps with beryllium coating, τ_n = 889.0±3.1 s for the traps with oxygen coating. The validity of extrapolation is confirmed by the χ^2 value of 0.81, calculated from the oxygen data. The final result, obtained for the neutron lifetime is τ_n = 888.4±2.9 s, the corresponding value of λ (G_A to G_V ratio of weak interaction constants) is λ = -1.2677±0.0025.

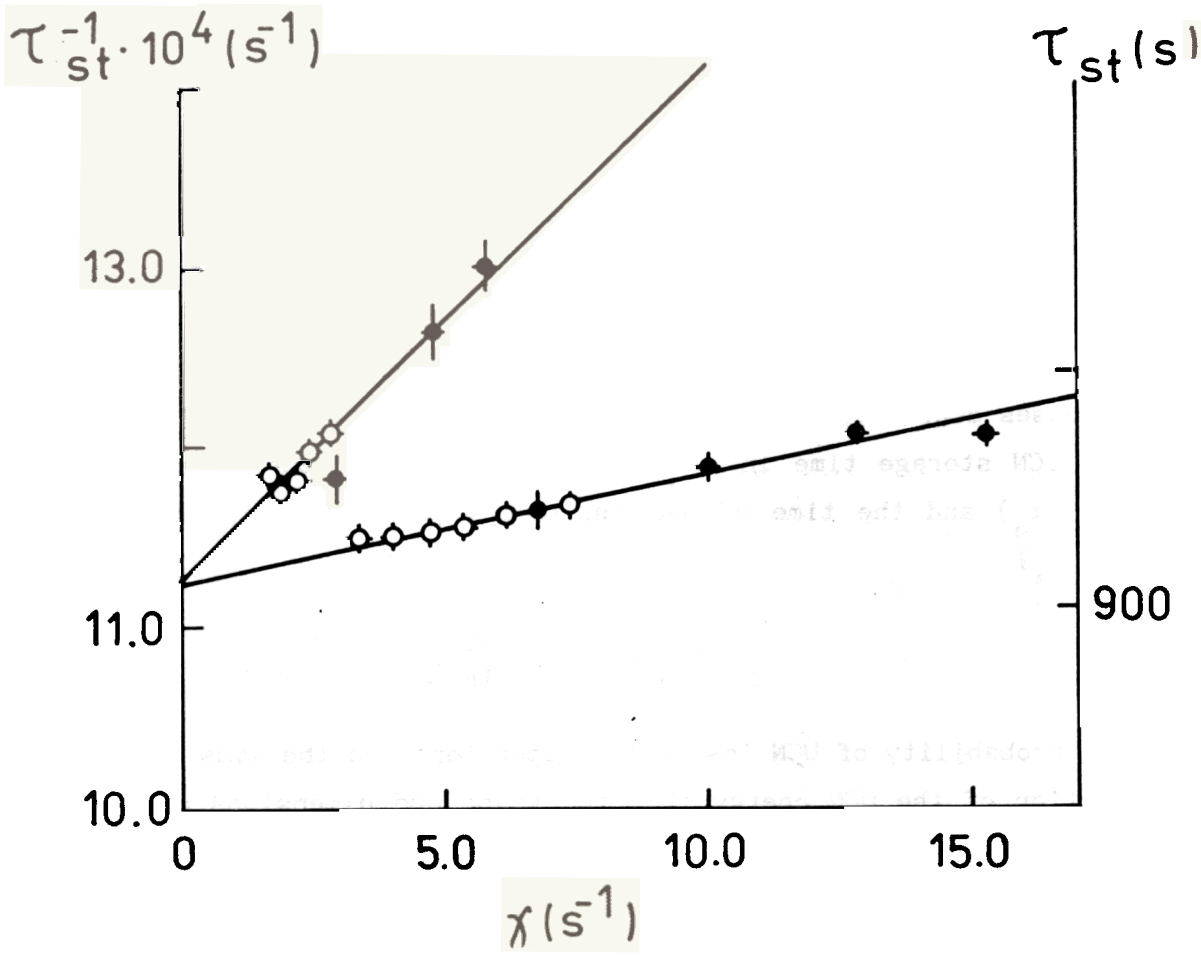

Results of the UCN storage time measurements (τ_{st}^{-1}) as the function of the parameter γ. 1(Be), the extrapolation from beryllium traps data. 2(O_2) the extrapolation from the oxygen traps data. ⊕ - results of measurements with spherical traps; - ◆ results of measurements with cylindrical traps.

INVESTIGATION OF PARITY VIOLATION IN NEUTRON RESONANCES OF Rb AND ^{113}Cd

V.P.Alfimenkov, Yu.D.Mareev, L.B.Pikelner, V.R.Skoy, V.N.Shvetsov

Laboratory of Neutron Physics, JINR, Dubna

The spectrometer POLYANA for experiments with polarized resonance neutrons and nuclei has been recently modernized to obtain a higher neutron flux. It has been removed to a more intense neutron beam of the IBR-30 booster and closer to the moderator. As the result, the neutron flux through the polarized proton target increased by approximately 20 times. Now the intensity of neutrons leaving the target with polarization f_n=0.6 is 3 $10^5/E^{0.9}$ n/sec eV. The new high efficient multisection proportional neutron counter with ^{3}He was manufactured for measurements of the transmission through a target of neutrons with opposite helicities. This counter can be installed at three flight paths 17, 30 and 52 m. The multisection design allows accumulation of time-of-flight spectra from any combination of the counter's sections and of the integral spectrum. The new IBM PC AT/286 based system was organized for the spectra acquisition and processing.

On this modernized spectrometer there were made experiments on the search for parity violation effects in polarized neutron transmisson in p-resonances of Rb natural isotope mixture at E_o=9.6 eV and ^{113}Cd E_o=7.0 and 21.9 eV. The effect reveals itself as the difference between the transmissions of neutrons with opposite helicities. The statistically significant value of $P_p=(-9.8\pm3.0)10^{-3}$ was obtained only for the ^{113}Cd p-resonance E_o=7.0 eV. Comparison of this result with the results of other experiments allowed the calculation of a matrix element for different parity compound states mixing. For the other resonances of ^{113}Cd and Rb the parameters Γ and $g\Gamma_n$ ($ag\Gamma_n$ for Rb) were obtained.

MEASUREMENTS OF PARITY VIOLATION IN RESONANCE NEUTRON-CAPTURE REACTIONS

E. I. Sharapov, Yu. P. Popov
Laboratory of Neutron Physics, JINR, Dubna
S. A. Wender, S. J. Seestrom, C. D. Bowman
Los Alamos National Laboratory, Los Alamos, USA
H. Postma
University of Technology, Delft, The Netherlands
C. R. Gould
North Carolina State University, Raleigh, USA
A. Wasson
National Institute of Science and Technology, Washington, USA

Experiments on the study of parity violation in total (n,γ) cross sections were performed on ^{139}La and ^{117}Sn targets at the LANSCE pulsed neutron source using longitudinally polarized neutrons and a BaF_2 detector. The effect of parity nonconservation in the $^{139}La(n,\gamma)$ reaction for the resonance at E_n = 0.73 eV was confirmed. New results were obtained for p-wave resonances in the $^{117}Sn(n,\gamma)$ reaction. Capture and transmission techniques for measuring parity violation effects are compared.

Table

Parity-Violating Asymmetries Measured in Neutron Capture

Sample	n (10^{22} atom/cm^2)	E_n (eV)	ε_γ (%)
La	3.1	0.73	8.6±0.5
La	6.8		5.8±0.4
^{117}Sn	2.9	1.33	1.1±0.2
^{117}Sn	2.9	26.4	-1.3±1.6
^{117}Sn	2.9	34.0	0.45±0.49

ON SOME PECULIARITIES OF INDEPENDENT FRAGMENT YIELDS IN THE FISSION OF ^{239}Pu INDUCED BY RESONANCE NEUTRONS

A.A.Bogdzel, N.A.Gundorin, U.Gohs, A.Duka-Zolyomi,
J.Kliman, V.Polgorski, A.B.Popov, Dao Anh Minh
Laboratory of Neutron Physics, JINR, Dubna

Interest in peculiarities of resonance neutron induced fission is connected with the possibility of developing a multi-mode-fission model on the ground of new experimental data.

Necessity to investigate peculiarities of resonance neutron induced fission arises from the A.Bohr's theory of fission channels[1]. Available experimental data on fragments' kinetic energy, gamma and neutron multiplicities, mass and charge distributions come mainly from the fission of ^{235}U[2]. However, the Rigier's R.B.[3] and Cowan's G.A.[4] results have demonstrated more dramatically changes in P/V parameter of the fragments mass distribution from the fission of ^{239}Pu induced by resonance neutrons with energies from 0.3 eV to 15 eV.

We have employed the discrete prompt gamma-ray spectroscopy method to measure independent yields of fission fragments of ^{236}U on the beam of the reactor IBR-30 in Dubna[5]. Similar investigations continue with ^{240}Pu.

In 1990-1991 the aim of our work was to measure independent yields of fragments from the neutron resonance fission of ^{239}Pu by means of the gamma-ray spectroscopy method.

EXPERIMENT

The fission gamma-ray spectrum from 100 keV to 1.6 MeV contains over 100 photo-peaks.

These photo-peaks are used for the identification of fission fragments. The yields determination consists in the calculation of the ratio:

$$Y_i^{exp} = (\Sigma_k N_{co}^k)_i / (\Sigma_k N_f^k)_i * (K^{eff})^{-1}$$

for each resonance, where the resonance areas $(\Sigma_k N_f^k)_i$, and $(\Sigma_k N_{co}^k)_i$ were taken from fission and coincidence TOF spectra, respectively, K^{eff} is the absolute efficiency of FIGARA which was determined using the standard calibration set.

Relative changes in yields of individual resonances were calculated by the algorithm:

$$\delta Y_i^{exp} = (Y_i^{exp} - Y_c)/Y_c,$$

Y_c - the recommended independent yields for thermal neutron-induced fission[6].

RESULTS

1. Independent yields of some fragments from the fission of ^{239}Pu by resonance neutrons with the energy from 0.2 eV to 230 eV were measured (Table).

2. The experimental data obtained for thermal (Y_t) and resonance (Y_{res}) neutrons were compared with recommended independent yields from thermal neutron fission[6]. Resonance neutron fission has revealed the peculiaruty: the yield decreases with mass number near standard I and increases - near standard II as demonstrated in Fig. The inverse peculiarity was found for the resonance neutron-induced fission of ^{235}U by F.-J.Humbsch et al.[2].

3. Relative changes in some independent yields to 11-th resonances with spin 1^+ and 4-th resonances with spin 0^+ were demonstrated. Weighed mean values for two groups of light and heavy fragments were calculated from these data as a function of $1/\Gamma_f$.

4. Using the well-known weighing method, we have obtained average parameters of gamma-rays spectrum: multiplicity N_γ = 7.26±0.19, the total energy E_t = 6.68±0.12 MeV and the mean energy $\varepsilon = E_t/N_\gamma$=0.92±0.03MeV.

5. In addition to multiplicity, total and mean energy of fission gamma-rays, independent yields of some fragments from the resonance neutron-induced fission of ^{239}Pu can be measured within the error of 5-25 percent by means of the gamma-spectroscopy method.

6. The experimental data on individual resonances do not deny the possibility of the correlation between fission fragment yields and fission widths, possibly connected with the (n, γf) process, but can supply no evidence in favor due to considerable experimental errors. So higher precision measurements of independent yields of individual resonances are necessary.

1. A.Bohr. Proc.Int.Conf. on Peaceful Uses of Atomic Energy, 1956, vol.2, p.151.

2. F.-J.Hambsch. et al. Nucl.Phys., A491 (1989) 56.
3. R.B.Rigier et al. Phys.Rev., 119 (1960) No.6.
4. G.A.Cowan et al. Phys.Rev., 144 (1966) No.3.
5. A.A.Bogdzel et al. Comm.JINR, P15-88-385, Dubna, 1988
6. Arthur C.Wahl. Atomic Data and Nuclear Data Tables, 39 (1988) 118-121.

Table

Independent yields of Fission Fragments from resonance neutron-induced fission of ^{239}Pu

Fragment Z-FR	Mass A	Transition energy E(keV)	Transition spin J^{π}	Recommended independent yield thermal neutrons) Y_c(%)	Experimental independent yield thermal neutrons Y_T(%)	Experimental independent yield (resonance neutrons) Y_{res}(%)
36-KR	88	775	2^+-0^+	0.79±0.03	0.80±0.21	0.77±0.23
	90	707	2^+-0^+	1.18±0.05	1.10±0.19	1.58±0.27
38-SR	94	837	2^+-0^+	3.14±0.16	2.92±0.32	2.65±0.33
40-ZR	98	1223	2^+-0^+	2.85±0.14	2.75±0.28	2.78±0.29
	100	212	2^+-0^+	4.76±0.24	4.50±0.23	3.95±0.20
	102	152	2^+-0^+	1.19±0.12	1.19±0.15	0.99±0.14
42-MO	104	192	2^+-0^+	4.12±0.21	3.99±0.20	4.02±0.20
	106	171	2^+-0^+	2.06±0.10	1.80±0.20	1.48±0.21
52-TE	132	975	2^+-0^+	2.36±0.07	2.32±0.28	1.79±0.23
	134	1279	2^+-0^+	4.70±0.51	3.42±0.35*	2.70±0.28*
54-XE	136	1313	2^+-0^+	3.02±0.36	2.86±0.30	1.83±0.17
	138	589	2^+-0^+	4.08±0.33	3.89±0.27	3.56±0.28
56-BA	142	359	2^+-0^+	3.27±0.26	3.09±0.25	3.49±0.32
	144	199	2^+-0^+	2.05±0.23	2.39±0.14	2.51±0.15
58-CE	146	259	2^+-0^+	0.95±0.01	0.79±0.13	1.13±0.18
	148	159	2^+-0^+	1.09±0.12	1.29±0.12	1.70±0.16

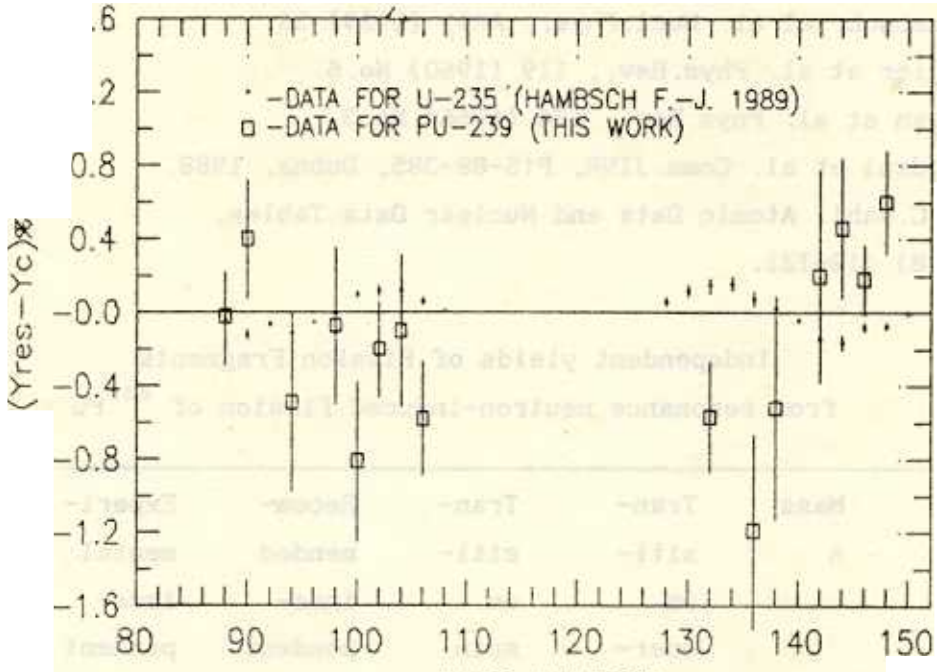

The difference (Y_{res}-Y_c) vrs fragment mass

EVALUATION OF TOTAL FISSION CHARACTERISTICS FOR ^{235}U AND ^{239}Pu IN THE LOW ENERGY REGION

U.Gohs

Laboratory of Neutron Physics, JINR, Dubna

Energy conservation consistent evaluations of total fission characteristics $\bar{X}_\lambda$ were performed for $J^\pi = 4^-$ neutron resonances of ^{235}U /1/ and $J^\pi = 1^+$ neutron resonances of ^{239}Pu /2/ on the basis of a phenomenological multimode model. If one considers the contribution of the (n, γf) process with an average width $\bar{\Gamma}_{\gamma f}$ (without account for channel effects), the average values of the total kinetic energy $\overline{TKE}$, the average number of promptly emitted neutrons $\bar{\nu}_n$, the multiplicity of γ-rays $\bar{N}_\gamma$, and the total energy of γ-rays $\bar{E}_\gamma$ can be expressed by

$$\bar{X} = (\bar{\Gamma}_{\gamma f}/\Gamma_{f\lambda})\Sigma W_{d\lambda}\overline{X_d} + (1 - (\bar{\Gamma}_{\gamma f}/\Gamma_{f\lambda})\Sigma\Sigma P_{k\lambda} W_d^k \overline{X_d},$$

where $P_{k\lambda}$ represents the relative contribution of the fission channel k to a given resonance λ with an average fission width $\Gamma_{f\lambda}$. W_d^k is the relative population of the mode d for the channel k, $W_{d\lambda}$ is the relative population of the mode d for the resonance λ. In the case of ^{239}Pu the channel effects do not exist since the $J^\pi = 1^+$ strength is represented by one fission channel.

According to the present evaluations, the (n, γf) process is characterized by the following averages

$J^\pi = 4^-$ resonances of ^{235}U

$$\bar{\Gamma}_{\gamma f}\bar{N}_{\gamma f} = (0.42\pm0.10)\ \text{meV},$$

$$\bar{\Gamma}_{\gamma f}\bar{E}_{\gamma f} = (410\pm120)\ \text{eV}^2$$

$J^\pi = 1^+$ resonances of ^{239}Pu

$$\bar{\Gamma}_{\gamma f}\bar{N}_{\gamma f} = (1.5\pm0.5)\ \text{meV},$$

$$\bar{\Gamma}_{\gamma f}\bar{E}_{\gamma f} = (2150\pm650)\ \text{eV}^2.$$

It has been shown that the observed experimental fluctuations in total fission characteristics for $J^{\pi} = 4^{-}$ resonances of ^{235}U can be explained within a multimode fission model with account for the (n, γf) process (Fig.1). By including the influence of fission modes we can get information about the (n, γf) process ($\bar{\Gamma}_{\gamma f}$ and $\bar{E}_{\gamma f}$) from measurements of $\bar{\nu}_n$, $\bar{E}_{\gamma}$, and $\bar{N}_{\gamma}$. Then one may fairly conclude that the neutron number as the function of fragment mass depends on the contribution of fission modes, which influences the calculation of the preneutron emission mass distribution from measured fragment kinetic energies.

In the case of $J^{\pi} = 1^{+}$ resonances of ^{239}Pu the observed experimental fluctuations in $\bar{\nu}_n$, $\bar{E}_{\gamma}$, and $\bar{N}_{\gamma}$ result from the competition between the (n, f) reaction and the (n, γf) process (Fig.2). Our results indicate a larger contribution of fission mode standard I for $J^{\pi} = 1^{+}$ resonances in comparison with thermal neutron induced fission.

1. U.Gohs. In: Proc. of Int.Conf. on Nucl.Data for Science and Technology. Jûlich, May, 1991 (in press).
2. U.Gohs. In: Proc. of Int. Workshop on Dynamical Aspects of Nuclear Fission. Smolenice, June, 1991 (in press).

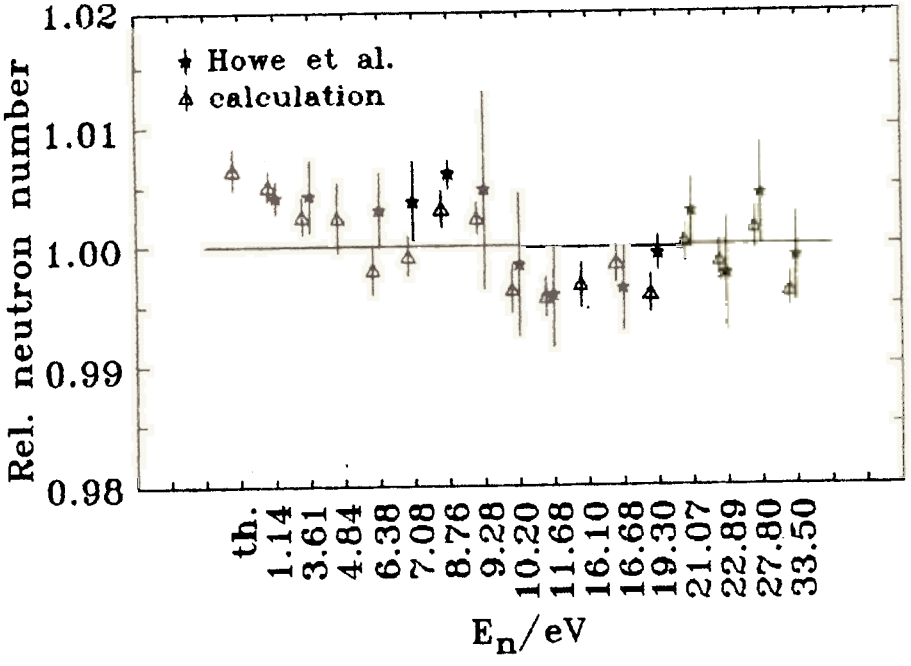

Fig.1. Relative $\bar{\eta}_n$ as the function of resonance energy E_n

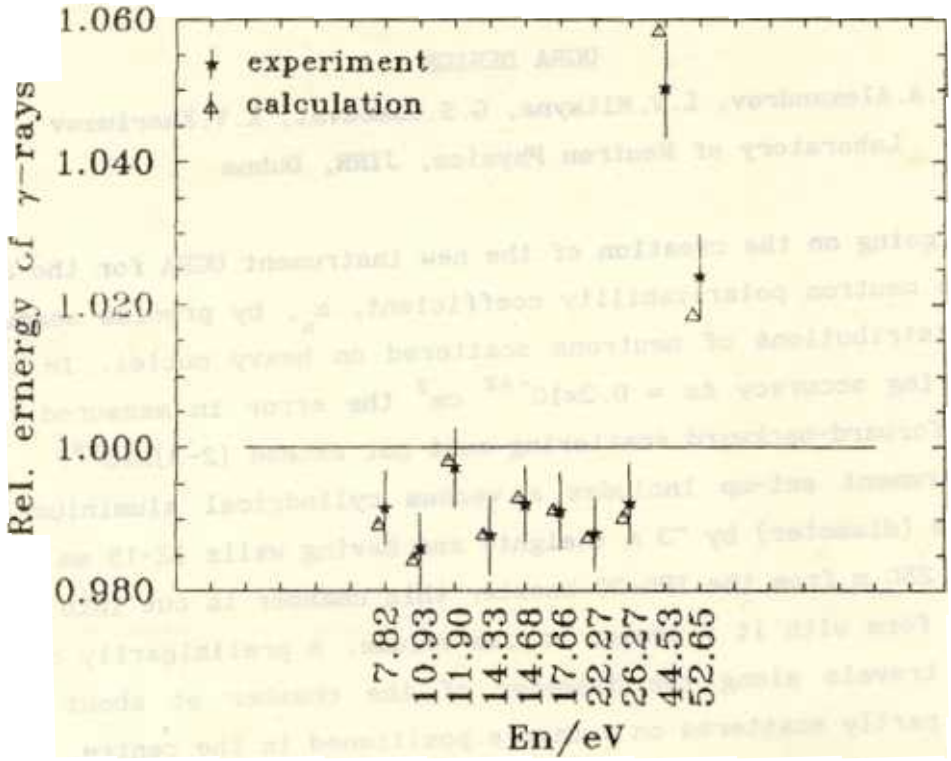

Fig.2 Relative $\bar{E}_\gamma$ as the function of resonance energy E_n.

UGRA

UGRA DESIGN

Yu.A.Alexandrov, L.V.Mitsyna, G.S.Samosvat, K.V.Khariuzov
Laboratory of Neutron Physics, JINR, Dubna

Work is going on the creation of the new instrument UGRA for the determination of the neutron polarizability coefficient, α_n, by precise measurements of angular distributions of neutrons scattered on heavy nuclei. In order to have a measuring accuracy $\Delta\alpha \simeq 0.3\times10^{-42}$ cm^3 the error in measured relative asymmetry of forward-backward scattering must not exceed $(2-3)\times10^{-4}$.

The instrument set-up includes a vacuum cylindrical aluminium chamber measuring ~3 m (diameter) by ~3 m (height) and having walls 12-15 mm thick. At a distance of 250 m from the IBR-30 booster this chamber is cut into a neutron guide tube to form with it a common vacuum volume. A preliminarily collimated neutron beam travels along the diameter of the chamber at about half its height and is partly scattered on a sample positioned in the centre. Scattered neutrons are counted by detectors mounted on a rotating platform parallel to the chamber bottom.

Two modes of scattered neutrons detection are planned to be used, ionization and scintillation. In the first mode sixteen detectors will be scanning the sample. Each of them is a set of proportional counters filled with ^{3}He gas at 10 atm with a total volume of about 8ℓ. Every detector is to be positioned at a level of 70 cm below the neutron beam inside the shielding having an input channel made so that it"sees" only the sample and part of the chamber wall behind it. At a booster power of 10 kW, the sample area of 200 cm^3 and a 30% probability of neutron scattering on the sample, the above indicated measuring accuracy can be achieved in about 20 days of the instrument running time. At that, every detector will register about 2×10^6 scattered neutrons in the energy interval of 28-30 keV. In the scintillation mode, in order to have the same counting rate it suffices to have two liquid (containing about 10% of ^{10}B) scintillation detectors. The detecting layer is 12.5 cm in diameter and 3 cm thick. Both detectors are enclosed in shields with input channels and positioned near the central horizontal plane of the chamber so that one of them does not "see" the shielding details of the other.

Besides the neutron polarizability measurements the UGRA can be used for:

- search for light scalar particles transferring interaction;
- search for and investigation of mixed (s+d) wave resonances;

- determination of spin channels mixtures in p-wave resonances;

- measurement of the strength functions for $P_{1/2}$ wave neutrons and of scattering radii of P-wave neutrons;

- applied research; nondestructive quantitative analysis of samples for hydrogen.

ON THE CORRECTNESS OF ESTIMATES OF THE (n, e)-AMPLITUDE AND THE NEUTRON POLARIZABILITY FROM TOTAL CROSS SECTIONS OF Bi AND Pb

V.G.Nikolenko, A.B.Popov

Laboratory of Neutron Physics, JINR, Dubna

At present there exist two essentially different results for the (n, e)-scattering amplitude (a_{ne}) obtained from the energy dependence of total cross sections and the data on coherent scattering lengths for lead and bismuth: $(1.32\pm0.04)\times10^{-3}$ fm (Bi, Pb)[1] and $(1.59\pm0.04)\times10^{-3}$fm (Bi)[2], which lead to two values with opposite signs for the neutron mean square charge radius 0.12(2) fm and -0.11(2) fm, respectively.

Our analysis of used in[1] and [2] methods of a_{ne} extraction has shown that the reason of the discrepancy between the a_{ne} values (which, in fact, were obtained from the same experimental data) are conditioned by different mathematical descriptions of these data. In the formulae in ref.[2] unlike[1] there were lost interresonance interference terms. We confirm the more grounded value of a_{ne} = -1.32 mfm of the authors[1] and pay attention to the fact that in ref.[1] the expression for the coherent scattering length does not contain the term taking into account the contribution of the imaginary part, which becomes essential at higher neutron energies. One might think that the imaginary part corrections lead to a very small change in a_{ne} values, but they essentially influence the estimates of the neutron charge mean square radius

$$\langle r^2\rangle^{1/2} = \frac{3h^2}{me^2}\,(a_{ne} - a_F$$

(where the Foldy's term a_F = -1.468 mfm), and push its value from 0.12 fm to 0.04 fm (Bi) and 0.09 fm (Pb).

Corrections for the imaginary part of the scattering length are especially essential when the neutron polarizability coefficient, α_n, is estimated from the experimental data under discussion. Within the formally achieved statistical error $\Delta\alpha_n \approx 3$ (in units 10^{-3} fm^3) the obtained estimates of α_n change from -8 to +36 in dependence on the way the imaginary part of the scattering length, the resonance contribution and the accepted nuclear scattering radius are accounted for.

1. L.Koester et al. Physica, 137B (1986) 282; Z.Phys.A., 329 (1988) 229.
2. Yu.A.Alexandrov et al. JINR, E3-85-135, Dubna, 1985; Sov.J.Nucl.Phys., 44 (1986) 900.
3. V.G.Nikolenko, A.B.Popov. JINR, P3-90-568, Dubna, 1990.
4. V.G.Nikolenko, A.B.Popov. JINR, E3-91-106, Dubna, 1991.
5. V.G.Nikolenko, A.B.Popov. To be published in Z.Phys.A.

SCATTERING OF NEUTRONS WITH ENERGIES FROM 1 TO 300 keV ON KRYPTON AND XENON

A.M.Govorov, L.V.Mitsyna, G.S.Samosvat
Laboratory of Neutron Physics, JINR, Dubna

Differential cross sections for the elastic scattering of neutrons with energies up to about 300 keV on gaseous krypton and xenon are measured. Oxygen is used as a standard.

Gases at about 40 atm filled three stainless-steel containers, each 1.9ℓ in volume. These three gas-filled containers and one gas-free container were placed in turn in the neutron beam. The experimental setup and the measuring method used are described in [1].

Neutron strength functions S^0, $S^1_{1/2}$, $S^1_{3/2}$ and distant levels contributions R^∞_0, R^∞_1 are extracted from the cross sections data by the least squares method (see, for example, [2]).

Obtained values make complete the earlier data for 34 nuclei in the atomic mass region 48<A<144. The most interesting are the data on p-wave scattering radii $R'_1=1.35\ A^{1/3}\ (1 - 3R^\infty_1)$ fm illustrated in the Figure. In krypton measurements we have refined the A-dependent behavior of p-wave scattering radii in the region of A ≅ 70-90, where the neutron p-wave phase shift has an anomalous positive sign. Investigations with xenon point to the anomaly of R'_1 (A≃ 128).

1. V.A.Vagov et al. JINR Comm., P3-82-770, Dubna, 1982 (in Russian).
2. G.S.Samosvat. Particles and Nucleus, v.17 (1986) p.713 (in Russian).

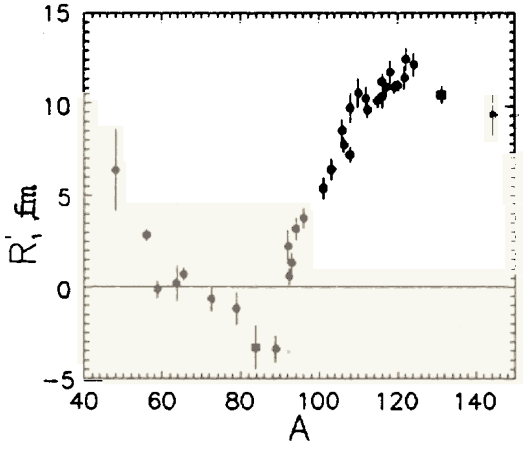

Experimental values of R'_1. For Kr and Xe - dark squares

ON THE STUDY OF NEUTRON RESONANCES IN ^{147}Sm

G.P.Georgiev, Yu.S.Zamyatnin, V.I.Ivanov,
L.B.Pikelner, I.A.Sirakov
LNP, JINR, Dubna
Yu.V.Grigoriev
Physics-Power Engineering Institute, Obninsk, USSR
G.V.Muradian
Institute of Atomic Energy, Moscow, USSR
N.B.Yaneva
Institute of Nuclear Research and Nuclear Power, Sofia
Bulgaria

The pulsed booster IBR-30 (JINR, Dubna) was used as the neutron source in experiments on the study of multiplicities of γ-rays following radiative neutron capture in ^{147}Sm in the energy range from 15 eV to 900 eV. These experiments were performed by the time-of-flight method using a multisectional 4-π detector of γ-rays, which allows one to measure multiplicity spectra in individual resonances. Correlation between the multiplicity spectrum and spin of the resonance was investigated. Spins were assigned to about 90 resonances and radiative widths of about 30 resonances were measured.

This article describes the multiplicity spectrometer built on the basis of the high intensity pulsed neutron source at the Laboratory of Neutron Physics, JINR, and reports on the first results obtained with this method in the ^{147}Sm experiment.

In the experiment the multisectional scintillation γ-detector, Romashka - the given name[1], was installed on the 500 m flight path of the pulsed neutron booster IBR-30. Mean booster power is 10 kW and the multiplication coefficient - 200. At that the neutron pulse generated has the duration of about 4 μsec and a resolution of 8 ns/m. The pulse repetition rate is 100 p.p.s.

The detector consists of 16 independent sections, crystals of NaI(Tl), measuring 122x122x152 mm^3, each viewed with a photomultiplier. The detector has a through vacuum channel for the collimated beam to pass through and a sample be positioned inside the detector (Fig.1).

Samples were made from ^{147}Sm oxide enriched to 96.4%. They were prepared either 3.58×10^{-4} atom/barn or 8.94×10^{-5} atom/barn thick and put into thin-wall aluminium containers 100 mm in diameter.

The neutron time-of-flight and γ-quanta coincidence multiplicity were measured for every neutron capture event. The events will be stored in the memory of the measuring module, if the sum energy of registered γ-quanta lies in the interval from 2 MeV to 8 MeV. The pulse detection threshold of each section is 100 keV.

This registration scheme allows us to simultaneously measure 16 time-of-flight spectra corresponding to coincidences of different multiplicities and to obtain γ-multiplicity distributions for every resonance.

In addition, the boron n-γ converter, positioned inside the detector, gave the opportunity to detect neutron scattering events by measuring mono-energy γ-quanta from the $^{10}B(n, \alpha)$ reaction. Moreover, it served to decrease the detector sensitivity to scattered neutrons.

In result of the determination of areas under resonance peaks in spectra of different multiplicities, K, at K varying from 1 to 7 we have found the multiplicity distribution and average multiplicity value, <K>, for every resonance, (Fig.2). As is seen in the figure the resonances form two clearly distinguishable groups with respect to the <K> value. These groups correspond to 3^- and 4^- spin values for the resonances with earlier known spins (at energies up to ~400 eV)[2,3].

This made it possible to assign spins to about 90 resonances in ^{147}Sm in the energy interval from 15 eV to 900 eV and confirm most of the earlier made spin assignments. It is suggested to revise spin assignments for five resonances (161.0; 161.8; 359.2; 362.3 and 412.0 eV). Some of the resonances (61.5 and 257.0 eV) appeared to have intermediate <K> values. A per-channel examination of <K> values has shown that these resonances are the earlier unresolved double resonances with various spins (Fig.3). Additional measurements conducted with the ^{148}Sm isotope have prooved the resonance at 94.8 eV to belong to this isotope and not to ^{147}Sm.

Simultaneous measurement of the time-of-flight spectra of neutron capture and neutron scattering has allowed us to make estimates on radiative neutron widths for a considerable number of resonances. These estimates were derived from the comparison of under-peak areas in neutron capture, S_γ, and neutron scattering, S_n, spectra with account for the relative effectiveness of detection of these two processes.

In this way we have obtained the preliminary Γ_γ values for some 30 resonances at energies from 15 eV to 900 eV.

1. G.P.Georgiev et al. JINR Comm., P3-88-555, Dubna, 1988.
2. S.F.Mughabghab. Neutron Cross Section, v.1, Part B, Academic Press, 1984.
3. A.B.Popov, K.Trzeciak, Hvan Cher Gu. Sov.J.Nucl.Phys., 32 (1980) 603.

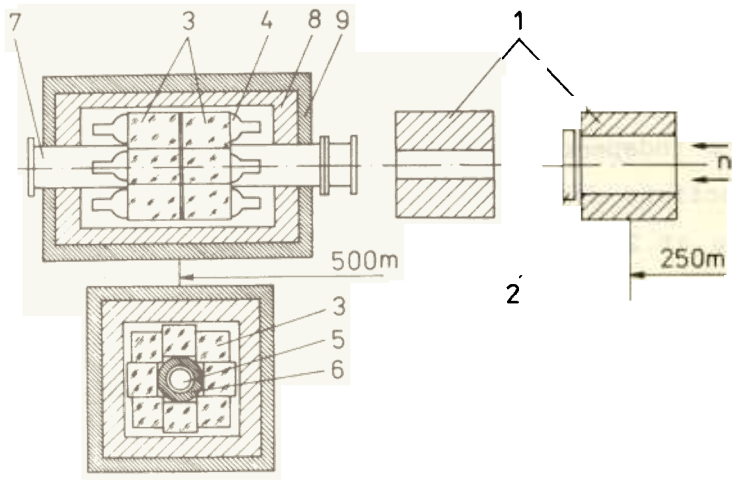

Fig.1. Longitudinal and transversal section view of the multisectional scintillation γ-detector "Romashka" (not in scale): 1 - collimator; 2 - filter; 3 - NaI(Tl) crystals; 4 - photomultipliers FEU-110; 5 - sample; 6 - converter; 7 - vacuum tube for sample positioning; 8 - lead shielding; 9 - B_4C shielding.

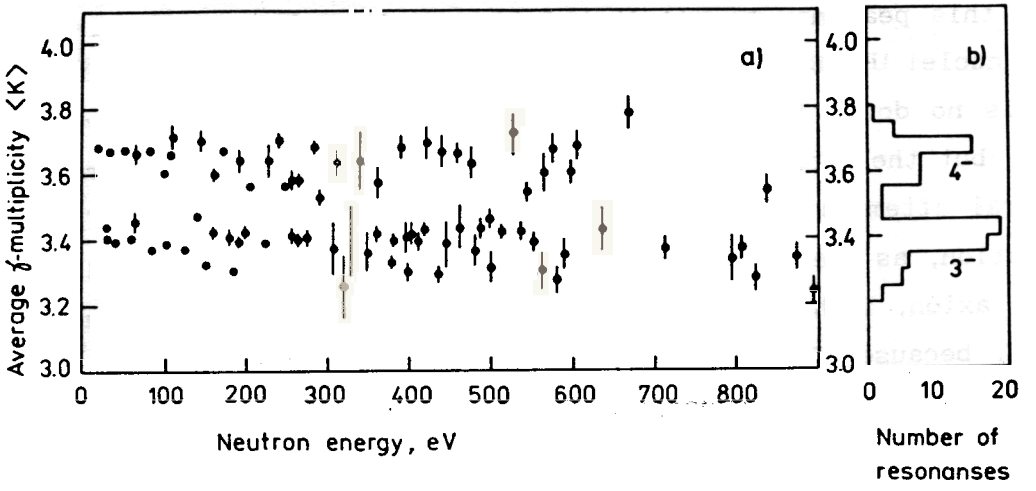

Fig.2. Experimental average values for γ-ray multiplicity <K>; a) <K> values of resonances at energies from 15 eV to 900 eV; b) number of resonances as a function of <K>.

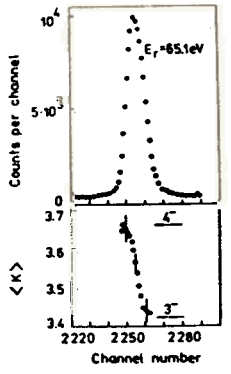

Fig.3. Per-channel determination of the average γ-ray multiplicity value in the vicinity of the 65.1 eV resonance. A sharp deviation in <K> value from the value characteristic of resonances with spin 4^- towards that corresponding to spin 3^- evidences the presence of two unresolved resonances with different spins.

A SEARCH FOR 180°-CORRELATED PAIRS OF GAMMA-QUANTA IN α-DECAY OF Pu-239

S.B.Borzakov, Yu.N.Pokotilovskij, I.M.Salamatin

Laboratory of Neutron Physics, JINR, Dubna

In collisions of very heavy nuclei (Z > 82) at energies close to the Coulomb barrier in experiments at UNILAC (GSI) two groups have observed e^+ and correlated e^+e^- peaks with invariant masses ~1630, ~1780 and ~1830 keV and widths 24-40 keV[1,2]. Energies of the peaks (slightly different in different publications) and their widths are independent of the total charge of colliding nuclei, while their cross-sections depend noticeably on charges of nuclei. As these peaks are seen also at $Z < Z_c = 173$, there appears no direct connection of these phenomena with the spontaneous positron creation in a supercritical Coulomb potential.

Besides e^+e^- peaks there was observed in the experiment[3] in collisions U + Th a 180°-correlated $\gamma\gamma$-peak at a total energy of 1062 keV with the width 2.5 keV. However, a more recent publication of this group[4] reports on the fact that this peak may be attributed to radiation from high spin states of scattered nuclei U-238.

There is no doubt in the experimental reliability of the above-mentioned phenomena, but their rigorous interpretation is still absent. There have been made several attempts to interprete these experimental results. The earliest interpretation, as the decay of a new light neutral particle - scalar or pseudoscalar - axion, is hardly probable, first, because of several peaks present, and second, because of null results of searches for such particles in nuclear reactions and "beam-dump" experiments[5].

The hypothesis based on the pure electromagnetic interaction[6,7] explains observed peaks as interference between different processes of positron creation. However, exact calculations are very complicate here and all estimates are made in the simplest models.

It is appropriate to note also the prediction[8] of a very rich spectrum of quasistationary levels, obtained in the solution of a relativistic Coulomb problem of two bodies on the ground of the quasipotential method in the model of scalar particle interaction.

The most bold proposition was made by several groups about the formation of the new phase of QED in strong electromagnetic fields[9-12]. According to this hypothesis correlated e^+e^- peaks and $\gamma\gamma$-pairs are caused by the decay of a bo-

und e^+e^- state analogous to positronium, which is formed in this new phase with a coupling constant ~1. Perhaps there are no hard theoretical grounds for this hypothesis at present, but the problem is explored intensively. It is assumed, that the new phase is metastable: the bubble of this phase, produced as a result of high electromagnetic fields of colliding nuclei, lives after creation for a long time as compared to the characteristic collision time (10^{-21}s).

There is another suggestion, that a nucleus of the new phase may exist near the nuclear surface before collision[13,14], the latter serves as the trigger mechanism for the decay of the blob into e^+e^- or annihilation to a $\gamma\gamma$-pair. Under assumption of this phenomenon occurence the decay of the new phase may be triggered not only by a heavy nuclei collision, but also by the decay of a nucleus with a change of the charge.

For example, in publication[14] the process like β-decay of heavy nuclei is considered. In experiment[15] a search has been undertaken for 180°-correlated $\gamma\gamma$-pairs in the fission process of Cf-252. The established limit for the probability of creation of a particle with a mass in the range 1.4÷2 MeV which decays into $\gamma\gamma$-pairs is less than 8×10^{-7}.

Besides it is interesting, with the hypothesis left aside, to verify experimentally, if some phenomena similar to those in heavy nuclei collisions take place in other processes with a sharp change of an electromagnetic field near the nucleus.

In this work we sought for 180°-correlated $\gamma\gamma$-coincidences in α-decay of Pu-239. A sample of metallic Pu-239 ø47x3 mm in a 2 mm thick lead jacket for absorption of soft γ-radiation and a lead collimator 15 mm in diameter were placed between two Ge(Li) detectors at a distance of 7 cm from each detector. The energy and total absorption peak efficiency calibration was made with standard γ-sources. Absorption of γ-rays in Pu and in the lead jacket was taken into account by calculation. The two-dimensional spectrum [E1,E2] of coinciding pulses (resolution time of coincidences is 0.1μs) was investigated, and the energy resolution of the spectrometer taken into account. In the Figure a diagonal slice is presented in accordance with the conditions (E1-E2)< 10 keV, E1+E2 = E. In the spectrum a smeared peak at 1022 keV due to positron annihilation is seen and there are no other singularities over the whole energy interval of 1 MeV < E < 2 MeV. Processing of the spectrum with account for the source intensity, the efficiency of the apparatus and the time of the experi-

ment (120 hours) gives the upper limit for the probability of creation of an object decaying into $\gamma\gamma$-pairs equal to 1.2×10^{-11} for E = 1.06 MeV with a monotonous decrease to 0.3×10^{-11} for E = 2 MeV (at a 95% confidence level).

1. T.Cowan et al. Phys.Rev.Lett., 56 (1986) 444;
   H.Bokemeyer. Report GSI-88-1, p.173.
2. P.Kienle. Ann.Rev.Nucl.Part.Sci., 36 (1986) 605;
   R.Koenig et al. Phys.Lett., B218 (1989) 12.
3. K.Danzmann et al. Phys.Rev.Lett., 59 (1987) 1885.
4. K.Danzmann et al. Phys.Rev.Lett., 62 (1989) 2353.
5. A.Chocos. Comm.Nucl.Part.Sci., 17 (1987) 211.
6. W.Lichten, A.Robatini. Phys.Rev.Lett., 54 (1985) 781;
   Ibid., 55 (1985) 135; T. De Reus et al. J.Phys., C12 (1986) L303; J.H.Bang et al. Z.Phys., A330 (1988) 431.
7. S.Schramm et al. Z.Phys., A323 (1986) 275; Yu.N.Demkov., S.Yu.Ovchinnicov. JETPh Lett., 46 (1987) 14 (in Russian);
   D.Carrier, L.M.Kraus. Phys.Rev., C38 (1988) 1225;
   A.E.Lobanov. JETPh Lett., 50 (1989) 161 (in Russian).
8. B.A.Arbusov et al. Preprint of Moscow Univ.Nucl.Phys. Inst., 89-1/76 (in Russian).
9. L.S.Celenza et al. Phys.Rev.Lett., 57 (1986) 55;
   Phys.Rev., D36 (1987) 2144.
10. B. Muller et al. J.Phys., C12 (1986) L109.
11. D.G.Caldi, A.Chodos. Phys.Rev., D36 (1987) 2876.
12. Y.J.Ng, Y.Kikuchi. Phys.Rev., D36 (1987) 2880.
13. D.G.Caldi et al. Phys.Rev., D39 (1989) 1432.
14. M.Inoue et al. Preprint of Hiroshima Univ. HUPD-8809 (1988).
15. B.J.Valley et al. Z.Phys., A333 (1989) 313.

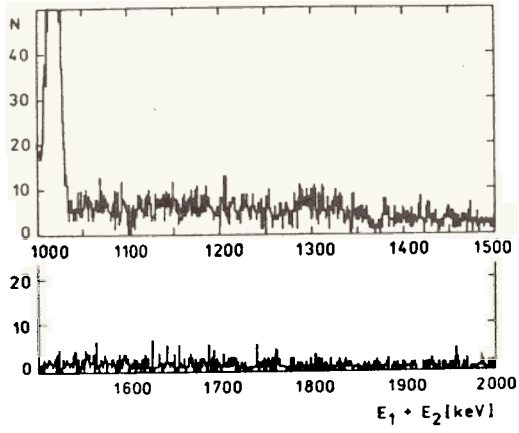

The spectrum obtained from the two-dimensional distribution of coinciding pulses under the condition (E1-E2)< 10 keV, E1+E2 = E.

EXPERIMENTAL ESTIMATE ON THE PROBABILITY OF γ-RADIATION WITH THE ENERGY E_γ > 20 MeV FOLLOWING THE SPONTANEOUS FISSION OF ^{252}Cf

Yu.N.Pokotilovskii

Laboratory of Neutron Physics, JINR, Dubna

Authors of ref.[1] reported on the observation of γ-radiation, following the spontaneous fission of ^{252}Cf, with energies up to $E_\gamma \sim 160$ MeV and the intensity behaving as E_γ^{-1} at E_γ > 20 MeV. They have interpreted the result as being due to bremsstrahlung arising at the flying apart of two fission fragments. Our work had the aim to check this result. Gamma-rays from the ^{252}Cf source producing 0.7×10^7 events/sec were measured by a single-crystal NaJ(Tl) spectrometer having the size of 150x150 mm. For cosmic muon background suppression we have used a set of anticoinciding plastic counters around the NJ crystal. No effect has been observed at E_γ > 20 MeV. So our conclusion was that the upper limit to be imposed on the probability of γ-radiation in the range of 20-160 MeV must be over an order of magnitude below the result reported in ref.[1].

1. J.Kasagi et al. Proc. V Conf. Clustering Aspects in Nuclear and Subnuclear Systems, Kyoto, 1988; J.Phys.Soc. Jap., 58 (1989) 620.

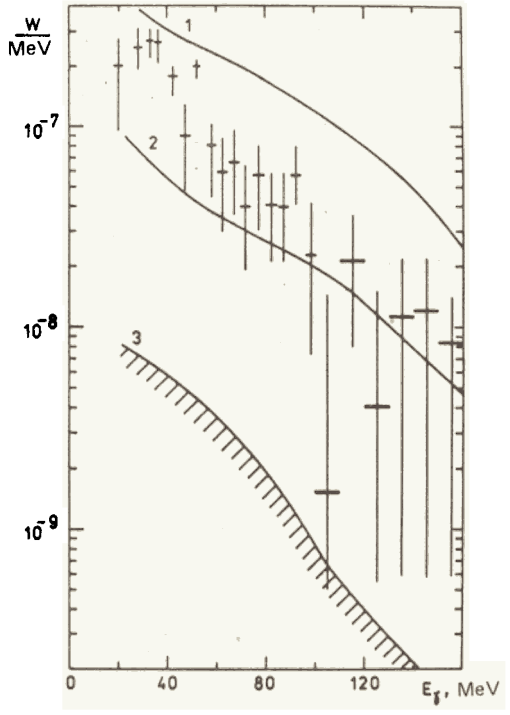

The spectrum of γ-radiation following the spontaneous fission of ^{252}Cf. Experimental points from ref.[1]. Curves: 1 - calculated in the sudden acceleration model, 2 - the same in the Coulomb acceleration model, both from[1], 3 - the upper estimate of the probability of γ-radiation obtained at LNP (one standard deviation).

POSSIBLE CHOPPER-MONOCHROMATOR FOR COLD NEUTRONS

Yu.N.Pokotilovskij

Laboratory of Neutron Physics, JINR, Dubna

A method is proposed for the chopping and monochromatization of a beam of cold neutrons by alternating magnetization/demagnetization of ferromagnetic foils inserted in the beam. As is known[1], slow neutrons, on traversing a ferromagnetic, experience small angle scattering on magnetic inhomogeneities. For cold neutrons the main mechanism of this scattering is the refraction of neutrons on ferromagnetic domain interfaces. As it follows, for example, from[1] the total width at half maximum of the angular distribution of transmitted neutrons looks as follows:

$$\Gamma_\theta = ((4.7\mu B)/E)\ (\tau/2\delta)^{1/2} \qquad (1)$$

where μ is the magnetic moment of the neutron; B. the value of the magnetic induction of the ferromagnetic; E, the energy of the neutron; τ, the thickness of the sample; δ, the size of a domain. At λ = 20 Å, $\tau = 5.10^{-2}$ cm, $\delta = 5.10^{-4}$cm, $\mu B = 1.2 \times 10^{-7}$eV eq.(1) yields $\Gamma \sim 2.10^{-2}$. In various experiments there has been observed a considerable decrease in the angular broadening of the transmitted neutron beam distribution under the action of an external saturated magnetic field applied to the ferromagnetic sample. By exploring this fact and the method of pulsed magnetization and demagnetization of thin plates from magnetically soft materials it is possible to realize the pulsed intensity modulation and monochromatization of a cold neutron beam. This procedure enjoys especial convenience, if performed in a pulsed source of cold neutrons.

A chopper monochromator based on this principle can be arranged as follows: few ferromagnetic foils in pulsed magnet environment are placed successively in the cold neutron beam at the distance ℓ_i from the neutron source which satisfies the condition:

$$\ell_i = vt_i, \qquad (2)$$

where v is the cold neutron velocity; t_i. the time, with respect to the neutron pulse, at which an i-th ferromagnetic foil gets magnetized for a short period. In between the foils there are to be positioned soller neutron collimators with the smallest possible angles of collimation. With the angle of collimation 10^{-3} and the beam broadening on transmission through a demagnetized

sample of 2.10^{-2}, the outgoing intensity from the collimator will be 20 times smaller, than in the case of a magnetized ferromagnetic sample. When a set of choppers is used, the degrees of intensity modulation are multiplied. It is shown that it is possible, in principle, to reach a very high degree of monochromatization of cold neutrons: $\sim 10^{-8}$ eV for $\lambda \sim 20$ Å.

A. J. Allen, D. K. Ross. J. Phys. D. - Appl. Phys., 17 (1984) 99.

CONDENSED MATTER

SMALL-ANGLE NEUTRON SCATTERING INVESTIGATION OF INVERTED MICELLAR SYSTEMS AOT + $X^*(H,D)_2O$ + $C_{10}D_{22}$ AND AOT + $X^*(H,D)_2O$ + $C_{10}H_{22}$ BY INTERNAL CONTRAST VARIATION

N.Gorski, Yu.M.Ostanevich, LNP, JINR, Dubna

As we reported previously[1], the inverted micelles of type "surfactant + water in oil" in a small molecular weight solvent - benzene - were restricted in the water content by value of $X = [H_2O]/[AOT] \cong 8$. This restriction is somewhere at $X \cong 100$ if the decane is used as a solvent. If the remarkable friability of the inverted micelles, observed by us in benzene at the smallest water concentrations, realizes in decane also, we would get a possibility to follow the cease of this interesting property as the water content is increased. Besides of this problem, it seems worth to try investigate the possibilities of the variation of "internal contrast" by change of the isotope composition of the water nucleus only.

All experiments were carried out at the time-of-flight small-angle scattering spectrometer "MURN" at the pulsed reactor IBR-2, as it was described in[1]. The following main experimental results could be mentioned at the moment:

- the method of variation of the "internal contrast" is elaborated in the case of inverse micelles;
- this method was applied to the system AOT + $X^*(H,D)_2O$ + $C_{10}D_{22}$ at X = 20, 40, 60 at temperatures 17, 24, 27, 32, and 37°C, and to AOT + $X^*(H,D)_2O$+$C_{10}H_{22}$ at X = 4, 8, 70, at temperatures 23, 27, 31, 34, and 41°C;
- at these conditions we have determined the forward scattering differential cross-sections in absolute scale, the radii of gyration R_g, the match-points B_{aq}, the aggregation numbers N, the number concentrations of the micelles n, the radii of the spherical water nuclei r_{H_2O} the surface of the water nucleus per a single polar group of the surfactant, the volume of single micelles and the volume, occupied by a single water molecule in the micelle v_{H_2O};
- at most of the above-mentioned conditions and compositions (with the exception of smallest water contents X= 4 and X = 8) well developed regions of validity of the Porod law ($d\Sigma/d\Omega \simeq 1/Q^4$) were observed, which allowed us to find the total surface of contrasting parts of the micelles;

- this surface is identified as the total surface of the water nuclei of the micelles;
- when pure D_2O used as a water nucleus, it was possible to observe the first subsidiary maximum of the micellar form-factor.

1. N. Gorski, Yu. M. Ostanevich. Ber. Bunsenges. Phys. Chem., 94 (1990) 737.

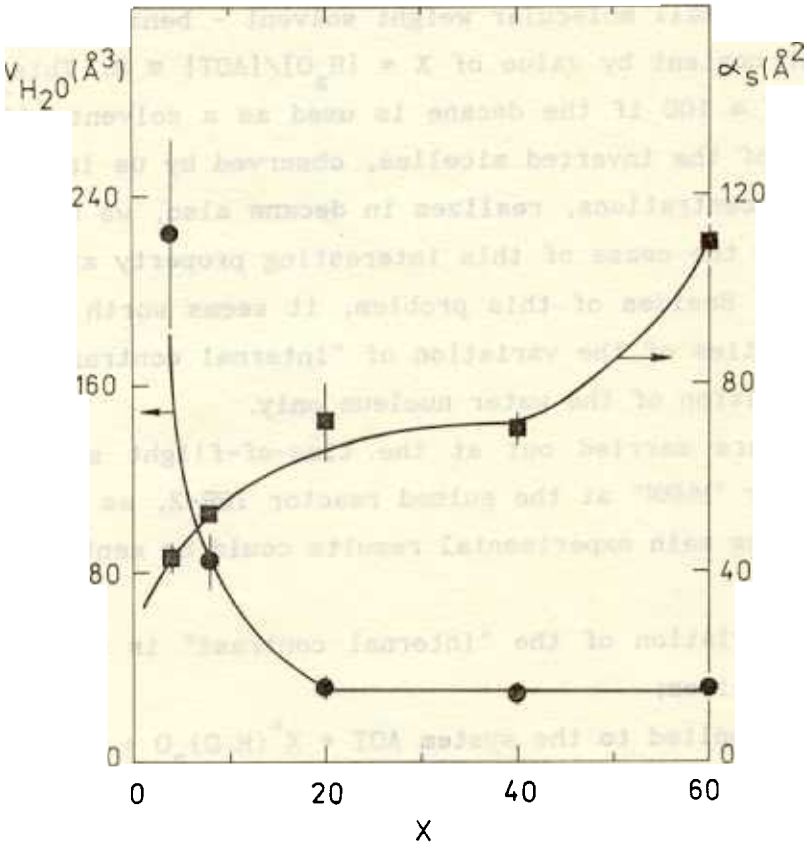

Fig. 1. The volume, occupied by a single water molecule in the micelle V_{H_2O} (·) and the area of the water core surface per single AOT head group a_s(□) versus the molar ratio $X=[H_2O]/[AOT]$ in the $AOT+X^*(H,D)_2O+C_{10}(H,D)_{22}$ systems. The solid lines are eye guides only.

SMALL-ANGLE NEUTRON SCATTERING STUDY OF POLY(OXYETHYLENE - OXYPROPYLENE - OXYETHYLENE) BLOCK COPOLYMER MICELLES IN AQUEOUS SOLUTION

J.Plestil, Institute of Macromolecular Chemistry, Prague, Czechoslovakia

H.Pospisil, JINR, Dubna

Block copolymers in selective solvents (a good solvent for one type and a precipitant for the other type of the block) form the micelles[1] consisting of a dense core, which contains mainly the insoluble component of the copolymer, and a shell composed of the swollen soluble component. For the oxyethylene-oxypropylene block copolymers in water solutions, the quality of the solvent can be easily modified by changing its temperature. At low temperatures, the copolymer is molecularly dispersed (unimer), while at higher temperatures, both the polymolecular aggregates (micelles) and the unimers are present[2]. In Ref.2, the results of both static and dynamic light scattering investigations of the commercial poly (oxyethylene-oxypropylene-oxyethylene) block copolymer, Pluronic L64, were reported. Small-angle X-ray scattering has proved to be very useful in characterizing the micellar system[3]. In this contribution, the small-angle neutron scattering (SANS) study of Pluronic L64 is reported. The reason for the use of neutron scattering was a much higher contrast for neutrons in comparison with that for X-rays. The SANS curves for Pluronic L64 in heavy water (copolymer concentration 0.001-0.30 g/ml, temperature range 20-50^{o}C) were measured with a time-of-flight SANS spectrometer MURN at the IBR-2 reactor. The solution was placed in a 1 mm quartz cell. The incoherent contribution to the scattering was estimated by measuring the scattering from D_2O/H_2O mixtures containing the same number of protons as the solutions. The example of the SANS curves is shown in Fig.1.

The following characteristics have been determined from the scattering data: critical micelle concentration (Fig.2); radius of gyration (Fig.3a), mass and second virial coefficient (Fig.3b) of the unimer; the weight fraction of unimers (Fig.4); micellar mass and second virial coefficient (Fig.5a) and radius of gyration (Fig.5b). The degree of swelling of the micellar core (Fig.6) was evaluated from the mean-square fluctuation of the scattering density (determined from the integrated scattering intensity)[4,5]. Structure parameters based on a core-shell model have been calculated for micelles at 45^{o}C.

1. Z. Tuzar, P. Kratochvil. Adv. Colloid Interface Sci., 6 (1976) 201.
2. Y. Zhou, B. Chu. Macromolecules, 21 (1988) 2548.
3. J. Plestil, J. Baldrian. Makromol. Chem., 176 (1975) 1009.
4. J. Plestil. Makromol. Chem., Macromol. Symp., 15, (1988) 185.
5. J. Plestil, D. Hlavata. Polymer, 29 (1988) 2216.

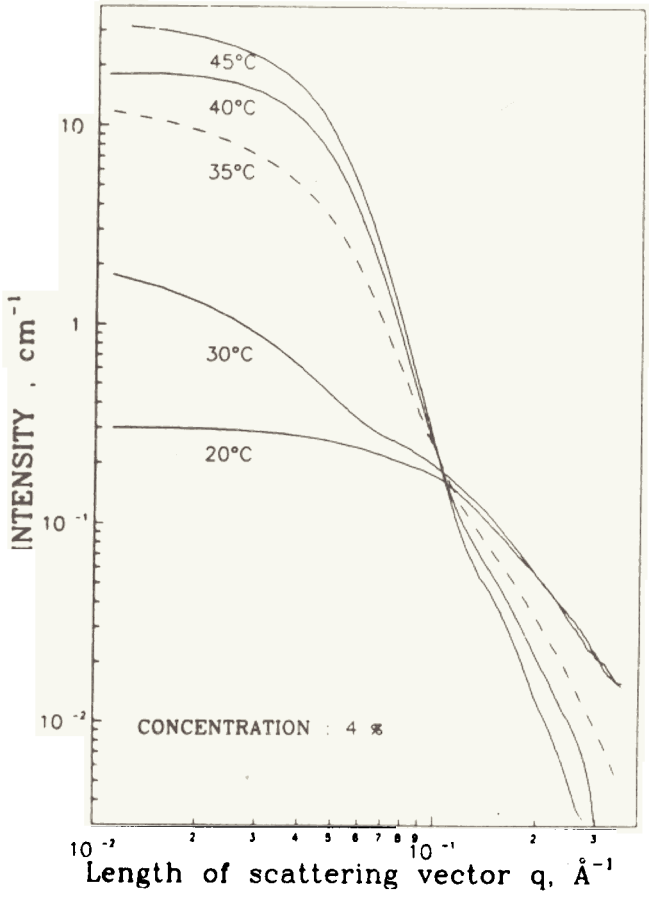

Fig. 1. Log-Log plot of the differential scattering cross-section per unit sample volume, I(q), for Pluronic L64 in D_2O (c = 0.045 g/ml) at different temperatures.

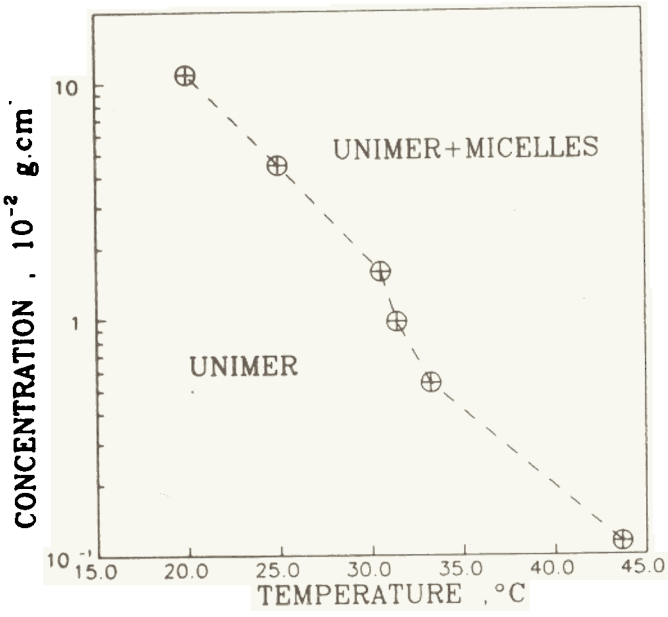

Fig.2. Critical micelle concentration as a function of temperature.

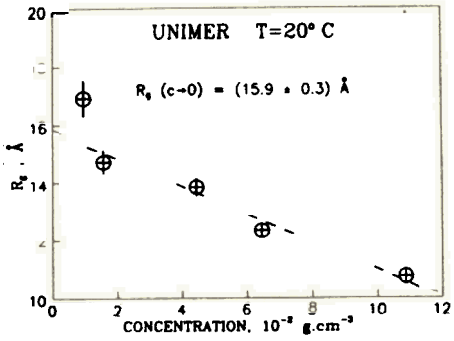

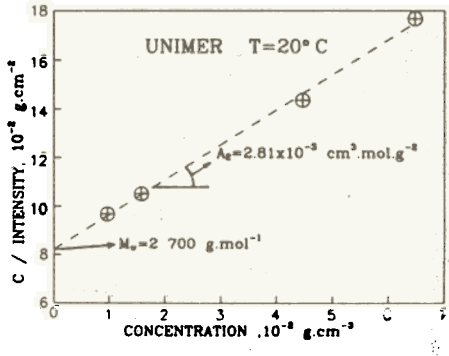

Fig.3. a) Extrapolation of the radius of gyration of unimers to infinite dilution. b) Determination of the weight-average molar mass of the unimer and second virial coefficient at 20°C.

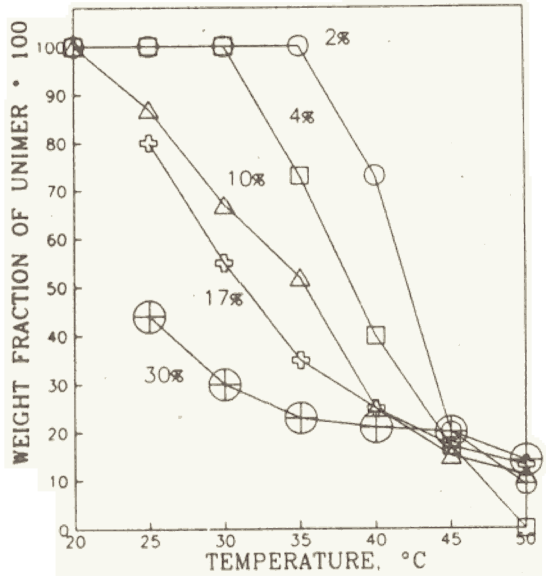

Fig.4. Temperature dependence of the weight fraction of unimers for various copolymer concentrations.

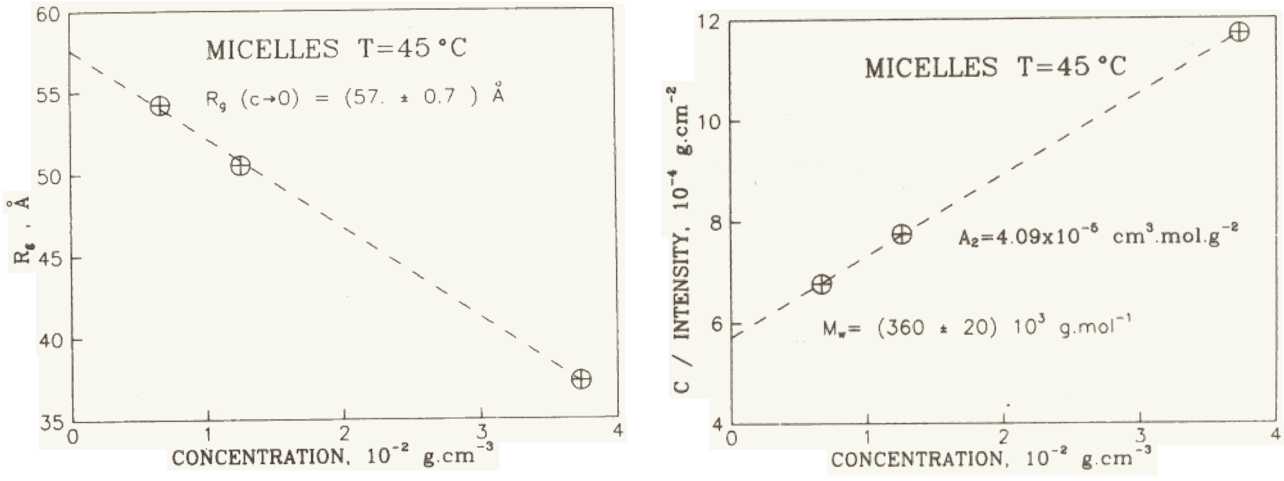

Fig.5. a) Extrapolation of the micellar radius of gyration to infinite dilution. b) Determination of the weight-average molar mass of the micelle and second virial coefficient at 45°C.

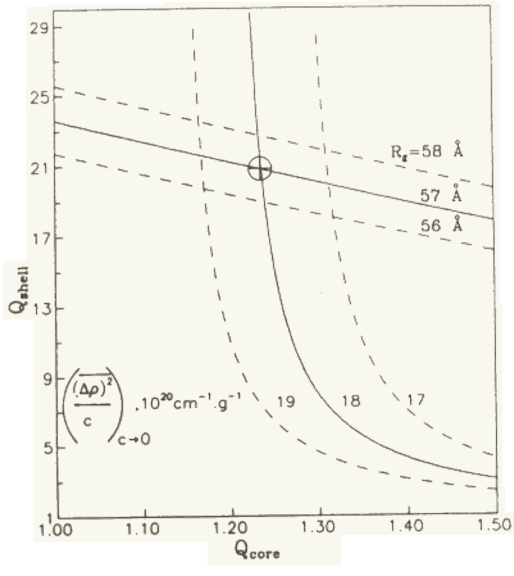

Fig.6. Determination of the swelling factors: Q_{core} = 1.24; Q_{shell} = 20.7; radius of core R = 47 Å and micellar radius R=103 Å.

SMALL ANGLE NEUTRON SCATTERING IN DILUTED WATER SOLUTIONS OF TETRAMETHYLUREA

A.I.Kuklin, Yu.M.Ostanevich, Laboratory of Neutron Physics, JINR,Dubna
L.Cser, T.Grosz, G.Jancso, Central Research Institute for Physics, Budapest, Hungary

In our previous publication[2] we have reported on the possibilities of investigating the properties of water solutions of the rather small, mainly hydrophobic molecule, tetramethylurea (TMU) (M.W. = 116.16), by small-angle neutron scattering (SANS). This technique appears to be rather sensitive to solute-solute as well as to solute-solvent interactions in the solution, if the solute molecules are small enough. The case of a nonelectrolyte solute seems to be especially interesting, in that one can hope to learn something about so-called hydrophobic interactions. In this field remarkable efforts were undertaken recently by Y.Koga. His investigation of excess partial molar enthalpies of tert-butanol in water-tert-butanol mixtures led to a conclusion about the existence of long-range repulsive solute-solute interaction in highly dilute solutions of tert-butanol[2]. So, it seems worthwhile to investigate the concentration dependence of the SANS parameters in the region of high dilutions, down to mole fraction of the solute X = 0.001.

Scattering experiments were done at the time-of-flight SANS spectrometer "MURN" at pulsed reactor IBR-2. Sample H-TMU-D_2O solutions covered the concentration range of 0.05-1.0 aquamolarity, and all precautions described in[1] were taken into account. Main results - the apparent forward scattering differential cross-section per single molecule of TMU and the apparent radius of gyration versus concentration - are shown in fig.1 and fig.2. The figures also show the results expected in a simplified model of solution, in which the interparticle interaction is not taken into account.

At the moment it is difficult to come to certain conclusions about the existence of the long range interactions between solute molecules assumed in[2]. Though the small difference between the calculated and observed cross-sections at the zero concentration easily can be explained by consideration of such a repulsive interaction, the calculated values strongly depend on the partial volume of TMU which is not known at the lowest concentrations. Besides, the quite unexpected growth of the radius of gyration with concentration needs some other explanation. As a first alternative one can assume some degree of dimerization of TMU molecules. A detailed quantitative analysis and more exact measurements of the partial volume of the high dilution

region of TMU solutions in D_2O are needed before any firm conclusions be drawn.

1. V. Yu. Bezzabotnov, T. Grosz, Yu. M. Ostanevich, L. Cser, G. Jancso. Preprint JINR, P14-90-419, Dubna, 1990 (in Russian).
2. Y. Koga. Can. Journ. Chem., 66 (1988) 1187.

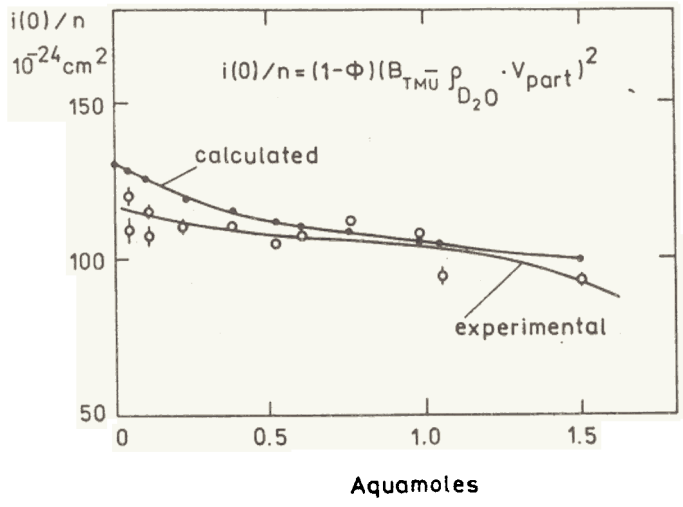

Fig. 1. The apparent forward scattering cross-section per single molecule of tetramethylurea (TMU) in D_2O versus total concentration of TMU. The upper line shows the model calculation without taking into account any kind of interparticle interactions (as shown in equation in the fig.), the lower one is an eye guide through the experimental values.

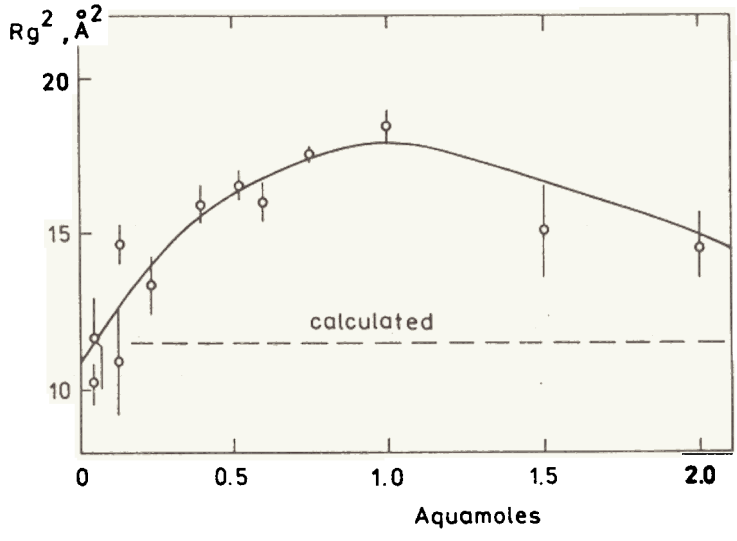

Fig. 2. The squared apparent radius of gyration of tetramethylurea (TMU) in D_2O versus total concentration of TMU in the solution. The dashed line is a calculated one according to the structure of a single TMU molecule, without taking into account any interparticle interactions.

SMALL-ANGLE NEUTRON SCATTERING ON CLINKER MINERALS AND HARDENED CEMENT PASTE

F.Haußler, Laboratory of Neutron Physics, JINR, Dubna
H.Baumbach, Leipzig University of Technology,FRG
F.Eichhorn, Institute for Nuclear Research, Rossendorf, FRG

Portland cement paste contains many crystalline and non-crystalline phases in various ranges of sizes. The crystalline phases (e.g.Portlandite, Calcite) are embedded in the amorphous phases of hydration products. The kernel of the hydrating grain consists of unreacted Portland cement.

In SANS-experiments, carried out at the spectrometer MURN-TEXT in Dubna (USSR), samples of hardened cement paste, dry clinker, or dry Portland cement powder were investigated. The phase composition and granulometric data of the used cement powder are described in /1/. Because of the generally accepted fact, that the properties of concrete are determined largely by the cement stone /2/, the investigations using SANS are restricted to hardened cement paste samples. For a better interpretation of the scattering data the samples were produced from grains of clinker minerals and ordinary Portland cement having diameters in a very small range.

A detailed description of the used SANS-spectrometer MURN-TEXT is given in /3-5/. Several experimental results show the absence of a Guinier region. At large scattering angles (large Q) the Porod approximation is applicable. From the scattering curves represented in the Porod plot ($[d\Sigma/d\Omega . Q^4]$ versus Q) the Porod constant is obtainable by a straightforward procedure.

A wide collection of SANS-curves of both dry powder (clinker minerals and ordinary Portland cement) and hardening cement paste are measured. The hardened cement paste was of the SCC-type with a water-cement ratio of 0.38. A mixture of 62 vol % H_2O and 38 vol % D_2O was produced. All samples were put into a container which consisted of two circular slices of optical quartz glass. The obtained SANS-data for all the samples studied have been plotted on graphs of $[(Q^4 \cdot d\Sigma/d\Omega)/\text{Å}^{-4}\text{cm}^{-1}\text{sterad}^{-1}]$ versus $\ln[Q/\text{Å}^{-1}]$. Thus, the perfect Porod scattering (potential law $\propto Q^{-4}$) is a straight horizontal line. Another potential behavior is also represented by straight lines.

The Porod's potential law holds for the samples of the clinker minerals C_3A and C_4AF (see figs.1 and 2). In the measured Q-region the main clinker phase C_3S, ordinary Portland cement, and hardening cement paste do not show a Porod-like behavior of the SANS-curves (see fig.3 and Table 2). By means of the program INVAR /6/ the Porod constants are calculated. In Table 1, K_p

stands for the porod constant; S,the surface area; V_g,the volume; and m_g,the mass of the sample.

The potential behavior given in Table 2 is comparable with the data measured by Kriechbaum et al.[7]. Obviously the sizes of the ordinary Portland cement grains do not essentially influence the formation of the hydration products detectable by the SANS measurements.

1. F. Haußler et al. Cement and Concrete Research, 20 (1990) 644.
2. S. Rohling, M. Nietner. Proc. VTT Symp., VTT-115, 1990, p. 5.
3. Yu. M. Ostanevich. Macromol. Chem., Macromol. Symp., 15 (1988) 91.
4. Yu. M. Ostanevich. Preprint JINR, P13-87-407, Dubna, 1987.
5. V. Yu. Bezzabotnov, Yu. M. Ostanevich. Physica B 156&157 (1989) 595.
6. J. Plestil. Private communication, Dubna, 1987.
7. M. Kriechbaum et al. Progress in Colloid & Polymer Science 79 (1989) 1.

Table 1

Specific surface measurements of powder fractions

Characteristics		$K_p/10^{36}m^{-5}sr^{-1}$	$S/m_g/m^2g^{-1}$	$S/V\ /10^6m^{-1}$
C_4AF	<27 μm	0.95+/-0.17	0.39+/-0.08	0.58+/-0.09
	27-45 μm	0.55+/-0.03	0.20+/-0.02	0.34+/-0.02
	45-63 μm	0.53+/-0.15	0.17+/-0.05	0.32+/-0.09
	>63 μm	0.59+/-0.11	0.19+/-0.04	0.36+/-0.07
C_3A	<27 μm	0.45+/-0.04	0.41+/-0.04	0.49+/-0.04
	>63 μm	0.12+/-0.01	0.10+/-0.01	0.13+/-0.01

Table 2

The exponential behavior of the SANS-curves

Characteristics	Q_{min}/Q_{max} nm^{-1}	Expon.	Q_{min}/Q_{max} nm^{-1}	Expon.
8-14 µm/3 days	0.15/0.27	-2.9	0.27/0.4	-2.1
27-45 µm/3 days	0.15/0.27	-2.8	0.27/0.4	-2.1
8-14 µm/241 days	0.16/0.5	-3.1		
14-20 µm/241 days	0.16/05	-3.3		
27-45 µm/241 days	0.18/0.5	-3.4		

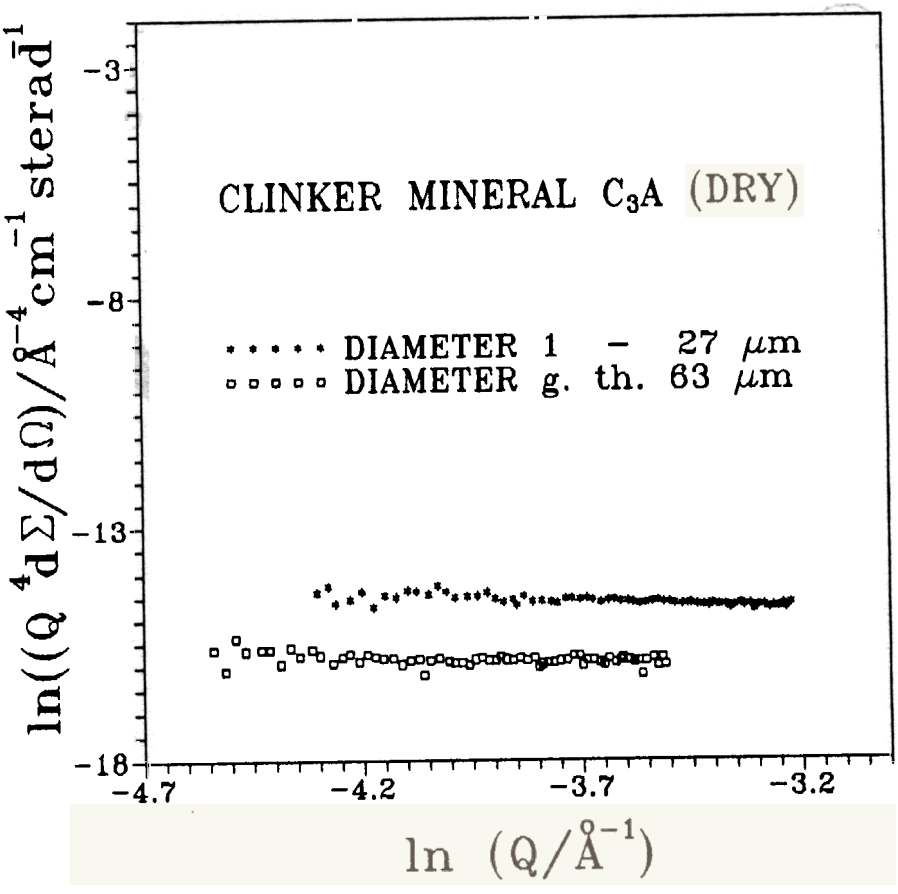

Fig.1 Porod plot of fractioned dry clinker minerals C_3A.

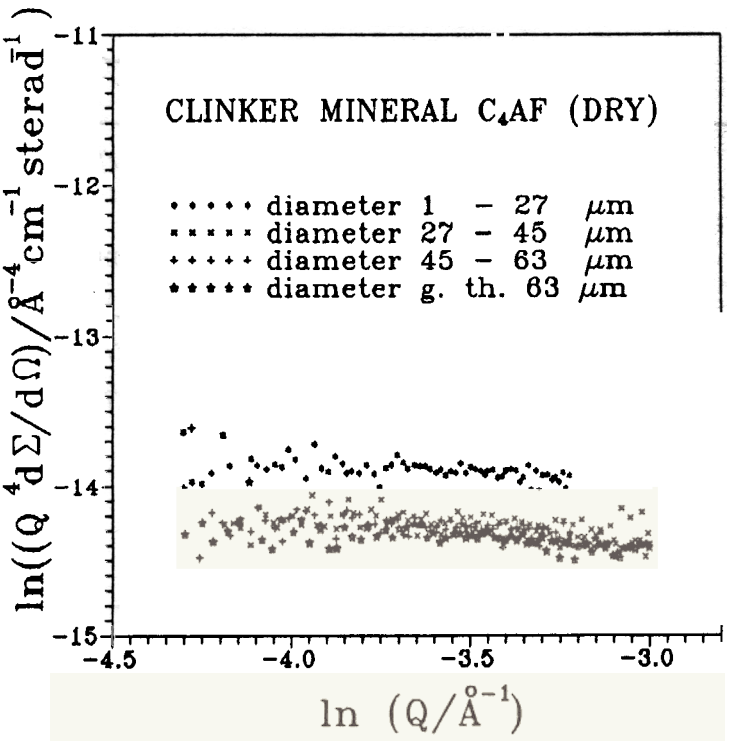

Fig. 2. Porod plot of fractioned dry clinker minerals C_4AF.

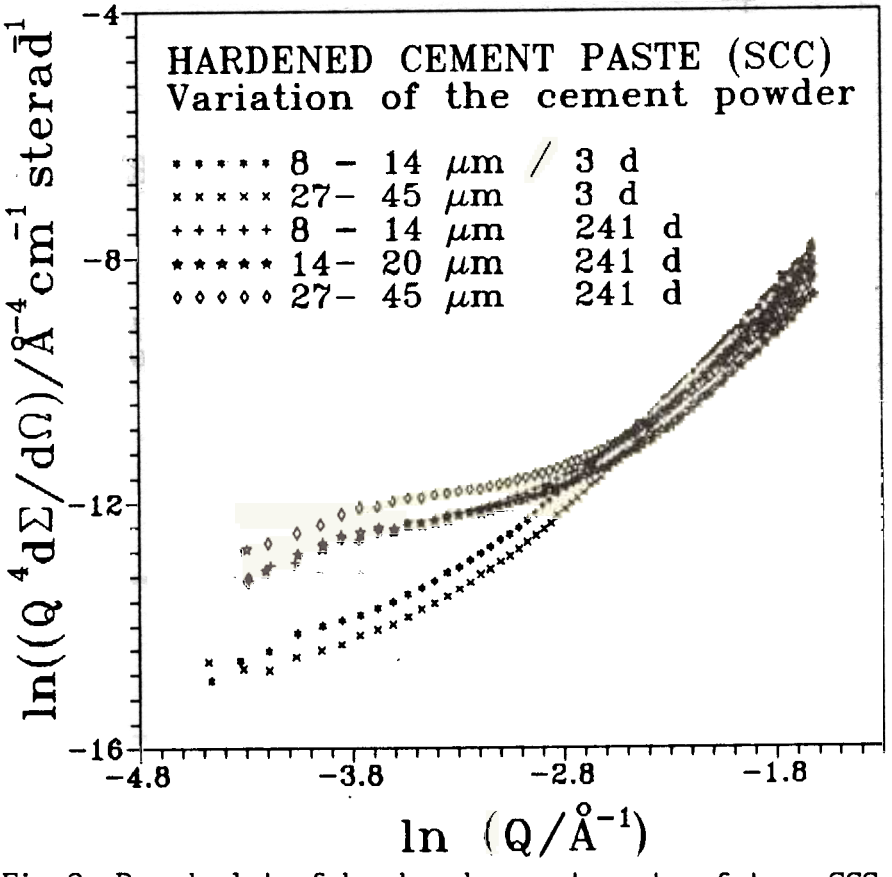

Fig. 3. Porod plot of hardened cement paste of type SCC.

STUDY OF THE SUPERSTRUCTURE OF $YBa_2(Cu_{1-x}Fe_x)_3O_{6+\delta}$ IN THE RANGE 80-680 K

A.M.Balagurov, G.A.Bonch-Osmolovsky
Laboratory of Neutron Physics, JINR, Dubna

In the case of the compound Y123-Cu/Fe several experimental methods, including neutron diffraction and Mossbauer spectroscopy, are used to study the atomic and magnetic ordering of dopant cations. Recently it was found[1] that for high iron concentrations ($x \geq 0.20$) the diffraction patterns include many additional peaks if compared with the initial ($x = 0$) pattern. On the analogy of the Y123-Cu/Co system[2] one may expect the long-range magnetic ordering to arise in Y123-Cu/Fe, as revealed by the Mossbauer studies[3]. As some of the additional peaks could be due to some other reasons, i.e. foreign materials and excess oxygen ordering, only the temperature dependence of the peak intensity could help decision about their magnetic nature.

Neutron diffraction patterns were measured at the DN-2 TOF diffractometer at several scattering angles simultaneously in the d-spacing range from 1 up to 20 A. We used the following samples and conditions:

- cooling down to 8 K of (0.15, 1), (0.23, 1) and (0.27,1) samples;
- heating up to 680 K of (0.23, 1), (0.27, 1) (0.30, 1) and (0.30, 0.50) samples. The first figure in parenthesis is the iron concentration (x), the second one is the formal value for δ. The samples were cooled in the He-refrigerator and heated in a furnace with a large inner volume and large incoming and outgoing windows.

As an example of the experimental pattern Fig.1 shows spectra from the (0.30, 0.5) sample measured at various temperatures. One may see that at $T \leq 200$ K a new peak arises at d = 4.73 A and the peak at d = 5.16 A gets essentially higher. Some peak intensities as the function of the temperature are shown in Fig.2.

We can enunciate the next results.

In the diffraction patterns of all the samples with high oxygen content ($\delta \geq 1$) the lines of the Y123 phase are nuclear in origin. It means that in Y123-Cu/Fe, differently from Y123-Cu/Co, the long-range magnetic order is absent.

After oxygen removal ($\delta \leq 0.5$), antiferromagnetic peaks arise, for example, (1/2, 1/2, 1) and (1/2, 1/2, 3/2), which correspond to the doubling of all lattice parameters. This picture resembles the situation with Y123-Cu/Co[4]

and can be explained by the ordering of magnetic moments both in planes and in chains. The Neele temperature of this phase is about 470 K.

The diffraction lines at d = 5.16 A as well as at d = 4.73 A, which have exhibited the temperature dependence, cannot be attributed to the Y123 phase. It is quite clear now that the 5.16 A peak belongs to a new phase as well as the many other peaks. This tetragonal phase has $a_f = b_f = 3.88$ A and c = 7.70 A (or 15.4 A), i.e. $a_f \approx a_{123}$, $c_f = 2a_f$ (or $c_f = 4a_f$), unlike the Y123 phase, where $c \approx 3a$. Thus, the 5.16 A peak is the magnetic peak (0 0 3/2) or (0 0 3) of this new phase, which has the same Neele temperature as Y123 for low δ.

The nature of the 4.73 A peak is still unclear. The best way to understand it, as well as to refine the structure of the new phase is to use the higher resolution diffractometer with $\Delta d/d \leq 0.002$.

1. A.M.Balagurov et al. Superconductivity, 3 (1990) 557.
2. P.F.Micelli et al. Phys.Rev., B39 (1989) 12375.
3. I.S.Lyubutin et al. Phys.Lett. A137 (1989) 144.
4. R.Sonntag et al. Physica C, 159 (1989) 141.

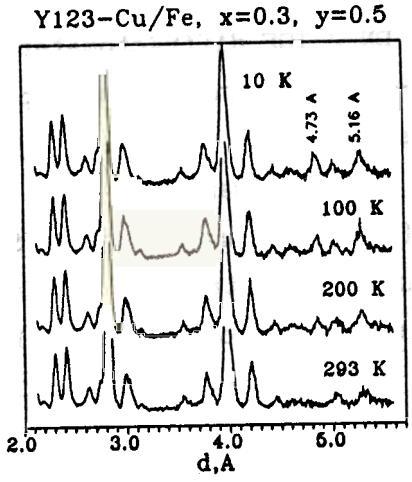

Fig.1. Diffraction patterns of $YBa_2Cu_{2.1}Fe_{0.9}O_{6.5}$ measured in the range 10-293 K. The superstructure peaks at d > 4.2 A are clearly seen. If the sample is cooled, the new 4.73 peak arises and the intensity of the 5.16 A peak increases.

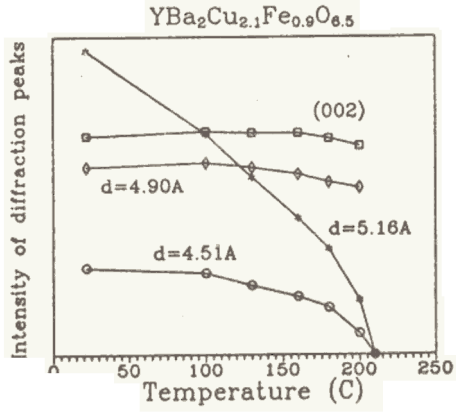

Fig.2. The intensity of some diffraction (nuclear and magnetic) peaks as a function of temperature during the heating of the sample.

OXYGEN DIFFUSION PROCESS IN $YBa_2Cu_3O_{6+\delta}$-CERAMICS

A.M.Balagurov, N.V.Vuong, L.C.Quy, T.A.Quan,
V.I.Luschikov, V.H.Tuong, P.Q.Trieu
Laboratory of Neutron Physics, JINR, Dubna

A combined (theoretical and experimental) study has been undertaken of oxygen diffusion in Y123-ceramics, which plays the crucial role in the formation of the superconducting phase of this compound. The one-dimensional diffusion equation was used to describe the diffusion process, which occurs at the annealing of samples at constant temperature as well as at linear heating or cooling.

The model applicability seems quite satisfactory as illustrated in Fig.1, which shows the experimental data on oxygen content variation during the heating of the sample at the oxygen pressure of P_0 = 1 atm and the heating rate of 1 deg/min (TGA data), and the calculated curve. In the calculation the following parameters of the model were used: the diffusion length L = 0.003 cm, the diffusion coefficient in the form $D = D_0 * \exp(-E/kT)$ with D_0 = $2.1 \times 10^{-4} cm^2/sec$, E=0.6 eV.

The investigated samples were prepared from Y_2O_3, $BaCO_3$ and CuO by the standard procedure. They were annealed in air or in oxygen flow having the rate of 100 ml/min. The X-ray analysis was performed on the diffractometer DRON-3. The determination of oxygen content and the structure parameters refinement were made by using the neutron diffraction data (diffractometer DN-2). In addition, the samples quality was checked by measuring the temperature dependence of resistivity and magnetic susceptibility.

The analysis of the obtained results allows one to make the following conclusions:

1. Intense diffusion of oxygen from ambient atmosphere into samples occurs during the annealing of Y123 at the comparatively low temperature of 350°C. Furthermore, there also takes place the restoration of the Y123 phase, which was partially decomposed at the cooling of the samples in air from the synthesis temperature down to room one.

2. Oxygen diffusion at 350°C is accompanied by the oxygen ordering in Cu-O chains along the b-axis of the lattice, while at the linear cooling or heating (especially at large rates, V ≥ 1 deg/min) the chain occupation with oxygen along the a and b axes is different from its equilibrium state.

3. In the oxygen diffusion process the state of the starting sample, having a near zero value of δ, undergoes three stages:

- formation of its solid solution with oxygen. The structure of this stage

is tetragonal and the diffusion coefficient in the intervals 200-700°C of temperature and 1.4-1.7 atm of oxygen pressure can be expressed as:

$$D = (2.3 - 4.6)\times10^{-7} \times (P_0^{1/2} - 0.7)^2 \times \exp(-0.14/kT),$$

where D is in cm^2/sec, P_0 in atm, kT in eV;

- further development of the system retaining the tetragonal phase disordered over Cu-O chains. In this phase the diffusion coefficient is estimated as

$$D_2 = (0.84 - 3.4)\times10^{-4} \times \exp(-0.6/kT);$$

- transition to the orthorhombic phase, in which the diffusion coefficient decreases gradually to zero as the δ-value nears unity.

4. This proposed and tested variant of "hot grinding" for the preparation of Y123, reduces essentially the influence of granular surfaces on the establishment of oxygen content in the volume of the sample. At that, diffusion proceeds much faster and the transition temperature T_c of 91-94 K is established in the sample in about an hour.

The investigations performed are reported in:

1. N. V. Vuong. Description of the Oxygen Diffusion Process in Y123-Ceramics JINR, P17-91-341, Dubna, 1991.
2. A. M. Balagurov et al. Oxygen Diffusion in Y123-Ceramics. JINR, P17-91-340 Dubna, 1991.
3. A. M. Balagurov et al. Oxygen Diffusion in Y123-Ceramics During the Heating To be published.
4. N. V. Vuong et al. Influence of the Granular Surface on the Oxygen Uptake in Y123-Ceramics. JINR, P17-91-342, Dubna, 1991.

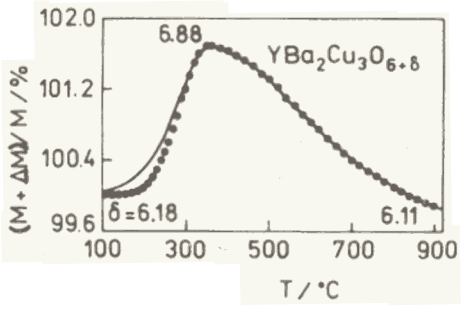

Fig. 1. The dependence of the oxygen content, in reference to the weight change of the starting sample $YBa_2Cu_3O_{6.18}$, on the heating temperature, changing at the rate of 1 deg/min at oxygen pressure of 1 atm. It shows the experimental points (TGA- data) and the calculated curve in the one-dimensional diffusion model.

NEUTRON POWDER DIFFRACTION STUDY OF $YBa_2(Cu_{1-x}Ni_x)_3O_{7-\delta}$

A.M.Balagurov, Laboratory of Neutron Physics, JINR, Dubna
J.Piechota, A.Pajaczkowska, IF PAS, Warsaw, Poland

Numerous studies of a series of compounds $YBa_2(Cu_{1-x}M_x)_3O_{7-\delta}$, where M = Fe or Co, have shown that:

- the crystal lattice symmetry changes from orthorhombic (Pmmm) to tetragonal (P4/mmm) at $x \approx 0.03$,
- approximately one extra oxygen is incorporated in the Cu(1)-O plane for every two Fe or Co atoms which substituted Cu in Y123,
- Fe and, especially, Co atoms occupy preferentially the Cu(1) site.

The problem of substitution of divalent impurities, Ni or Zn, for Cu in Y123 is also very interesting. These dopants, contrary to Co or Fe, have valence 2^+, the most likely valence of Cu in Y123. Unfortunately, in the case of Ni, the available studies yield limited and contradictory data. For example, in /1/ it was found that the Ni dopants occupy only the Cu(1) site for x = 0.066, but in /2/ and /3/ it was demonstrated that Ni impurities are distributed about equally over the Cu sites. Moreover, in /4/ it was shown that Ni may get dissolved in the Y123 matrix up to x = 0.04, and precipitates as NiO at higher x. We undertook a neutron powder diffraction study of the samples of $YBa_2(Cu_{1-x}Ni_x)_3O_{7-\delta}$ containing ^{58}Ni (x = 0.05, 0.09) or a natural mixture of Ni isotopes (x = 0.06, 0.15) /5/. The results obtained allow the suggestion that nickel substitutes copper at least up to the concentration of x = 0.07, and for all x studied the structure resembles that of an undoped $YBa_2Cu_3O_{7-\delta}$ compound. The structure retains its orthorhombic symmetry without any significant change in relative coordinates of atoms. The distribution of Ni over the Cu(1) or Cu(2) sites is about equally probable. The precipitation of part of nickel into the NiO phase already at concentrations $x \geq 0.05$ (Fig.1) supports the idea of limited solubility of Ni in the Y123 phase, differently from Fe and Co.

1. T.Kajitani et al. Jap.J.Appl.Phys. 27 (1988) L354
2. J.F.Bringley et al. Phys.Rev. B38 (1988) 2432.
3. R.S.Howland et al. Phys.Rev. B39 (1989) 9017.
4. M.Quian et al. Phys.Rev. B37 (1988) 5932.
5. A.M.Balagurov et al. Sol.St.Comm. 78 (1991)

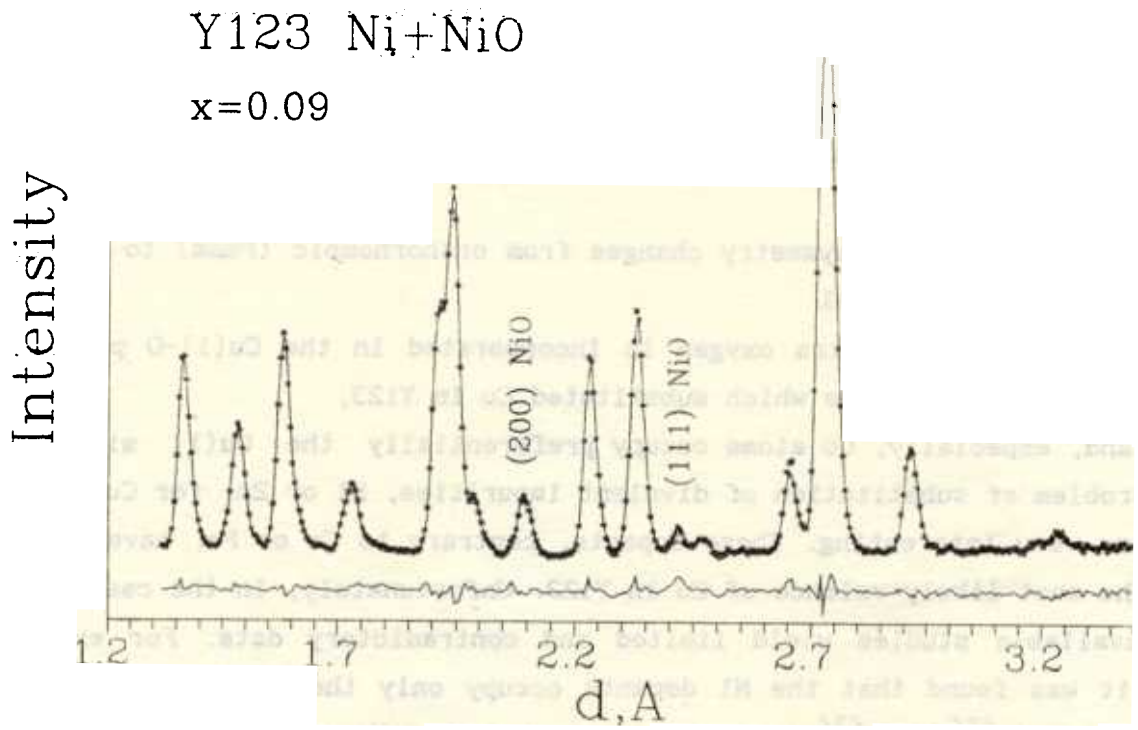

Fig. 1. Observed (stars) and calculated (solid line) neutron profile intensities for Y123-Cu/Ni with x = 0.09. The diffraction peaks of the second phase, NiO, are clearly seen.

NEUTRON DIFFRACTION STUDY OF PHASE TRANSITIONS IN METASTABLE ICE OF HIGH PRESSURE

A.M.Balagurov, G.M.Mironova, Laboratory of Neutron Physics, JINR, Dubna

O.I.Barkalov, A.I.Kolesnikov, E.G.Ponyatovsky, V.G.Sinitsyn, V.K.Fedotov
Institute of Solid State Physics, Chernogolovka, USSR

In ice, as it was shown recently[1], in addition to some crystal phases, two amorphous phases of different density, lda and hda, do also occur. These amorphous phases can be extracted from hexagonal ice of high pressure. Some other possibility to obtain lda and hda from the quenched high pressure tetragonal phase VIII was reported in[2], where a series of transitions was observed: VIII -> lda -> Ic -> Ih, here Ic is the cubic phase, Ih is the hexagonal phase. It was suggested that the low density phase, lda, was formed from the high density phase, hda, but attempts to observe this process have failed.

We studied[3] phase transitions of heavy ice from the quenched phase VIII, when heated from 94 to 240 K, by the real time neutron diffraction method with the temporal resolution of 5 min to find the transition VIII->hda. The sample (99% D_2O, weight 0.3 g) was pressed at room temperature to the pressure of 2.6 GPa, held for 1 hour to attain equilibrium, cooled down to 100 K and then shut off pressure. Neutron diffraction patterns were measured on the DN-2 time-of-flight diffractometer at the IBR-2 pulsed reactor.

The starting phase VIII was observed up to 130 K. In the interval between 130 and 135 K during 5 min the diffraction lines of this phase diminished and two broad peaks at Q=1.72 A^{-1} and 2.09 A^{-1} together with a very low-intensity peak at Q=1.63 A^{-1} appeared. These momentum transfers are the same as observed previously, namely, 1.63 A^{-1}, 2,10 A^{-1} and 1.72 A^{-1}, which correspond to two amorphous phases hda and lda and the diffraction line (111) for the cubic phase Ic. The phase mixture kept unchanged up to 150-160K, then the transition to the cubic phase Ic took place and, later, to the hexagonal one, Ih (fig.1). The transition Ic-->Ih has the complicated nature: in the beginning the ordering of D_2O in the basic plane of Ih occurs, then these planes are ordered with respect to each other.

Thus, in this experiment the transition of ice VIII to amorphous ice, hda, was first observed. It was found that two amorphous phases, high and low de-

nsity, may coexist and the complicated nature of the transition between cubic and hexagonal phases was established.

1. O.Mishima, L.D.Calvert, E.Whalley, Nature, 314 (1985) 76
2. D.D.Klug et al, J.Chem.Phys., 90 (1989) 2390
3. A.M.Balagurov et al, JETP Letters, 53 (1991) 30

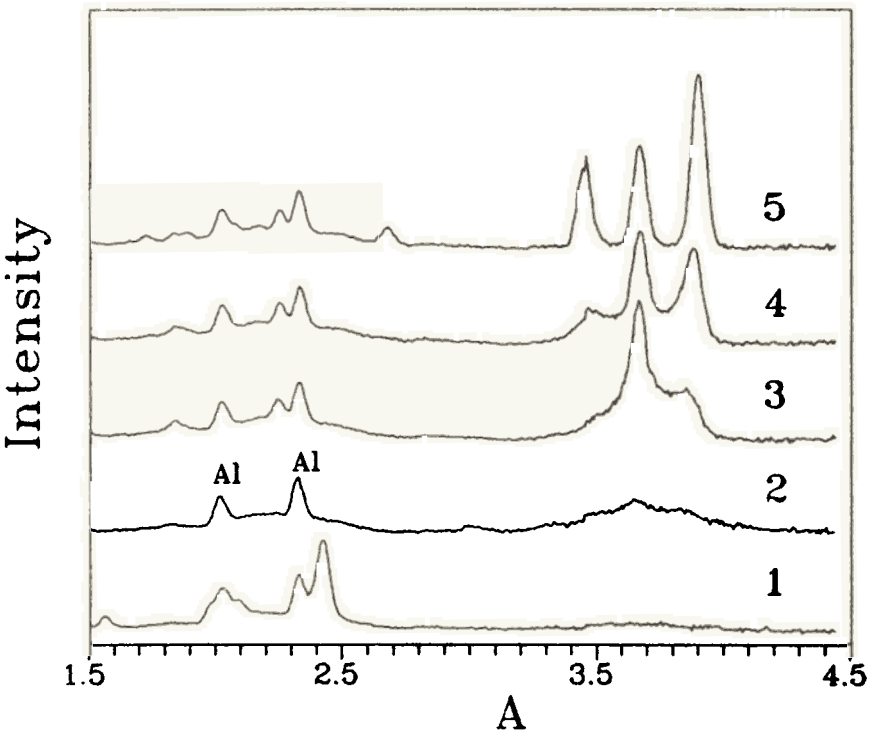

Fig.1. Neutron diffraction patterns measured during the heating of ice from 94 up to 240 K: 1 - high pressure ice VIII (T=94-130 K), the peak (200) at d=2.41 A is clearly seen, 2 - amorphous state (T=130-150 K), the peaks from Al walls of the cryostat are marked, 3 - cubic ice Ic (T=160-170 K) together with the intermediate phase, 4 - the intermediate state Ic-->Ih, 5 - hexagonal ice Ih (T ≥ 230 K).

REAL TIME NEUTRON DIFFRACTION STUDY OF THE Σ-δ PHASE TRANSITION IN $TiD_{0.74}$

A.M.Balagurov, G.M.Mironova, Laboratory of Neutron Physics, JINR, Dubna
I.O.Bashkin, A.I.Kolesnikov, V.Yu.Malyshev, E.G.Ponyatovsky, V.K.Fedotov
Institute of Solid State Physics, Chernogolovka, USSR

The complex, yet unclear, nature of the ε-->δ phase transition in TiH_x has been demonstrated in numerous experiments (see, for example, /1/). In particular, the structure of the intermediate superconducting δ'-phase and the reason of intense small angle neutron scattering during the transition to a final state were unknown.

To clarify these questions we have studied transitions in high pressure quenched ε-$TiD_{0.74}$ during the heating from 80 K to 293 K using the real time method for simultaneous collection of diffraction and small angle scattering patterns /2/. The experiment was carried out on the DN-2 diffractometer with the temporal resolution of 30 s. The initial ε-phase was prepared by squeezing the sample up to 60 kbar, heating it up to 620 K, holding in these conditions for 10 min, quenching down to liquid nitrogen temperature during 20 min, then the sample was shut off pressure.

During the heating of the sample from 80 K up to 137 K the diffraction pattern was in agreement with that of the ε-phase of TiD, where deuterium atoms occupy the octahedral sites in the structure. In the interval between 142 and 205 K the transition into δ'-phase took place, namely, deuterium passed slowly to occupy the tetrahedral sites and was ordered in (110) planes. Simultaneously the volume of the elementary cell increased. At T=205-220 K the d-spacing d_{111} changed abruptly. It was the evidence of the δ' to δ phase transition. First indication of a small angle neutron scattering (SANS) rise was detected at T=180-200 K in the range of momentum transfer of Q = =0.02-0.05 A^{-1}. At 200 K SANS increased to a marked degree, then the SANS intensity got stabilized at 215 K. As it was established in the structure analysis, at that moment the stoichiometric δ-phase of TiD was created and metallic α-Ti was separated. Fig.1 shows the result of Rietveld refinement of the final phase at room temperature. This diffraction spectrum corresponds to a mixture of 81% δ-phase (sp.gr. Cccm, a=4.168, b=4.234, c=4.577 A), with 96% occupancy of the T-sites for deuterium, and 19% α-Ti (sp.gr. $P6_3/mmc$, a=2.952, c=4.688 A).

Thus, the ε--δ phase transition in $TiD_{0.74}$ was investigated and the region of occurrence of the δ'-phase established. It was shown that during the hea-

ting the deuterium content in the δ'-phase grew slowly, at the δ'-- δ phase transition, the *c*-period of the cell changed abruptly, and after that, the separation of α-Ti was initiated. The content of the final state was very close to that of the stoichiometric one.

1. A.San-Martin, F.D.Manchester, Bulletin of Alloy Phase Diagrams, 1987, v.8, p.30 and p.81.
2. A.M.Balagurov et al, FTT, 1991, to be published

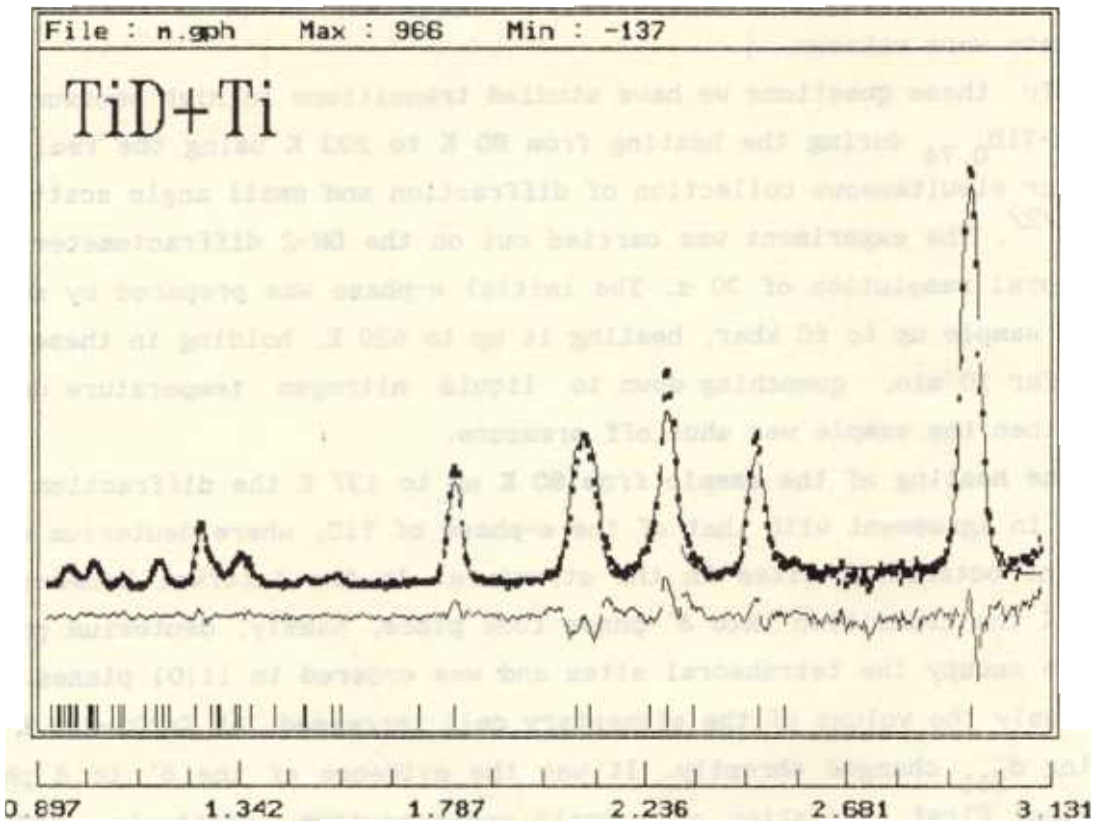

Fig.1. Rietveld refinement of two phase diffraction patterns: δ-$TiD_{0.96}$ and α-Ti. Experimental points, the calculated line and the difference curve are shown.

REAL TIME NEUTRON DIFFRACTION STUDY OF THE PHASE TRANSITION IN $Cu(Li,V_{0.4})Fe_{1.6}O_4$

A.M.Balagurov, E.P.Kozlova, G.M.Mironova, Laboratory of Neutron Physics, JINR, Dubna

I.Jacyna-Onyszkiewicz, IF PAN, Poznan, Poland

At high temperatures ($T \geq 760^{\circ}C$) the compound $CuFe_2O_4$ crystallizes into a space group Fd3m and has the inverse spinel structure. The ions Fe^{3+} occupy the tetrahedral sites and, what is more, the tetrahedra FeO_4 are undistorted. Accordingly, a certain part of Cu and Fe cations occupy the octahedral sites. At room temperature the $Cu(Fe)O_6$ octahedra are slightly distorted and the symmetry of the structure reduces to $I4_1/adm$. The parameter of tetragonal distortion c/a, is higher than unity ($c/a \simeq 1.06$). If iron is fully substituted by Cr, the symmetry of the structure will remain tetragonal, but $c/a \approx 0.91 < 1$.

Systematic studies of iron substitution by other cations with different valences are being carried out at the Institute of Physics, PAN in Poznan. The major aim of these studies is the clarification of the reasons why distortion of the cubic symmetry occurs in these compounds and the estimation of the crystal field effects.

A real time neutron diffraction experiment with the temporal resolution of 80 s was performed on the TOF diffractometer DN-2 to examine the tetragonal-cubic phase transition in $Cu(Li,V_{0.4})Fe_{1.6}O_4$ during the heating, to determine the order of the transition and to study hysteresis phenomena. The sample was prepared at the IF PAN.

Figure 1 shows thermodiffractograms (near $d_{hkl} = 2.5$ A) measured at temperatures from $T = 120^{\circ}C$ (the beginning of a time scale) up to $510^{\circ}C$ and down back to $120^{\circ}C$. One may clearly see tetragonal splitting of the diffraction peak at a lower temperature and its intensity increasing at the transition to a cubic phase. To better illustrate the fact, the time dependence of the tetragonal peak (103) integral intensity is shown in Fig.2. In the initial state the parameter of tetragonal distortion is equal to 1.04, i.e. slightly lower than in a pure $CuFe_2O_4$ compound. The difference $\gamma = c/a-1$ can be taken as the order parameter and its value decreases gradually to zero.

Two unexpected effects were observed. Firstly, the transition is accompanied with very large temperature hysteresis: at the heating the transition is completed at $T_c = 500^{\circ}C$, while at the cooling the starting temperature of the

reverse transition is about 400°C. Secondly, the width of diffraction peaks in the cubic phase is almost twice as small as in the tetragonal phase (Fig.3). It can be explained, if one assumes some additional orthorhombic distortion of the structure at a lower temperature. To justify the above assumption a measurement with a much better resolution is needed.

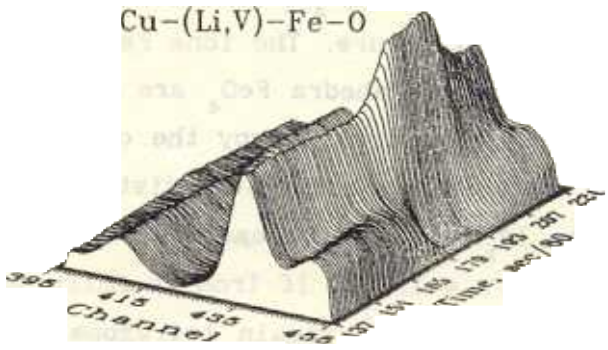

Fig.1. Neutron diffraction patterns in the vicinity of the cubic (311) peak of the compound $CuLi_{0.2}V_{0.2}Fe_{1.6}O_4$ measured during the heating of the sample from 120°C (the beginning of a time scale) up to 510°C and the cooling down to the initial temperature. The temporal resolution was equal to 80 s.

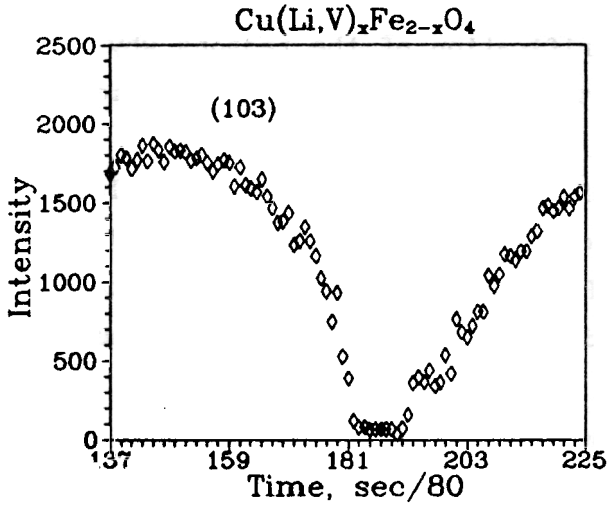

Fig.2. Integral intensity of the tetragonal (103) diffraction peak (the small peak in the right-hand side of Fig.1) vs. time. The transition to the cubic phase and the reverse transition are illustrated.

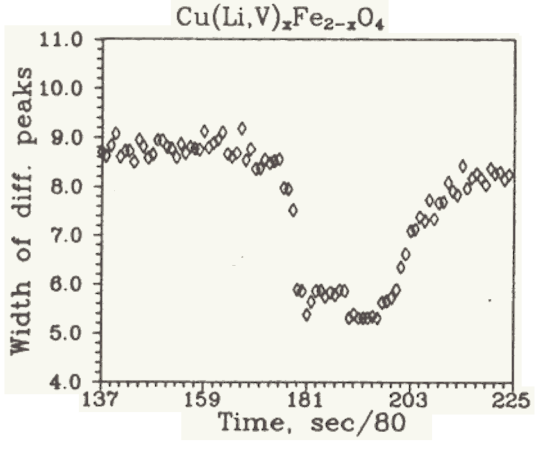

Fig.3. The change of the diffraction peaks width during the phase transition. The widening of the peaks can be related to additional orthorhombic distortion of the lattice at a lower temperature.

HIGH TEMPERATURE PHASE STRUCTURE OF CESIUM DIHYDROGEN PHOSPHATE

A.I.Beskrovnyi, Laboratory of Neutron Physics, JINR, Dubna

A.I.Baranov, L.A.Shuvalov, Institute of Crystallography, Moscow, USSR

I.D.Datt, Mendeleev Chemico-Technological Institute, Moscow, USSR

Ferroelectric CsH_2PO_4 was investigated in detail by several authors in the temperature interval 4 to 560 K to study its physical properties and ferro(para) phase crystal structure ($T_{c1} \simeq 150K$)[1,2]. The temperature dependence curve of the dielectric constant and the DTA-curves point to the existence of two more high temperature phase transitions ($T_{c2} \simeq 503$ K, $T_{c3} \simeq 540$ K). The X-ray quantitative analysis of them appeared impossible because of the cesium metaphosphate formation on the sample surface. However, it allows the conclusion that their symmetry is not higher than monoclinic[3].

Neutron diffraction measurements were carried out on single crystal samples of CsH_2PO_4 on the DN-2 diffractometer at the IBR-2 reactor. The room temperature data were obtained in agreement with literature (the monoclinic symmetry, $P2_1/m$). At T ~ 510 K the number of diffraction lines diminished and kept constant with the further increase of temperature up to 550 K. Then the conclusion follows that only one high temperature phase takes place in this case. The whole host of monocrystal and powder data evidence in favour of the cubic symmetry of the high temperature phase. Taking into account that only small distortions in PO_4 tetrahedron geometry and real hydrogen bonds configurations can occur, the initial crystal structure model is suggested. Treatment of the neutron powder data with the Rietveld profile method has allowed us to get the crystal space group (Pm3m, a = 4.966(3)Å, Z = 1). It turned out that the crystal structure is highly disordered both with respect to oxygen and hydrogen atoms O-12(h), H-24(ℓ) with the occupation parameter g= 1/6. A different from unity g-parameter points to the possibility of PO_4-configuration rotations and as a consequence to the dynamical disorder in the hydrogen bonds system.

The existence of unoccupied proton positions in the bound system allows the assumption about the high proton conductivity of the high temperature phase in CsH_2PO_4. It is possible also that conductivity anisotropy is absent in this case because of the high crystal structure symmetry of the phase.

1 Matsunaga H., Itoh K., Nakamura E. J.Phys.Soc.Jap., v.48 (1980) 2011

2. Itoh K., Hagiwara T., Nakamura E. J.Phys.Soc.Jap., 52 (1983)
3. Rashkovich L.N., Meteva K.B. Kristallographiya, 24, 4 (1978) (in Russian).

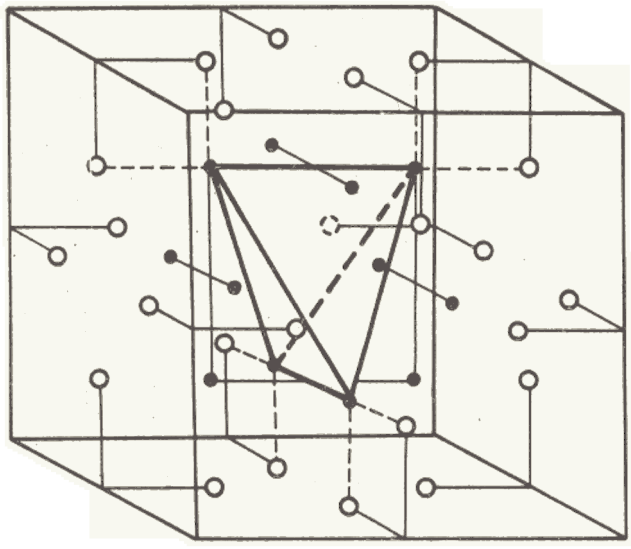

Fig.1. The structure of the high temperature phase of CsH_2PO_4. Apexes of the cube are occupied by Cs-atoms. One of the six possible orientations of the PO_4 tetrahedron is shown. Dotted lines - possible hydrogen bonds for a given tetrahedron orientation. The proton occupies only one position (open circles) in every pair of the nearest to oxygen positions.

NEUTRON DIFFRACTION STUDY OF THE LOW TEMPERATURE DOMAIN STRUCTURE IN $LiKSO_4$

B.N.Savenko, D.Sangaa, LNP, JINR, Dubna
D.A.Keen, C.C.Wilson, RAL, Chilton, Didcot, U.K.
B.Mroz, Inst. of Phys., UAM, Poznan, Poland

In the last few years great attention has been paid to the low-temperature phase transitions in $LiKSO_4$ (LPS). The investigations made by different methods (see, for example, [1]) in the range from room temperature to 5 K have established several phase transition points. The different phases and corresponding transition points from melting point to liquid helium temperature can be numbered as follows:

```
  940K     700K      240K     180K    38K
I------II------III------IV------V------VI.
```

It is known that LPS is hexagonal at room temperature with a space group $P6_3$. For the rest phases, even the question of the point group is still open. The symmetries of phases IV are up to now controversy.

We have tried to solve some open questions concerning the existence of transitions and symmetries of phases in LPS. The domain structure in ferroelastic phase V should reflect the symmetry in phases IV and V. The domain formation is accompanied by the splitting of the reciprocal lattice nodes. The number and distribution of the splitting components in this new composite cell[2] are related with the symmetries in the ferro- and paraphase. A detailed symmetry analysis for LPS has been performed in paper[3] for the transitions from group 6mm or 6 into mm2, 2 or 1.

The measurements were performed on single crystal samples having the shape of a rectangular prism over the temperature range from 5 to 293 K. The samples were grown in the Institute of Physics, UAM, Poznan, Poland. The majority of the experiments were performed with the help of the time-of-flight single crystal diffractometer SXD at ISIS[4]. Some previous experiments were performed at the diffractometer installed at the pulsed reactor IBR-2[5].

On cooling the LPS crystal from room temperature to 189 K (the transition point into phase V) the position and profile of the diffraction peaks remain unchanged. When the crystal passes to phase V, the splitting of the nodes in the reciprocal lattice is produced accompanied by the intensity increase. Examples of the measured cross-section of the $(1\bar{2}0)$ node in $(\lambda, 2\Theta)$ space

are given in Fig.1 for three different temperatures. The splitting is increasing with the temperature decreasing. But no change was observed for the nodes (001).

As it follows from[3], three point groups are possible for phase V, namely, mm2, 2 or 1. The triclinic symmetry for phase V was rejected from the beginning, observing that the peaks (0 0 2n+1) which were extinguished in phase III, remained extinguished in phase V, too. For choosing between the groups mm2 and 2, we have used the symmetry analysis[3]. We may conclude that the transition IV - V is of the type 6mm - mm2.

Appearing at 189 K the splitting diffraction pattern remained unchanged at cooling down to 15 K and the 38 K phase transition, observed by the optical method, was not revealed in our experiments.

1. B.Mroz, J.A.Tuszynski, H.Kiefte, M.J.Clouter. J.Phys.: Condens.Matter, 1 (1989) 5965.
2. G.S.Parry. Acta Cryst., 15 (1962) 596.
3. A.M.Balagurov, N.C.Popa, B.N.Savenko. phys.stat.sol.(b), 134 (1986) 457.
4. C.C.Wilson, J.B.Forsyth. RAL Report, RAL-89-005, 1989.
5. I.M.Frank, P.Pacher. Physica B120 (1983) 37.

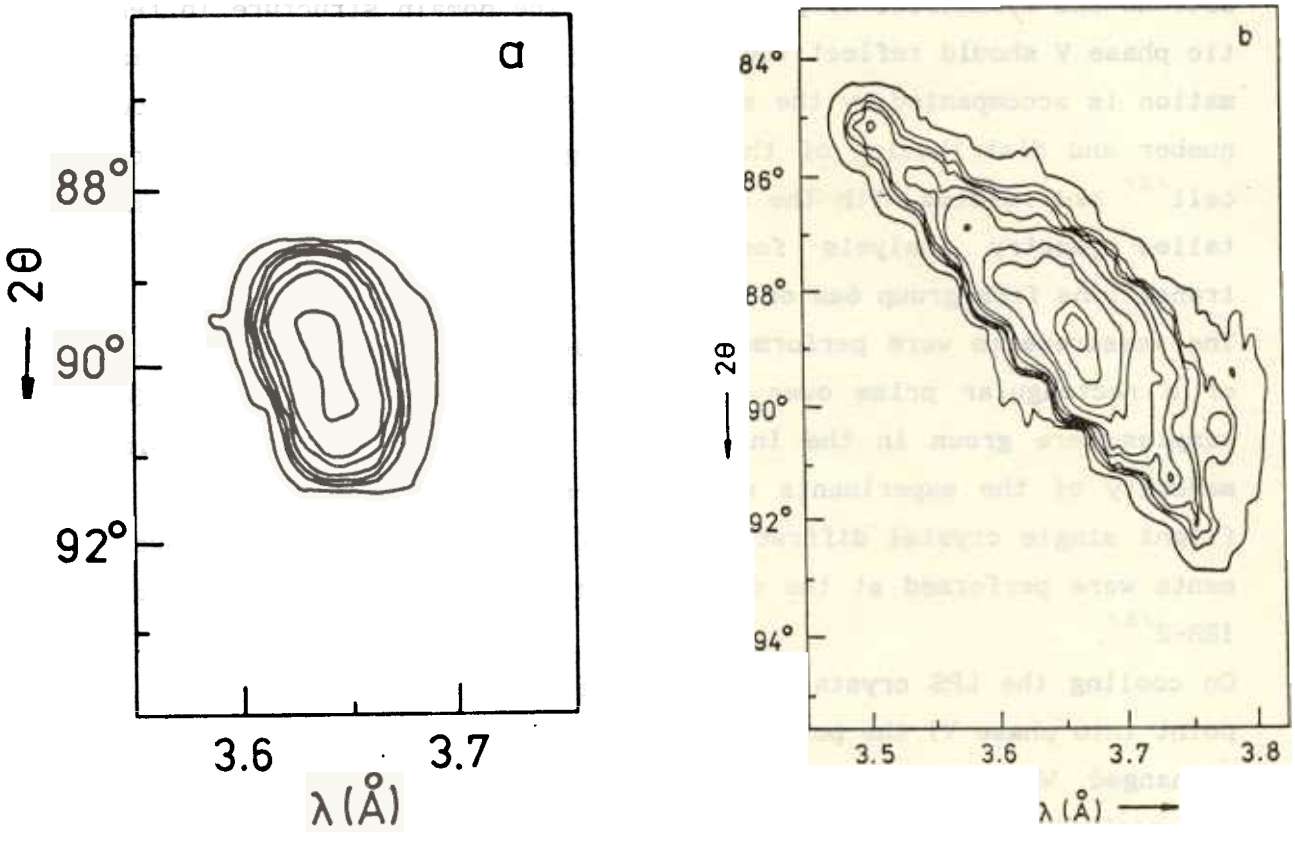

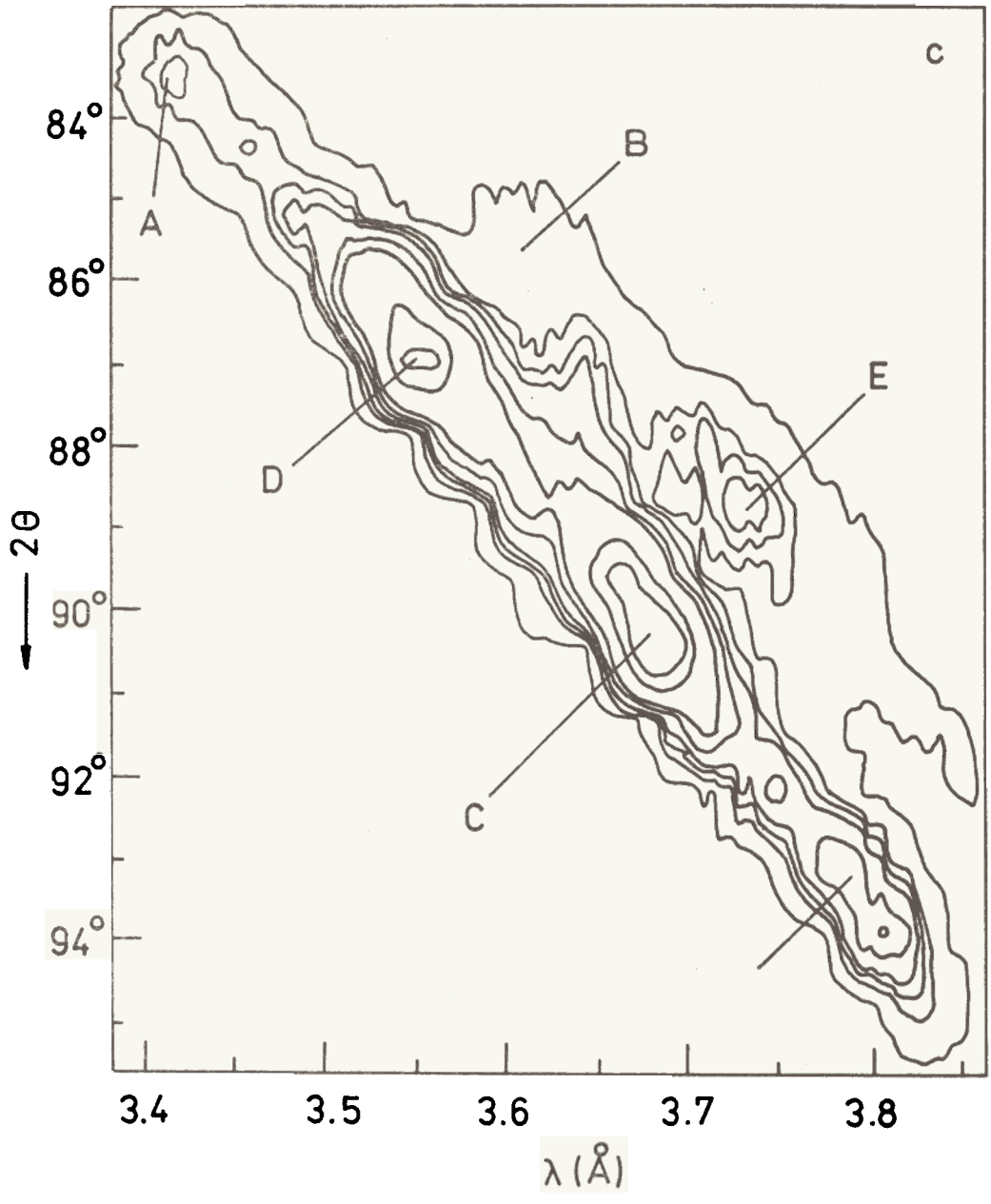

Fig. 1. Cross-section of the node $(1\bar{2}0)$ in $(\lambda, 2\Theta)$ coordinates: a) for T = =190 K (phase IV), b) for T = 180 K, c) for T = 99 K (both phase V).

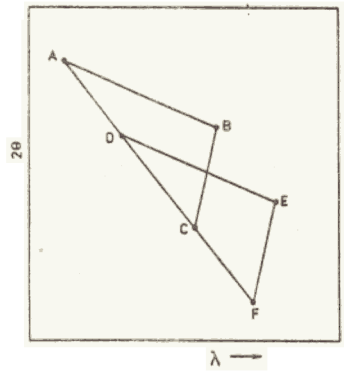

Fig. 2. Picture of the splitting of the $(1\bar{2}0)$ node at the transition into phase V in coordinates $(\lambda, 2\Theta)$.

HIGH PRESSURE RESEARCH OF $LiKSO_4$ PHASE TRANSITIONS

D.Sangaa, B.N.Savenko, LNP, JINR, Dubna
A.N.Ivanov, Inst. of High Pressure Phys., Troitsk, USSR
B.Mroz, Inst. of Phys., UAM, Poznan, Poland
L.S.Smirnov, ITEP, Moscow, USSR

Since there were reported two structural phase transitions of lithium-potassium sulphate $LiKSO_4$ (LPS) occuring between 100 and 293 K[1,2], and especially, the ferroelastic phase transition at 189 K found on cooling at atmospheric pressure[3], much attention has been given to the low temperature phases of LPS. LPS has at least three polymorphic modifications in the temperature region from 100 to 293 K at atmospheric pressure; these phases are denoted as phase I (room temperature phase), II (intermediate phase) and III(low temperature phase) in the order of the temperature decrease. LPS has hexagonal symmetry with the space group $P6_3$ at room temperature[4]. The space groups in phases II and III are probably the hexagonal $P6_3mc$ and the orthorhombic $Cmc2_1$ one, respectively[5]. The II-III phase transition is of the first order because of a sharp anomaly in lattice parameters[5] and thermal hysteresis[6] at II-III phase transition temperature. In phase III ferroelastic domain structure appears[3] and the splitting of diffraction peaks is observed[7]. In work[8] the pressure-temperature phase diagram of LPS (Fig.1) was investigated in wide temperature and pressure regions. It is seen in Fig.1, that the range of stability of the intermediate phase II decreases with increasing pressure and the phase II vanishes at the I-II- III phase triplet point (4.3 kbar, 287 K). Thus the phase transition changes from the II-III into the new pressure-induced I-III one at 4.3 kbar with increasing pressure.

The measurements were performed on single crystal samples having the shape of a rectangular prism. The sample dimensions were 4x4x5 mm^3. All experiments were performed on the diffractometer DN-2[9]. The high pressure cylinder-piston chamber was used with freon-11 as the pressure-transmitting fluid[10].

In Figs.2,3 there are shown the cross-sections of the diffraction peak (120) at atmospheric pressure and at 6 kbar, respectively. With pressure increasing to 3.5 kbar the position and profile of the diffraction peaks remain unchanged (Fig.2). At further increasing pressure to 8 kbar the peak (120) gets split, proving thus the existence of the ferroelastic domain structure in this phase (Fig.3). In work[11] it was reported that the transition to

the ferroelastic phase III is accompanied by the splitting of the diffraction peak (120) into six components. The lack of three components in Fig.3 can be explained by insufficient DN-2 resolution, large absorption of neutrons in the high-pressure chamber walls and, possibly, by a relatively small number of domains of this kind.

Thus a new pressure-induced transition into phase III was observed at room temperature.

1. D.P.Sharma. Pramana, 13 (1979) 223.
2. M.L.Bansal et al. Solid State Comm., 36 (1980) 1047.
3. B.Mroz et al. Ferroelectrics, 42 (1982) 71.
4. A.J.Bradley. Phil.Mag., 49 (1925) 1225.
5. P.E.Tomaszewski, K.Lukaszewicz. Phase Transitions, 4 (1983) 37.
6. T.Breczewski, T.Krajewski, B.Mroz. Ferroelectrics, 33 (1981) 9.
7. A.M.Balagurov et al. phys.stat.sol.(a), 96 (1988) 25
8. S.Fujimoto, N.Tasuda, H.Hibino. Phys.Lett., 104A (1984) 42.
9. A.M.Balagurov et al. JINR, 3-14-291, Dubna, 1984.
10. A.N.Ivanov et al. ITEP Report, 40-91, Moscow, 1991.
11. A.M.Balagurov, N.C.Popa, B.N.Savenko. phys.stat.sol.(b), 134 (1986) 457.

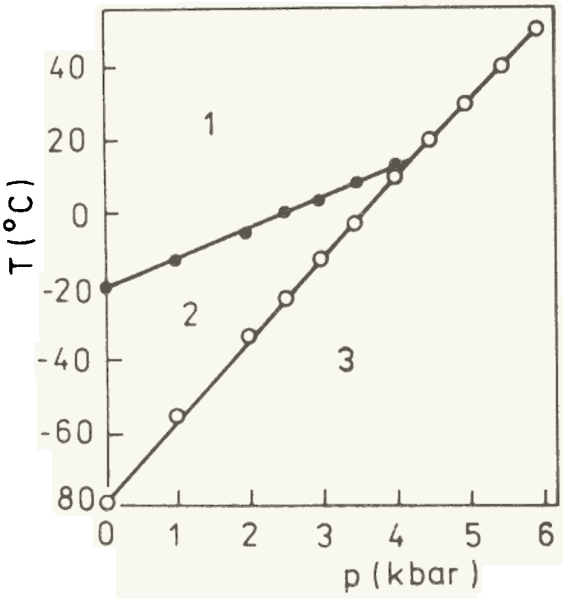

Fig.1. The pressure-temperature phase diagram of $LiKSO_4$.

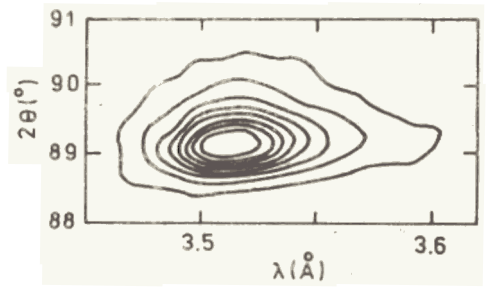

Fig.2. Cross-section of the node (120) in (λ, 2θ) coordinates at atmospheric pressure.

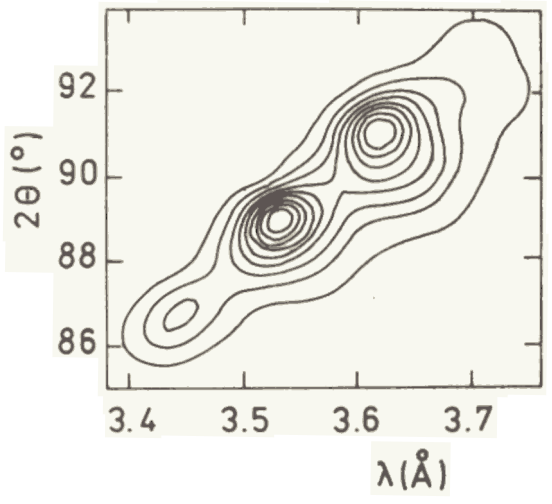

Fig.3. Cross-section of the node (120) in (λ, 2θ) coordinates at 8 kbar pressure.

NEUTRON SCATTERING IN DISORDERED PEROVSKITE-LIKE CRYSTALS

S.B.Vakhrushev, A.A.Naberezhnov, N.M.Okuneva
Leningrad Phys.-Tech. Institute, USSR
B.N.Savenko, D.Sangaa, LNP, JINR, Dubna

Recent years have demonstrated the increasing interest in the investigation of structure phase transitions in disordered crystals such as RbH_2PO_4-$NH_4H_2PO_4$ (RDP-ADP) $K_{1-x}Li_xTaO_3$ and some others[1]. The so-called ferroelectrics with diffuse phase transitions (DPT) constitute one of the most interesting groups of these compounds[2]. The $PbMg_{1/3}Nb_{2/3}O_3$ (PMN) crystal could be considered as a model object to study DPT. In spite of the tremendous number of papers devoted to investigation of the PMN the microscopic mechanism of the phase transition is not clear yet. The main reason for the observed peculiar properties of the ferroelectrics with DPT is a random distribution of nonisovalent ions (Mg^{+2} and Nb^{+5} in the case of PMN) over the symmetry equivalent positions. This random distribution of ions results in random, at least in values, coupling of neighbouring dipole moments and in the appearance of frozen electric fields, random both in directions and values. The properties of such systems are similar to some extent to those of spin glasses[3]. Our previous neutron studies[4] have revealed a glass like behaviour of the low temperature phase of the PMN, but some important questions remained unclear.

We have undertaken additional neutron scattering measurements of the PMN single crystal on the DN-2 TOF diffractometer with a positional sensitive detector. This instrument enables us to study two-dimensional distributions of the intensity of both Bragg and diffuse scattering in the vicinity of several reciprocal lattice points simultaneously. Our measurements have shown, that, when the PMN is cooled without any external electric field, there is no substantial widening of Bragg peaks and the longitudinal component of diffuse scattering does not appear also. This experimental result allows us to reject the hypothesis about the microdomain character of the low temperature phase.

In our, earlier experiments performed on the triple-axis spectrometer it was shown, that the cooling of the PMN crystal in the external electric field results in strong enhancement of the intensities of Bragg peaks. The limited amount of data have not enabled us to give an unambiguous answer to the question, if this enhancement is connected with the decrease of an anomalously large Debye-Waller factor due to the ordering of polar ion shifts, or

it is due to extinction changes. Our measurements have shown, that the most strongly increasing peaks are those of the (2h+1, 2k, 21) and (2h+1, 2k+1, 21) types with large h,k,l; that is, the peaks for which the extinction is minimum. So we could make the conclusion, that the cooling of a PMN crystal in electric field results in the ordering of ion shifts, and, moreover, the removal of the field from the field cooled crystal produces no change of intensities, and so the obtained state is stable at low temperatures. We are also doing real time experiments to study the structure relaxation in PMN. For this purpose to a zero-field cooled crystal an electric field is instantly applied and the time dependence of the intensity of both Bragg and diffuse scattering studied. We have found out, that in addition to the previously observed relaxation of Bragg intensity, the relaxation of the diffuse scattering did also exist. At present the quantitative results of these real time experiments are under evaluation.

1. U.T. Hochli, K. Knorr, A. Loid. Adv. in Phys., 39 (1990) 405.
2. G.A. Smolensky et al. Ferroelectrics and Related Materials. 1984, 736 p.
3. S.L. Ginzburg. Irreversible Phenomena of Spin Glasses. Moscow, 1989, 152 p.
4. S.B. Vakhrushev et al. Ferroelectrics, 90 (1990) 173;
S.B. Vakhrushev et al. Physica B, 156&157, (1989) 90.

NEUTRON DIFFRACTION EXPERIMENTS WITH PULSED MAGNETIC FIELDS AT IBR-2

D.Georgiev, V.V.Nietz, G.Pasazhev, A.A.Yakovlev
Laboratory of Neutron Physics, JINR, Dubna

1. THE COHERENT SPIN-FLOP TRANSITION IN AN ANTIFERROMAGNET WITH UNIAXIAL ANISOTROPY

The kinetics of the spin-flop transition in the single crystals of CrO_3 and α-Fe_2O_3 is being investigated on the spectrometer SNIM-2. The phase transition is induced by magnetic field sinusoidal pulses having the duration of 1 ms and the amplitude of up to 150 kOe. Changes in magnetization vector orientation were determined by means of neutron diffraction measurements. The typical differential neutron diffraction pattern is shown in Fig.1 together with the magnetic field versus time pattern (time channels are numbered along the X-axis).

The main peculiarities of the phase transition revealed in Cr_2O_3 experiments are:

1. Coherence, i.e. synchronism of magnetic reorientation over the whole sample volume (about 1 cm^3). No formation stage of the phase domains.

2. Slow-down of the process of magnetization orientation rotation in experiments with pulsed magnetic fields.

3. Independence of the magnetization rotation angle at a given field strength of the magnetic field change rate in the limits of the experiment.

4. Increase in magnetic field strength corresponding to a given angle of magnetization rotation with increasing temperature.

Observed coherence of phase reorientation is in deep contradiction with the traditional idea of the kinetics of the first order phase transition. Theoretical analysis has shown that peculiarities 2,3,4 disagree completely with the representation of the spin-flop transition as the isothermal process in the presence of a pulsed magnetic field.

A theoretical basis for the explanation of effects observed lies in the idea of an adiabatic behavior of an antiferromagnet in an external magnetic field and in the assumption of the existence of some intermediate, quasiequilibrium state in the spin-flop transition. A corresponding model has been developed. However, numerical calculations have to be made to compare its predictions with the results of the experiment.

The spin-flop transition was measured in the other crystal, α-Fe_2O_3, which has the same crystalline and analogous magnetic structure. The phase transition in α-Fe_2O_3 has exhibited similar to Cr_2O_3 main peculiarities of behavior. Its temperature behavior was different in correspondence with some difference in magnetic phase diagrams. An attempt was made to derive a qualitative relationship between the antiferromagnetism vector rotation angle and the magnetic field strength in the adiabatic spin-flop transition, which failed in the case of Cr_2O_3. In this attempt we used a well studied phase transition in α-Fe_2O_3, induced by a field perpendicular to the rhombohedronic axis, to have calibrated the intensity as the function of the rotation angle for the further use in the spin-flop transition analysis. It is hoped that finally we shall have the qualitative characteristics of the transition convenient for comparison with theory.

2. INVESTIGATION OF MAGNETIC FIELD INDUCED STATES IN $HoFeO_3$

Diffraction experiments to investigate a single crystal of $HoFeO_3$ have been made in the temperature range from 26 to 170 K in the presence of a pulsed magnetic field of about 175 kOe.

It was an attempt to register antiferromagnetic ordering in sublattices of rare earths, which, in principle, might be induced by an external magnetic field (holmium ions are in a paramagnetic state in the given temperature range). Diffraction peaks (102), (104) and (302), which are absent in zero magnetic field at temperatures $T > 60$ K were successfully measured. Temperature and magnetic field dependences of induced antiferromagnetism were obtained. Typical reflection from a field intensity dependences (102) are shown in Fig. 2. In relatively weak fields the dependence is a quadratic function, which fact points to the proportionality between the field strength and the value of the induced antiferromagnetism vector. At lower temperatures the behavior of $HoFeO_3$ becomes more complex. Figure 3 shows the dependences of the (302) reflections on the field strength. Though some complications should have been expected beforehand in connection with the known phase transition at 60 K, the whole picture remains unclear. It is possible that a complete data treatment will help to clear up the reasons of some inconsistency of the experimental results with the existing model representations of orthoferrites.

In the theoretical aspect it is not an unexpected fact that antiferromagnetizm can be induced by an external field. It follows directly from the theory of weak ferromagnetism in antiferromagnetic compounds. However, it is important to have the possibility to detect and investigate this effect in practice. In the case of rare earth orthoferrites and orthochromites this will allow one to directly obtain exchange integrals values, which are the characteristics of the interaction between the ions of rare earths and transition metals, the possibility much hindered in other methods.

Another problem connected with $HoFeO_3$ is the orientation phase transition of the first order, $\Gamma_2 \rightarrow \Gamma_4$, induced by an external magnetic field at $T < 40$ K. This transition is connected with a distinguishable shift of rare earth ion levels under the action of an external magnetic field. This transition is well enough argumented in theory and described in scientific literature. Some publications are known reporting investigations of some situation in $HoFeO_3$, which they interprete (to our opinion without sufficient grounds for) as the observation of this transition.

Our SNIM-2 experiments gave the negative answer to the question about the first order phase transition, at least in the way formulated in literature. It is early to make definite conclusions as the experimental data are not still processed and understood completely. However, obtained results are probably the consequence of a more complex behavior of orthoferrites at low temperatures and they point to the necessity of revising the $HoFeO_3$ phase diagram (and diagrams of related substances) in a magnetic field.

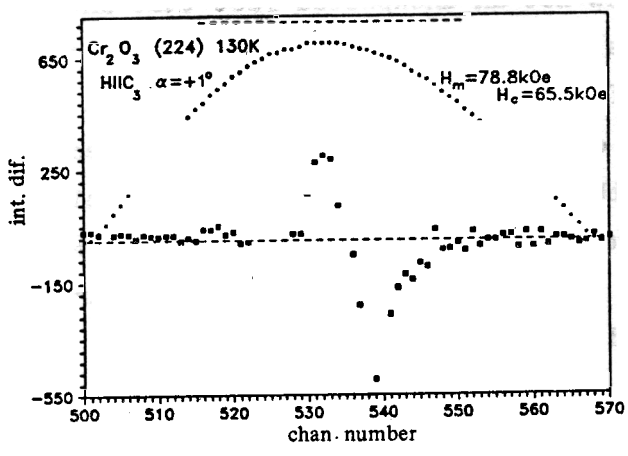

Fig. 1. The differential neutron diffraction pattern (I_H and I_0 are the intensities with and without field, respectively) for the diffraction peak (224) measured on the single crystal Cr_2O_3 together with the time dependence of the magnetic field having an amplitude H_m = 84.2 kOe (the time window duration is 16 msec). The magnetic field direction is along the rhombohedric axis.

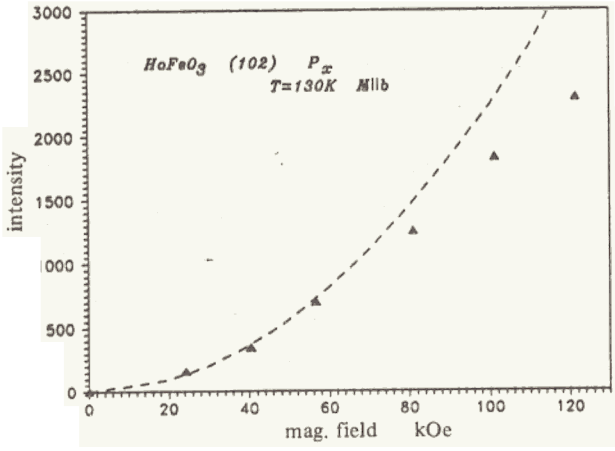

Fig. 2. The dependence on the magnetic field of the diffraction peak (102) connected with induced antiferromagnetism in a single crystal of $HoFeO_3$. The magnetic field direction is along the Y-axis.

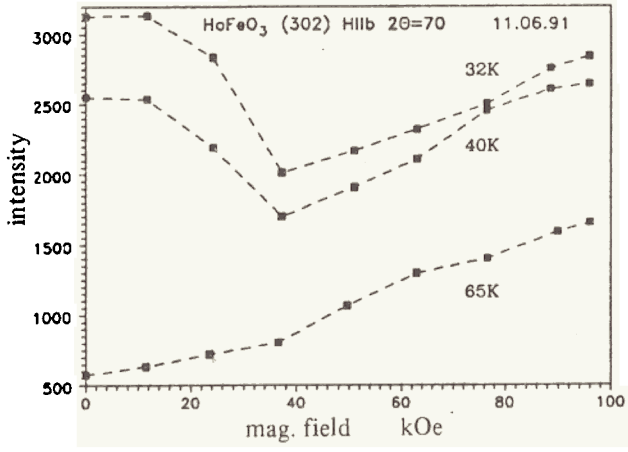

Fig. 3. The dependence on the magnetic field of the (302) peak intensity for $HoFeO_3$ at given temperature values.

THE MEASUREMENT OF POLE FIGURES OF GEOLOGICAL SAMPLES WITH LOW CRYSTAL SYMMETRY

K.Helming, W.Voitus, K.Walther, LNP, JINR, Dubna

The time-of-flight diffractometer NSWR is situated on a long flight path of beam line 7A of the pulsed reactor IBR-2 and is mainly used for the measurement of pole figures. The layout is shown in Fig.1. After escaping the core (1) the fast neutrons are slowed down in the moderator (2). An additional disk-chopper (4) synchronized with the reactor reduces the background between the pulses. The neutrons are guided by a Ni-coated straight neutron guide (7,8) which has a cross section of 50x170 mm^2. The first part of the neutron guide (≈18 m) is filled with argon gas, the other part is evacuated. The total flight path is 104.66 m[2]. The thermal neutron flux on the sample is greater than $1x10^6$n $cm^{-2}s^{-1}$.

To measure the pole figures of geological samples one had to overcome some difficulties[1]:

- most geological samples are coarse grained and inhomogeneous and require the use of neutrons instead of X-rays;
- because of the low crystal symmetry (tricline...trigonal) the diffraction patterns show a lot of peaks which are often overlapped. A diffractometer with a high resolution like NSWR is therefore necessary.

The spectrometer is equipped with a central sample desk, carrying the texture goniometer. A platform (a sector of a circle, angle of the sector: 120°) can be turned around the sample desk. On the platform 7 detectors in shielding tanks are guided by rails concentrically in reference to the sample. The minimal angular distance (in 2ϑ-scale) between two detectors is about 14° and the maximal one is about 20°.

The experiment is remote controlled by a PC/AT via an inserted module linked with a CAMAC-controller.

Step motors serve for a high precision in angle setting. The texture goniometer allows one to measure large samples (plates up to 25 cm ø, 1 cm thick), but samples having spheric or cubic shape (ø or side length about 3 cm) are prefered. In this case the samples are completely embedded in the incoming neutron beam (always the same irradiated sample volume). Furthermore, the sample causes no "shadow" region and all the seven detectors can be used simultaneously: the first detector is set at $2\vartheta = 160°$, the second at $2\vartheta = 145.6°$ and the seventh at $2\vartheta = 73.6°$. The normal to the sample is also the axis of rotation (angle φ) in steps of 7.2° and is at an angle of

3.6° with the scattering vector $\vec{k}$ (which belongs to the scattering angle $2\vartheta = 160^\circ$). This results in pole figures, where at 3.6° from the equator are located the measured points of the seventh detector (pole angle $\theta = 86.4^\circ$) and at 7.2°-intervals follow on concentric circles - the measuring net of the other detectors (with the pole angle $\theta = 43.2^\circ$ for the first detector). The inner parts of the pole figures are not measured. In Fig.2 a pole figure is shown where the points of the sampling mesh are represented.
Figure 3 shows a time-of-flight spectrum of a sample taken from the super-deep drilling (KTB) at Windischeschenbach. This sample contains nearly 60% quartz, and 15% oligoklase and 15% biotite. The other accomplishing materials are less than 1% and are not visible in the diffraction pattern. The intensity of the Bragg-peaks has to be corrected for the sensitivity of the detectors, reflectivity and intensity due to the reactor spectrum.
Table 1 shows a compilation of samples which were measured in the period of October 1990 to June 1991. Here it must be pointed out that up to now in quartz containing samples there was obtained only the texture of the quartz fraction. From the samples from the bore hole of the super deep drilling at Windischeschenbach (FRG) there were investigated also the textures of the mica and feldspar fraction. The quartz and mica fractions are texturized, the feldspar fraction is without texture.

1. V. Damm et al. Texture and Microstructures, 12(1990) 15.
2. M. Betzl et al. Int. Conf. Adv. Meth. in X-Ray and Neutron Structure Analysis of Materials. Prague, Aug. 20-24, 1990 (poster).
3. A. N. Nikitin et al. Abstracts: VI All-Union Conf. "Textures and Recrystallization", Sverdlovsk, 1991.
4. T. I. Ivankina et al. Symp. Deformation Process and the Structure of Lithosphere. Potsdam, May 3-10, 1990.

Table 1

Sample	Phases	Symmetry	Co-operation
olivine[3]	olivine	orthorhombic	IPE, Moscow
quartz[4]	quartz	trigonal	IPE, Moscow
gneiss	quartz	trigonal	CIPE, Potsdam
	oligoclase	triclinic	
dolomite	dolomite	trigonal	Univ.,Gottingen
	calcite	trigonal	
	biotite	triclinic	
calcite	calcite	trigonal	Univ.,Gottingen
amphibolite	hornblende	monoclinic	Univ.,Gottingen
	oligoclase	triclinic	
	quartz	trigonal	
KTB	quartz	trigonal	CIPE, Potsdam
(super-deep	oligoclase	triclinic	Univ.,Gottingen
drilling	biotite	triclinic	
meteorit	kamencite	cubic	IPE, Moscow

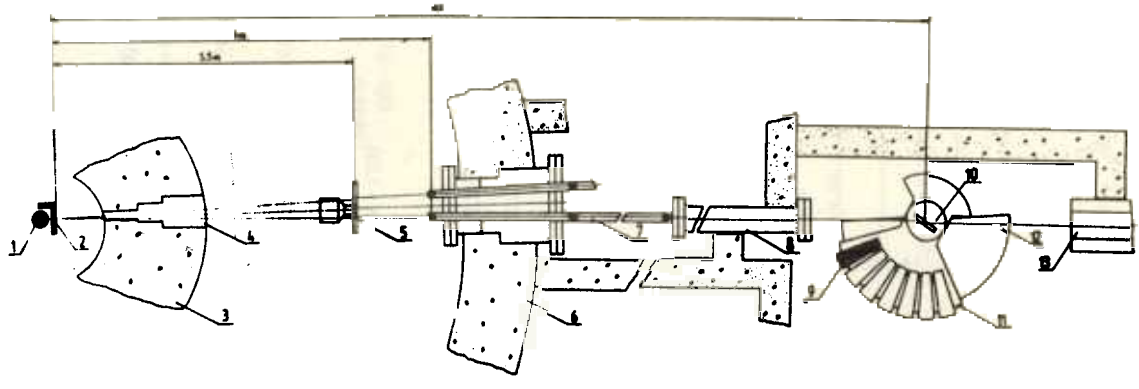

Fig. 1. The layout of the diffractometer NSWR on beam 7A of the reactor IBR-2. 1 - core of reactor; 2 - moderator; 3 - inner corridor; 4 - beam lock; 5 - disk chopper; 6 - biological shield; 7 - first part of neutron guide, Ar-filled; 8 - second part of neutron guide, vacuum; 9 - detector shield; 10 - texture goniometer; 11 - platform, turnable; 12 - base of spectrometer; 13 - beam stop.

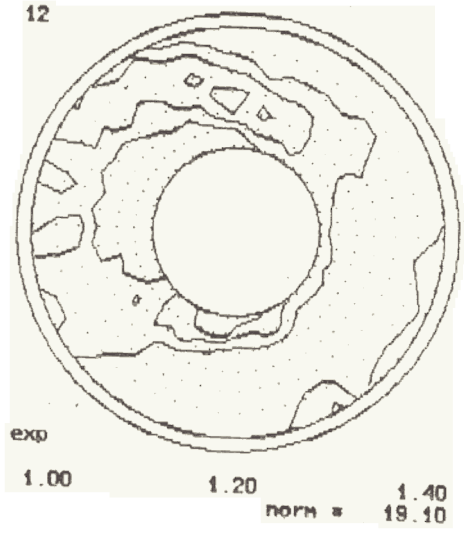

Fig.2. The sampling mesh of the pole figures. The pole angles of the concentric circles in the pole figure differ by 7.2 degrees. The inner part of the pole figure may not be measured because the same information is included in the outer part of the pole figure (minimal pole density set).

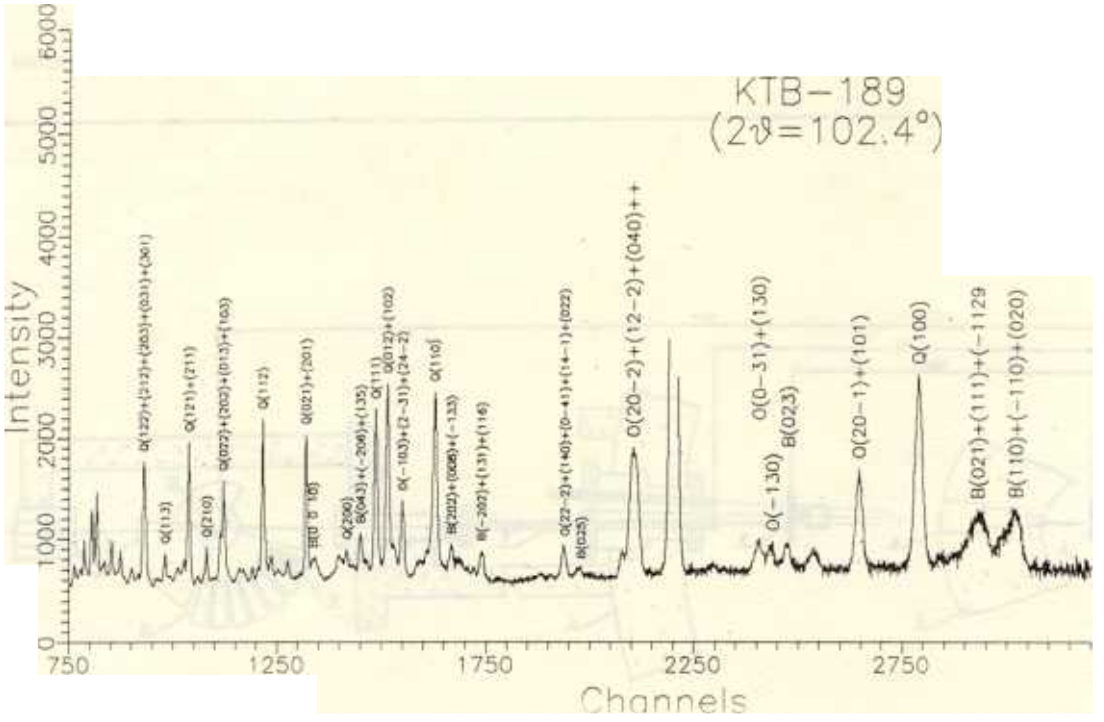

Fig.3. Time-of-flight pattern of a sample from the bore-hole of the super-deep drilling at Windischeschenbach (FRG). Flight-path: 104.66 m, channel width: 64 ms, scattering angle: 102.4°. Dominant reflexes are indicated for: Q - quartz, B - biotite, O - oligoclase. The unindexed strong peak is Q - (101)+(011) and B (600).

THE DYNAMICS OF WATER ABSORBED IN SILICA

A.A.Tumanov, Institute of Physics and Power Engineering,
Obninsk, USSR

On the time-of-flight spectrometer DIN-2PI we have investigated spectra of neutrons scattered from highly dispersed pyrogenic aerosil As (mean particle diameter ~100 Å, specific areas ~300 m^2/g) and from porous silica Sp (mean pore size ~90 Å and specific areas ~450 m^2/g). The results were obtained for hydrated and dehydrated samples of silica.

Experimental conditions: incident neutron energy E_0 = 4.2 meV; scattering angles from 11 to 134°; temperature 290 K.

The spectrum of the absorbed water shell was determined as the difference of hydrated and dehydrated silica spectra.

The results of quasielastic neutron scattering:

1. The quasielastic neutron scattering spectrum of hydrated silica consists of the elastic scattering peak from the silica matrix and the diffusion broadening peak from the absorbed water shell. The shape and dispersion (or width ΔE) of the neutron scattering distribution for the SO_2-matrix are equivalent to the resolution function width ΔE = 150 μeV.

2. The differential scattering law corresponds to convolution of the experimental resolution function (determined by scattering from vanadium) with the Lorentzian function (Fig.1). Analysis of scattering dispersion calculated within the limits of the energy interval $\pm\varepsilon_0$ with $Q \leq 1$ $Å^{-1}$ make it possible to determine the water self-diffusion coefficient, D. Its value decreases with decreasing water concentration and $D = 1.2\times10^{-5} cm^2/s$ at the humidity of 0.15 $gH_2O/gSiO_2$; $D = 6\times10^{-6}$ cm^2/s at 0.06 $gH_2O/gSiO_2$.

3. The angular dependence of quasielastic neutron scattering intensity, J_{qe}, for silica witnesses in favour of the small angle scattering and coherent scattering in the region around $Q \simeq 1.5$ $Å^{-1}$ due to the first maximum of the radial distribution function SO_2 (Fig.2). The slope of the function $\ln J_{qe}(Q^2)$ for water absorbed in As and Sp points to a considerably smaller value of the proton mean square displacement in comparison with bulk water. The quasielastic scattering intensity $J_{qe}(Q)$ behavior does not obey the simple Debye-Waller scattering law.

The inelastic neutron scattering from silica and absorbed water was investigated earlier in [1].

1 E.F.Sheka et al. Journal. of Electron Spectroscopy and Related Phenomena, 54/55 (1990), 855-876.

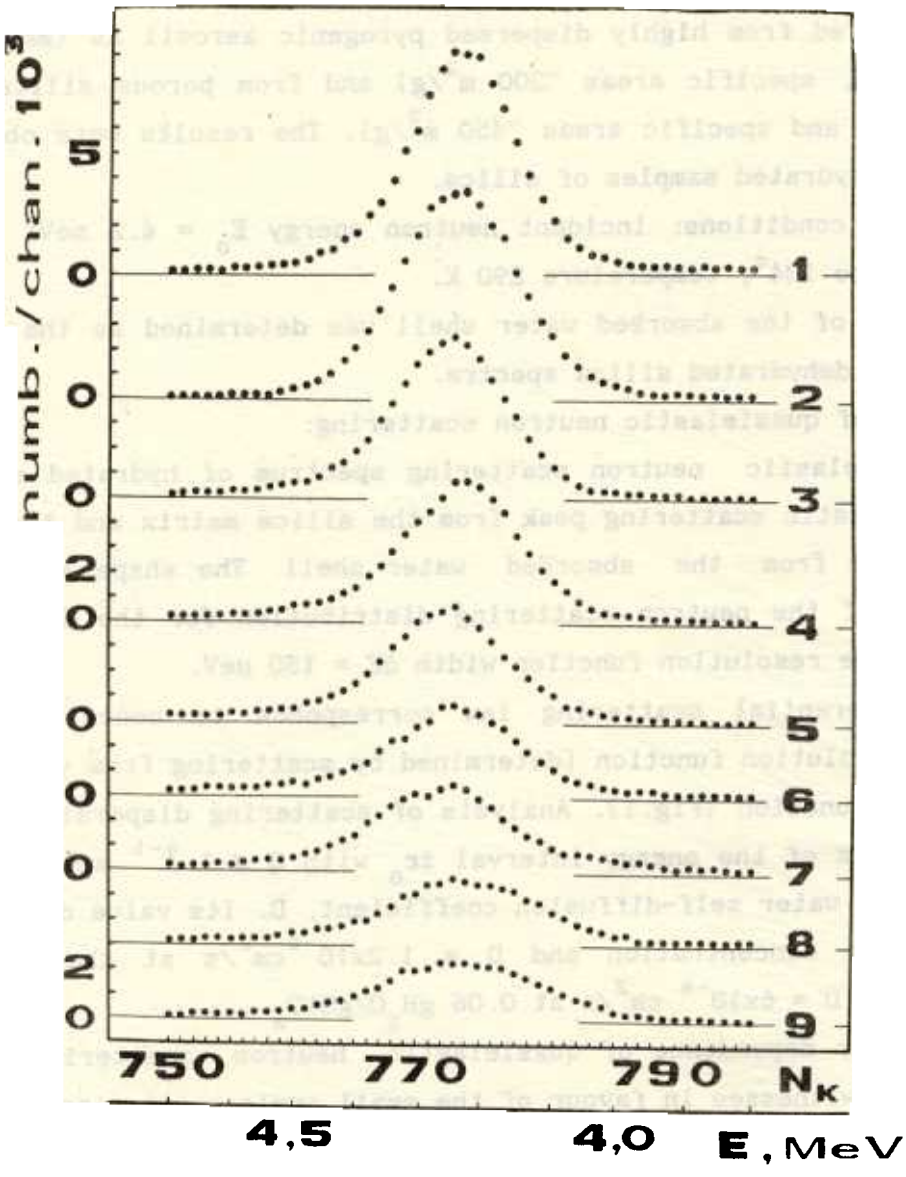

Fig.1. Spectra of quasielastic neutron scattering from water absorbed in silica (aerosil). The scattering angles: 1-11°, 2-21°, 3-28°, 4-43°, 5-47°, 6-71°, 7-86°, 8-114° and 9-134°. The amount of absorbed water constitutes 4.9 mass %.

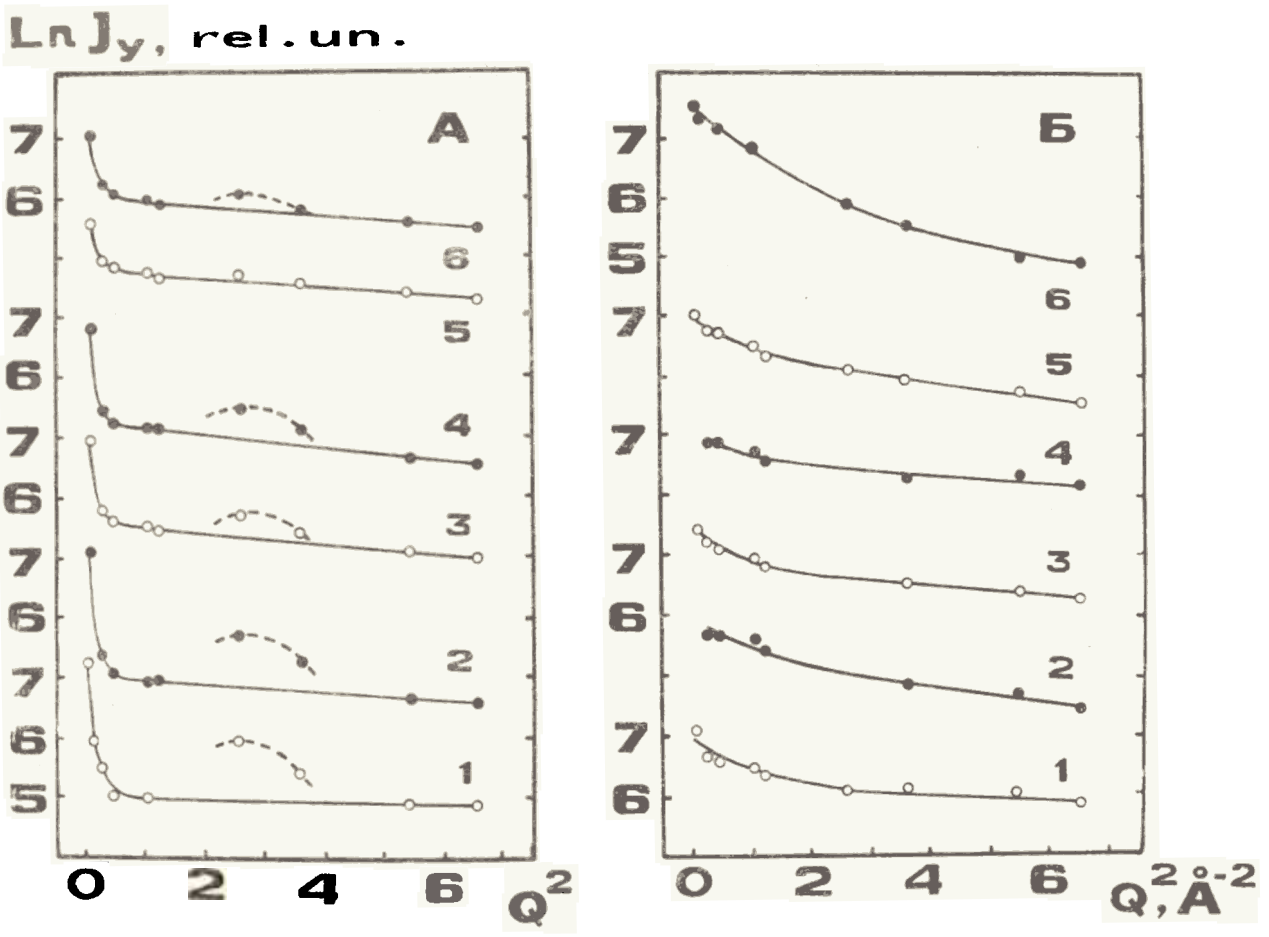

Fig.2. Quasielastic peak intensities for silica (A) and absorbed water (B) at 290 K. A: 1 and 2 - dehydrated aerosil (As) and porous silica; 3 and 5 - hydrated Sp at the humidity of 0.149 and 0.082 g H_2O/g Sp; 4 and 6 - hydrated As at 0.059 and 0.037 g H_2O/g As. B: 1 and 4 - water absorbed in Sp at the humidity of 0.082 and 0.149 g H_2O/g Sp; 2 and 3 - at 0.037 and 0.059 g H_2O/g As; 5- at the humidity of about 0.2 g H_2O/g As; 6 - hydro-jelly aerosil. The amount of silica is about 10 mass %.

THE DYNAMICS OF LIQUID METALS WITH IMPURITIES

M.V.Zaezhev, M.N.Ivanovski, V.A.Morozov, A.G.Novikov,
V.V.Savostin, N.K.Fomichev, A.L.Shimkevich
Institute of Physics and Power Engineering, Obninsk, USSR

Preliminary results of the study of a liquid K-O system include those of inelastic neutron scattering measurements on a potassium - oxygen melt at T = 550 K for three oxygen concentrations: C_1 = 1.8; C_2 = 5.1; C_3 = 8.5% at, and on a pure potassium sample at three temperatures: 340 K, 440 K, 550 K.

The experiments were carried out on the DIN-2PI double time-of-flight neutron spectrometer on neutron beam No.2 of the IBR-2 pulsed reactor[2]. Incident neutron energies were E_0= 7.5 meV and 4 meV at elastic peak resolutions of E_0= 0.35 meV and 0.16 meV, respectively. Nine detectors of scattered neutrons were scanning the angle range from 7^o to 134^o. The sample was a loop with liquid metal curculating in it (Fig.1). A thin wall (0.2 mm), stainless steel cylinder measuring D = 100 mm by H = 160 mm was installed into the neutron beam. The metal circulation was maintained by the DC pump. In order to have a desirable oxygen concentration in liquid potassium a diffusion-type cold trap filled with K_2O was used. The oxygen concentration in liquid potassium was determined by measuring the metal temperature on the K - K_2O interface in accordance with the equation:

$$\lg C_0 = 2.37 - 799/T, \text{ at.\%}.$$

Figure 2 shows experimental double-differential scattering cross-sections for pure liquid potassium at 550 K and the corresponding values calculated in the incoherent approximation[2]. The frequency distribution spectrum of liquid potassium atoms extracted from the experimental cross-sections data in the frame of this approximation is presented in Fig.3. The analysis of the experimental results obtained at lower temperatures requires coherent effects to be taken into account.

The double-differential scattering cross-sections data on the K - O melt are illustrated in Fig.4. One can see that the effect of oxygen scattering reveals itself both in the inelastic and quasielastic part of the cross-section curve and increases with growing oxygen concentration. Qualitative information about the impurities behavior can be obtained by subtraction of experimental curves corresponding to different oxygen concentrations. The resolution corrected half-width of the quesielastic scattering peak observed for these dif-

ferential curves versus squared momentum transfer, k^2, is presented in Fig.5. The oxygen diffusion coefficient, determined from the slope of $\Delta E(k^2)$ at smallest k^2, is $D=(10-15).10^{-5}$ cm^2/s and approximately equals the self-diffusion coefficient of potassium at this temperature. The reduction of the $\Delta E(k^2)$ slope with growing k^2 can be qualitatively interpreted either as the evidence for the "solid state" nature of oxygen diffusion or as the growth of the effective mass of diffusing oxygen caused by chemical binding. A more detailed analysis is under way now.

1. A.V.Abramov et al. Atomnaya Energiya v.66, No.5. (1989) p.316-321 (in Russian).
2. Yu.V.Lisichkin et al. Jadernye Konstanty, No.33 (1979) p.12-24 (in Russian).
3. R.Cowley, A.Woods, G.Dolling. Phys.Rev., v.150 (1966) No.2, p.487.
4. J.Miranda. J. of Phys. v.16F, No.1 (1986) p.1.

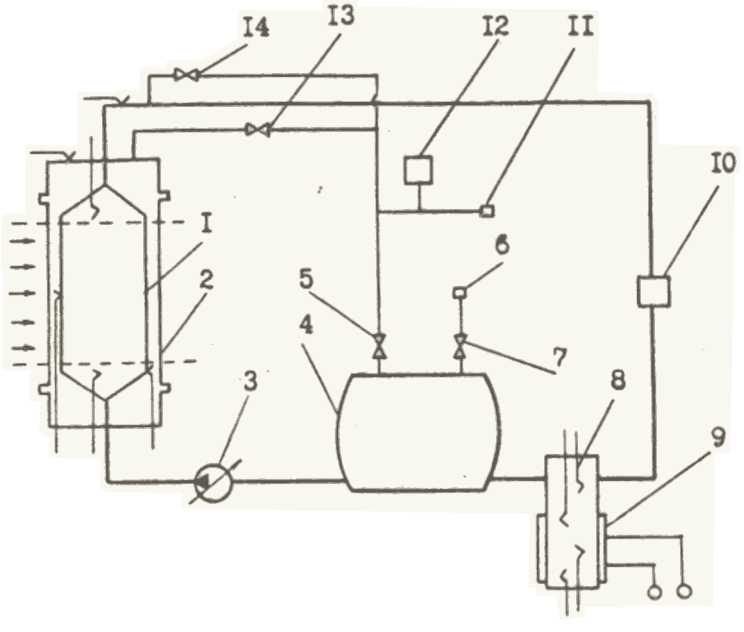

Fig.1. Technological scheme of sample: 1 - container; 2 - aluminium shell; 3 - DC pump; 4 - expansion tank; 5,7,13,14 - valves; 6,11 - vacuum seals; 8 - diffusion-type cold trap; 9 - water refrigerator; 10 - flow meter; 12 - manometer.

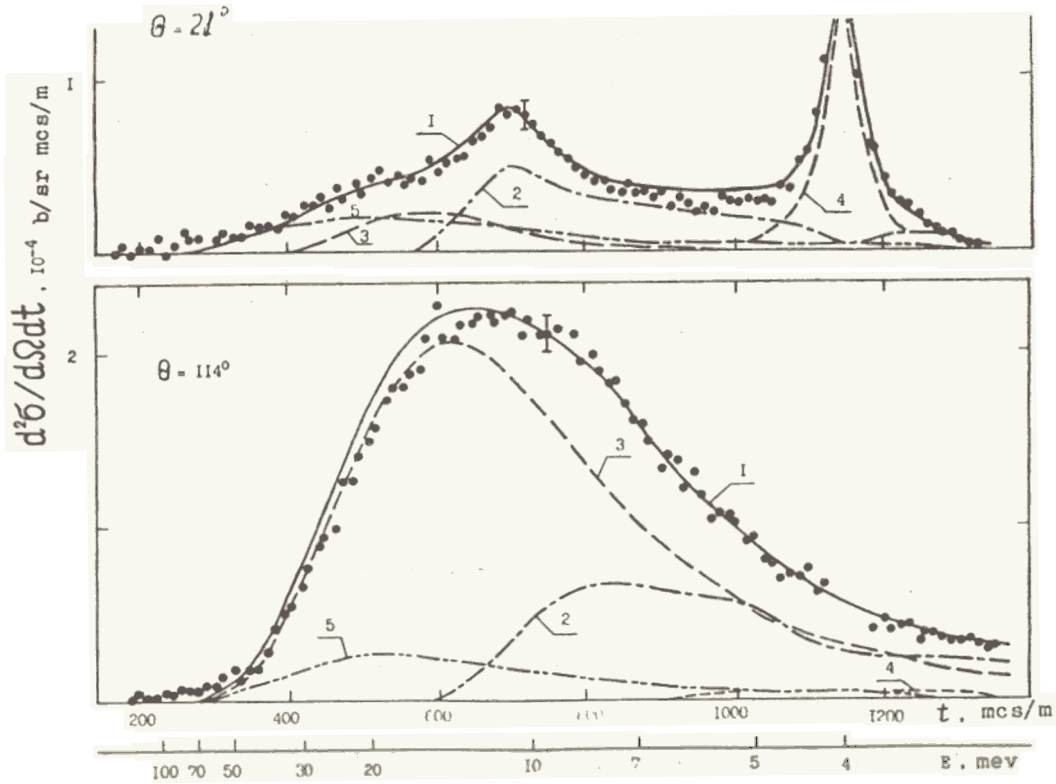

Fig. 2. Double-differential scattering cross-sections for pure potassium, E_0 = 4 meV, T = 550 K. o - experiment; 1 - model calculation; 2 - single-phonon scattering; 3 - multiphonon scattering; 4 - quasielastic scattering; 5 - multiple scattering.

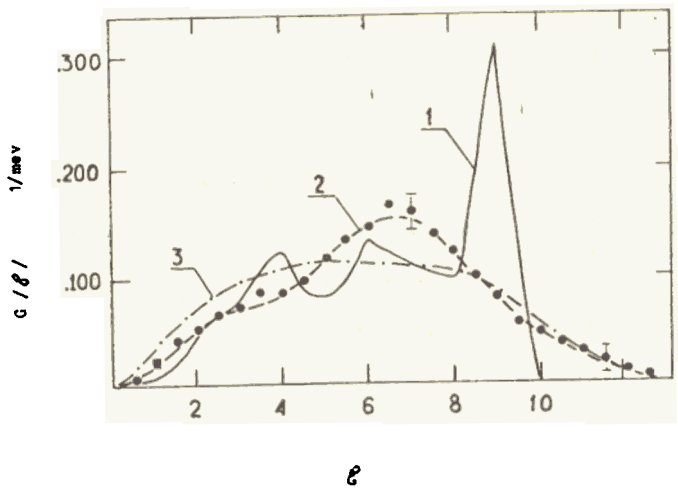

Fig. 3. The frequency distribution spectrum of liquid potassium, T = 550 K. o - experiment; 1 - initial model (solid potassium, T = 9 K, calculation[3]); 2 - superposition of two Lorentzians; 3 - molecular dynamical calculation, T = 340K[4].

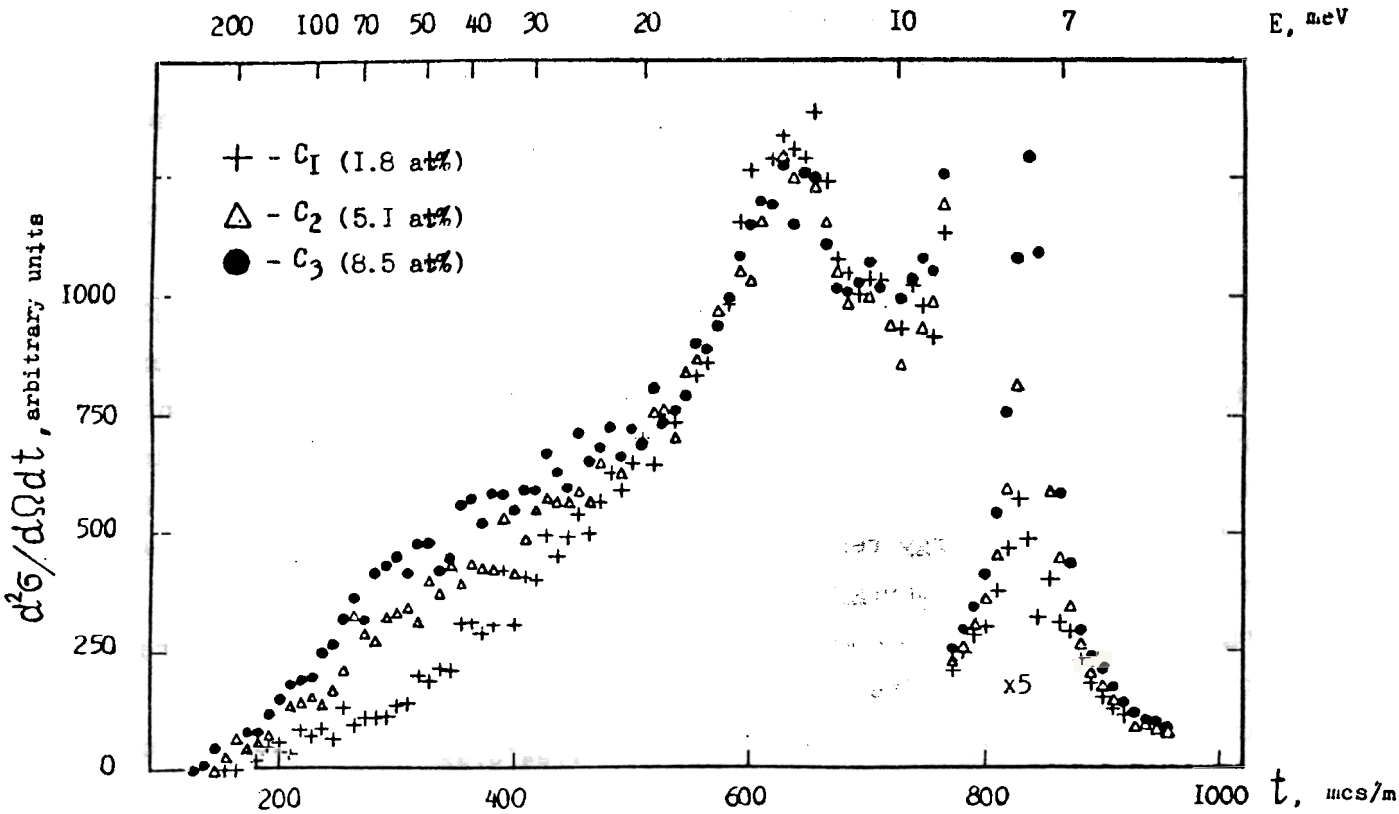

Fig. 4. Slow neutron scattering double-differential cross-sections of K-O system for 3 oxygen concentrations and the scattering angle $\theta = 28^{\circ}$.

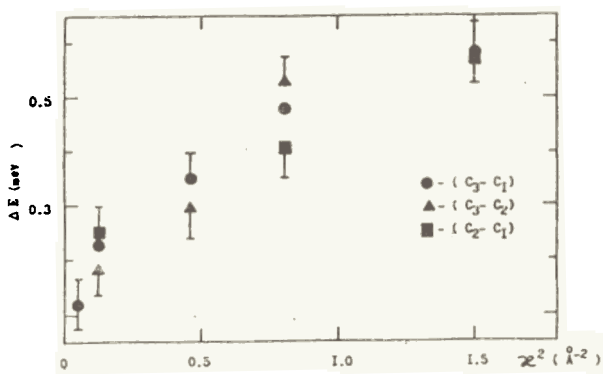

Fig. 5. The width at half maximum of quasi-elastic spectrum of scattering neutrons for differential curves.

INELASTIC SCATTERING STUDY OF ThO_2, UO_2 AND $ZrH_xU_{0.32}$ COMPOUNDS

Zh.A.Kozlov, Laboratory of Neutron Physics, JINR, Dubna

I.Padureanu, S.N.Rapeanu, Gh.Rotarescu, Central Institute of Physics, Bucharest, Romania

V.A.Semenov, Institute of Physics and Power Engineering, Obninsk, USSR

Inelastic neutron scattering spectra of polycrystalline samples of ThO_2, UO_2 and $ZrH_xU_{0.32}$ (x = 1.6 and 1.84) have been measured at different temperatures on the TOF-spectrometer DIN-2PI at the IBR-2 reactor. The measurements were carried out in the region of scattering angles of 4^o to 134^o at the incident neutron energy E_0 = 7.4 meV and 10.34 meV for ThO_2 and E_0 = 10.34 meV for UO_2 and $ZrH_xU_{0.32}$. The energy resolution of the spectrometer $\Delta E/E$ was less than 4% in the whole region of energy transfers.

Using the Breadow-Oskotsky method and the one-photon approximation frequency spectra $g(\omega)$ were determined (Figs.1,2).

Figure 1 shows the frequency spectrum of $ZrH_{1.84}U_{0.32}$ at room temperature. It is like that for zirconium hydride. Acoustic modes and optic modes are well separated. The acoustic modes (ω < 40 meV) are connected mainly with the oscillations of zirconium and uranium atoms, while the optic modes with hydrogen oscillations. The addition of uranium leads to some transformation of the acoustic spectrum and to the increase of the optic spectrum width.

Figure 2 shows frequency spectra of ThO_2 at room temperature and at 1278 K. The spectrum structure at room temperature consists of maxima located at the energy transfer of 12, 20, 34, 53 and 72 meV. The maxima at 12, 20 and 34 meV are attributed to thorium oscillations and the maxima at 53 and 72 meV to oxygen oscillations. Experimental spectra of ThO_2 and UO_2 (not shown) are compared with the frequency distribution for UO_2 calculated by J.A.Young to show good coincidence in the positions of maxima.

At 1278 K (Fig.2) the function $g(\omega)$ ThO_2 changes seriously both the acoustic and optic spectrum. An increasing number of oxygen oscillators should be mentioned as well as some modification of the vibrational spectrum of thorium atoms at small energies.

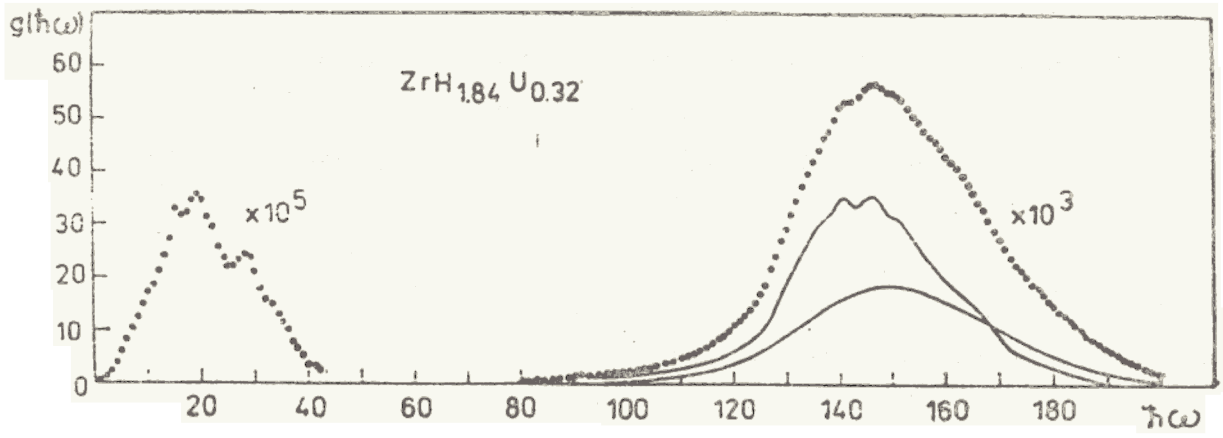

Fig. 1. The frequency spectrum of $g(\omega)$ of $ZrU_{0.32}H_{1.84}$. First and second order phonon contributions are shown by a solid line.

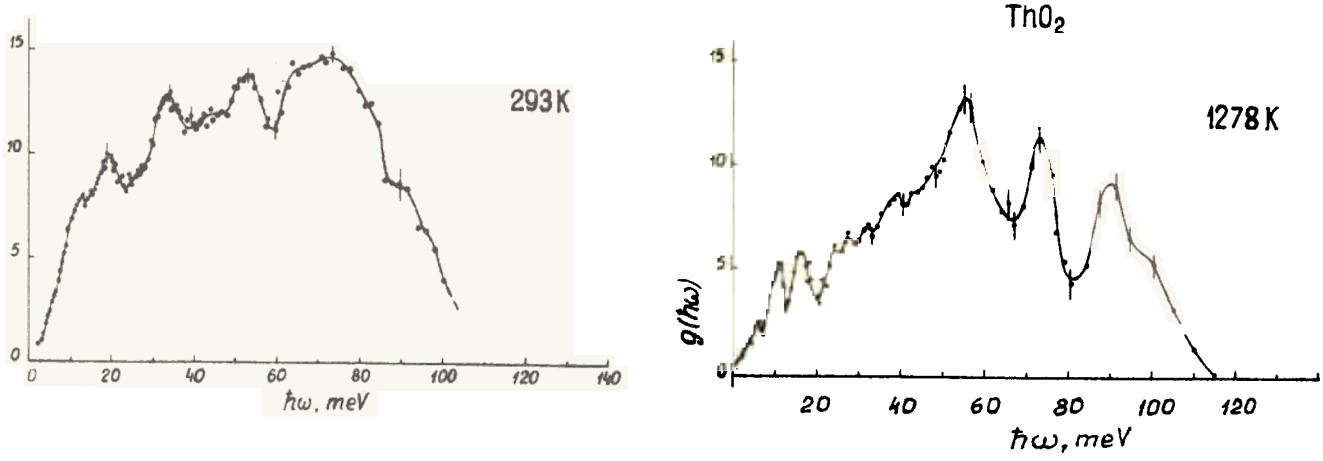

Fig. 2. The spectral function $g(\omega)$ for ThO_2 at 293 and 1278 K.

INTERSTITIAL ALLOYS

S.A.Danilkin, V.P.Minaev, Institute of Physics and Power Engineering, Obninsk, USSR

V.V.Sumin, Institute of Physical Chemistry, Moscow, USSR

INS study of the lattice dynamics of interstitial alloys provides information on frequency distributions of metal atoms and local vibrations of interstitials. Metal-metal and metal-interstitial interaction parameters (or potentials) can be derived from these data.

During the last years under investigation were the binary solid solutions V-O, V-N, a ternary system TaV_xN_y and carbon and nitrogen austenitic steels[1-3].

The experiments have shown that with increasing interstitial atom content phonon spectra of metal atoms became harder in VO_x, VN_x, NbO_x, TaN_x solid solutions as illustrated in Fig.1 on the example of VO_x alloys. In nitrogen Fe-Mn austenitic steels the concentration dependence of the second moment of the frequency distribution $\langle\varepsilon^2\rangle$ has maximum at ~1.2% at N. (This part of work was made in collaboration with V.G.Gavriluk, S.P.Efimenko, Yu.N.Yagodzinski, Institute of Metal Physics, Kiev). These results show that the effect of interstitials on the host lattice consists of two components with opposite signs, one results in the hardening and the second in the dilatation and softening of the metal-metal interaction. Lattice dilatation caused by an interstitial is completely compensated in V, Nb and Ta solid solutions by oxygen and nitrogen. Partial compensation (at lowest concentrations) was observed in nitrogen austenitic steels. Probably, the hardening of the spectrum is connected with variation of electron properties of metals caused by interstitials[2,3].

Local vibrations of oxygen and nitrogen interstitials in BCC transition metals and of nitrogen and carbon in austenitic steels have frequencies above the boundary of the metal spectrum[1-3]. As the example, the frequency spectrum of oxygen atoms in $VO_{0.06}$ is shown in Fig.2[1]. The spectrum contains two peaks corresponding to interstitial atoms vibrations (ε = 57 and 86 meV).

Computer simulation of the V-N solid solution lattice dynamics was performed. It was found that after some modification the V-N interatomic potential of Johnson et al.[4] gives good description of nitrogen atoms frequencies. Calculations of the V-O solid solution frequency spectrum show that a weak peak at 45 meV (Fig.2) corresponds to the vibrations of vanadium

atoms that are neighbours to interstitial atoms. With this potential lattice distortions around the interstitial atom and the energy of stress-induced interaction of pairs of interstitials were calculated.

1. Danilkin S.A., Minaev V.P., Sumin V.V. Proc. of the Int.Conf. on Neutron Scattering, 21-25 January, 1991, Bombay; Physica B, 1991, to be published.
2. Danilkin S.A. et al. Fiz.Tverd.Tela, 31 (1989) 8.
3. Sumin V.V. et al. Metallophysica, 12 (1990) 100.
4. Johnson R.A. et al. Acta Metall., 12 (1964) 1215.

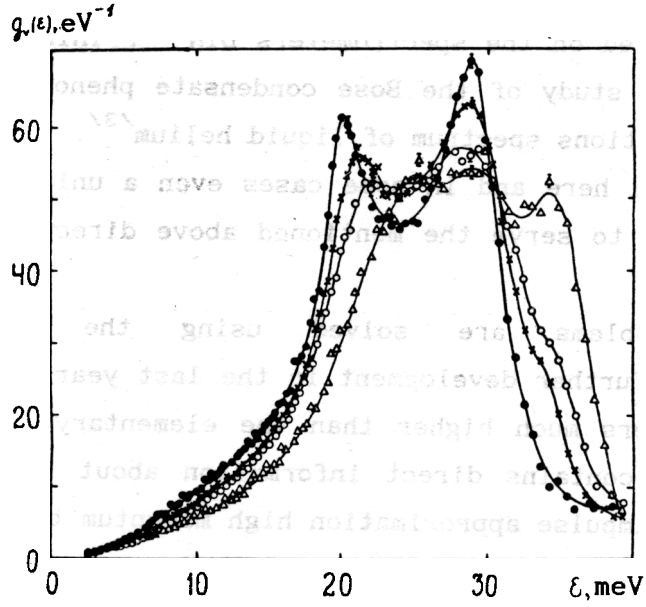

Fig.1. Vanadium atom frequency spectra in VO_x solid solutions: · - vanadium; x - $VO_{0.03}$; o - $VO_{0.06}$; Δ - $VO_{0.11}$

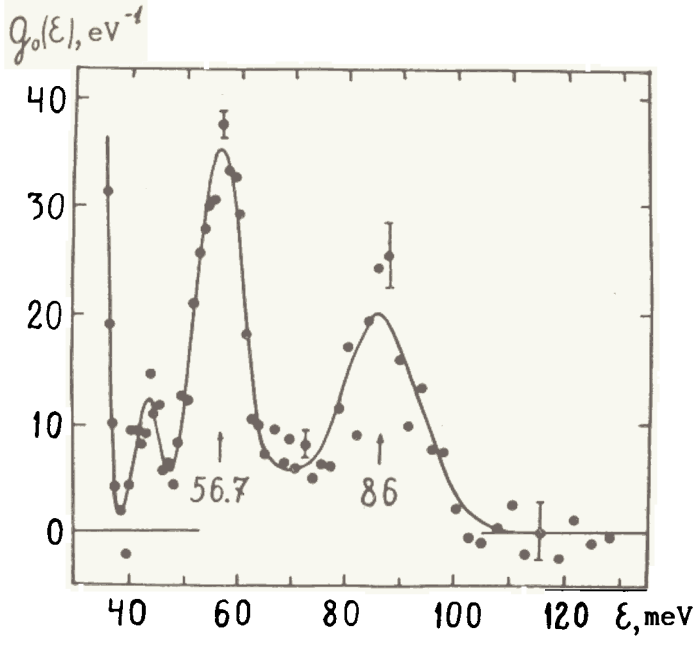

Fig.2. Frequency spectrum of oxygen atoms in $VO_{0.06}$.

INVESTIGATION OF QUANTUM PROPERTIES OF LIQUID HELIUM

N.M.Blagoveschenskii, A.V.Puchkov
Institute of Physics and Power Engineering, Obninsk, USSR
I.V.Bogoyavlenskii, L.V.Karnatsevich, V.G.Kolobrodov
Institute of Physics and Technology, Kharkov, Ukraine
J.A.Kozlov
Laboratory of Neutron Physics, JINR, Dubna

It is for 20 years already that microscopic properties of superfluid and normal helium are being investigated on the spectrometers DIN[1]. This investigation goes in two directions - study of the Bose condensate phenomenon[2] and study of the elementary excitations spectrum of liquid helium[3]. The neutron scattering is a powerful tool here and in some cases even a unique one. The neutron experiment parameters to serve the mentioned above directions of research are of rich variety.

The first direction problems are solved using the impulse approximation[4], which received further development in the last years. It is believed that at momentum transfers much higher than the elementary excitations energy the scattering law contains direct information about the Bose condensate density. To apply the impulse approximation high momentum transfers and high resolution are required. We have attempted to have them on the DIN-2PR-spectrometer. The main challenge of the experiment is to measure the liquid helium dynamic structure factor at temperatures below the λ-point in the condition when the momentum transfer, the instrument resolution, and the "helium peak" width are optimized. We choose the incident energy E_0 = 200 meV, when the resolution broadening is one forth of the "helium peak" width and it is smaller than the broadening due to final state interaction effects (according to modern theory estimates).

The measurements were performed in the range of scattering angles 90-160° (detector's area is 400x465mm^2, the sample - detector distance is 10 m). The sample temperature was 4.2 K and 1.4 K and the resolution at "helium peak" maximum 6-9 meV for the 160-90° angles, respectively.

72 hours of sample exposition time at each temperature were required to obtain adequate statistics and 42 hours with an empty cryostat. Typical spec-

tra at two scattering angles are shown in Fig.1. The total count at "helium peak" is approximately 350000.

On the DIN-2PR there is the possibility to measure neutron spectra at several incident energies simultaneously. Then the "second" incident energy is 53 meV. An example of the neutron scattering spectrum of the same sample is shown in Fig.2.

It is planned to analyze neutron scattering spectra by means of fitting models, as usual (the special program COMPIL) and by means of the treatment proposed in /5/.

In the second direction of helium investigations a preliminary experiment on the spectrometer DIN-2PI at an incident neutron energy of 2 meV was performed. A typical neutron spectrum is shown in Fig.3. The sample is powderlike $ZrH_{1.8}$ (3% scatterer). The background-chopper rotates at 300 rpm, the DIN-2PI-chopper (velocity selector) at 1500 rpm (the radius of curvature is 2.5 m, the slit-width 4 mm). The elastic peak FWHM (210 channel) - 250 μsec. It is remarkable that there is a very low background in the range of energy transfers 0-1.9 meV. It is very important for the elementary excitations investigations. Weak peaks in channels 200 and 800 arise due to fast neutrons of the first and second IBR-satellites. The smooth rise of background in the spectrum tail is caused by the background-chopper.

1. A.V.Abramov et al. Atomnaya Energiya, 66 (1989) 1316 (in Russian).
2. I.V.Bogoyavlenskii et al. Sov.J.Low Temp.Phys., 16 (1990) 137.
3. N.M.Blagoveshchenskii et al. Sov.Phys.JETP Lett., 31 (1980) 14.
4. P.C.Hohenberg, P.M.Platzman. Phys.Rev., 152 (1966) 198.
5. T.R.Sosnick et al. Europhys.Lett., 99 (1989) 1707.

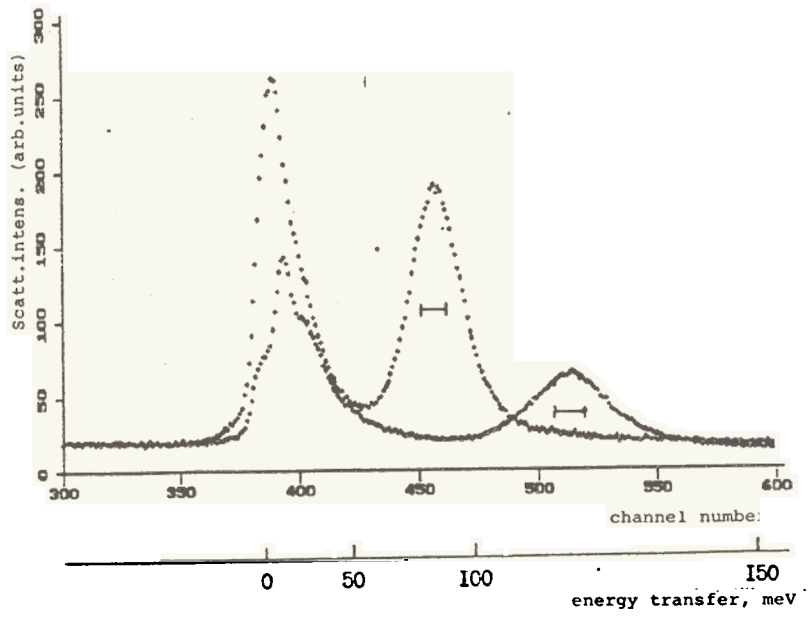

Fig.1. Typical neutron spectra of liquid helium at T = 1.4 K. The scattering angles are 100° and 160°, the incident neutron energy E_0 = 200 meV. The interval from 380 to 410 channel shows the elastic and inelastic scattering on the cryostat material (Al), 425-600 channel - the scattering on liquid helium ("helium peak"). Instrumental resolution in the range of the "helium peak" is 6-9 meV. The sample exposition time is 72 hours. The time-analyzer channel is 8 μsec wide.

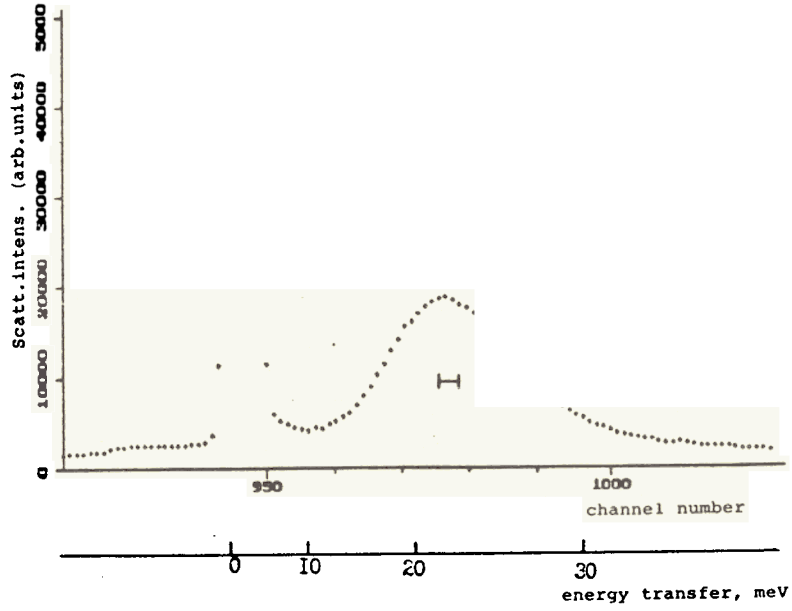

Fig.2. An example of the neutron spectrum of liquid helium at 1.4 K. The scattering angle is 100°. The incident energy is E_0= 53 meV. The spectrum is measured simultaneously with the E_0 = 200 meV measurements (Fig.1). The instrumental resolution in the range of the "helium peak" is 1.5 meV. The time-analyzer channel is 32 μsec wide.

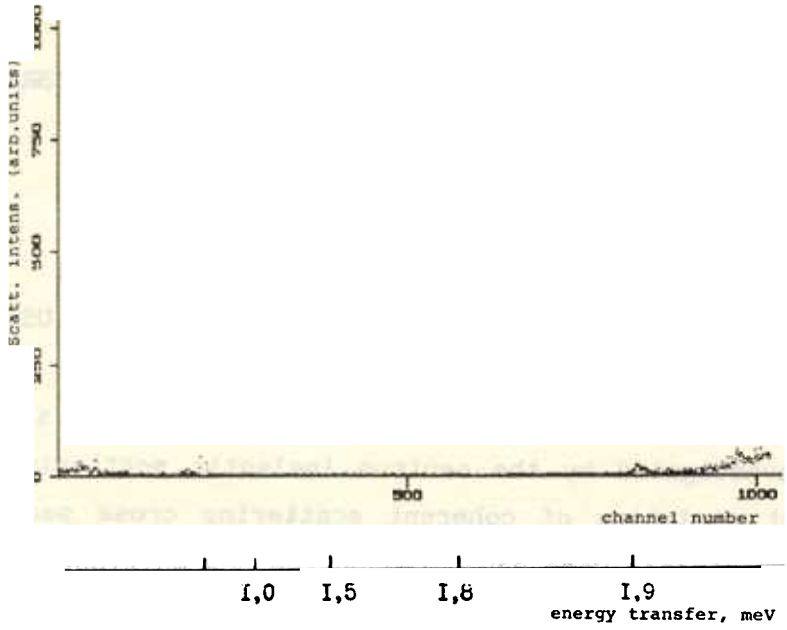

Fig. 3. Neutron elastic scattering at E_0 = 2 meV on the 3% scatterer ($ZrH_{1.8}$). It shows the possibilities of the spectrometer DIN-2PI to serve the neutron scattering study at small negative energy transfers down to 1.9 meV. The instrumental resolution is much dependent on the sample geometry and may be estimated as 30-40 μeV in the energy transfer region 1-1.5 meV. The measuring time is 1.5 hour, the time-analyzer channel is 64 μsec wide.

NERA

NEUTRON SCATTERING STUDY OF COPPER AND OXYGEN ATOM VIBRATIONS IN YTTRIUM HTSC CERAMICS

I.Natkaniec, J.Mayer, J.Krawczyk
Laboratory of Neutron Physics, JINR, Dubna
V.K.Fedotov, A.I.Kolesnikov, E.G.Ponyatovskii
Institute of Solid State Physics, Chernogolovka, USSR

Some peculiarities of the dynamics of copper and oxygen atoms in "1-2-3" ceramics were investigated by the neutron inelastic scattering method using isotopic contrast variation of coherent scattering cross sections (3:1) of ^{65}Cu and ^{63}Cu. Experiments were conducted on the new multipurpose neutron spectrometer NERA at the IBR-2 pulsed reactor. Time-of-flight INS spectra (Fig.1) from two isotopic samples of $YBa_2^{65}O_{6.95}$ and $YBa_2Cu_3^{63}O_{6.95}$ were measured at temperatures T = 80, 290 K on a 109 m incident neutron flight path with the Be-filter for energy analysis of scattered neutrons. The differential spectrum represents the vibrational spectrum of copper atoms in the superconducting ceramics. The generalized phonon density of states function, $G(\omega)$, for the 1-2-3 superconducting ceramics (Fig.2a) and partial contributions from oxygen (Fig.2b) and copper atoms (Fig.2c) show a weak dependence on temperature that can be explained by the difference in Debye-Waller factors at T = 80 K and 390 K. The phonon density of states of Cu atoms occupies mainly the energy interval from 0 to 40 meV in agreement with ref.[1]. The excess spectral density at 40 to 75 meV can be attributed to the multiphonon scattering of neutrons. However, the preliminarily calculated multiphonon contribution (the dashed line in Fig.3) does not describe completely the behaviour of the spectrum in this region. There is observed an analogous situation in phonon spectra of "1-2-3" oxygen deficient copper (Fig.4). A decrease in oxygen content leads to the softening of the copper spectrum in the acoustic region, to splitting of the peculiarity at ω = 19 meV (Fig.3) and little enhancement in a harder spectral region.

P.P.Parshin et al JETP Lett., 51 1990) p.380

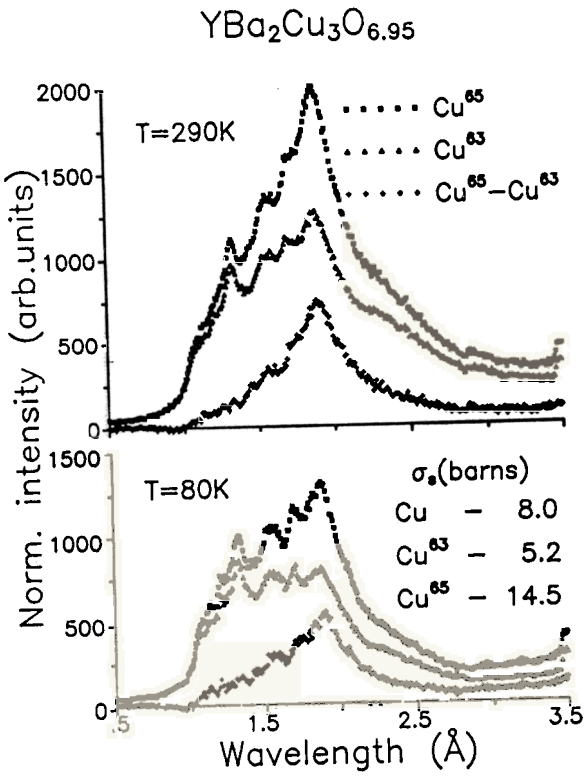

Fig. 1. TOF INS spectra for two copper isotopic compositions (^{65}Cu and ^{63}Cu) of the ceramics $YBa_2Cu_3O_{6.95}$.

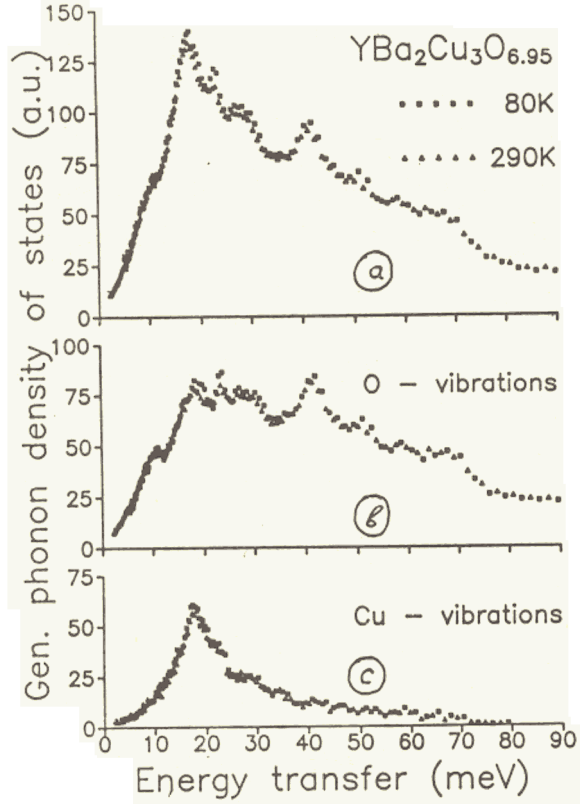

Fig. 2. Generalized phonon density of states functions, $Ge(\omega)$: a - the spectrum of the $YBa_2Cu_3O_{6.95}$ ceramics; b, c - partial contributions from copper and oxygen atoms.

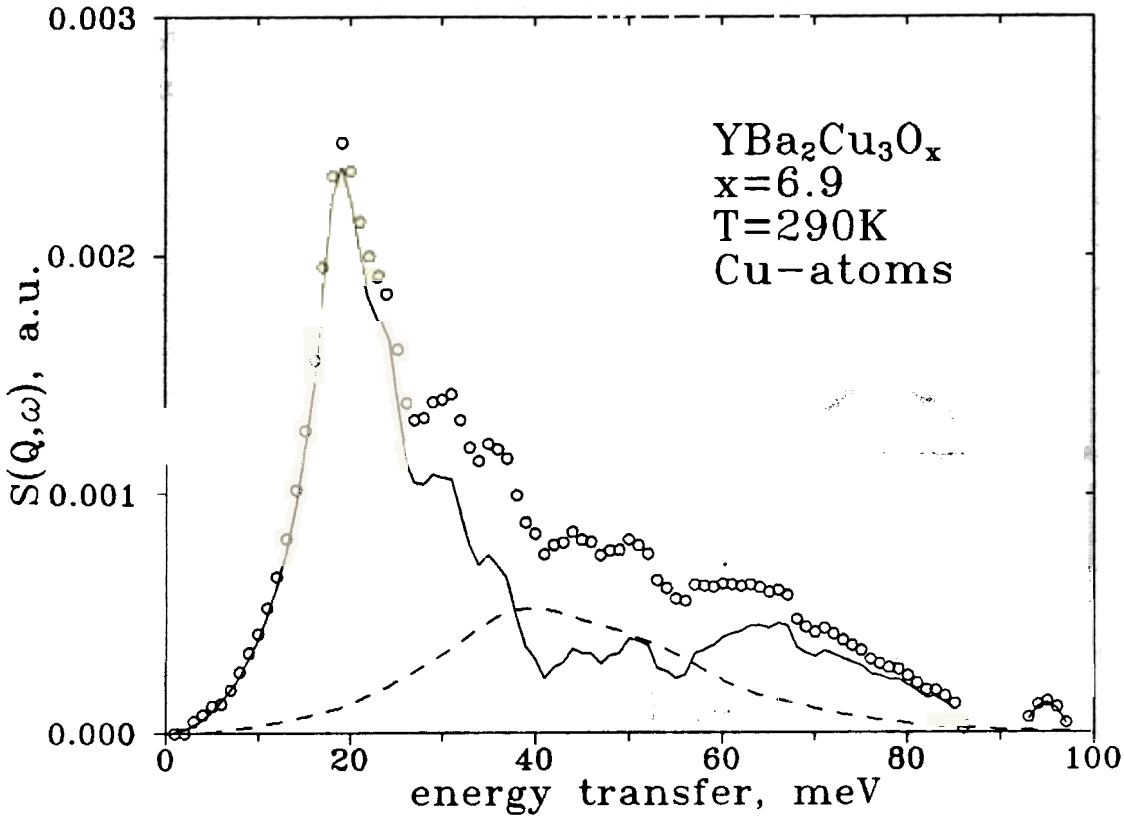

Fig.3. The generalized phonon density of states function of copper atoms in the $YBa_2Cu_3O_{6.95}$-ceramics: points - experiment; dashed line - multiphonon neutron scattering contribution; solid line - their difference.

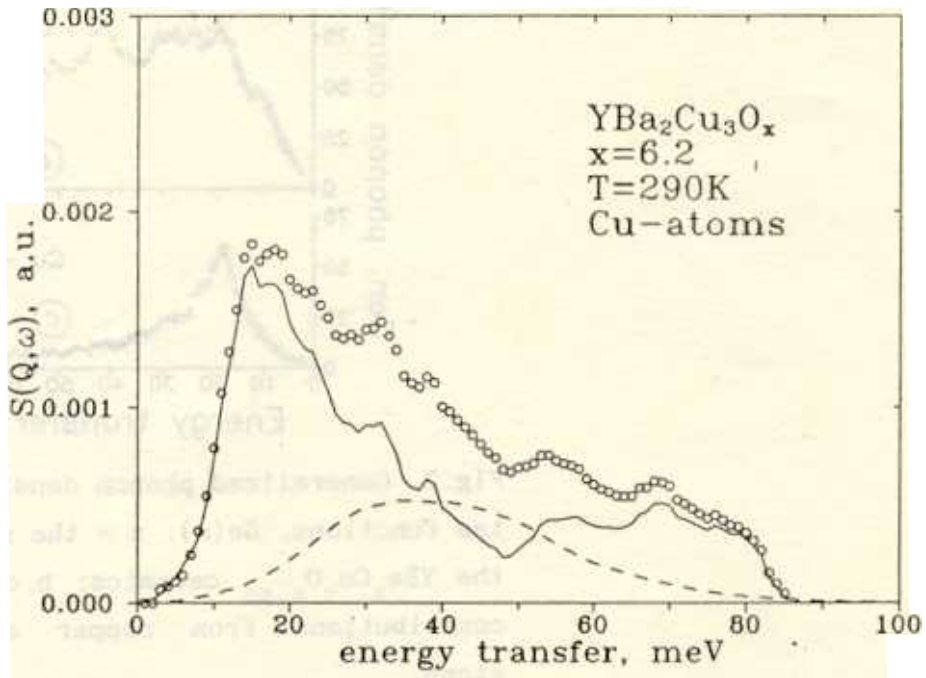

Fig.4. The same as in Fig.3 for the case of $YBa_2Cu_3O_{6.2}$

INVESTIGATION OF THE REORIENTATION OF 4-N-PENTHYLPHENYL-4'-N-HEPTYLOXYTHIOBENZOATE ($\bar{7}$S5) MOLECULES IN THE NEMATIC PHASE

J.Chrusciel, J.Krawczyk, J.Mayer, LNP, JINR, Dubna

The quasielastic neutron scattering (QNS) is a good method of investigation of fast stochastic motions, both translational (diffusion) and rotational, of molecules in condensed phases (liquids, liquid and plastic crystals, superionic conductors). This method was used to investigate the reorientation of $\bar{7}$S5 molecules in the nematic phase. The QNS spectra were measured on the time-of-flight (TOF), inverted geometry spectrometer NERA-PR. The energy of the neutrons scattered from the sample was fixed by the Bragg scattering from the (111) plane of the Cu monocrystals in the almost backward direction. Due to backscattering the resolution (width of elastic peak at half maximum) was reduced to 48 μeV.

Spectra were measured simultaneously at three scattering angles of 30, 50 and 80°, that correspond to the momentum transfers κ = 0.86, 2.01 and 3.06 A^{-1}. TOF spectra obtained at two temperatures of the sample in the nematic phase are shown in the figure. One may see a strong decrease in elastic contribution to the spectra with the increase of κ. On the other hand, the broadening of the quasielastic part almost does not change. It means that the correlation time τ, describing the speed of reorientation, is constant. The estimated value of τ is of the order of 10^{-11}s. Careful model fitting processing of the spectra should give an answer to the question if the QNS spectra result from the reorientation of the whole molecule or of two benzene rings around their para-axes. Additionally, the temperature dependence of τ should make it possible to assess the activation energy of the process.

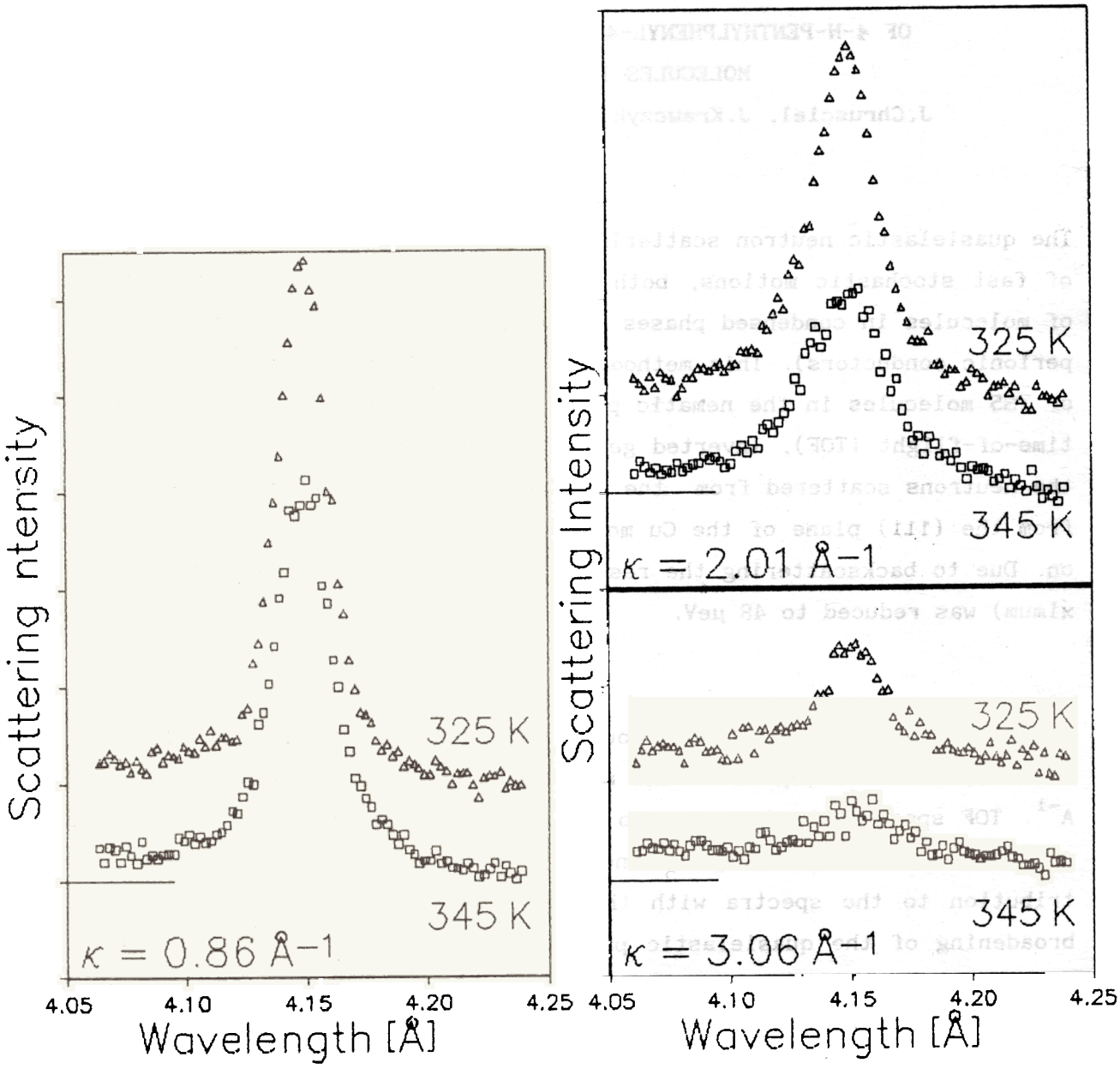

Fig. 1. QNS spectra of nematic 7S5 obtained for two temperatures and three scattering angles.

PRESSURE DEPENDENCE OF VIBRATIONAL SPECTRA OF ICE

O.I.Barkalov, A.I.Kolesnikov, V.V.Sinitsyn, Institute of Solid State Physics, Chernogolovka, USSR

A.N.Ivanov, Institute of High Pressure Physics, Troitsk, USSR

D.F.Litvin, Institute of the Physics of Metals, Moscow, USSR

L.S.Smirnov, Institute of Theoretical and Experimental Physics, Moscow, USSR

I.Natkaniec, Laboratory of Neutron Physics, JINR, Dubna

The P-T phase diagram of ice at temperatures up to 350 K and pressures up to 350 Kbar has 9 phase regions corresponding to different crystal structures (Fig.1). It should be noted that in some phases hydrogen atoms are disordered, while in others they are either partly or fully ordered. The small value of the moment of inertia of a water molecule leads to largely separated in energy translational and librational modes in the vibrational spectrum of ice. The phonon density of states of ice is studied experimentally by incoherent inelastic neutron scattering (IINS)[1,2].

IINS spectra of some ice modifications were investigated at liquid nitrogen temperature in the range of pressures up to 20 Kbar. Ice modifications at the pressure up to 10 Kbar were measured using a fixed high pressure cell[3]. The ice phase at 20 Kbar was obtained by quenching. IINS spectra of ice at the pressure up to 10 Kbar were measured on the NERA-PR spectrometer and of the quenched sample of ice VI on the KDSOG spectrometer at the IBR-2 reactor. Figures 2 and 3 show measured spectra of ice Ih, II and VI.

In the translational part of the spectrum of ice phase Ih four bands at 7, 17.7, 26.6 and 34.7 meV can be identified. The librational mode zone lies far apart from the translational one and its left-hand edge is at the energy of about 65 meV. IINS spectra of ice phase II were measured using a Be-filter on the NERA-PR spectrometer and corresponded to pressures near the left-hand side and right-hand side boundaries of existence of this phase. Pressure affects considerably the vibrational spectra: translational bands shift towards higher energies with increasing pressure and in the librational zone there appears a low energy band (about 60 meV) which energy is below the librational zone of phase Ih. This observation is in agreement with the results of IINS experiments made in RAL to study ice phases[1,2].

It is characteristic of the vibrational spectrum of phase VI that in the translational zone one can see three bands at 10.3, 23.4 and 36.9 meV. The low

energy boundary of the librational subzone is at 53.5 meV. The splitting of the librational zone of ice phase VI increases in comparison with the case of ice phase II. Measurements conducted show that vibrational spectra of ice phases Ih, II and VI are modified as follows: the translational part becomes harder, while the librational one softer (these zones are moving towards each other). Within one ice phase II the whole spectrum, including the vibrational and translational parts, shifts towards higher energies. This result was obtained for the first time.

1. J.C.Li et al. Physica B, 156-157 (1989) p.376.
2. J.C.Li et al., to be published.
3. A.N.Ivanov et al. Report ITEP, No.40-91, Moscow, 1991

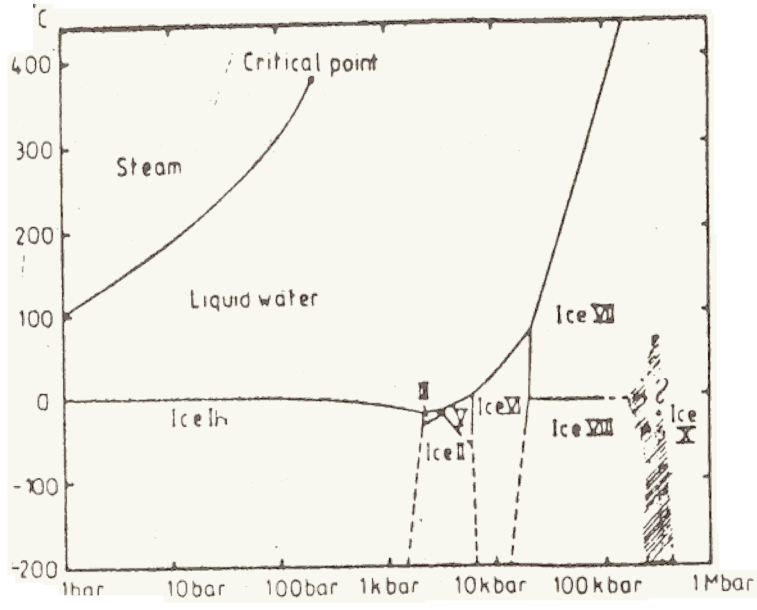

Fig.1. The P-T phase diagram of ice

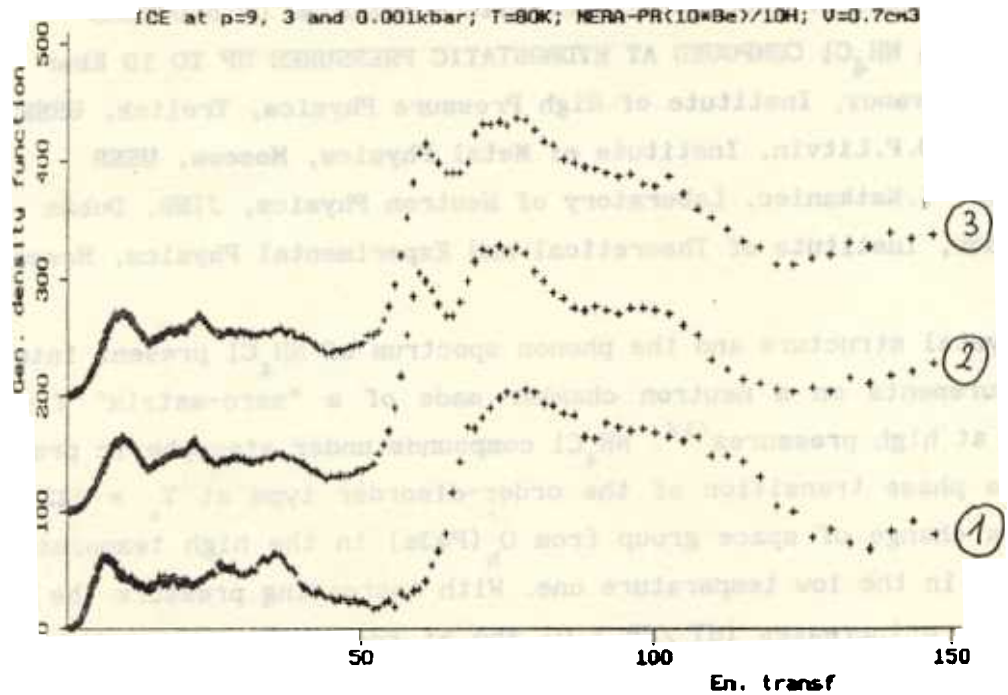

Fig.2. Pressure effect on vibrational spectra of ice: 1 - ice Ih, 2 and 3 ice II, at 3 and 9 Kbar, respectively.

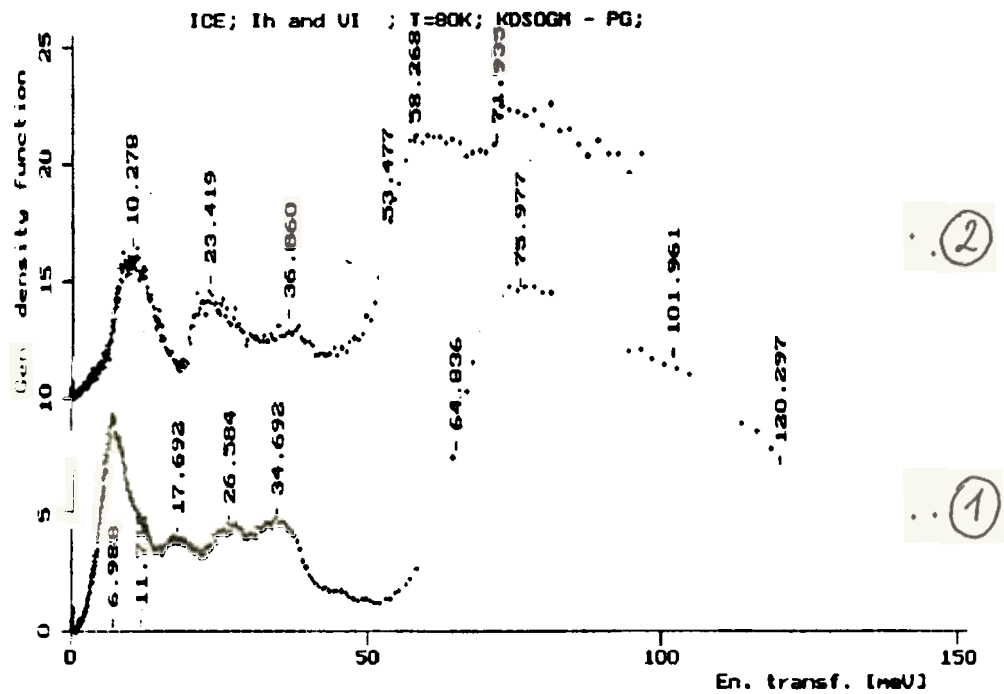

Fig.3. Generalized phonon density of states of ice Ih (1) and ice VI (2)

STUDY OF INCOHERENT INELASTIC SCATTERING OF NEUTRONS ON A NH_4Cl COMPOUND AT HYDROSTATIC PRESSURES UP TO 10 Kbar

A.I.Ivanov, Institute of High Pressure Physics, Troitsk, USSR
D.F.Litvin, Institute of Metal Physics, Moscow, USSR
J.Mayer, I.Natkaniec, Laboratory of Neutron Physics, JINR, Dubna
L.S.Smirnov, Institute of Theoretical and Experimental Physics, Moscow, USSR

The crystal structure and the phonon spectrum of NH_4Cl present interest for test measurements on a neutron chamber made of a "zero-matrix" Ti-Zr alloy operating at high pressures[1]. NH_4Cl compounds under atmospheric pressure experience a phase transition of the order-disorder type at T_c = 242.7 K followed by a change of space group from $O_h'(Pm3m)$ in the high temperature phase to $T_d'(P43m)$ in the low temperature one. With increasing pressure the transition temperature increases ($dT_c/dP > 0$) and at room temperature the transition occurs above 5 Kbar[2,3]. In the NH_4Cl spectrum one distinguishes easily the modes corresponding to librational vibrations of NH_4 groups. Incoherent inelastic neutron scattering (IINS) allows one to follow the effect of high pressures on both librational and translational modes in an ordered and disordered state of NH_4Cl.

IINS spectra were measured on the NERA spectrometer positioned on the 109 m flight path at the IBR-2 reactor. A 1.3 g NH_4Cl sample preliminarily pressed into a 7 mm diameter cylinder 18 mm high was placed into a fixed pressure cell of the cylinder-piston type. The hydrostatic pressure up to 10 Kbar at room temperature was achieved with the help of freon-11 used as the high pressure transmission medium. The HP-cell was connected via a copper heat linepipe to a cryogenic vessel of the cryostat. With the lowering temperature down to 80 K the pressure in the cell decreased down to about 7 Kbar. IINS spectra measured at T = 290 K and 80 K are shown in Fig.1. The IINS spectra characteristic of NH_4Cl can be clearly seen against the background from the freon-filled chamber. This fact allows the conclusion that the tested HP-cell is quite applicable for investigating IINS spectra at high pressures.

It is shown in Fig.2 how temperature and pressure affect the generalized vibrational density of states in NH_4Cl. Table 1 illustrates the influence of these factors on the energy and librational bandwidths of NH_4 groups. Detailed data analysis can be found in ref.[4]. The experiments have demonstrated the possibility to investigate with the NERA-PR the generalized phonon density of

states of hydrogen containing materials in the low temperature range at pressures up to 10 Kbar.

1. A.N. Ivanov et al. ITEP Preprint No.40-91, Moscow, 1991 (in Russian)
2. I.J.Fritz, H.Z.Cummins. Phys.Rev.Lett., v.28 (1972) p.96.
3. Y.Ehisuzaki, M.Niol. Chem.Phys.Lett., v.3, No.7 (1969) p.480.
4. A.N. Ivanov et al. ITEP Preprint No.80-91, Moscow, 1991 (in Russian)

Table 1

Influence of temperature and pressure on the libration mode energy E_R, on the full width at half maximum, FWHM, of the peak in G(E) and the corrected for spectrometer resolution D-value

Phase	T, K	P, Kbar	E_R, meV	FWHM, meV	D, meV
II	290	0	42.3	10.2	9.8
III		10	45.3	8.2	7.8
III	80	0	46.8	5.5	4.8
III		7	47.9	4.9	4.1

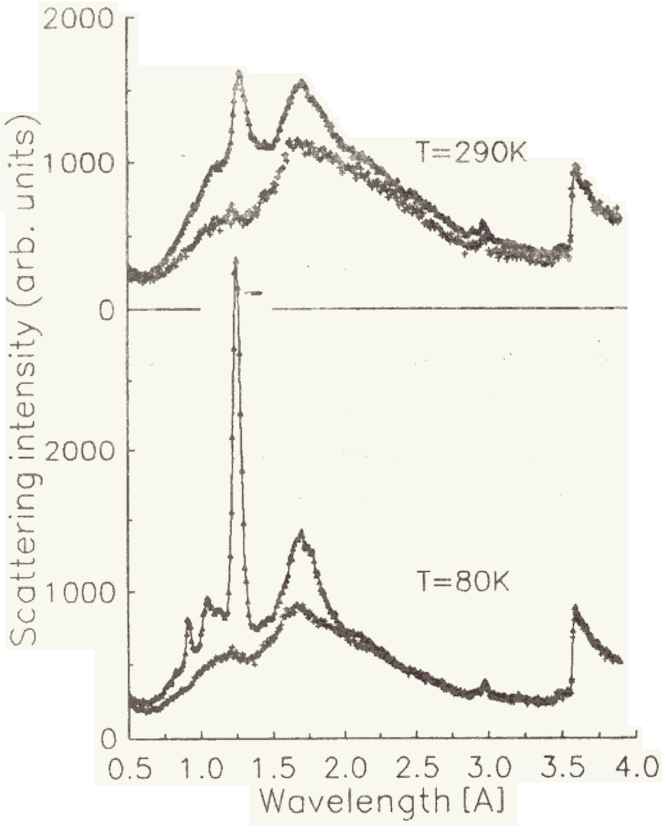

Fig. 1. Time-of-flight IINS spectra of the Ti-Zr high pressure cell filled with freon-11 (crosses) and of NH_4Cl (triangles) at 290 and 80 K.

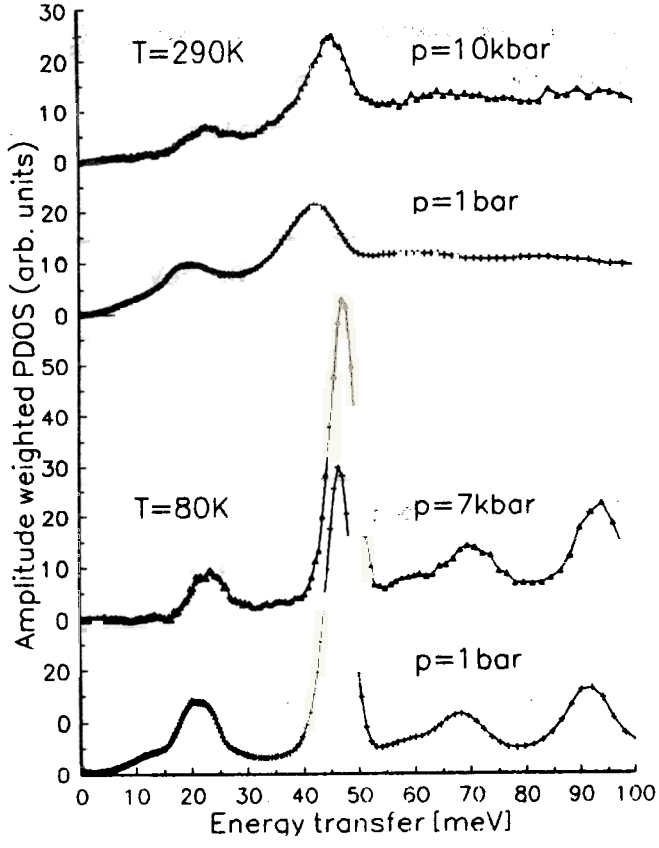

Fig. 2. Generalized phonon density of states G(E) of NH_4Cl obtained from experimental IINS spectra measured at different temperatures and pressures.

STUDY OF $Ba_{1-x}K_xBiO_3$ LATTICE DYNAMICS BY NEUTRON SCATTERING AND COMPUTER SIMULATION

A.V.Belushkin, A.V.Vagov, Laboratory of Neutron Physics, JINR, Dubna
P.P.Parshin, M.G.Zemlyanov, Kurchatov IAE, Moscow, USSR

The discovery of the superconductive state of $Ba_{1-x}K_xBiO_3$ (BKBO) has attracted both the theoretic and experimental physicists' attention to these systems despite their relatively low critical temperature ($T_c \simeq 30K$) in comparison with cuprates. Unlike that of cuprate copper oxides, the superconductive phase of BKBO is a simple cubic perovskite and does not possess metal-oxide planes which play an important role in the formation of the superconductive state in HTc materials. Recent experimental and theoretical investigations point to the significant role of phonons in structural phase transitions and in establishing superconductive properties of BKBO.

The goal of the work undertaken was to investigate the $BaBiO_3$ and $Ba_{0.6}K_{0.4}BiO_3$ lattice dynamics with the aid of computer simulations based on a simple model for interatomic potential and inelastic neutron scattering.

1. On the basis of a simple model for interatomic potential we managed to explain structural instabilities of the simple cubic $BaBiO_3$ phase with respect to phase transitions to lower symmetry phases connected with BiO_6 octahedra rotations.
2. It is predicted that the R3c symmetry phase is likely to exist in $BaBiO_3$.
3. Computer dispersion curves allow us to suppose that the peak at about 40 meV in the optical scattering spectra is due to the density of states peculiarity rather than to oscillations in the center of the Brillouin zone.
4. The results of the neutron scattering experiments confirm the conclusion about strong interaction between oxide octahedra breathing modes and electrons. This interaction must play a very significant role in establishing superconducting properties and in the mechanism of phase transitions via charge density waves.
5. The density of states computed with this model describes well the main singularities of the experimental functions of the generalized density of states and is in agreement with recent molecular dynamics computer simulation data.

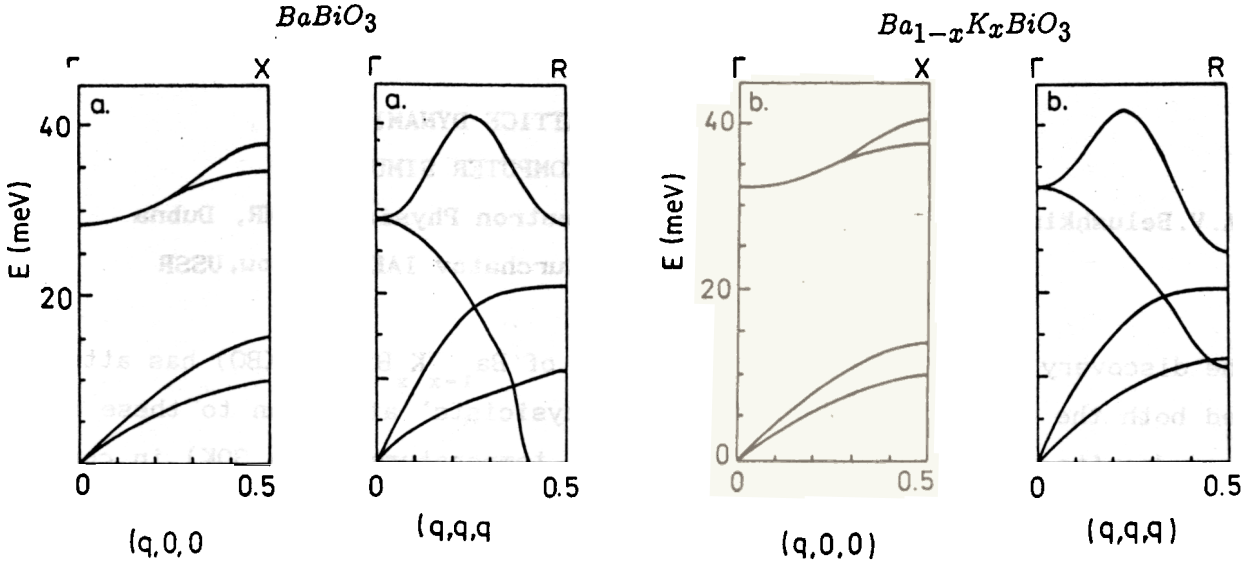

Fig. 1. Calculated phonon dispersion curves for $BaBiO_3$(a) and $Ba_{0.6}K_{0.4}BiO_3$. Only acoustic and BiO_6 vibration curves are shown for clarity. One can see that while in (q,0,0) direction lattice dynamics is stable for both systems, in (q,q,q) directions the cubic phase is unstable with respect to BiO_6 vibrations. The same is true for (q,q,0).

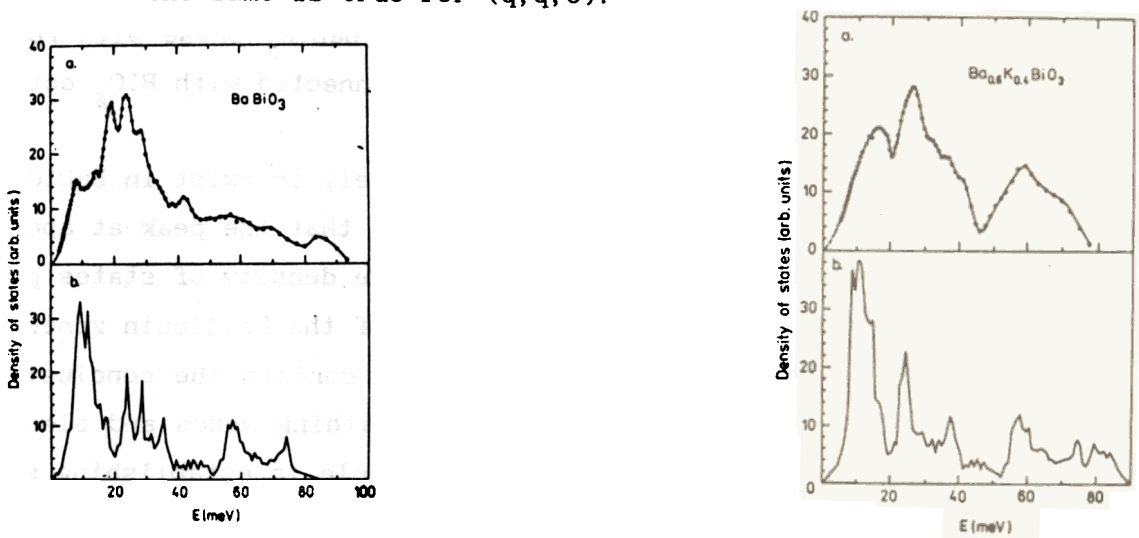

Fig. 2. Comparison between the calculated phonon density of states (lower curves) and the experimental generalized phonon density of states.

CRYSTAL ELECTRIC FIELD OF THE Nd_2CuO_4 COMPOUND

A.Yu.Muzychka, E.A.Goremychkin, I.Natkaniec, I.L.Sashin
Laboratory of Neutron Physics, JINR, Dubna
M.Divis
Charles University, Prague, CSFR
V.Nekvasil
Institute of Physics, Prague, CSFR

We use the inverted geometry spectrometer KDSOG-M to investigate the crystal electric field of the compound Nd_2CuO_4 by inelastic magnetic scattering of neutrons (IMSN).

Similar investigations have been undertaken by other groups[1-3] to produce the results which interpretation did not allow a comprehensive description of the bulk properties of the compound. The aim of this work is the CEF parameters refinement.

It is an essential improvement of the IMSN data that two peaks (5.3 meV, 11.9 meV) in the spectrum at T = 80 K were identified in this work as connected with transitions from CEF excited levels. The IMSN data interpretation with account for the mixing of the main and first excited multiplet has yielded a good description of the data (Fig.1) together with the quantitative description of experimentally measured magnetic susceptibilities (Fig.2).

The CEF Hamiltonian in this case has the form:

$$H_{cef} = B_2^0 \cdot \hat{O}_2^0 + B_4^0\hat{O}_4^0 + B_6^0\hat{O}_6^0 + B_4^4\hat{O}_4^4 + B_6^4\hat{O}_6^4,$$

where $\hat{O}_{2n}^{2m}$ are the equivalent Stevens operators acting in the space $|J = 9/2, J_z\rangle$, $|J = 11/2, J_z\rangle$ (the matrix elements shape is reported in[4]),

$$B_{2n}^{2m} = [V_{2n}^{2m}(\delta_J^{9/2} + \delta_J^{11/2})] \cdot \Theta_{2n}^J, \quad \delta_J^x = \begin{cases} 1, x = J \\ 0, x \neq J \end{cases}, \quad \Theta_{2n}$$

are the Stevens factors (their values see in[4]), V_{2n}^{2m} are the CEF parameters under determination in this work.

The best agreement between the calculated and experimental data has the set $\{V_{2n}^{2m}\}$:

$$V_2^0 = -(20.3\pm0.9)\ \text{meV}, \qquad V_4^0 = -(34.1\pm0.15)\ \text{meV},$$

$V_6^0 = (1.67 \pm 0.04)$ meV, $V_4^4 = (203.2 \pm 0.6)$ meV,

$V_6^4 = (135.1 \pm 0.3)$ meV

or in terms of $B_{2n}^{2m} = V_{2n}^{2m} \Theta^{9/2}_{2n}$:

$B_2^0 = (13 \pm 0.6) \cdot 10^{-2}$ meV, $B_4^0 = (9.93 \pm 0.04) \cdot 10^{-3}$ meV,

$B_6^0 = -(6.3 \pm 0.14) \cdot 10^{-5}$ meV, $B_4^4 = -(5.92 \pm 0.04) \cdot 10^{-2}$ meV,

$B_6^4 = -(5.09 \pm 0.02) \cdot 10^{-3}$ meV.

1. P.A.Alekseev et al. Sov. Journ.Superconductivity: Physics, Chemistry, Technology (1989), v.2, No.10, p.163 (in Russian).
2. A.T.Boothroyd et al. Physica C (1990) 17-24.
3. U.Staub et al. Sol.St.Comm. (1990), v.75, No.5, 431-433.
4. S.A.Altshuler, B.M.Kozyrev. Electric Paramagnetic Resonance in Intermediate Compounds. "Nauka", Moscow, (in Russian).
5. J.-M.Tarakson et al. Phys.Rev.B (1989), v.40, No.7, 4494-4502.

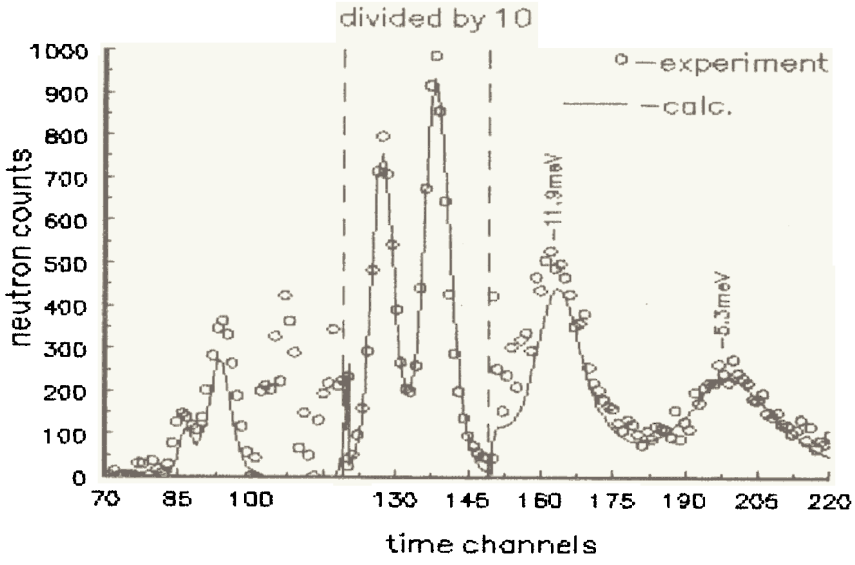

Fig. 1. The magnetic response of the Nd_2CuO_4 at T = 80 K as obtained by the IMSN method. Additional, not calculated peciliarities of the spectrum are connected with the use of the La_2CuO_4 spectrum as phonon substrate. The temperature dependent behaviour of these peculiarities has a nonmagnetic character (the intensity is increasing with increasing temperature).

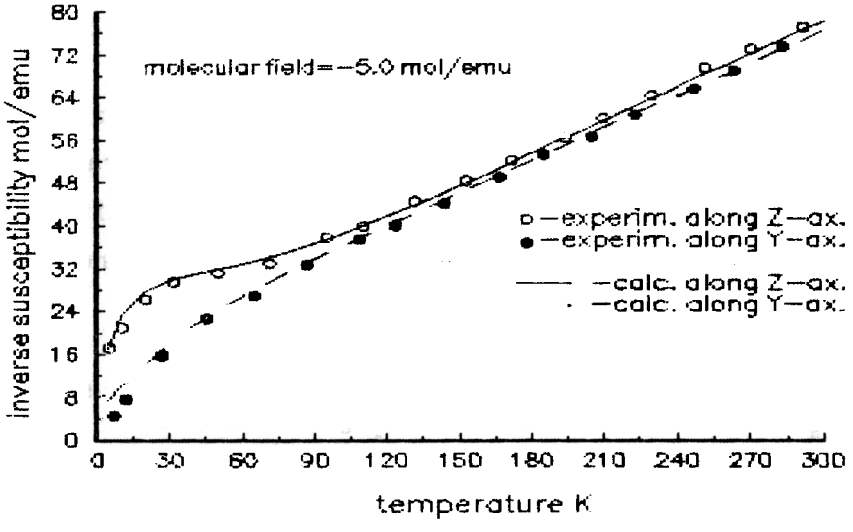

Fig. 2. The measured temperature dependence of the inverse magnetic susceptibility[5] and the results of the calculation based on the CEF parameters set determined in this work.

CRYSTAL ELECTRIC FIELD IN $Re_{0.05}Y_{0.95}Ni_2$ COMPOUNDS

I.L.Sashin, E.A.Goremychkin

Laboratory of Neutron Physics, JINR, Dubna

At present it appears impossible to calculate reliably the parameters of the crystal electric field in rare earth metallic compounds on the basis of a model. This impossibility is connected, in the first turn, with our not exact knowledge of what particular contribution to the effective CEF potential plays the most important role.

Studies of the families of isostructural REM compounds, RNi_2, RNi_5 and RAl_2 [1,2], have demonstrated no regularity in the behaviour of CEF Hamiltonian parameters, A_ℓ^m, inside given families.

In this connection it is interesting to continue investigating CEF in isostructural RE metallic compounds strongly diluted with nonmagnetic ones, as there we have a "clean" interaction of the 4f-shell with CEF.

Spectra of a series of isostructural Laves phase compounds $R_{0.05}Y_{0.95}Ni_2$ (R = Nd, Pr, Tb, Tm, Er, Dy, Ho) were measured on the spectrometer KDSOG-M by thermal neutron inelastic scattering. For this case the CEF Hamiltonian has the form:

$$H_{cef} = B_4^0 (O_4^0 + 5O_4^4) + (O_6^0 - 21O_6^4),$$

where B_ℓ^m are the CEF parameters and O_ℓ^m are the Stevens operators.

Figure 1 shows experimental and calculated INS spectra of the compound $Nd_{0.05}Y_{0.95}Ni_2$. Two magnetic peaks correspond to the transitions: $\Gamma_6-\Gamma_8^1$ (6.59 meV) and $\Gamma_8^1-\Gamma_8^2$ (4.58 meV). Most consistent data were obtained for the CEF Hamiltonian parameters:

$$B_4^0 = (-2.0\pm0.04)\times10^{-3}\text{meV and } B_6^0(1.48\pm0.07)\times10^{-5}\text{meV}.$$

The data on the other parameters are in the process of processing.

1. E.A.Goremychkin, E.Mûhle. In: V Int. School on Neutron Physics. Dubna, 1987, p.467.
2. B.Fuck, M.Loewenhaupt. Z.Phys.B (1986), v.63, p.213.

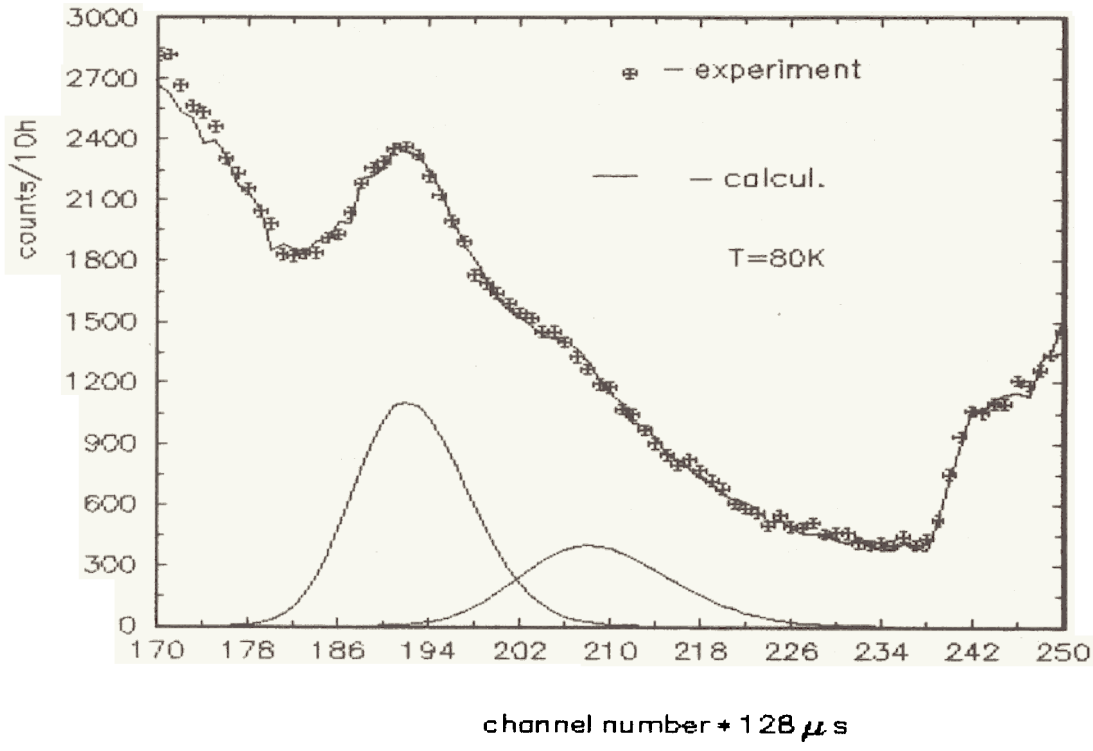

Fig.1. The INS spectrum of the $Nd_{0.05}Y_{0.95}Ni_2$ compound at 80K(+). The solid line represents the spectrum calculated with account for the phonon spectrum. Two Gaussian-like lines correspond to transitions between CEF levels of the main multiplet of the ion Nd^{3+}.

CRYSTAL FIELD EXCITATIONS IN $CeCu_2Si_2$

E.A.Goremychkin, Laboratory of Neutron Physics, JINR, Dubna
R.Osborn, RAL, Chilton, Didcot, U.K.

$CeCu_2Si_2$ was the first heavy fermion compound, with an electronic specific heat contribution γ of 1.1 J/mole/K^2, discovered to have a superconducting ground state below T = 0.5 K[1]. It has since been the subject of numerous investigations of both its bulk and microscopic properties[2]. In common with all f-electron systems, the crystal field (CF) potential of heavy fermion compounds is an essential component in determining the ground-state properties (specific heat, magnetic susceptibility, transport properties, etc.). In addition, it has been suggested that the CF potential itself is due to the hybridization interaction between the localized f-electron states and band states that is responsible for the heavy fermion behaviour[3].

The only direct experimental method for determining the CF in a metallic compound is inelastic neutron scattering (INS), with the cross section being proportional to the dynamic magnetic susceptibility, and there have been four previous studies of $CeCu_2Si_2$[4-7], although two of them were polarized neutron studies with very poor energy resolution. The results have been controversial because the CF level scheme proposed by the first INS investigation[4] is inconsistent with specific heat[8] and single crystal magnetic susceptibility[9] measurements.

The main challenge in interpreting measured neutron spectra is to derive correctly the phonon contribution either by a careful analysis of the angular dependence of the scattering or by using an isostructural non-magnetic compound (e.g. containing La instead of Ce). This is a particularly serious problem in the case of $CeCu_2Si_2$ since the nuclear (i.e. phonon) cross section is very strong, especially below 20 meV in the energy range of the proposed lower doublet. In the light of the above-mentioned discrepancies between INS and other studies, it is very important, to assess the reliability of the earlier conclusions based on INS data.

We have therefore performed new measurements on stoichiometric samples of $CeCu_2Si_2$ and $LaCu_2Si_2$ on the neutron time-of-flight spectrometers HET, at the pulsed spallation neutron source ISIS (Rutherford Appleton Laboratory, U.K.), and KDSOG at the pulsed reactor IBR-2 (JINR, USSR). HET is a chopper spectrometer which combines very high energy resolution with a wide range of energy transfer ω and wavevector transfer Q. These characteristics allow us

to estimate the magnetic contribution by a scaling procedure described by Murani[10] using the low and high Q data of the La compound to determine the Q-dependence of the Ce phonon contribution. The level of multiple phonon scattering, which dominates over the nuclear contribution at lower scattering angles, has been assessed by Monte Carlo simulation. Measurements of Ce and La samples on KDSOG, an inverse geometry spectrometer with high intensity and moderate resolution, have allowed the use of direct subtractions because multiple scattering is much less significant in this scattering geometry. The complementary use of these two spectrometers with different methods of estimation of the magnetic scattering provides some justification for our main conclusions.

Our main result is that, contrary to the conclusions of previous INS investigations but in accord with the specific heat results, there is only one CF transition at 30 meV, which is very broad. It has a Lorentzian lineshape with a width of Γ = 8.4 meV at 2 K. There is also evidence for magnetic quasi-elastic scattering (Γ = 1.9 meV at 10 K) in good agreement with previous low energy investigations[4]. The combined tails of the quasi-elastic scattering and the broad inelastic scattering produce significant magnetic intensity in the range 10 to 20 meV but this is not enough, in our view, to support the suggestion of a second CF transition in this region.

1. F.Steglich et al. Phys.Rev.Lett. 43 (1979) 1892.
2. G.R.Stewart. Rev.Mod.Phys. 56 (1984) 755.
3. P.M.Levy, S.Zhang. Phys.Rev.Lett. 62 (1989) 78.
4. S.Horn et al. Phys.Rev. B23 (1981) 3171.
5. E.Holland-Moritz et al. Phys.Rev. B39 (1989) 6409.
6. C.Stassis et al. Phys.Rev. B33 (1986) 1680.
7. Y.J.Uemura et al. Phys.Rev. B33 (1986) 6508.
8. C.D.Bredi et al. J.Mag.Mat. 47&48 (1985) 30.
9. B.Batlogg et al. J.Appl.Phys. 55 (1984) 2001.
10. A.P.Murani. Phys.Rev. B28 (1983) 2308.

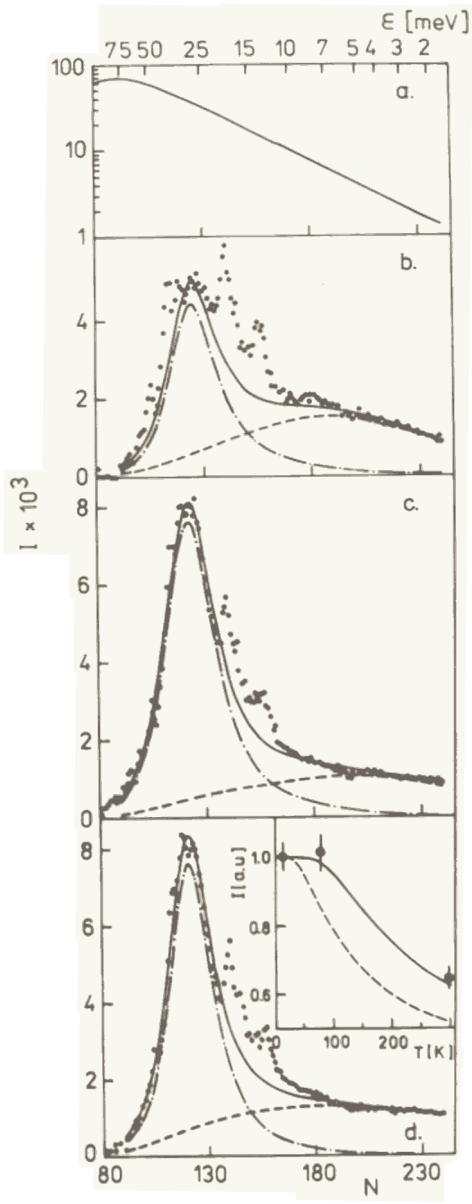

Fig. 1. The magnetic scattering (points) from $CeCu_2Si_2$ measured on KDSOG at 300 K (b), 77 K(c) and 10 K (d). The dashed (dot dashed) line is the estimated quasi-elastic (inelastic) scattering. Fig. 1(a) is the incident flux distribution. The temperature dependence of the CF transition intensity predicted by our CF model is shown as the solid line in the insert to Fig. 1(d) where it is compared to the experimental points. The dashed line shows the intensity variation of the CF model from /4/.

NEUTRON SPECTROSCOPY OF $CeCu_{5-x}Al_x$ (x = 1,2) AND $CeCu_4Ga$ HEAVY FERMION SYSTEMS

E.A.Goremychkin, A.Yu.Muzychka, I.Natkaniec, I.L.Sashin
Laboratory of Neutron Physics, JINR, Dubna
D.D.Chistyakov, N.B.Kolchugina
Baikov Institute of Metallurgy, Moscow, USSR

Earlier investigations of substitution of Cu by Al or Ga in the hexagonal compound $CeCu_5$ (P6/mmm) indicated a cross-over from a magnetically ordered Kondo compound $CeCu_5$ to a non-magnetic heavy fermion state in $CeCu_3Al_2$ and $CeCu_3Ga_2$ [1,2]. They have shown that $CeCu_4Al$ and $CeCu_4Ga$ in this series behave exceptionally and demonstrate a huge electronic contribution to specific heat.

We investigated the evolution of magnetic responses of these compounds by inelastic neutron scattering (INS). Magnetic parts of INS spectra were obtained by subtraction of phonon scattering spectra measured for compounds that contained La instead of Ce atoms. INS experiments were performed at 10 and 80 K on the time-of-flight inverted geometry spectrometer KDSOG-M installed at the IBR-2 high flux pulsed reactor[3]. The experimental INS spectra are shown in Fig.1, while the magnetic parts from cerium compounds are presented in Fig.2.

In the INS spectra of $CeCu_5$ a well defined peak at an energy transfer of 17.5 meV caused by transitions between crystal field (CF) levels was observed in agreement with ref.[4]. Additionally, a weak quasielastic contribution was also seen. The substitution of Cu for Al or Ga in $CeCu_5$ leads to drastic changes in magnetic neutron scattering: the CF transition shifts to much lower energies of about 5-4 meV and becomes significantly broader, a strong, broad quasielastic contribution is clearly observed. The magnetic INS spectra of these compounds at 80 K are well fitted by one Lorentzian reflecting a broad quasielastic scattering distribution only. The similar behavior shows the magnetic scattering on $CeCu_3Al_2$ at 80 and 10 K. The transition energies (ε) and the corresponding line widths ($\Gamma/2$) are listed in Table 1. Apparently, these changes in magnetic neutron scattering on $CeCu_5$ under substitution of Cu for Al or Ga are due to substantial enhancement of s-f hybridization associated with the filling of the conduction band with extra electrons supplied by Al and Ga atoms

1. J.Kohlmann, E.Bauer, K.Winzer. Physica B, 163 (1990) p.188.
2. E.Bauer et al. Physica B, 163 (1990) p.686 and references therein.
3. Neutron Experimental Facilities at JINR, Dubna, 1991, p.20.
4. E.A.Goremychkin et al. Sol.State Comm., 64 (1987) p.1473.

Table 1

	$CeCu_4Al$		
	ε(meV)	Γ/2(meV)	Intensity (a.u.)
10 K	0	2.3±0.4	32±3
	4.7±0.3	3.3±0.4	4.9±0.5
T = 80 K	0	5.0±0.5	16±2
	$CeCu_4Ga$		
T = 10 K	0	4.5±0.3	31±3
	4.0±0.2	2.6±0.3	6.5±0.5
T = 80 K	0	4.1±0.4	14±2

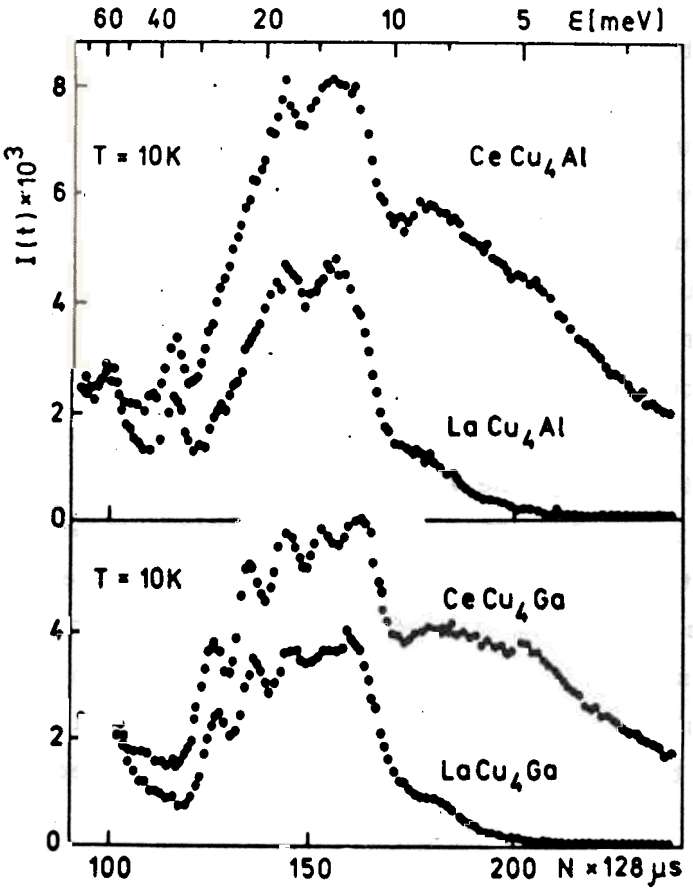

Fig.1. Experimental INS spectra from $CeCu_4Al$, $LaCu_4Al$, $CeCu_4Ga$ and $LaCu_4Ga$ at 10 K; N denotes the number of TOF channels, I - the normalized neutron counts and ε is the energy transfer.

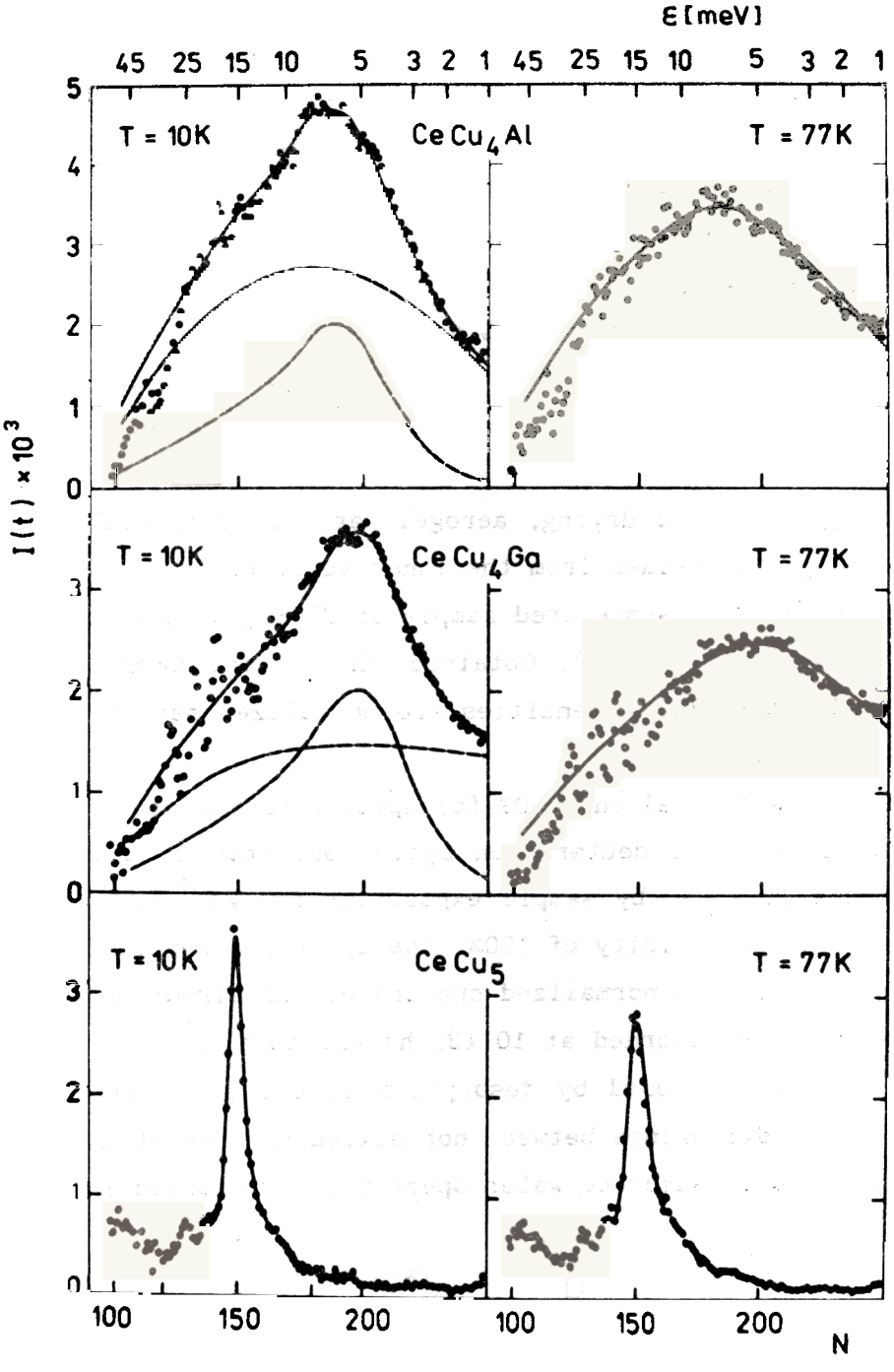

Fig. 2. Magnetic parts of INS spectra of $CeCu_4Al$ and $CeCu_4Ga$ compared with calculated spectra taking into account the resolution function of the spectrometer, positions of the transferred energy lines, their widths and intensities are given in Table 1. The experimental INS spectra of $CeCu_5$ are also shown for comparison.

VIBRATIONAL SPECTRA OF DISPERSED AMORPHOUS SILICAS: AEROGEL

E.F.Sheka, I.V.Markichev, P.B.Nechitaylov

Patrice Lumumba Peoples' Friendship University, Moscow, USSR

I.Natkaniec, A.Yu.Muzychka

Laboratory of Neutron Physics, JINR, Dubna

V.D.Khavryutchenko, V.M.Ogenko

Institute of Surface Chemistry, Kiev, Ukraine

J.Fricke, G.Reicheauer

Physikalisches Institut der Universität Wurzburg, Germany

Aerogel is the product of base- or acid-catalysed hydrolysis of tetraethoxysilane in alcohol solutions at 300-350°K. After the sol-gel process and subsequent hypercritical drying, aerogel was heated to 600°C for about 24 hours to remove organic resides from the inner surface.

The INS spectra of the as-prepared sample of 27.8 g were recorded at 10 (20 h), 80 (14.2 h) and 290 K (11 h). Obtained TOF (a) and AWDS (b) spectra are shown in Fig.1. The spectral intensities are normalized per 100 g of mass and 1 hour of measuring time.

Figure 2 shows the TOF (a) and AWDS (b) spectra of the deuterated air-dried sample at 10 K (21 h). The deuteration cycle consisted of sample heating at 100°C for 12 hours followed by sample exposition for 24 hours in heavy water vapours with a relative humidity of 100%. The cycle was repeated twice.

The TOF (a) and AWDS (b) normalized spectra of the air-dried sample kept at 100°C for 20 hours were recorded at 10 (31 h) and 80 K (11.5 h) and are shown in Fig.3. The mass loss caused by desorption is 0.5 g. Differential spectra corresponding to the difference between normalized spectra of air-dry and air-dried samples related to adsorbed water spectra are presented in Fig.4 for two temperatures.

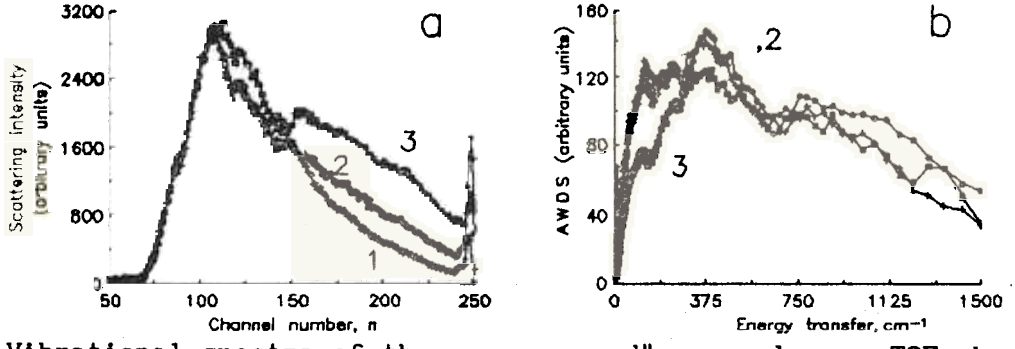

Fig.1. Vibrational spectra of the as-prepared" aerogel: a - TOF, b - AWDS, 1 - 10, 2 - 80, 3 - 290 K.

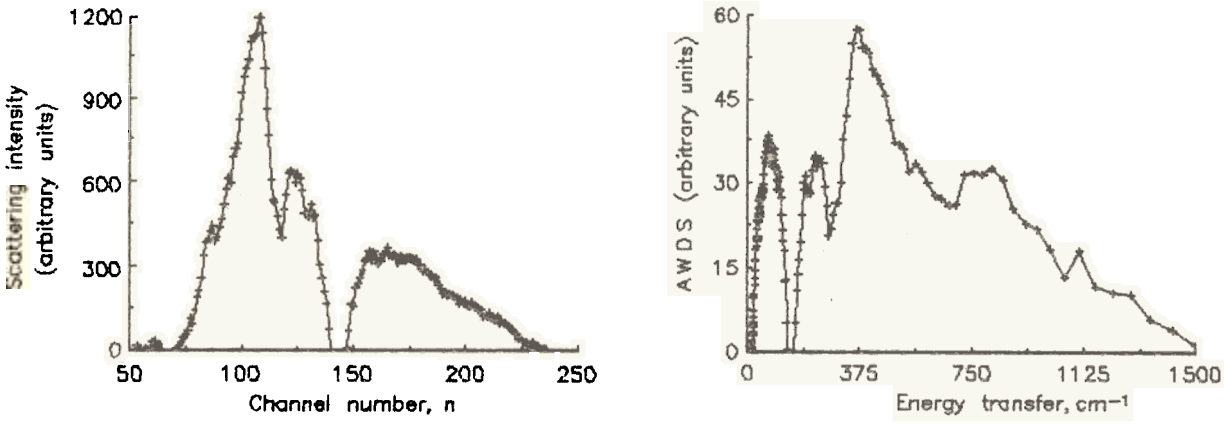

Fig.2. The vibrational spectrum of deuterated aerogel: a - TOF, b - AWDS, 10 K.

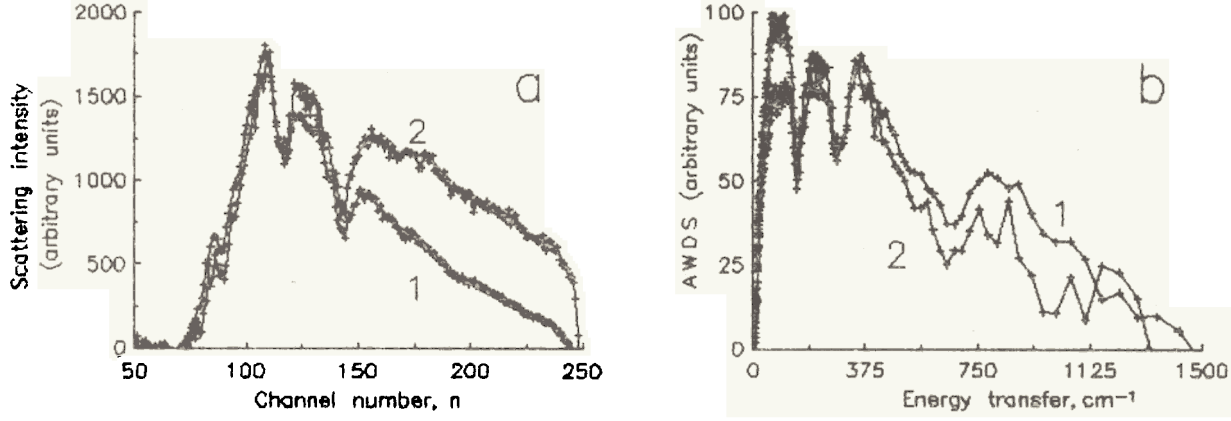

Fig.3. The vibrational spectrum of dried aerogel: a - TOF, b - AWDS, 1 - 10, 2 - 80 K.

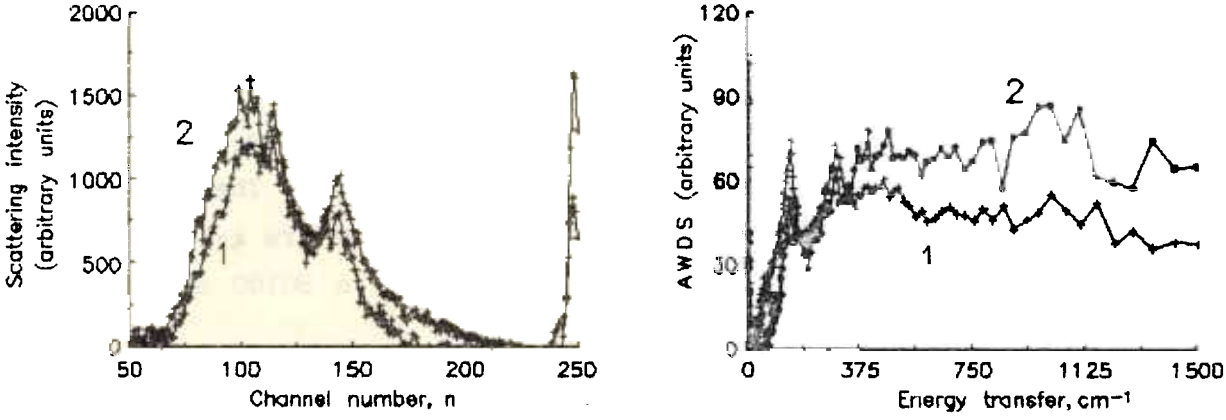

Fig.4. The vibrational spectrum of water adsorbed on this aerogel" a - TOF, b - AWDS, 1 - 10, 2 - 80 K.

VIBRATIONAL SPECTRA OF DISPERSED AMORPHOUS SILICAS: SILICA GEL

E.F.Sheka, I.V.Markichev, P.B.Nechitaylov
Patrice Lumumba Peoples' Friendship University, Moscow, USSR
I.Natkaniec, A.Yu.Muzychka, J.Krawczyk
Laboratory of Neutron Physics, JINR, Dubna
V.D.Khavryutchenko, V.M.Ogenko
Institute of Surface Chemistry, Kiev, Ukraine

A comparative INS study of vibrational spectra of a set of dispersed amorphous silicas, different by origin, has been initiated a year ago. So-called "as-prepared" or air-dry commercial products form the first group. The other group form air-dried samples treated in ambient atmosphere under specific for every sample conditions. The study is aimed at advancing the microscopic conception to the atomic structure of samples on the basis of experimental and calculated spectra of adsorbed water.

By now the INS spectra have been measured for two massive samples of quartz glass and of glass sintered from aerosil - A380 and for three dispersed products: aerosils A175 and A380 and silica gel SG20[1].

Silica gel SG100, the object of the current investigation, has been produced at about 300 K by polycondensation of a silicon acid in water solutions. The mean pore size is 100 Å. The spectra of the as-prepared product were reported earlier in[1]. The sample of 60.5 g was dried at 120°C for 72 hours. The mass loss is 1.6 g.

Figure 1 represents the time-of-flight (TOF) spectra (a) along with the amplitude weighed density of states (AWDS) spectra (b) of air-dried SG100 at 10 (13.7 h), 80 (21 h) and 290 K (12.7 h). The mass loss is assumed to be related to retained and/or adsorbed water released on drying. The differential spectra of the as-prepared sample[1] and the air-dried one are related to this water. The spectra of retained and/or adsorbed water in SG100 are shown in Fig.2 for three temperatures.

Deuterated samples have been studied to reveal the contribution from their siloxane cores.

The samples of SG20 and SG100 were dried at 100°C for 24 hours and then placed into heavy water vapours for 24 hours at the relative humidity of 100%. This procedure has been repeated 3 times for SG100 and 5 times for SG20.

The INS spectra of thus prepared deuterated air-dried samples have been measured on the KDSOG-1M at 10 (20 h) and 80 K (13 h) for SG20 and at 10 (19.5 h), 80 (12.5) and 290 K (11.5 h) for SG100. The sample masses were 77.5 and 43 g, respectively.

The INS spectra normalized per 100 g of mass and 1 hour of measuring time are shown in Figs.3 and 4.

1. E.F.Sheka et al. J.Electr.Spectr.Rel.Phenom., 54/55 (1990) p.855.

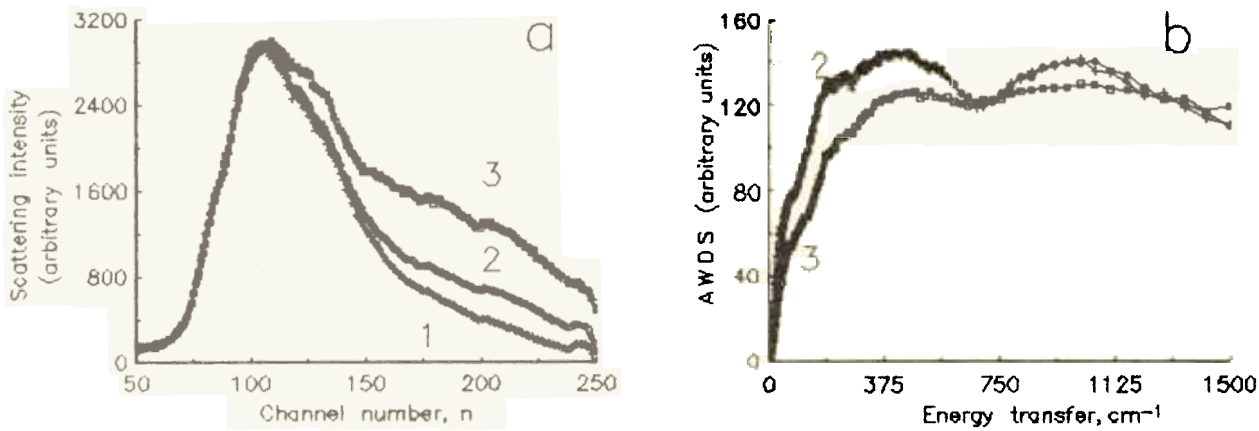

Fig.1. Vibrational spectra of dried silica gel SG100: a - TOF, b - AWDS, 1 - 10, 2 - 80, 3 - 290 K. The spectra are normalized per 100 g of mass and per 1 hour of measuring time.

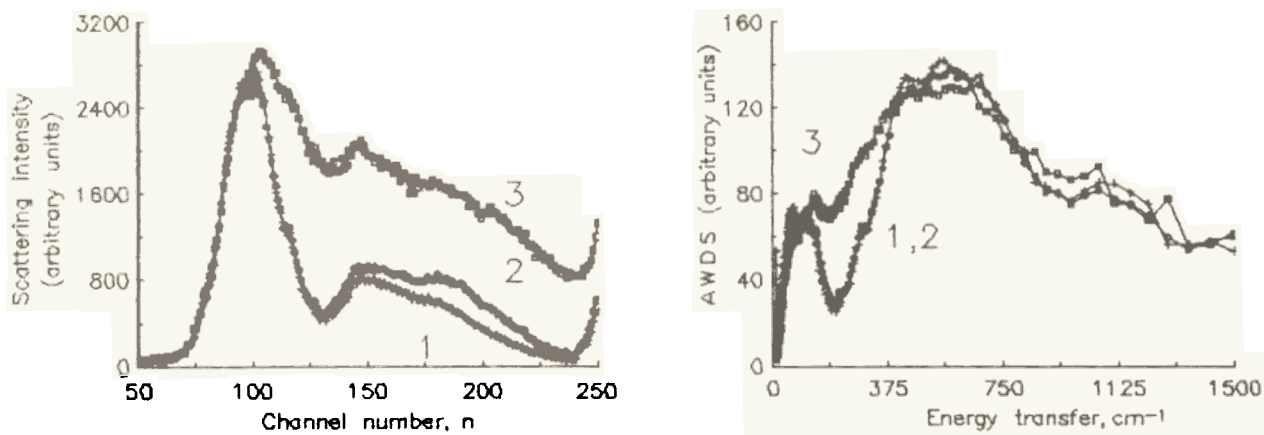

Fig.2. Vibrational spectra of water hold in SG100: a - TOF, b - AWDS, 1 - 10, 2 - 80, 3 - 290 K.

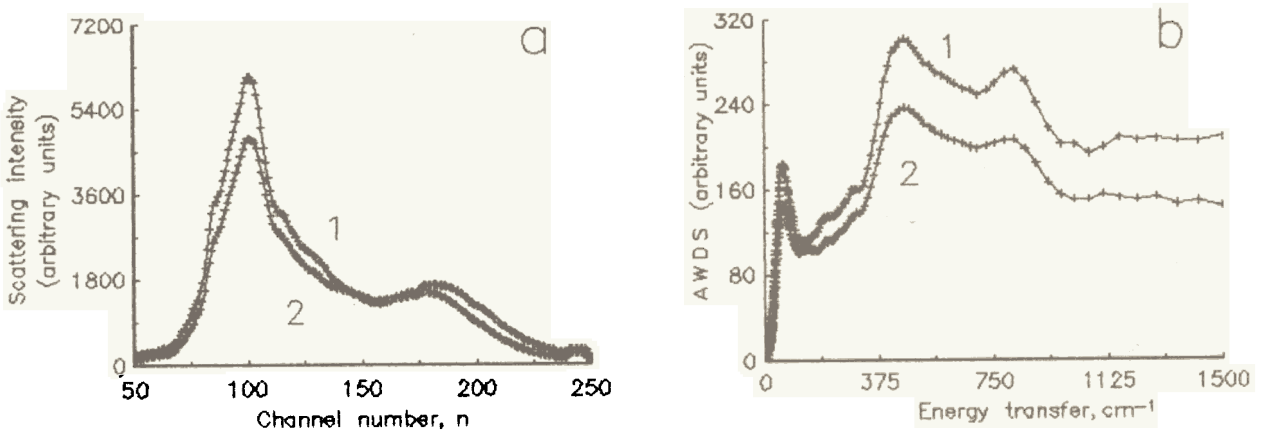

Fig.3. The vibrational spectrum of deuterated silica gel SG20: a - TOF, b AWDS, 1 - 10, 2 - 80 K.

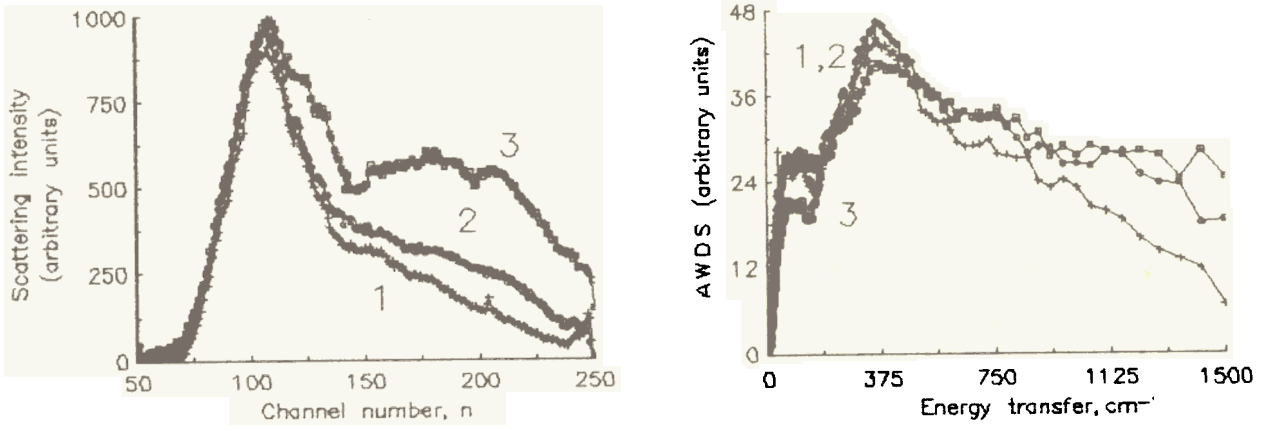

Fig.4. Vibrational spectra of deuterated SG100: a - TOF, b - AWDS, 1 - 10 2 80, 3 - 290 K.

VIBRATIONAL SPECTRA OF DISPERSED AMORPHOUS SILICAS: SILOCHROM

E.F.Sheka, I.V.Markichev, P.B.Nechitaylov
Patrice Lumumba Peoples' Friendship University, Moscow, USSR
I.Natkaniec, A.Yu.Muzychka
Laboratory of Neutron Physics, JINR, Dubna
V.D.Khavryutchenko, V.M.Ogenko
Institute of Surface Chemistry, Kiev, Ukraine

Silochrom is a special type amorphous dispersed silica. It is produced by mixing aerosil with water to gel formation. Gel is kept in an autoclave at 150-170°C for some hours and then it is air-dried at 100-120°C for the same time.

The vibrational spectra of the as-prepared sample of 70 g in weight were recorded at 10 (22 h), 80 (12.5 h) and 290 K (13.5 h) on the KDSOG-M spectrometer. Figure 1 represents obtained TOF (a) and AWDS (b) spectra, normalized per 100 g of mass and 1 hour of measuring time. Their intensities are similar to those of the as-prepared aerosil spectra[1]. This means that the amount of adsorbed water is about the same in these samples. Obtained spectra differ considerably from the spectra of the other dispersed silicas[1].

1 E.F.Sheka et al J.Electr.Spectr.Rel.Phenom., 54/55 (1990) p.855.

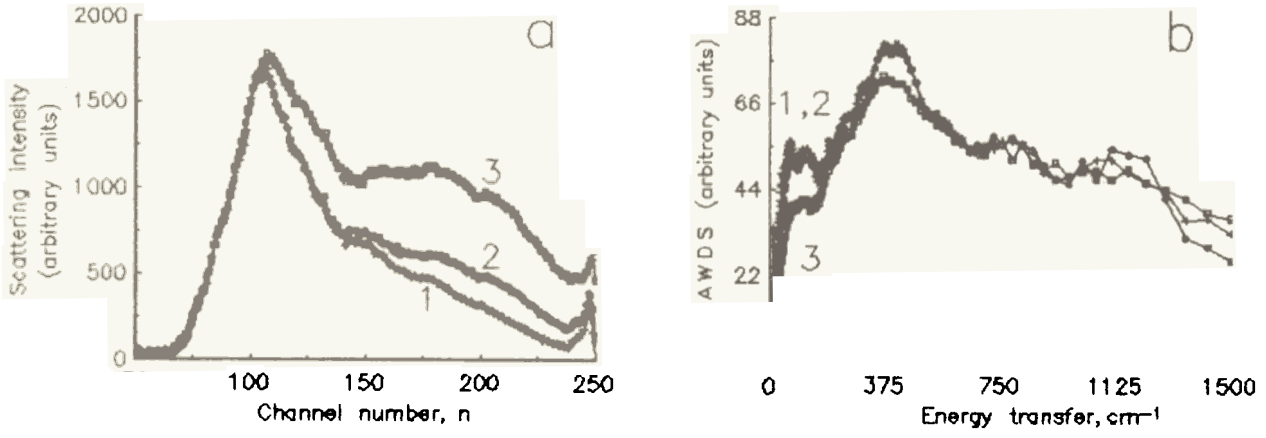

Fig.1. Vibrational spectra of 'as-prepared' silochrom a - TOF, b - AWDS, 1 10, 2 - 80, 3 - 290 K.

MEASUREMENT OF THE LOSS COEFFICIENT OF ULTRACOLD NEUTRONS IN BERYLLIUM POWDER

V.V.Golikov, V.K.Ignatovich, E.N.Kulagin
Laboratory of Neutron Physics, JINR, Dubna

In the previous years the new method for measuring the loss coefficient μ per single reflection of ultracold neutrons (UCN) from a solid surface was proposed and checked in the Neutron Physics Laboratory. In this method the reflection of UCN's from powder samples of different thickness is measured. To get the μ from the reflection coefficient, R_∞, measured for a powder sample of infinite thickness, the generally accepted notions for neutron diffusion were used, from which it comes out that

$$\mu = 0.75\ ((1-R_\infty)/(1+R_\infty))^2. \qquad (1)$$

In accordance with this expression it was obtained, that after high temperature outgasing the loss coefficients for graphite and beryllium were in agreement with theory, the known capture and inelastic scattering cross-sections of nuclei in these substances being taken into account. The result was in contradiction with the data of UCN storage experiments in sealed vessels. So an additional analysis of the applicability of the generally accepted neutron diffusion theory to the UCN transport in powder is required.

During the reported period the new theoretical and experimental investigation of UCN diffusion in dispersed media was undertaken. It was understood that for the description of the UCN transport in the case of total reflection from powder grains of sizes (several μm) considerably larger than the neutron wavelength, the packing density and the connected with it reflection ρ from the powder monolayer were important to be taken into account. With the help of the new theory the expression (1) was generalized:

$$\mu \simeq 0.75\ ((1-R_\infty)/(1+R_\infty))^2(1-\rho)^{-2}. \qquad (2)$$

New measurements of UCN reflection from a powder at different thickness of layers and at different packing densities were performed. The values of μ and ρ were extracted. The new theory data and the data of preceding experiments helped to obtain a reduced loss coefficient η for beryllium at room temperature after high temperature outgasing. Its value, $(6.4\pm2.5).10^{-5}$, is nearly an order of magnitude higher than the theoretical one and it is in agreement with the results of UCN storage experiments.

STUDY OF INHOMOGENEOUS MAGNETIC FLUXES IN A SUPERCONDUCTING CERAMICS $YBa_2Cu_3O_{6.9}$

V.L.Aksenov, E.B.Dokukin, Yu.V.Nikitenko,
A.V.Petrenko and S.A.Sergeenkov
Laboratory of Neutron Physics, JINR, Dubna

It is known [1] that superconductors show a number of magnetic properties: the Meissner effect, magnetic relaxation, surface magnetism, etc. The recently discovered [2] high-temperature superconductors (HTS) exhibit, due to smaller coherence lengths, even a more complicated magnetic behavior [3]. Thus, it seems rather important to use polarized neutrons as a tool to directly investigate the magnetic flux inside a bulk material. These experiments are few, however, due to the difficulty of their realization [4,5,6].

Here we discuss the investigation of the magnetic flux distribution in the superconducting ceramics $YBa_2Cu_3O_{6.9}$ via polarized thermal neutron transmission technique. Similar studies but of low temperature II-type superconductors have been undertaken by Weber [4]. He has shown that the dependence of polarization P(H) on magnetic field showed a region confined within the characteristic fields, H_{c1} and H^+, where polarization reached minimum at H^*. At $H>H_{c1}$, the field starts to inhomogeneously penetrate into the superconductor, and polarization decreases. For high enough fields, when $H^+<H\leq H_{c2}$, the pinning forces are overcome and polarization tends to its initial behavior. At last in the intermediate point H^*, these tendencies compensate each other and polarization achieves its minimum.

The results of paper [4] have been confirmed in [5], where the ceramics $YBa_2Cu_3O_{6.9}$ has been treated in the temperature range from 4.2t to 44.5K up to a maximum magnetic field of 16.5KOe. We studied the superconducting ceramics $YBa_2Cu_3O_{6.9}$ in the range from 78.6K to 88.9K. The specific resistivity of our sample has vanished at T=89K. In the dependence P(H), we found , in addition to the first minimum at $H=H_1^*$ due to field penetration into grains, the second minimum at $H=H_2^*$. The figure shows the temperature dependences $H_1^*(T)$ and $H_2^*(T)$. Both minima shift to smaller fields with increasing temperature. But, if $H_1^*=0$ at $T=T_1=90.5K$, then $H_2^*=0$ at $T=T_2=89.2$ K. It is seen also that the dependence of the second minimum position on temperature is stronger than that of the first one. Both minima, as it was established, have similar dependences of depolarization $D(\lambda)=1-P(\lambda)$ via neutron wavelength λ, namely: $D(\lambda)=1-\exp\{-\beta\lambda^2\}$. This dependence was predicted by Halpern and Holstein [7] in 1941. The value of the parameter β is connected with induction fluctuations perpendicular to

mean magnetization $\delta B_\perp$, the size of the magnetic domain d, and the concentration n of these fluctuations, via the relation $\beta \sim \delta B_\perp^2 d^2 n$.

It is quite possible that the second minimum corresponds to the field penetration into a subgrain region. This hypothesis seems quite reasonable. For instance, papers [8,9] give evidence in favor of the existence of these subgranular regions in the ceramics $YBa_2Cu_3O_{6.9}$ in connection with the registration of the second maximum of the field dependence of the critical current.

The authors are indebted to E.Fisher for testing the sample.

1. M.Tinkham, Introduction to Superconductivity. New York: McGraw-Hill, 1975.
2. Bednorz J.G., Muller K.A., Z.Phys.,1986,v64,p189.
3. Malozemoff A.P., Physical properties of high temperature superconductors I, World Scientific, London, 1989.
4. Weber H.W., J.Low Temp.Phys., v.17,N1/2, 49(1974).
5. R.P.Dmitriev,R.Z.Jagood,N.K.Zhuchenko,M.P.Volkov and E.I.Leyarovski, Z.Phys.B,83,155-159(1991).
6. E.B.Dokukin, D.A.Korneev, A.V.Petrenko. JMMM,90-1,p.637
7. O.Halpern, T.Holstein, Phys.Rev.,59,960(1941).
8. H.Kupfer et.al. International conference on critical currents in high-temperature superconductors. Snowmass Village, Colorado, USA, 16-19 August, 1987.
9. H.Kupfer et.al. International conference on critical currents in high-temperature superconductors. Birmingham, 16 May, 1988.

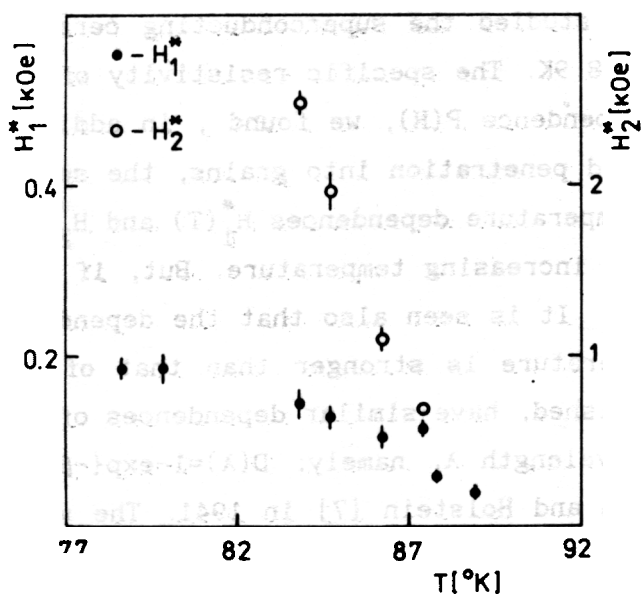

Fig. The dependence on temperature of the minima positions in the polarization on field dependence P(H), o- position of the first minimum, ·- position of the second minimum.

MEASUREMENT OF MAGNETIC FIELD PENETRATION DEPTH IN NIOBIUM POLYCRYSTALLINE FILMS BY POLARIZED NEUTRON REFLECTION METHOD

L.P.Chernenko, D.A.Korneev, A.V.Petrenko,
N.I.Balalykin, A.V.Skripnik
Laboratory of Neutron Physics, JINR, Dubna

As shown in the literature[1], the specular polarized neutron reflection may be used as a direct method of measuring the absolute value of the magnetic field penetration depth of a superconductor (s.p.d.). However, the s.p.d. as determined by measuring the direct current in Josephson junctions in a weak magnetic field[2] has given a value in niobium films (91 nm, T = 4.6 K) which is well over than that obtained by polarized neutron reflection[1] (43 nm, T = 4.6 K). The present experiment was started to throw light on causes of this difference.

We carried out experiments on two niobium films of various thickness and roughness prepared with the same sputtering technique. The experiments have been conducted on the spectrometer of polarized neutrons (SPN) in a reflectometry mode[3] at the IBR-2 reactor. Two measurements have been carried out sequentially. At room temperature the specular reflection spectra were measured to obtain neutron-optical parameters (thickness, roughness) of films. Then we carried out the measurements once more at T = 4.9 K in the field of 500 Oe. Before the measurements were performed, the reflectometer was turned to the grazing angle θ = 4.0 mrad with $\Delta\theta/\theta$ = 0.025. For data handling we used the new method of calculation of the reflection factor described in[4]. The method consists of replacing the continuous one-dimensional neutron-optical potential of the film with the discrete series of Fermi quasi-potentials to model the reflection of plane waves from inhomogeneous media. Unlike the traditional approach[1], we took roughness into account by introducing in the calculation of the reflectivity increasing amplitudes of Fermi potentials. These were distributed according to the Gaussian error curve with dispersion equal to the roughness parameter (σ) square. Actually the results of the two techniques are in excellent agreement for pure nuclear potentials. The two methods to evaluate roughness become different only when both nuclear and magnetic potentials are present[4].

In view of the geometric arrangement of the sputtering apparatus, the "thin" film of 28x50 mm^2 (sputtered on a silicon plate) had a graded thickness with an average value of 255(+/-15) nm, σ = 0.5 nm. The "thick" film - 700 nm in

thickness - was obtained by slanted sputtering on the ceramic substrate (95% Al_2O_3), σ = 8 nm. The critical temperature for both films was 8.95 K. Since a decrease of the critical temperature of niobium films is expected at a film thickness lower than 200 nm the samples seemed satisfactory. This was confirmed by the analysis of the composition of initial material for niobium sputtering, and the films themselves, using the neutron activation analysis. The analysis did not reveal noticeable amounts of impurities in the films.

To analyse the experimental data we used the diamagnetic profile of a superconducting film according to London's local electrodynamics of superconductors. An extra ingredient of the model was the assumption of the existence of some "dead" layer in niobium close to a substrate, which at T = 4.9 K does not pass to a superconducting state.

The figure shows the relation of reflection factors of neutrons with opposite polarization (flipping ratio) depending on a normal component of a neutron wave length. If the model does not consider the "dead" layer on the boundary with a sublayer, the experimental spectra are described by theoretical curves (see fig.) at the value of s.p.d. equal to 145(+/-15) nm for a "thin" film, and 90(+/-10) nm for a "thick" one, respectively. The value of a s.p.d. equal to 43 $nm^{/1/}$ describes our data adequately only for a "thin" film in a model with a "dead" layer 100 nm in thickness.

The analysis of systematic factors leading to a possible shift of s.p.d. has shown that the obtained values at T = = 4.9 K of 145 nm and 90 nm are the low values of s.p.d. for the thin films investigated. We believe that the hypothesis of a "dead" layer 100 nm in thickness, bringing the value of s.p.d. to that of 43 nm (T = 4.9 K) is not well based for two reasons. Firstly, the analysis of the depth composition of a film by backward scattering of accelerated ions of helium with an energy from 3.0 MeV to 3.2 MeV has shown that there is neither oxygen nor other impurities across the whole width of the thin film. Secondly, the films 100 nm in thickness at T = 4.9K are superconducting.

We conclude that our measurement of s.p.d. by neutron reflectometry method on the niobium polycrystalline films gave the s.p.d. that is different from the s.p.d. in bulk niobium. At T = 4.9 K the s.p.d. for the "thin" film and that for the "thick" film are 145 nm and 90 nm, respectively.

The studies of the film contents by neutron activation analysis and backward scattering of He ions did not confirm hypothesis of the existence of "dead" layer in the "thin" film, which was introduced to explain the experimental data with s.p.d. of bulk niobium.

1. G.P.Felcher, R.T.Kampwirth, K.E.Gray and R.Felici. Phys.Rev.Lett., 52 (1984) 1539.
2. M.Russa. J.Low Temp.Phys., 50 (1983) 301.
3. D.A.Korneev, V.V.Pasyuk, A.V.Petrenko and E.B.Dokukin. "Neutron reflectivity studies on superconducting, magnetic and absorbing thin films on the polarized neutron spectrometer at the pulsed reactor IBR-2". 2nd Int.Conf. Surface X-Ray and Neutron Scattering. Bad-Honef, Germany, June 25-28, 1991. Springer Verlag, Berlin, 1991.
4. D.A.Korneev, L.P.Chernenko. JINR Rapid Comm.. 4[30]-88 and Poverhnost'. Fizika, himija, mehanika, 9, 61 (1990) (in Russian).

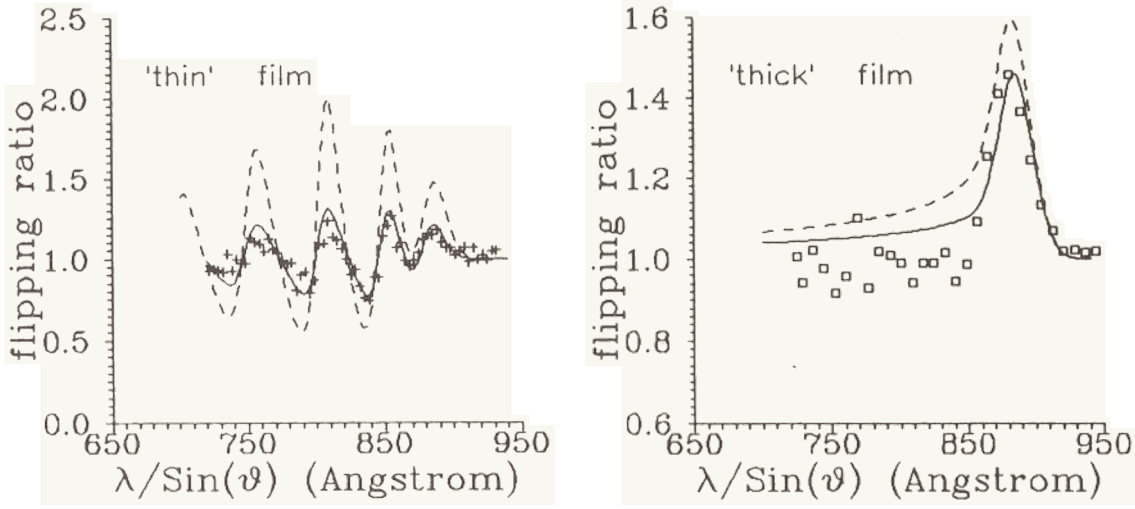

Experimental values of the flipping ratio: crosses are for the film 255 nm in thickness; squares are for the film 700 nm in thickness. Lines correspond to theoretical calculations considering the corrections for polarization and resolution of the reflectometer. Dashed lines are for the s.p.d. of 50 nm.

NEUTRON REFLECTIVITY INVESTIGATIONS of MAGNETIC FeCo and ABSORBING BTi THIN FILMS to IMPROVE the POLARIZING ABILITY of MAGNETIC MIRRORS

V.V.Pasyuk, D.A.Korneev, A.V.Petrenko, H.Jankovski*

Laboratory of Neutron Physics, JINR, Dubna

*Institute of Electronics, AMM, Cracow, Poland

To improve the polarizing ability of the magnetic mirrors used in the polarizing neutron guides the magnetic film and the absorbing sublayer were studied separately. The measurements of the reflectivity from Fe50Co50 thin films with the thickness of 150 nm and 110 nm sputtered on the float-glass substrate were carried out for the values of the external magnetic field equal to 300 Oe and 400 Oe. Figure 1(a) shows the reflectivity profiles R+ and R- for the 150 nm FeCo thin film in an external magnetic field of 300 Oe. Neutron scattering length density depth profiles got after the data fitting are shown in Figure 1(b). To obtain a highly effective polarizing thin film mirror it is necessary to exclude the reflection of neutrons with an unwanted spin state, i.e. to obtain R- =0. The investigated magnetic film has not been compensated in the sense that the neutron scattering length density Nb for the unwanted spin state is not zero. The film was not homogeneous in depth and we assumed that the near surface layer was enriched with cobalt. So the problem still remains of further selecting the composition and sputtering conditions for the Iron-Cobalt alloy.

It is worth to emphasize that for the FeCo film the "-" spin reflectivity (if compared to the "+" spin one) is very informative, and allows one to find more details of the interfacial neutron scattering length density profile.

The second requirement for the ideal thin film polarizing mirror is that the absorbing sublayer should be non-reflecting for the unwanted spin state. To elucidate the cause of the mentioned above polarization decrease in the large wavelength part of the neutron spectrum (λ>0.4nm) the reflectivities from Gd and GdTi thin films were measured [2]. It was shown that a fundamental barrier to obtaining a weakly reflecting alloy in a wide region of neutron wavelengths on the base of Gd is the presence of the low-lying resonances in the scattering cross-section which result in a strong dependence of the Gd scattering length on the neutron wavelength. This inconvenience is absent for Boron. So one can expect that the boron-based alloys will decrease the reflectivity of the absorbing sublayer and will improve the polarizing ability of magnetic polarizers. Calculated reflectivity profiles optimized for the minimum of reflection for BTi and BV thin films are shown in Figure 2. The very first ex-

perimental data we have got for a BTi thin film are shown in the insert to Figure 2. Now we are on the way to the sputtering optimization of the BTi and BV thin films.

1. D.A.Korneev, V.V.Pasyuk, H.Rzany, A.F.Schebetov: JINR Rep. P3-81-546 (1981) and P3-81-547 (1981)
2. D.A.Korneev, V.V.Pasyuk, A.V.Petrenko, H.Jankovski: in print at Nucl.Instr.Meth.

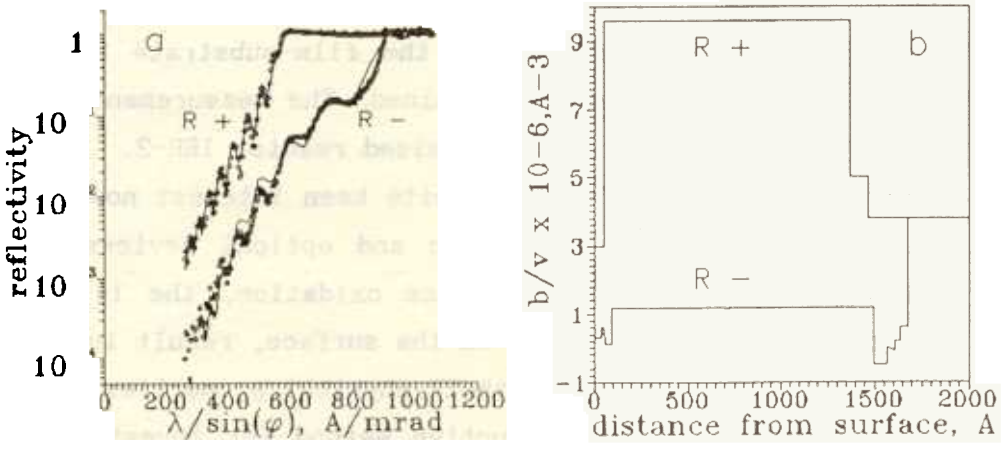

Fig.1. (a) Spin reflectivities for a 150 nm FeCo film on a float-glass substrate in an applied magnetic field of 300 Oe. The solid line is a theoretical fit to the data. (b) The neutron scattering length density profiles obtained from the least- squares fit to the experimental data are shown in figure 1(a).

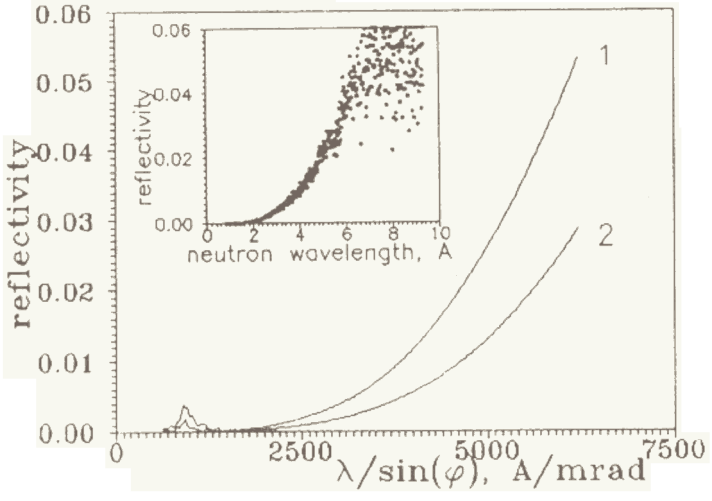

Fig.2. The reflectivity data for BTi (curve 1) and BV (curve 2) thin films optimized for the thickness and concentration for the minimum of reflection. The first experimental reflectivity profile for a BTi thin film measured at the glancing angle φ=5.0 mrad is shown in the insert.

A NEUTRON REFLECTIVITY STUDY OF TITANIUM THIN FILM AGING

V.V.Pasyuk, D.A.Korneev, A.V.Petrenko
Laboratory of Neutron Physics, JINR, Dubna
H.Jankovski
Institute of Electronics, Academy of Mining and Metallurgy
Cracow, Poland

The application of the neutron specular reflection to investigate the surface and interface of a 1630 Å Ti film is described. The thickness of the surface oxidized layer, interdiffusion at the film-substrate boundary and its alteration within two years were determined. The measurements were carried out on the spectrometer SPN-1 at the pulsed reactor IBR-2.

Thin films and multilayer structures excite keen interest now because of their being used extensively in electronic and optical devices. The processes of film aging, in particular surface oxidation, the layers interdiffusion, adsorption of light elements on the surface, result in film depth composition changes and, as a rule, in their physical properties alteration. The neutron reflectivity is a nondestructive method for investigating both surface and interfacial boundaries, and is a technique which helps to assess the interface density profiles and determine the layer density and thickness. The neutron specular reflection gives information on the neutron- optical potential profile normal to the reflecting surface, which is proportional to the spatial density of neutron-nucleus scattering lengths of the elements of the film.

In this work the neutron specular reflection was used to study thin Ti film aging. High sensitivity of the neutron reflection to oxygen presence in this film is due to a strong contrast of the negative neutron-optical potential of titanium and the positive one of oxygen.

Using the time-of-flight method at a fixed neutron incidence angle θ, we have measured the reflectivity spectral dependences within the wavelength range from 0.7 to 11 Å with the angle dispersion of 3%. The 1630 Å *Ti* film was sputtered on the float glass substrate [1]. The first reflectivity measurements were made two weeks after the film preparation, the second measurements were made in two years. The reflectivity spectral dependences are shown in figure 1. Observed reflectivity changes are connected with the neutron-optical potential (or the neutron scattering length density *Nb*) profile alteration. The sample consisted of a single layer on a substrate, how-

ever, in order to examine any surface and interfacial profiles the model of a series of discrete layers was used to have a good fit to the experimental data. The neutron scattering length density profiles are plotted in Fig.2.We have revealed, that there is a layer with the positive scattering length density near the surface. We suppose that after the film preparation the oxidized layer with a thickness of about 90 $\mathring{A}$ was formed. After being kept in air for two years, this layer thickness became equal to 120 $\mathring{A}$. Our suggestion is in accord with the conclusions of R.Pretorius et.al. [2], and M.A.Taubenblatt and C.R.Helms [3] who have shown that at room temperature a thin TiO_2 layer is formed on the Ti surface . The neutron scattering length density of the Ti film we have got is $b/v = -1.25 \times 10^{-6}$ $\mathring{A}^{-2}$. It is lower than the table value for bulk Ti $b/v = -1.945 \times 10^{-6}$ $\mathring{A}^{-2}$. So we may conclude that an admixture with a positive scattering length density is uniformly distributed in the Ti film. Most likely it is oxygen. A relatively broad titanium-glass interface is caused by the inhomogeneous structure of the glass, as it has been shown in [1]. Small but remarkable changes of the neutron scattering length density profile with aging are connected with the interdiffusion of Ti and SiO_2.

1 Korneev D.A., Pasyuk V.V., Petrenko A.V., Jankovsky H. Proceedings of XXV School on Physics "Condensed matter studies by nuclear methods", 1990, Singapore

2. R.Pretorius, J.M. Harris and M.A.Nicolet, Solid-State Electron, 21 1978, p.667

3 M.A.Taubenblatt and C.R.Helms, J.Appl.Phys.,53,1982,p.6308

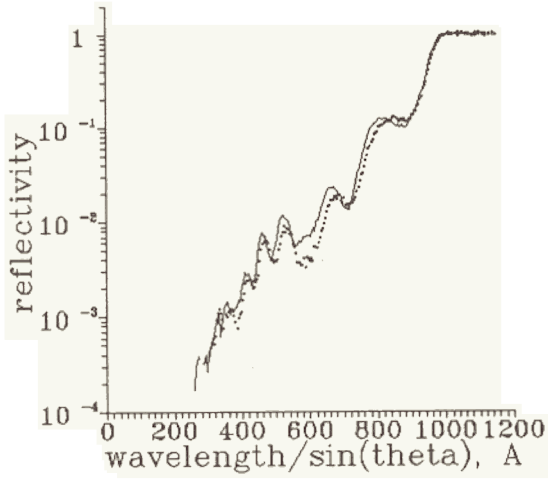

Fig.1. Reflectivity profiles for a Ti film on a float glass substrate measured in two weeks after the film preparation (points) and in two years after the film preparation (line).

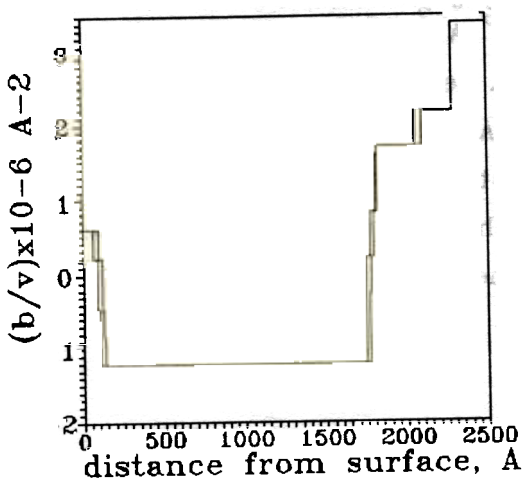

Fig.2. Neutron scattering length density profiles for a Ti film sputtered on a float glass substrate, as obtained from the least squares fit to the experimental data from fig.1.

Nuclear Physics with Neutrons

Within the scope of the field scientists of the Laboratory of Neutron Physics continued to study fundamental properties of the neutron, parity violation effects arising in the interaction of slow neutrons with nuclei, various decay channels of neutron resonances, the mechanism for the neutron nucleus interaction. Experiments were performed both on the high efficient time-of-flight spectrometer at the IBR-30 booster, JINR, and on neutron sources of the other research centers (PNPI, Gatchina, USSR; Los Alamos Laboratory, USA).

In the period reported in the Laboratory there have been accomplished measurements of the lifetime of ultracold neutrons in a gravitational trap. A team of LNP (Dubna) and PNPI (Gatchina) scientists has succeeded in suppressing significantly UCN losses during their storage in a trap and came up to the direct observation of the neutron decay exponent. The original procedure has allowed them to obtain the most precise for the present value for the neutron lifetime τ_n=888.4 sec and the corresponding to it value of the axial to vector component ratio of 1.2677±0.0025.

Modern estimates of the scattering amplitude of neutrons on electrons and of the polarizability of the neutron on its interaction with heavy nuclei (lead, bismuth) were analysed. It was concluded that the difference in these estimates made by Dubna and Jülich groups and in derived from them neutron mean square charge radius values: (+0.12(2) fm and −0.11(2) fm), is due to different mathematical approaches used to interprete the data. In particular, corrections for the imaginary part of the scattering length appear to be of significance in the extraction of the neutron polarizability coefficient from the neutron scattering cross section data.

The POLYANA instrument for resonance neutron polarization has been reconstructed to give a tenfold increase of efficiency. The search for parity violation effects in p-wave resonances continued. The resonances E_o=9.6 eV (Rb) and E_o = 7.0 eV, E_o = 21.9 eV (^{113}Cd) were investigated. Parity violation has been detected only in the resonance E_o= 7 eV ^{113}Cd: p = $(-9.8\pm3.0)\times10^{-3}$. The sign of the effect is of interest. It confirms the regularity of the effect behavior in various nuclei. This fact speaks in favour of the validity of the modern point of view on the mechanism for parity violation.

LNP-PNPI joint experiments continued on the observation of parity violation effects for few-nucleon systems in (n, p) and (n, α) reactions. These experiments have the aim to identify contributions of charged and neutral weak currents and to have estimated weak interaction constants. An upper estimate of $(-6.4\pm5.5)\times10^{-8}$ obtained for the ^{6}Li(n, α)^{3}H reaction is essentially lower in comparison with earlier estimates and with the theoretical estimate derived in the framework of the cluster model of ^{7}Li.

LNP scientists participated in the preparation of instrumentation for and in carrying out experiments on the LANSCE spectrometer (Los Alamos, USA) to study parity violation in radiative capture of polarized resonance neutrons. The latest value for parity violation effect in lanthanum has been confirmed and the new value of $(1.1\pm0.2)\times10^{-2}$ obtained for the resonance ^{117}Sn(n, α) E_o=1.33 eV. For resonances E_o = 26.4 eV, 34.0 eV there have been obtained only upper estimates of the effect.

Accomplishments in the measuring procedure development have permitted significant back-

ground suppression in experiments on the study of population of states at energies larger than 1 MeV in the gamma-decay of compound states of heavy nuclei. The new method has been developed for the construction of complex level schemes of heavy compound nuclei decay on the basis of the (n, α) and (n, 2α) data. This method allows one to construct decay schemes of complex nuclei up to excitation energies of 3–4 MeV at the nowadays best level of confidence. At that unambiguous identification of transition and level multiplets takes place.

Lower (but near to real) estimates on the total radiative strength function (RSF) were obtained for primary (E1+M1) gamma-transitions with energies above 0.5 MeV to show that:

- RSF's are better described in the framework of the model for the giant electric dipole resonance with the width Γ_G dependent on the temperature of the final state of nucleus and the energy of γ-quanta (as suggested by LNP and Voronezh State University theorists), than in the framework of the generally accepted model assuming the width Γ_G to be constant.

- To describe the RSF energy dependence one has to take into account enhanced γ-transitions between single particle 4S-3P neutron shells, whose contribution is very large. Gamma-multiplicity fluctuations in some resonances of ^{147}Sm in the energy range from 15 to 900 eV were measured using the NaJ(Tl) based 4π-detector of γ-quanta. Distinct correlation between the resonance multiplicity spectrum and resonance spin was observed to help spin assignments to 90 resonances.

Investigations of the scattering of 1–300 keV neutrons from gaseous samples of krypton and xenon have provided data on the neutron strength functions $S^1_{1/2}$ and $S^1_{3/2}$ and contributions of far-lying levels R^∞_0 and R^∞_1. In krypton experiments there has been refined the behaviour of the $R_1(A)$ curve at A=70–90 showing an anomalous sign of the neutron p-wave phase shift.

Experiments continued on the study of (n,p) and (n,α) reactions on stable and radioactive nuclei. LNP scientists in cooperation with a group from the Institute for Nuclear Research of the Ukranian Academy of Sciences have measured thermal neutron cross sections on rare isotopes,^{36}Ar(n,α)^{33}S and ^{50}V(n,p)^{50}Ti.

The collaboration with Peking University scientists has yielded the experimental procedure and test measurements of charged particle spectra from reactions with fast neutrons resulting in the improvement of the multisection ionization chamber capable of energy and range of particles analysis.

Fission scientists investigated yields of certain fragments in certain ^{239}Pu resonances from 0.2 eV to 230 eV by measuring characteristic γ-transitions of fission fragments. A peculiarity in the mass dependence of relative fission fragments yields in resonances has been observed to be in antiphase with the analogous dependence from ^{235}U experiments by Hambsch et al.

Average parameters of fission γ-quanta multiplicities were calculated by weighing to be n_γ=7.26±0.19, E_{tot}=6.68±0.12 MeV and the average energy E_γ=0.98±0.03 MeV.

Model estimates of fission characteristics of ^{235}U and ^{239}U in the low energy range were analysed. For the average characteristics of the (n, γ, f) process there have been obtained the following values: ^{235}U resonances with $J^\pi = 4^-$:

$$\overline{\Gamma}_{\gamma f}\overline{N}_{\gamma f} = (0.42 \pm 0.10) meV,$$

$$\overline{\Gamma}_{\gamma f}\overline{E}_{\gamma f} = (410 \pm 120) eV^2$$

^{239}Pu resonances with $J^{\pi} = 1^{+}$:

$$\overline{\Gamma}_{\gamma f}\overline{N}_{\gamma f} = (1.5 \pm 0.5)meV,$$

$$\overline{\Gamma}_{\gamma f}\overline{E}_{\gamma f} = (2150 \pm 650)eV^2$$

It is shown that experimentally observed fluctuations of characteristics of total fission in 4^{-} resonances of ^{235}Pu can be explained in the framework of the multimode fission model taking into account the (n, γf) process.

At the Laboratory there are going construction works on the UGRA instrument for the determination of the neutron polarizability coefficient, (α_n) by high precision measurements of angular distributions of neutrons scattered on heavy nuclei. An error in measured relative asymmetry of forward-backward scattering must not exceed the value of $(2\text{–}3)\times10^{-4}$ to reduce the error in α_n down to 3×10^{-43}cm^3. This instrument can be also used for:

- the search of light scalar particles, the interaction carriers;
- the search for and investigation of mixed (s+d) resonances;
- the determination of spin channels mixtures in p-wave resonances;
- the nondestructive quantitative analysis of samples for hydrogen present in them.

The new chopper-monochromator for cold neutrons based on small angle neutron scattering alteration by means of magnetized/demagnetized foils has been proposed. An "inelastic" adiabatic spin-flipper version has been developed for the case of cold neutrons.

Condensed Matter Studies by Neutron Scattering

In the season of 1990-1991 experiments were mainly conducted on eight spectrometers positioned on 6 beam-lines of the IBR-2 reactor. With respect to the method used the experiments can be classified as follows:

- diffraction studies on the spectrometers DN-2, NSVR and SNIM-2;
- SANS studies on the MURN spectrometer;
- polarized neutron reflection studies on the SPN spectrometer;
- neutron spectroscopy measurements on the DIN, KDSOG-M and NERA-PR spectrometers to study inelastic scattering of neutrons.

Investigations of crystal structures with neutron diffraction methods at the IBR-2 reactor are carried out in the directions:

- structure study experiments on single- and polycrystals;
- phase transitions in superconductors, ferroelastics and superionic samples;
- phase transitions in the presence of strong external magnetic fields;
- structure of lipid membranes;
- transition phenomena investigated by diffraction techniques.

They, for the most part, are the traditional directions of research for LNP, where it enjoys well established cooperation with numerous scientific institutions active in the field.

Of structure works a noticeable role belongs to HTSC studies. In experiments on a single crystal A.I.Beskrovnyi and colleagues investigated modulated structure in $Bi_2(Ca, Sr)_3Cu_2O_{8+\gamma}$. Though with a very small single crystal ($1.5\times10\times0.03$ mm^3) they have succeeded in measuring (in a wide temperature range) satellite peaks in number sufficient to develope a model. In spite of expectations the structure modulation does not change observably in the temperature range 8 K to 920 K.

With $YBa_2Cu_3O_7$ a detailed study of structure effects connected with the substitution of copper by iron or nickel was undertaken. In order to enhance the substitution effect and thus increase the diffraction data reliability the contrast variation technique was applied with the use of ^{57}Fe and ^{58}Ni isotopes (A.M.Balagurov et al.). The results have confirmed an earlier guess that copper substitution by other 3-d metals, which leads to fast degradation of superconductive properties, reflects preferential substitution in the CuO_2 plane. It has been shown that both nickel and iron (at concentrations $\geq$10%) penetrate actively into the Cu_2O plane. At that, however, the decrease in T is not so sharp as in the case of Cu by Co substitution, that occurs only in CuO chains. Then the conclusion follows that it is not only the substitution site that is of significance, but also some purely structural characteristics play the important role here, the bond length value, in particular.

With Y123 ceramics a series of experiments were conducted to study oxygen diffusion in samples that were cooled at different cooling rates, annealed at constant temperature or heated slowly. The one-dimensional model of diffusion appeared to be sufficient to describe oxygen diffusion. Estimates of diffusion coefficients were made for each of the above-mentioned regimes of sample treatment.

A comparatively new branch of research at the IBR-2 reactor are the real time experiments. Quite a number of interesting data have been obtained in them. Of recent ones the emphasis should be laid on the study of phase transitions in different compounds, e.g. titanium hydrate, $Cu(Li,V)_{0.4}Fe_{1.6}O_4$ spinel, high pressure heavy ice D_2O. The method developed by LNP scientists allows them to carry out these investigations in the second resolution range not achieved

yet at other neutron sources. The measurements were performed on the diffractometer DN-2, currently the most high luminosity and powerful diffractometer in the IBR-2 suit.

The NSVR diffractometer dedicated for texture studies is positioned on the 100 m flight path of the reactor. It has a lower luminosity but a three times higher resolving power that makes it very effective in investigating textures of complex low-symmetry materials. Textures of various geological samples were investigated on this diffractometer (K.Helming, W.Voitus, K.Walther et al.).

On the diffractometer equipped with a pulsed magnet, SNIM-2, there was investigated the kinetics of spin-flop transitions in single crystals of Cr_2O and α-Fe_2O_3 induced by a pulsed magnetic field of 1 msec duration and 150 KOe amplitude (D.Georgiev, V.V.Nietz et al.).

Works published in the past year reflect also efforts made by the Laboratory staff to upgrade now existing and build new neutron diffractometers. In particular V.L.Aksenov, A.M.Balagurov et al. report on the work being done to put into operation the new Fourier diffractometer with a resolving power at a level of 0.05%.

The Small Angle Neutron Scattering (SANS) spectrometer MURN is a high luminosity instrument built for the investigation of SANS in isotropic systems. It allows one to measure small scattering cross-sections in absolute units in rather a wide range (0.05–0.7 reciprocal Angstroms) of scattering vector lengths. Main activities in the season 90/91 were aimed at a search for new applications of its advantages.

In the ternary system AOT–Water–Benzene an alternative approach to the well-known contrast variation technique was approved. It is found, that variation of a so-called internal contrast (isotopic composition of the water nucleus in inverse micelles) do lead to the same results as external contrast variation, if measurements are done well inside the micelle stability gap on the phase diagram. However, near the gap's borders isotopic substitution affects strongly the structural properties of solutions and different ways of contrast variation reveal largely different structures. This observation seems to be very important for the safe interpretation of SANS data. Besides of this, investigation of the inverse micelle friability phenomenon, observed previously at lowest water contents, was continued with other solvents and in a widened range of water contents.

Properties of water solutions of small organic molecules is another new field of SANS application. This year we have tried to find SANS evidence of the existence of a long range repulsive interaction between solute molecules at very high dilutions (mole fraction as small as 0.001), recently proposed on the basis of calorimetric experiments. Though the SANS experiments were rather accurate, no important signs of the assumed repulsion were observed.

The third micellar system investigated recently was the (oxyethylene-oxypropylene-oxyethylene) block copolymer in water. Very detailed experiments in a wide range of temperatures and concentrations allowed one to determine experimentally a number of characteristics of this system, with the degree of swelling of a hydrophobic micellar nucleus among them.

A rather unexpected field of SANS application is connected with an attempt to investigate the Porod region of the scattering cross-section from components of cement (the clinker minerals) and from cement pastes at different steps of their aging. Results, obtained to-date, show, that in chemical transformations which are the essence of cement pastes hardening, there occur very important changes in spatial arrangement of phase boundaries, responsible for small angle scattering observed. Important changes are also detected in scattering curves during the aging of a cement paste to the age of up to 241 days.

The whole host of results obtained are in many relations new and their interpretation in

terms of the physical chemistry of solutions and solids requires some efforts to be made.

The time-of-flight spectrometer of polarized neutrons SPN was found to be a very effective instrument for the investigation of magnetic properties of surfaces of thin films in the reflectometry mode. Among the results obtained during the season 90/91, the most interesting, perhaps, is the observation of the dependence of the magnetic field penetration depth in superconducting niobium on the thickness of the niobium film. The dependence was discovered to be rather strong (the penetration depths of 43 nm, 90 nm and 145 nm in a massive sample and in films 700 nm and 255 nm thick, respectively, are quoted). However, up-to-date there is no satisfactory theoretical explanation of this phenomenon.

An interesting and important step was done towards the realization of the "non-reflecting mirror", an important component of ideal neutron mirror-polarizer. The reflection of unwanted spin from known constructions of polarizing mirrors is the important factor that sets limit on the application of these otherwise nice devices. First experiments with absorbing sub-layers made of thin films of titanium and vanadium borides have shown that in this way the properties of polarizing mirrors can be improved drastically.

Another interesting possibility opens with the reflectometric observation of aging of a thin (163 nm) titanium film. It was found that on the surface of metallic titanium at normal conditions during first two weeks the titanium oxide layer 9 nm thick appeared, while during the following two years this oxide layer has thickened to 12 nm.

Two direct geometry spectrometers, DIN-2PI and DIN-2PR for double analysis of neutron energy by time-of-flight act in parallel on one neutron beam-line at a distance of 20 m and 95 m from the reactor core, respectively. On the higher luminosity one, DIN-2PI, experiments on inelastic and quasielastic scattering of neutrons on samples of liquid helium, liquid metals and adsorbed water continued. Measurements of phonon spectra of V-O, V-N, TaV_xN_y continue the investigation of nitrogen and oxygen solid solutions in metals. For ThO_2, VO_2 and $ZrH_xU_{0.32}$ (x=16 and 1.84) dependences of the phonon density of states on room temperatures up to about 1300 K were measured. On the DIN-2PR a first series of experiments on the scattering of neutrons with an incident energy of 200 meV from liquid helium at T=4.2 K and 1.4 K has been conducted in continuation of the study of Bose condensate and elementary excitations in liquid helium at large momentum transfers and good energy resolution.

The new spectrometer, NERA-PR, that exploits the inverted geometry principle for inelastic and quasielastic neutron scattering studies was positioned at a distance of 109 m from the reactor core and began operations. Energy analysis of scattered neutrons by their reflection to an angle of 175° from a single crystal of Cu(111) allows one to investigate neutron quasielastic scattering with a resolution of $\Delta E = 0.05$ meV in rather a wide momentum transfer range from 0.5 to 5Å. Experiments were initiated to investigate stochastic reorientations of molecules in liquid crystals. The beryllium filter used in the spectrometer for energy analysis provides for high luminosity and good resolution at large momentum transfers ($50 \leq \Delta E \leq 500$) meV. Partial vibrational densities of copper and oxygen atoms in $YBa_2Cu_3^*O_{6+x}$ (x = 0.95, 0.25) were determined by measuring neutron inelastic scattering spectra with copper isotopes (^{65}Cu and ^{63}Cu) having different cross sections for neutron scattering. Measurements of phonon spectra of NH_4Cl and H_2O at T = 290 K and 80 K at pressures up to 10 Kbar have proved the beryllium filter method on the NERA-PR spectrometer to have high enough luminosity and resolution for investigating phonon spectra on pressure dependences.

On the KDSOG-M spectrometer, that also exploits the inverted geometry principle, the energy analysis of scattered neutrons is performed with the help of pyrolytic graphite plates

installed behind the beryllium filter. High luminosity and a relatively good resolution in the energy transfer range up to 200 meV allows effective study of inelastic scattering from hydrogen-free samples or samples with low hydrogen content that are the usual case in the spectroscopy of adsorbed molecules. A comparative study has been undertaken of vibrational spectra of a number of dispersed silicas (silicagel, aerogel, aerosil, silochrom). The data analysis has allowed identification of adsorbed or retained water in investigated samples. These spectra are much different and thus point to different configurations of adsorbing centers in investigated silica samples. Experimental data are compared with quantum mechanical calculations in the framework of a selfconsistent cluster approach to allow the conclusion about the polymorphism of dispersed silicas being in dependence on the sample manufacturing technology (see works by E.F.Sheka, V.Khavryutchenko, I.Natkaniec et al.).

In the past years the chief object of research on the KDSOG-M spectrometer were the crystal field excitations in rare-earths containing compounds and alloys. In the reported period there continued investigations of magnetic excitations in heavy fermion systems like $CeCu_4Al$, $CeCu_4Ga$ and $CeCu_2Si_2$. In them it was important to carefully take into account the phonon spectra that affect essentially the neutron inelastic scattering spectra. For that there were measured simultaneously spectra from stoichiometric lanthanum samples of $LaCu_4Al$, $LaCu_4Si_2$ showing no magnetic scattering. The characteristic feature of the magnetic scattering spectra of cerium containing heavy fermion compounds is the only one Lorentzian-like crystal field transition having a rather broad energy distribution and an intense contribution from quasielastic neutron scattering also with a broad energy distribution of the Lorentzian type (see works by E.A.Goremychkin et al.).

Study of the crystal electric field parameters continued with the metallic rare-earth compounds of the isostructural family $Re_{0.05}Y_{0.95}Ni_2$ (where R = Nd, Pr, Tb, Tm, Er, Dy, Ho). Rare-earth metals in this family are diluted strongly with nonmagnetic yttrium atoms and the 4-f shell interaction with crystal electric field can be studied in a most pure form.

By investigating crystal electric field transitions in Nd_2CuO_4 in dependence on temperature (from 10 to 300 K) it appeared possible to identify transitions from excited states. Data interpretation with account for the mixing between the ground and first excited state has for the first time yielded a satisfactory description of neutron inelastic scattering data as well as the qualitative description of the magnetic susceptibility measurement data.

In 1990-1991 the LNP scientists took part in joint experiments at the ISIS of RAL, UK. On the inelastic scattering spectrometers HET and MARI the temperature dependence of the widths of the crystal field transitions in $Y_{0.9}Tm_{0.1}Ba_2Cu_3O_{6+x}$ (x = 0.1 and 0.9) was measured. Results point to the formation of a gap in a spin excitation spectrum at temperatures about 20 K above T_c.

The HET record resolution at high energy transfer allowed investigation of intermultiplet transitions in a heavy fermion system $CeAl_3$. Splitting of the first excited CF multiplet was found to be three times stronger than that of the main one, in evidence of a considerable contribution of conductivity electrons into the CF potential.

On the quasielastic scattering spectrometer IRIS there was investigated the dynamics of NH_4 groups reorientations in the process of dipole glass formation in the system $K_{1-x}(NH_4)_xH_2PO_4$ (x = 0.4 and 0.9).

Domain structure formation following phase transitions in a ferroelectric crystal of $LiKSO_4$ was investigated on the SXD diffractometer.

Low Temperature Research

HTSC SQUID's and low temperature SQUID's

In the reported period at the Low Temperature Department the main objects of research were HTSC-SQUIDs and SQUID-based measurement systems. The work based on the study of the characteristic voltage of bridges from HTSC ceramics. Results obtained have shown that this characteristic voltage, i.e. the product of the critical current through bridge by its normal resistance, is constant and amounts to about 20 mV. In the framework of a simple model it appeared possible to explain this effect by the existence in HTSC ceramics of intergrain contacts (links) having the characteristic size of the order of the coherence length in HTSC materials .

The coherence length in HTSC's is of the order of ten angstroms and it is a hard task to build an artificial contact of a size. So it was only natural that we had to overcome many difficulties in creating thin film HTSC-SQUIDs. The existence in ceramics of intergrain contacts of the coherence length size allows one to give priority to creating SQUIDs operating at nitrogen boiling temperature as the application of these contacts .

Within the scope of this first priority concept the Low Temperature Department scientists have created HTSC SQUIDs operating at liquid nitrogen temperatures. These SQUIDs formed a convenient basis for building measurement systems like magnetic cardiometer-gradientometer, sensitive galvanometer and geophysical magnetometer, that are detailed below.

The intense use of conventional low-temperature SQUIDs has led to the creation of the magnetic susceptibility detector with a magnetic moment resolution of 10^{-12} Am^2 and of the superconducting quantum detector of weak magnetic moments. The latter provides important information on HTSCs and on the other weak magnetic materials. Its main parameters are given in the appendix.

Low temperature experiments

In this field the main activity was concentrated on investigation of HTSC properties. By using very high sensitivity device to measure small magnetic moments the method was developed for measuring magnetic moment long-time relaxation and critical Josephson currents in YBaCuO ceramics. Measurements performed have yielded the dependence J_c (H,T) and the temperature dependence of the first critical Josephson field.

For the HTSC SQUIDs applications it was found that the use of high quality magnetic screens is crucial for the SQUID operation. The investigation of hollow cylindrical screens at liquid nitrogen temperatures using a fluxgate teslameter has been undertaken. The critical parameters of the screens were measured and their behaviour in fields above the critical one examined to show the possibility of using these screens at liquid nitrogen temperatures. A test screen has been made from $YBa_2Cu_3O_{7-x}$ ceramics doped with Ag to have a break-down field of 12 Oe. On the basis of these investigations was built a high sensitive SQUID-based galvanometer operating at liquid nitrogen temperatures for measuring direct and low-frequency alternating currents. The galvanometer's direct current sensitivity is about 0.5 nA at the internal resistance of about 20 Ω. It has the energy resolution in the white noise region of 2×10^{-21}J/Hz. A gain in energy resolution in comparison with instruments operating at "warm" temperatures is over 4 orders of magnitude.

It was found that HTSC SQUIDs are rather sensitive to atmospheric conditions. To avoid this serious problem a HTSC SQUID from BSCCO ceramics was created with Pb addition operating at liquid nitrogen temperatures. The white noise spectral density is $4\times10^{-4}\Phi_o/Hz^{1/2}$. The 1/f noise prevails at frequencies lower than few tens of Hz. The advantage of this SQUID is the stable operation in atmospheric conditions.

Activation Analysis

This method on pulsed neutron sources has unique possibilities to investigate the traces of different elements, in particular rare earths in samples. This year a cycle of works were accomplished on the investigation of distributions of basic and trace elements, including rare earths (REE's) in geological structures of some oil extraction areas in Cuba. The results have indicated a significant increase in REE's contents at the level of 500-700 m before the oil stratum in a well. The fact that some REE's have strong neutron capture cross sections (hundreds, thousands of barns) allows the use of prompt neutrons, following thermal neutron capture in REE's, for the analysis of neutron logging data.

The Laboratory continued to widen the application of neutron activation analysis methods to the solution of environment protection problems. This work included:

- investigation of the role of mineral fertilizers (their toxic and REE components) in environment polution, including human beings;
- investigation of distributions of basic and trace elements, including toxic ones (Cu, Zn, As, Cd, Hg, etc.) and rare earths, in corn crops being raised in the main agricultural areas of this country.

The second investigation has in the main served the purpose of the production of ecologically pure food for children. Methods have been developed for the determination of the macro- and micro-element content of wheat, ray, rice, potatoes (starch) and buckwheat in natural samples and in ash residuals.

The results of both investigations have been reported at the International Conference on Modern Trends in Activation Analysis, MTAA-8, Vienna, Austria, September 1991 and will be published in the Conference Proceedings.

In 1991 design work on AZOT-1 and AZOT-2 instruments for express analysis of nitrogen content in protein of grains and animal feed has been accomplished and their large scale production started. Electronic equipment of the instruments has been transformed from IBM- PC based CAMAC to CAMAC free computer variant.

Radiation Research

In 1991 the LNP group in cooperation with a group from the Laboratory of Super High Energies, JINR, staged experiments on IBR-2 neutron beams to investigate:

- resistivity of solid state detectors (Si) to fission neutron radiation;
- U and Th contents in construction materials of the neutrino detector.

In 1991 methods of fast beam formation with a negligible X-ray contribution have been developed and a first set of Si-detectors and silicon samples irradiated. The procedure for impurity content determination in silicon and silicon-based products has been developed and tested on the REGATA instrument at the IBR-2 reactor.

Analysis of U and Th contents in some materials and in construction materials of the neutrino detector has shown that all they contain significant amounts of U at Th (units, tens of ppm). At the same time for a low background detector these contents must be 1000–10000 times less.

Studies of the Elemental Composition of Surfaces

Experimental procedures developed for measurements at Van de Graaf EG-5 were used to investigate near-surface layers in metallic glasses, superlattices, microelectronic elements, implanted samples, semi-conductors, etc. under contracts between institutes of JINR member-states.

In this year a systematic study of ceramics and HTSC films on various substrates was undertaken. HTSC samples manufactured in a number of USSR institutes and the other JINR member-states institutes were investigated using experimental procedures developed on the EG-5 generator basis. In PIXE experiments there was made a qualitative element analysis of investigated samples including the analysis for trace elements. In RBS experiments there were investigated depth penetration profiles of Y, Ba, Cu and O in films and of constituent elements of substrate materials. As the result, conclusions were made about stoichiometry of investigated samples, the thickness of superconducting layers and the extent of their diffusion into substrate materials. The FRD method was used to investigate the hydrogen content in near-surface layers.

In the reported year the method for measuring channelling RBS spectra was in the process of testing. During the test angular yield curves were measured for crystals of silicon and strontium titanate. Typical spectra and angular yield curves characteristic of channelling were obtained. Experiments with HTSC films have shown the imperfectness of their crystal structure that is nowadays interpreted as the essential disorientation of crystallites.

Other Activities

The process of the tetra-ortho transition in yttrium HTSC ceramics under processing in halogen vapours (Br, I) was investigated. X-ray and neutron diffraction experiments have demonstrated that in parallel with superconducting orthostructure recovery there occurs decomposition and amorphisation of a considerable sample volume and the orthophase is formed due to the sorbtion of released oxygen and not due to halogen intercalation into the crystal lattice. These experiments have also confirmed the high capability of the orthophase to recrystalize that was observed at irradiation of yttrium ceramics with charged particles at low temperatures.

The influence was investigated of heavy ions irradiation on the characteristics of HTSC-based microbolometers. Besides the fact that the answer was obtained to the question about the radiation resistance of these first instruments on the HTSC basis, it appeared possible to judge about low-temperature structural fluctuations in films materials from the behaviour of their noise characteristics.

The time-of-flight method was developed for measuring photoelectron spectra of HTSC's on their irradiation with laser pulses in a nanosecond range. The energy resolution of 50 meV was achieved and the photoemission threshold in polycrystal samples of $YBa_2Cu_3O_7$ HTSC ceramics was measured to be (5.5±0.5) eV.

JOINT INSTITUTE FOR NUCLEAR RESEARCH

HTSC SQUID - MAGNETOMETER

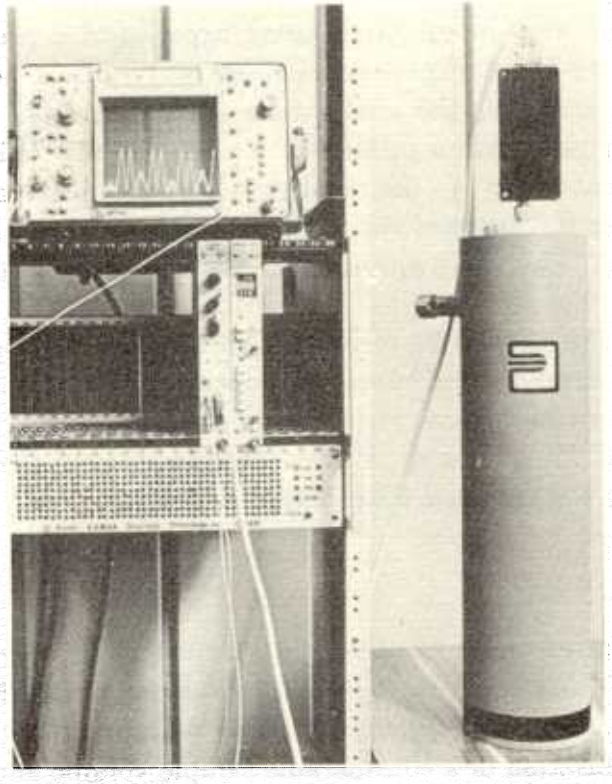

Purpose

The magnetometer is designed for geophysical investigations, magnetic anomalies search, experiments based on weak magnetic fields measurement.

Characteristic features

- use of liquid nitrogen as cooling medium
- automated entering into operating mode with the characteristics tuning display
- possibility of operation under field conditions with a LAPTOP computer
- Fourier-analysis of a signal with the spectrum shown in the display
- coordinated signal filtration and synchronous rejection of periodic noise

Instrument Details

1. Device operating temperature, K	77
2. Measurement dynamic range, not less, ϕ_o	$\pm 10^6$
3. Resolving power, not worse:	
on field, Tl/Hz$^{1/2}$	$1.2 \cdot 10^{-13}$
on flux, ϕ_o/Hz$^{1/2}$	$3 \cdot 10^{-4}$
4. Energy sensitivity, not worse, J/Hz	$9 \cdot 10^{-28}$
5. Digitizing error, not more, ϕ_o	$5 \cdot 10^{-4}$
6. Signal increment rate, not less, ϕ_o/S	1000
7. Bandwidth, Hz	0 - 150
8. Noise suppression with industrial frequency and its harmonics, not less, dB	60 (50Hz)

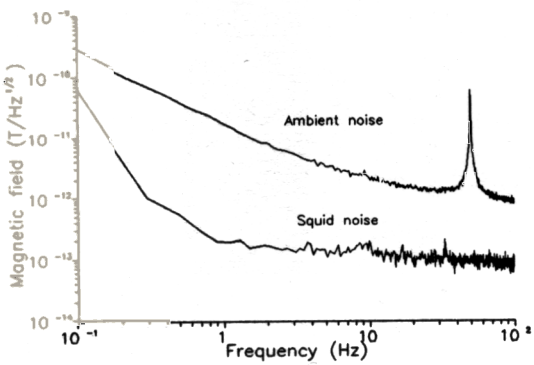

Example of a real geomagnetic field and SQUID noise (T=77K) measured with a HTSC magnetometer

Provisional users, please, apply to :

B.V.Vasiliev, Laboratory of Neutron Physics, JINR
141980, Dubna, Moscow district, USSR.
Phone: 926-22-96 (from Moscow), 62-789 (from Dubna)
E-mail number: bav56@lnp.jinr.dubna.su

JOINT INSTITUTE FOR NUCLEAR RESEARCH

SUPERCONDUCTIVE QUANTUM SMALL MAGNETIC MOMENT MEASUREMENT SYSTEM

Purpose

is designed for small magnetic moment measurement of the weakly magnetic samples in a wide temperature and field range.

Equipment

1. Cryogenic equipment components :
   - helium cryostat with a level gauge;
   - anti-cryostat with a temperature controller.
2. Magnetic system components :
   - superconducting solenoid;
   - magnetic flux stabilizer .
3. Sample transportation system .
4. Measurement and control equipment components :
   - SQUID with a magnetic flux transformer ;
   - CAMAC crate with a set of functional units and power supply.
5. Controlling computer, IBM PC/AT .
6. Software package for signal and system control .

Specifications

1. Magnetic moment dynamic range not less than , dB	160
2. Magnetic moment resolution , $A \cdot m^2 / Hz^{1/2}$	$3 \cdot 10^{-12}$
3. Magnetic field range , Oe	$10^{-3} \ldots 10^{2}$
4. Magnetic field stability not more than , $hour^{-1}$	10^{-6}
5. Time of entering to the regime of stable time not more than , min	10
6. Temperature range , K	4 . . . 300
7. Temperature stability not worse than , mK	± 5 (at 5 K)
8. Maximum sample diameter , mm	3
9. Total sample path, mm	60
10. Sample position accuracy not worse than	$2.5 \cdot 10^{-3}$
11. Maximum sample travel velocity , mm/s	2
12. Liquid helium capacity , l	30
13. Liquid helium consumption , l/day	4

Provisional users, please, apply to :

B.V. Vasiliev , Laboratory of Neutron Physics , JINR ,
141980 , Dubna , Moscow district , USSR .
Phone : 926-22-96 (from Moscow) , 62-789 (from Dubna) .
E - mail number : bav56@lnp . jinr . dubna . su

DATA ACQUISITION AND PROCESSING SYSTEMS

Computer Networks

During the year, possibilities were considered of using industrial electronic units and SU-produced optic cables in the network ETHERNET, the product of the DEC firm. In result, three electronic units and three types of optic cables were selected. They were tested by including them into the local network for a month. Their parameters have turned out to be no worse than analogous western units have.

Work continued on the development of the SONET LAN network:

- the "C" language procedures library was organized to enable remote access to files (this library is the basis for the realization of computer-aided distribution systems on the SONET-2 network hardware base).

Central Processor Computers

The Central Processor formed of the PDP-11/70 complex and two μVAX-II computers worked satisfactorily during the entire period of LNP reactors' scheduled operation time in the reported year. Our main concern was the lack of spare disks packs for 300 Mbyte drivers, as they might cause instability in Processer's performance. As the PDP-11/70 is aging fast both physically and morally, an urgent need is felt to substitute the aged for new, more perfect and reliable media of physical data archivization to be included into the ETHERNET or into the μVAX-II complex. To pursue the aim we continued developing terminal network of the PDP-11/70 and the μVAX-II.1991 works on the organization of electronic mail have brought new life to the JINET network of the JINR.

Physical Instrumentation

In 1990-1991, works were going on to convert LNP physical instruments to PC/XT, AT-aided ones and to develope further the software for some physical instruments already operated with PC's. The first phase of the TEKST project started work for the experiment.The DIFRAN and SPN-1 were switched on to the PC/AT-268. The instruments NERA-PR, SNIM-2, DN-2, DPP, NSVR, KDSOG have been modified. Works have been accomplished on arranging the lay-out for experiments with UCN. Preparatory work is going for the assembly of the HRFD on beam line 5 of the IBR-2.

To improve IBR-2 neutron beams additional systems for choppers phasing were mounted on beam line 5 (for the HRFD) and on beam line 7 (for the NERA-PR).

On IBR-30 beam-lines there were:

- accomplished works on the switching on to PC's and modification of the POLYANA and POISK lay-outs;
- put into operation the DN-3;

- put into operation the PC/AT-386 + CAMAC complex for the investigation of (n, 2γ) reactions.

Electronic Systems and Units

Hardware and software for thermostats control were developed, including:
- the CAMAC microprocessor controller;
- the programmable temperature regulator with keyboard control;
- the commutator for linking the terminal with automated microprocessor systems;
- to serve experiments on the DN-2 and DPP and to manufacture HTSC samples.

A fast electronics complex was created for the multisection plutonium chamber for experiments on the study of (n, γ, f) reactions.

A set of new CAMAC units have been developed, including:
- the 16-input unit for time spectra coding with extra functional capabilities;
- the on-off automated unit for the measuring module;
- the detector number coding unit;
- spectrometric ADC's for 1K and 8K channels with a frequency of 200 MHz.

Software

Work continued on the development of SONET-2 software for interactive access of a PC subscriber to directories and service files.

A programme has been developed for the analysis and processing of one-dimensional spectra on PC in a graphic mode. The programme is mainly dedicated to processing (per channel, per group) of the data from fission and transmission experiments. The programme performs addition, subtraction, multiplication, etc., of one-dimensional spectra and background generation according to different models specific for a given experiment.

In 1991 work has been accomplished on the development and upgrading of PC-aided measurement systems:
- for the spectrometers SNIM-2, DIFRAN, POISK, POLYANA;
- for the spectrometers TEKST and SPN-1 (software first phase);
- for the spectrometers DN-2 and DN-3 (for mechanical devices control);
- for the spectrometers NERA-PR and KDSOG-M (initial phase).

Organization and Communications

SEMINARS

"The Rutherford computer network and ISIS data acquisition system".
W.C.A.PULFORD, Rutherford Appleton Laboratory, U.K.

"The development status of the new high resolution neutron source at JINR".
L.B.PIKELNER, E.A.PERELSTEIN, V.L.LOMIDZE, JINR, USSR.

"Neutron scattering in single crystals".
S.Sh.SHILSTEIN, KIAE, USSR.

"The prospects for the Laboratory computing center development".
G.P.ZHUKOV, JINR, USSR.

"Precise experiments on neutron lifetime with ultra cold neutrons".
A.P.SEREBROV, LNPI, USSR.

"The electronic mail at JINR".
V.P.SHIRIKOV, JINR, USSR.

"Magnetic inelastic neutron scattering at ISIS".
R.OSBORN, RAL, U.K.

"The pressure of light".
M.A.OLSHANYJ, ISAN, USSR.

"Structural investigations of high-T_c materials at the Laboratory of Neutron Physics".
A.M.BALAGUROV, JINR, USSR.

"Structure and dynamics of quantum films on graphite".
H.LAUTER, ILL, France.

" About one possibility of improvement of thermal neutron extraction from moderators".
O.N.GONCHARENKO, INI, USSR.

"Excitation of atomic electron shells by neutrons".
I.N.MIKHAILOV, JINR, USSR.

"Daresbury synhrotron radiation facility".
J.P.DUKE, Daresbury Laboratory, U.K.

"What is C–60 ?".
A.V.ELETSKIJ, B.M.SMIRNOV, KIAE, USSR.

"Los Alamos neutron facilities".
Yu.P.POPOV, Yu.M.GLEDENOV, E.I.SHARAPOV, JINR, USSR.

Meetings

VI International School on Neutron Physics

8-18 October 1990, Alushta, the Crimea

This School dedicated to the memory of Professor I.M.Frank (23.10.1908–22.06.1990), the Nobel Prize Winner, was organized by the JINR with support from the Ministry of Atomic Power and Industry of the USSR. Specialists in neutron physics discussed modern trends of development of neutron sources, present status of experimental and theoretical research in the field of condensed matter and nuclear physics with neutrons as well as their great potential to be realized. General survey of scientific activities at already operating sources of neutrons and at those under construction in different countries has been presented. 251 scientists from 18 countries took part in this School.

The School Proceedings were published by the Publishing Department of JINR in 1991.

Investigation of Nuclei with Neutrons

12-14 March 1991, Dubna

The II Workshop was attended by 80 scientists, including 15 from the JINR Member States, 1 from the USA and 50 from the USSR. There was discussed the present state, perspectives and the program for physical investigations in the frame of the project of the new high resolution neutron source (HRNS). The results of joint experiments of LNP (JINR) and LNPI (Gatchina) on the determination with a record precision of the neutron lifetime by the UCN storage method were first reported. There were presented recent results in the physics of fission that permitted one to look differently at the descent of a fissioning nucleus from the saddle point. The cross section data for neutron induced reactions on unstable target nuclei were also reported. They are important in astrophysics.

The participants called for support for advanced studies in nuclear physics with neutrons and suggested that this Workshop should become traditional and of international status.

International Workshop on Advanced Pulsed Neutron Sources

25-27 June 1991, Dubna

The Workshop aimed at considering the possibilities of upgrading now operating and of creating new powerful sources of neutrons. The scientific leaders of all high intensity neutron sources took part in the Workshop. Among them were 9 scientists from the JINR Non-Member States and 50 from the JINR and the USSR. In a number of reports quite new ideas were advanced. It is acknowledged that financial support from the Institute of Nuclear Research in Troitsk has contributed much to the success of the Workshop organization.

USA-USSR Workshop on Condensed Matter Physics

18-21 June 1991, Upton, USA

The Workshop was organized by leading neutron centers of the USA and the USSR with the support of the Department of Energy of the USA Government. The Workshop was held at the Brookhaven National Laboratory, and it was attended by 10 scientists from the USA and 10 from the USSR. The USSR delegation consisted of 4 scientists from JINR, 3 from the Kurchatov Institute of Atomic Energy and 3 from the Petersburg Institute of Nuclear Physics. The USA neutron scientists were from Brookhaven, Oak Ridge, Los Alamos, Argonne National Laboratory and from

the National Institute of Standards and Technology. Discussions concentrated on most interesting results in the field of the physics of condensed matters obtained by neutron scattering methods in the USA and USSR, as well as on perspectives of cooperation in investigations at neutron sources. The emphasis was put on the study of high temperature superconductivity and development of the small angle neutron scattering method.

Training Center

The 1991 year marks the beginning of activity of the Dubna Training Centre of Moscow State University and Moscow Engineering and Physical Institute at the Joint Institute for Nuclear Research.

The Centre has the following directions of training:

- nuclear physics;
- particle physics;
- nuclear methods in condensed matter physics and in a high temperature superconductivity;
- radiobiology.

The training centre admits students in their senior years after finishing the general physics courses and listening to the primary special courses in the corresponding fields.

Students in the Centre listen to lectures that are given by leading scientists of the Joint Institute for Nuclear Research (JINR), the Moscow State University, the Moscow Engineering and Physical Institute and have a scientific practice at the laboratories of JINR. During this practice they get an experience of working at experimental facilities such as proton and heavy ion accelerators, a neutron pulsed reactor and a computer centre.

A normal duration of full program training at the Dubna centre is two years. It is quite possible to admit students for shorter periods too, including one or two months of intense courses on some selected topics. The working language for foreign students is English.

It is possible to admit post-graduated students also who could listen to lectures on some chosen subjects and take part in scientific researches at JINR laboratories.

Of JINR laboratories the Laboratory of Neutron Physics is the basic one in the fields of nuclear methods in condensed matter and in high temperature superconductivity. The Laboratory's scientists give courses of lectures in

- methods of investigating condensed matter at nuclear reactors and accelerators;
- fundamental neutron physics and the physics of neutron sources;
- low temperature physics;
- theoretical aspects of the physics of condensed matter;
- the physics of high temperature superconductivity;
- methods and instrumentation of experiments with neutrons, etc.

Besides that the students acquire experience in experimental data processing, work on modern personal computers and knowledge of the electronic equipment that serves the instrumentation suit of the Laboratory.

List of visitors from non-member states of the JINR in 1991

Name	Organization	Country	Dates of visit
Dr F Weidhase	TU, Dresden	FRG	15.01–19.01
			19.04–19.05
			20.09–30.09
Dr O Antson	ESPOO, Helsinki	Finland	11.02–14.03
Dr H Hartmut	TU, Kiemnitz	FRG	14.02–06.03
Dr W Boede	IFK, Rossendorf	FRG	25.02–08.03
			16.11–08.12
Dr P Reichel	IFK, Rossendorf	FRG	25.02–08.03
			16.11–08.12
Dr R Osborn	RAL, Chilton	United Kingdom	27.02–09.03
Prof P Hiismäki	ESPOO, Helsinki	Finland	11.03–14.03
			26.05–29.05
Prof S Raman	ORNL, Oak Ridge	USA	11.03–15.03
Dr H Lauter	ILL, Grenoble	France	08.04–13.04
			09.11–20.11
Prof Liu Zigzi	Academia Sinica, Bejing	China	22.04–26.04
Dr B Koenig	Institute of Physics, Leipzig	FRG	02.05–15.06
Dr R Benzing	Imperial College, London	United Kingdom	25.05–08.06
Dr W Birkholz	High Technical School, Leipzig	FRG	03.06–14.06
			10.11–25.11
Dr P Duke	Daresbury Laboratory, Daresbury	United Kingdom	13.06–14.06
Dr B Lippold	Institute of Physics, Leipzig	FRG	18.06–28.06
Prof Jian-Gao Zhao	Academia Sinica, Bejing	China	20.06–30.06
Prof Zhan Wen Shan	Institute of Physics, Bejing	China	20.06–30.06
Prof Liu Xiang Lin	Institute of Metallurgy, Shanghai	China	20.06–30.06
Prof Wu-yan Lai	Institute of Physics, Bejing	China	20.06–30.06
Prof Sun Shen Tai	Institute of Metallurgy, Shanghai	China	20.06–30.06
Dr Yang Linyuan	Institute of Physics, Bejing	China	20.06–30.06
Dr G Bauer	PSI, Zurich	Switzerland	24.06–28.07
Dr T Broome	RAL, Chilton	United Kingdom	24.06–27.06
Dr J Carpenter	IPNS, Argonne	USA	24.06–27.06
Dr K Noak	IFK, Rossendorf	FRG	24.06–27.06
Dr G Russel	LANSCE, Los Alamos	USA	24.06–27.06
Dr K Sumita	Osaka University, Osaka	Japan	24.06–27.06
Dr I Thorson	TRIUMF, Vancouver	Canada	24.06–27.06
Prof N Watanabe	KENS, Ibaraki-ken	Japan	24.06–27.06
Dr R Long	American Nuclear Society, Grand Park	USA	27.06
Dr B Kuenstler	IFK, Rossendorf	FRG	26.06–14.07
Dr H Heyne	IFK, Rossendorf	FRG	26.06–14.07
Prof Zhong Wenguang	Tsinghua University	China	01.07–31.07
Prof N MacMahon	Imperial College, London	United Kingdom	14.07–28.07
Dr M Hawe	Easthamstead Park School, London	United Kingdom	14.07–28.07
Dr G Striele	University of Tubingen	FRG	07.09–08.09
Dr C Wilson	RAL, Chilton	United Kingdom	02.10–05.10

Personnel

The Laboratory staff consists of permanent and non-permanent contract employees. Most employees from the USSR have permanent positions. A total of 580 staff posts were occupied in 1991. Staff details per departments are given in the Table. Under non-permanent contracts specialists from member states of the JINR and non-member states are working. Among them there are cadres from Bulgaria, Germany, Cuba, Czechoslovakia, Hungary, Korea, Mongolia, Poland, Romania and Vietnam.

Staff Situation in 1991

Departments	Scientists (permanent)	Scientists (non-permanent)	Engineers (permanent)	Engineers (non-permanent)	Technicians
Neutron Sources and Reactor Safety Sector	7	3	60	2	17
Condensed Matter	21	16	20	3	6
Nuclear Physics	29	13	13	–	11
Applied Research, Low Temp. Sector, Radiation Res. Sector	11	13	12	1	5
Computing	17	5	30	4	15
Technical and Administration Services	–	–	80	–	166
TOTAL	**85**	**50**	**215**	**10**	**220**

Finance

The Laboratory's expenditure for the financial year 1991 was 11.27 million roubles, the corresponding figure for 1990 was 9.02 million roubles (see Table 1). This was supported centrally by the budget of the Joint Institute for Nuclear Research, a constituent of which is the Laboratory of Neutron Physics, and, externally, by national programs funds and financial contributions on contracts. Part of the Laboratory's budget is assigned to the JINR for the Administration Division and common services. The other part covers the Laboratory's staff expenditure, research and development, neutron sources maintenance, buildings, etc.(see Table 2).

Positive balance between funds received (Table 1) and paid out (Table 2) formed thanks to national programs financing and contracts. It was at the disposal of the leaders of corresponding projects for them to be able to employ extra staff members on the short-term contract basis and to purchase necessary materials and equipment.

The materials, research and equipment development expenditure was reduced essentially this year in connection with the increased expenditure

on the other items of the budget caused by inflation. The Laboratory's Directorate made great efforts to find extra sources of financing as the Laboratory's resources were insufficient even to maintain and run satisfactorily the existing research facilities, to say nothing of the development of new instruments.

In 1991 the LNP Directorate applied to the JINR Directorate for the financial support of some projects of advanced neutron instruments and had received additionally (not indicated in Tables) for

- the upgrading of the IBR-2 reactor $ 352 th.
- the construction of the High Resolution Fourier Diffractometer $ 660.6 th.
- the development of the texture diffractometer $ 99.2 th.

Table 1. Comparison of 1990 and 1991 Budgets (Income)

Income	Income 1990 th. roubles	%	Income 1991 th. roubles	%	Change %
Laboratory budget from JINR	5348.8	59	7500.2	67	+40
National program on solid state physics	2000.0	22	2000.0	18	–
National program on high temperature superconductivity	1435.0	16	1389.0	12	−3
Other programs	235.4	3	381.5	3	+62
TOTAL	**9019.2**	**100**	**11270.7**	**100**	**+25**

Laboratory's fund distribution in 1991

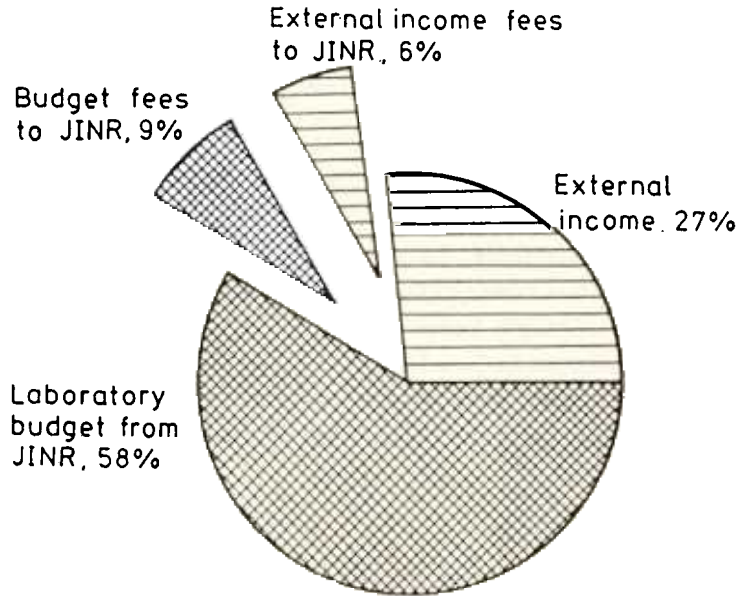

Table 2. Comparison of 1990 and 1991 Budgets (Expenditures)

Expenditure	Expenditure 1990 th. roubles	%	Expenditure 1991 th. roubles	%	Change %
Neutron sources					
IBR-2					
Staff costs	417.5	7	701.1	9	+68
Other expenditures	246.0	4	310.1	4	+26
IBR-30+LUE-40					
Staff costs	270.6	4	447.4	6	+65
Other expenditures	55.4	1	102.9	1	+86
Other Departments					
Staff costs	1788.3	28	2909.6	36	+63
Materials and equipment	1578.0	24	449.4	6	−72
Electric power, heat and water supply	213.4	3	342.7	4	+61
Buildings	179.3	3	197.6	2	+10
Long term supplies and services	155.0	2	310.2	4	+100
Short term supplies and services	142.3	2	71.3	1	−50
Travel	59.8	1	202.2	2	+238
Other investments	205.0	3	316.5	4	+54
Fees paid to JINR					
On laboratory budget	795.7	12	959.5	12	+21
On external income	353.8	6	720.9	9	+104
TOTAL	**6460.1**	**100**	**8041.4**	**100**	**+24**

PUBLICATIONS

THEORY

Nuclear Physics

Bunatian G.G. The Nucleon Size in Nuclear Matter. Nucl.Phys.A, 1990, v.509, p.736-756.

2. Bunatian G.G. On the Calculation of the Mean Square Charge Radius of the Nucleon in Nuclear Matter. Yad.Fiz., 1990, 51, v.4, p.995-1000 (in Russian).

3. Bunatian G.G. Description of the Nucleon in Nuclear Matter in the Frame of the Chiral Bag Model. Yad.Fiz., 51, 1990, v.5, p.2343-1257 (in Russian).

4. Furman W.I., Kliman J. The Relation between Fission Channels and Fission Modes. In: Proc. of the Int. Workshop on Dynamical Aspects of Nuclear Fission. Smolenice, Czechoslovakia, 17-21 June, 1991.

5. Ignatovich V.K. Physics of Ultracold Neutrons. Oxford,Clarendon Press, 1990.

6. Ignatovich V.K. To the Question of the Influence of Gravity on the Determination of the Neutron Lifetime in Experiments on UCN Storage. Yad.Fiz., 1991, v.53, issue 5, p.1297-2001 (in Russian).

7. Ignatovich V.K. On Linear Transport Problems. USSR Academy of Sciences Reports, 1991, v.318, issue 2, p.332 (in Russian).

8. Ignatovich V.K. An Algebraic Approach to the Propagation of Waves and Particles in Layered Media. In: Proc. of the Conf.: Analogies in Optics and Micro-Electronics. Eindhoven, the Netherlands, 1-4 May, 1991.

Condensed Matter Physics

1 Aksenov V.L. Glassy States in High-Temperature Superconductors. In: Ordering Phenomena in Condensed Matter Physics. (Eds. Z.M.Galasiewicz and A.Pekalski). World Scientific, 1991, p.2-23.

2. Aksenov V.L. Glassy Behaviour of High-Temperature Superconductors in External Magnetic Field. In: Int. Symp. on Nature of High-T_c Superconductors. World Scientific, 1991.

3. Bogolubov N.N., Aksenov V.L., Plakida N.M. On the Theory of High-Temperature Superconductivity. In: Selected Topics in Statistical Mechanics (Eds.: A.A.Logunov, N.N.Bogolubov, Jr., V.G.Kadyshevsky, A.S.Shumovsky). World Scientific, 1990, p.21-35.

4 Flach S., Plakida N.M., Aksenov V.L. A Theoretic Study of Lattice Instabilities in LaCuO. Int.J. of Modern Phys. B, 1990, v.4, p.1955-1973.

5. Golub A.A., Kabanov V.V., Mashtakov O.Yu. Magnetic Excitations in High-T_c Superconductors. Fiz.Tverd.Tela, 1991, v.33, No.6 (in Russian).

6. Golub A.A., Kabanov V.V., Mashtakov O.Yu. Magnetic Excitations in High-T_c Superconductors. Phil.Mag., 1991 (in press).

7. Kabanov V.V., Kornilovich P.E., Mashtakov O.Yu. Motion of Single Hole in the Framework of the Emery Model: Equivalence to the t-J Model. Physica C, 1991, v.176, No.4/6, p.559-566.

8. Kabanov V.V., Mashtakov O.Yu. Coherent Hole Motion in High-T_c Superconductors. Fiz.Niz.Temp., 1991 (in press) (in Russian).

9. Kornilov E.I., Litvin A.A., Priezzhev V.B. Thermodynamics of Melted Flux Liquids. Material Science Forum, 1990, v.62-64, p.197-198.

10. Kornilov E.I., Litvin A.A. On the Entropy Contribution to Thermodynamics of Melted Flux Liquids. Z.Phys.B - Condensed Matter, 1991, v.84, p.3-8.

11. Kornilov E.I. Lattice Model of Disordered Magnetic Flux System. III All Union Conference on High-Temperature Superconductivity. Kharkov, 15-19 April 1991.

12. Kornilov E.I. On the Entangled-Disentangled Transition in Magnetic Flux Liquids. Physica C, 1991 (submitted); Int. Conf. on Materials and Mechanisms of Superconductivity. High-Temperature Superconductors (M2S-HTSC), Kanazawa, Japan, 22-26 July, 1991.

13. Kornilov E.I., Pomjakushin V.Yu. On the Generalization of Kubo-Toyabe Formula. Phys.Lett.A, 1991, v.153, p.364-367.

14. Mishonov T.M., Simkin M.V. How to Measure the Cooper-Pair Effective Mass Using the Hall Effect in Thin HTSC Films. Fiz. Niz.Temp., 1991, v.17, No.11 (in press) (in Russian).

15. Plakida N.M., Aksenov V.L., Drechsler S.L., Galbaatar T., Stamenkovic S. Inelastic Neutron Scattering in the Anharmonic Model of High-T_c Superconductors. Modern Phys.Lett. B, 1990, v.4, p.341-346.

16. Sergeenkov S.A. Nonlinear CVC and Critical Current of the Superconductive Glass Model. Physica C, 1990, v.167, p.339.

17. Sergeenkov S.A. On Logarithmic CVC of High-T_c Superconductive Glass Model. physica status solidi (b), 1990, v.160, p.K137.

18. Sergeenkov S.A. On Excess Magnetoconductivity of a Superconductive Glass. Z.Phys.B: Condensed Matter, 1991, v.82, p.325.

19. Sergeenkov S.A. On Fluctuation-Induced Diamagnetism of a Superconductive Glass. Physica C, 1990, v.171, p.319.

20. Sergeenkov S.A. Memory Effects in a High-T_c Superconductive Glass Model. Physica C, 1991, v.174, p.519.

21 Sergeenkov S.A. Flicher-Noise Spectrum in Weak-Links-Containing Superconductor. In: Proc. of the IV Int. Conf. on Superconducting Quantum Effect Devices and Their Applications, SQUID'91. Berlin, Germany, 18-21 June, 1991. (To be published in Springer Proceedings in Physics).

22. Sergeenkov S.A. Thermoelectric Effects in Superconductors: the Role of Fluctuations and Weak Links. J.Superconduct., 1990, v.3, p.417.

23. Sergeenkov S.A. On Dislocation-Induced Reentrant-Like Behaviour in Deoxygenated High-T_c Superconductors. J.Superconduct., 1991, v.4, p.431.

24. Sergeenkov S.A. On Field-Induced Irreversibility Line Crossover in Deoxygenated Weak-Links-Containing Superconductors. Solid State Comm., 1991, v.79, p.863.

25. Simkin M.V. Plasma Waves in a Josephson Chain. Physica C, 1990, v.168, p.279-281

26. Simkin M.V. Josephson Oscillator Spectrum and the Reentrant Phase Transition in Granular Superconductors. Phys.Rev. B, 1991, v.44, p.7074-7077.

27. Simkin M.V. Fluxoid Quantization in SQUIDs Made from Granular Superconductors. Accepted by the Fourth International Symposium on Superconductivity. Tokyo, Japan, October 14-17, 1991.

28. Simkin M.V. Hall Effect in a Thin Superconducting Film - a Way to Measure the Cooper-Pairs Effective Mass. 1991 (Submitted to Europhys.Letters).

EXPERIMENTAL RESEARCH

Fundamental and Nuclear Physics

Alexandrov Yu.A., Samosvat G.S. Neutron Polarizability. In: Proc. of the VI Int. School on Neutron Physics, Alushta, 8-18 Oct., 1990. JINR, D3,14-91-154, Dubna, 1991, v.1, p.187 (in Russian).

2. Alexandrov Yu.A., Koester L., Samosvat G.S., Waschkowski W. Neutron ^{208}Pb Scattering and the Electric Polarizability of the Neutron. JINR Rapid Comm., No.6(45), Dubna, 1990, p.48-50.

3. Alfimenkov V.P. et al. The Results of Measurement of the Neutron Lifetime Using the UCN Trap. LINP Preprint, No.1629, Gatchina,1990; Letters to ZhETP, 1990, v.52, issue 7, p.984-989 (in Russian).

4. Alfimenkov V.P., Borzakov S.B., Mareev Yu.D., Pikelner L.B., Skoy V.R., Khrykin A.S., Sharapov E.I. P-Even Effects in the ^{113}Cd(n, γ) Reaction Near the E_p = 7 eV Resonance. Yad.Fiz., 1990, v.52, issue 4(10), p.927-932 (in Russian).

5. Alfimenkov V.P., Mareev Yu.D., Pikelner L.B., Skoy V.R., Shvetsov V.A. Investigation of Parity Violation Effects in Neutron Resonances of Rb and ^{113}Cd. JINR Preprint, 3-91-297, Dubna, 1991 (in Russian).

6. Alfimenkov V.P. et al. Method of Losses Calibration in Neutron Lifetime Experiment with UCN. Preprint LINP, No.1711, Gatchina, 1991.

7. Ali M.A., Bogdzel A.A., Khitrov V.A., Kulik V.D., Khiem L.H., Tuan N.T., Khang P.D., Popov Yu.P., Shilin V.N., Sukhovoj A.M., Vasilieva E.V., Vojnov A.V. Intense Two-Step Cascades Following the Decay of the ^{158}Gd Compound State. JINR Preprint, E3-91-428, Dubna, 1991 (submitted to Nucl.Phys.A).

8. Andrzejewski J., Gledenov Yu.M., Mitrikov M.P., Popov Yu.P., Sedyshev P.V., Chadraabal J., Li Ho Bom. Study of the ^{91}Zr(n,α)^{88}Sr and ^{187}Os(n,α)^{184}W Reactions on Resonance Neutrons. 7-th Int.Symp. on Capture γ-Ray Spectroscopy and Related Topics. Asilomar, California, USA, 14-19 Oct., 1990.

9. Andrzejewski J., Antonov A.D., Gledenov Yu.M., Mitrikov M.P., Popov Yu.P., Okunev I.S., Peskov B.G., Shal'gina E.V., Vesna V.A. Study of Parity Violation in the ^{6}Li(n,α)^{3}H Reaction with Polarized Neutrons. Ibid.

10. Andrzejewski J., Gledenov Yu.M., Popov Yu.P., Pshenichnyi V.A., Salatskii V.I. The Cross Section of the ^{7}Be(n,p)^{7}Li Reaction at the Neutron Energy 24.5 keV. JINR Preprint, P3-91-74, Dubna, 1991 (in Russian) (Submitted to Z.f.Phys.A).

11. Andrzejewski J., Gledenov Yu.M., Zamyslov G.V., Kislitskii A.I., Lyubanskii G.S., Pshenichnyi V.A., Salatskii V.I., Fedoseev N.P. Thermal Neutron Cross Sections of the ^{36}Ar(n,α)^{23}S and ^{50}U(n,p)^{50}Ti Reactions. JINR Comm., P3-91-244, Dubna, 1991.

12. Balabanov N.P., Vtiurin V.A., Gledenov Yu.M., Popov Yu.P. Measurement of α-Widths of Compound Nuclei. Particles and Nucleus, 1990, v.21, issue 2, p.317-363 (in Russian).

13. Bogdzel A.N., Grigoriev Yu.V., Gundorin N.A., Duka-Zolyomi A., Zo Sen Khen, Kliman J., Solomenkov P.S. Fast, Multisection, Plutonium-239 Containing Chamber. JINR Preprint, P3-90-395, Dubna, 1990 (in Russian).

14. Bogdzel A.N., Gundorin N.A., Polgorsky V., Kliman J., Kristiak J., Duka-Zolyomi A. Prompt Gamma-Ray Emission from Fission of ^{239}Pu by Resonance Neutrons. Proc. Int. Workshop on Dynamical Aspects of Nuclear Fission. Smolenice, Czechoslovakia, 17-21 June, 1991.

15. Bogdzel A.N., Gundorin N.A., Gohs U., Duka-Zolyomi A., Kliman J., Polgorski V., Popov A.B., Dao Anh Minh. Peculiarity of the Fission of ^{239}Pu by Resonance Neutrons. Proc. Conf. on Nucl.Data for Science and Technology. Jülich, FRG, 13-17 May, 1991.

16. Bogdzel A.N., Gundorin N.A., Popov A.B., Polgorsky V., Kliman J., Kristiak J., Gohs U. Prompt Gamma-Ray Yields at Individual Fission Resonances of ^{239}Pu. Proc. Int. Workshop on Dynamical Aspects of Nuclear Fission. Smolenice, Czechoslovakia, 17-21 June, 1991.

17. Boneva S.T., Khitrov V.A., Sukhovoj A.M., Vojnov A.V. Intensities of Two-Quanta Cascades at Different Excitation Energies of Compound Nuclei ^{146}Nd, ^{174}Yb and ^{183}W. Z.Phys.A, 1991, v.A338, p.319-323.

18. Boneva S.T., Vasilieva E.V., Popov Yu.P., Sukhovoj A.M., Khitrov V.A. Two-Quanta Cascades Following Radiative Neutron Capture. I.Spectroscopy of Excited States of Compound Nuclei in Neutron Binding Energy Range. Particles and Nucleus, 1991, v.22, p.479-511 (in Russian).

19. Boneva S.T., Vasilieva E.V., Kulik V.D., Le Khong Khjem, Popov Yu.P.,Sukhovoj A.M., Khitrov V.A., Kholnov Yu.V. Study of Two-Step Cascades and ^{180}Hf Compound State Decay Schemes in the Reaction ^{179}Hf(n, 2γ). USSR Academy of Sciences News Letters, Physics Series, 1990, v.54, p.1787-1789 (in Russian).

20. Boneva S.T., Vasilieva E.V., Kulik V.D., Le Khong Khjem, Popov Yu.P., Sukhovoj A.M., Khitrov V.A., Pham Dingkh Khang, Kholnov Yu.V. Construction of Complicate γ-Decay Schemes of Compound States on the Basis of Spectroscopic Data from (n, 2γ) and (n, γ) Reactions. USSR Academy of Sciences News Letters, Physics Series, 1991, v.55, p.841-849 (in Russian).

21 Boneva S.T., Vasilieva E.V., Kulik V.D., Le Khong Khjem, Popov Yu.P., Sukhovoj A.M., Khitrov V.A., Kholnov Yu.V. Spin of the ^{180}Hf Compound State Excited on Thermal Neutron Capture in ^{179}Hf. USSR Academy of Sciences News Letters, Physics Series, 1990, v.54, p.836-840 (in Russian).

22 Boneva S.T., Vasilieva E.V., Kulik V.D., Le Khong Khjem, Popov Yu.P., Sukhovoj A.M., Khitrov V.A., Kholnov Yu.V. Cascade γ-Decay of the ^{177}Yb Compound State. USSR Ac. of Sci. News Letters, Physics Series, 1990, v.54, p.822-830 (in Russian).

23. Borzakov S.B., Pokotilovskij Yu.N., Salamatin I.M. A Search for Correlated at 180° γ-Quanta Pairs in α-Decay of ^{239}Pu. Yad.Fiz., 1990, v.52(2), p.355-357 (in Russian).

24 Frankle C.M., Bowman C.D., Bowman J.D., Seestrom S.J., Sharapov E.I., Popov Yu.P., Roberson N.R. Neutron Resonance Spectroscopy in ^{113}Cd: the p-Wave Levels (submitted to Phys.Rev.C).

25. Gohs U. Evaluation of Total Fission Characteristics for ^{235}U in the Low Energy Region. In: Conf. on Nucl. Data for Science and Technology. Jülich, FRG, 13-17 May, 1991.

26. Gohs U. Evaluation of Fission Characteristics for ^{239}Pu in the Low Energy Region. In: Proc. Int. Workshop on Dynamical Aspects of Nuclear Fission. Smolenice, Czechoslovakia, 17-21 June, 1991.

27. Govorov A.M., Mitsyna L.V., Samosvat G.S. The Scattering of 1-300 keV Neutrons on Crypton and Xenon. Yad.Fiz., 1991, v.54, issue 5, p.1192-1196 (in Russian).

28. Grigoriev Yu.V., Manturov G.N., Sinitsa V.V., Georgiev G.P., Ivanov B.I., Sirakov I.A., Yaneva N.B. Theoretico-Experimental Investigation of Resonance Structure of the Total Cross Section and Radiative Neutron Capture Cross Section of Thorium-232 in the Energy Range from 4.65 to 46.5 keV. Preprint PhEI-2110, Obninsk, 1990 (in Russian).

29. Georgiev Yu.V., Koscheev V.N., Manturov G.N., Sirakov I.A., Sinitsa V.V., Yaneva N.B. On Determination of Resonance Structure Parameters of Uranium-238 Cross Section from Data on Total and Partial Transmission in the Energy Range from 0.465 to 200 keV. Preprint PhEI-2072, Obninsk, 1990 (in Russian).

30. Kulda J., Lukas P., Mikula P., Alexandrov Yu.A., Sedlakova L.N., Vrana M., Rauch H. Neutron Interferometry at a Pulsed Source. Nucl.Instr. Meth., 1991, v.A300, p.80-84.

31. Lyapin D.I., Salamatin I.M., Sirotin A.P., Skoy V.R., Tishin V.G., Sharapov E.I. Forward-Backward Asymmetry of 9325 keV γ-Yield from the ^{117}Sn (n, γ) Reaction in the Epithermal Region. JINR Comm., P3-90-125, Dubna, 1990 (in Russian).

32. Mitsyna L.V., Samosvat G.S. About Mixed Neutron Resonances. JINR Comm., P3-90-234, Dubna, 1990 (in Russian).

33. Nikolenko V.G., Popov A.B. On Different Values of the Neutron-Electron Scattering Amplitude and Neutron Mean Square Charge Radius Obtained from the Low-Energy Dependence of the Scattering Amplitude. JINR, E4-91-106, Dubna, 1991.

34. Nikolenko V.G., Popov A.B. The Revision of Estimates of the (n-e) Scattering Amplitude and Neutron Polarizability from Total Cross Sections of Bi and Pb. JINR, P3-90-568, Dubna, 1990 (in Russian).

35. Nikolenko V.G., Popov A.B. On the Correctness of Estimates on (n,e)-Amplitude and Neutron Polarizability from Total Cross Sections of Bi and Pb. Z.Phys.A. - Hadrons and Nuclei, 1991 (in print).

36. Pokotilovskij Yu.N. Experimental Limit of Measuring Probability of γ-Quanta with Energies $E_\gamma \geq 20$ MeV Following the Spontaneous Decay of ^{252}Cf. Yad.Fiz., 1990, v.52(4), p.942-943 (in Russian).

37. Pokotilovskij Yu.N. Possible Chopper-Monochromator for Cold Neutrons. JINR Comm., E3-91-413, Dubna, 1991.

38. Pokotilovskij Yu.N., Shelkova I.G., Oehler H. Calculated Version of Inelastic Adiabatic Spin-Flipper for Ultracold Neutrons. JINR Comm., P3-91-202, Dubna, 1991 (in Russian).

39. Pokotilovskij Yu.N. A Moving Converter as a Possible Tool for Producing Ultra-Cold Neutrons on Pulsed Neutron Sources. JINR Preprint, E3-91-414, Dubna, 1991 (submitted to NIM).

40. Sirakov I.A., Ukraintsev V.F. Modelling by the Monte Carlo Method of Resonance Structure of Neutron Cross Sections for Inelastic Scattering Channels. JINR Comm., P10-90-130, Dubna, 1990 (in Russian).

41 Sharapov E.I., Wender S.A., Postma H. et al. The Measurements of Parity Violation in Resonant Neutron-Capture Reactions. In: Capture Gamma-Ray Spectroscopy (Ed. by R.W.Hoff). AIP Conference Proceedings, 238, Americam Institute of Physics, New York, 1991.

42. Skoy V.R., Sharapov E.I. Total and Partial Neutron Cross Sections of ^{117}Sn at E $\leq$ 5 eV. JINR Comm., P3-90-126, Dubna, 1990 (in Russian).

43. Skoy V.R., Sharapov E.I. P-Even Angular Correlations in Resonance (n, γ) Reactions. Particles and Nucleus, 1991, v.22, issue 6, p.1400-1432 (in Russian).

44. Vesna V.A., Okunev I.S., Peskov B.G., Shulgina E.V., Antonov A.D., Andrzejewski J., Gledenov Yu.M., Mitrikov M.P., Popov Yu.P. Study of Parity Violation in the Reaction ^{6}Li(n, α)^{3}H. Lett to ZhETP, 1990, v.52, issue 1, p.660-662 (in Russian).

45. Wagner V., Mikula P., Lukas P., Scherm R., Sedlakova L.N. Bent Silicon as a Short-Wawelength Monochromator. Int.Conf. on Neutron Scattering. ICNS'91, Oxford, UK, 27-30 August, 1991.

46. Doctor's Thesis. Chadraabal J. Study with Slow Neutrons of (n, α) Reaction on Stable Nuclei Zr-91, Mo-95, Te-123. 1991.

Condensed Matter Physics

Aksenov V.L. Update on the pulsed reactor IBR-2 and its instruments at Dubna. Physica B, 1991, v.174, p.438-442.

2. Aksenov V.L. HTSC studies at high flux pulsed reactor IBR-2. Usp.Fiz.Nauk, 1991, v.161, p.179-182.

3. Aksenov V.L., Balagurov A.M., Simkin V.G., Trunov V.A., Hiismaki P. et al. The Neutron Fourier Diffractometer at the IBR-2 Reactor. JINR, P3-91-172, Dubna, 1991.

4. Antonov V.E., Belash I.T., Kolesnikov A.I., Mayer J. Neutron Scattering Study of Vibrational Spectrum of Manganese Hydrate. Fiz.Tverd.Tela, 1991, v.33(1), p.152-157 (in Russian).

5. Balagurov A.M., Prokert F., Sangaa D., Savenko B.N. Neutron Diffraction Studies of the Electric Field Influence on $Sr_xBa_{1-x}Nb_2O_6$. Ferroelectrics Letters, 1991, v.13, p.61-66.

6. Balagurov A.M., Vuong N.V., Quan T.A., Luschikov V.I., Tuong V.H., Lap B. Diffusion of Oxygen in the $YBa_2Cu_3O_x$. JINR, P17-91-378, Dubna, 1991 (in Russian).

7. Balagurov A.M., Bashkin I.O., Kolesnikov A.I., Malishev V.Yu., Mironova G.M., Ponyatovskii E.G., Fedotov V.K. Neutron Diffraction Study of the Kinetics of the ϵ to δ Phase Transition in $TiD_{0.74}$. Fizika Tv.Tela, 1991, 33, p.1256 (in Russian).

8. Balagurov A.M. New Diffractometers at the IBR-2 High Flux Pulsed Reactor. Physica B, 1991, v.174, p.542.

9. Balagurov A.M., Mironova G.M., Novozhilov V.E., Ostrovnoy A.I., Simkin V.G., Zlokazov V.B. The Application of the Neutron TOF Technique for the Real Time Diffraction Studies. J.Appl.Cryst., 1991, to be published.

10. Balagurov A.M., Vuong N.V., Quy L.C. et al. Oxygen Diffusion in Heated Y123 Ceramics. JINR, P17-91-340, Dubna, 1991 (in Russian).

11. Balagurov A.M., Mironova G.M. Real-Time Neutron Diffraction. Proc. VI Interna- tional School on Neutron Physics (Alushta, USSR, 1990). JINR, D3,14-91-154, v.2, p.16, Dubna, 1991 (in Russian).

12. Balagurov A.M., Mironova G.M. Real-Time Neutron Diffraction Studies. Kristallografiya, 1991, 36, p.314 (in Russian).

13. Balagurov A.M., Piechota J., Pajaczkowska A. Neutron Powder Diffraction on $YBa_2(Cu_{1-x}{}^{58}Ni_x)_3O_{7-\delta}$. Solid St.Comm., 1991, 78, p.407.

14. Balagurov A.M., Mironova G.M., Ponyatovskii E.G., Kolesnikov A.I., Sinitsyn V.G., Barkalov O.I., Fedotov V.K. Neutron Diffraction Study of Phase Transition in Metastable Ice VIII. JETP Lett., 1991, 53, p.30 (in Russian).

15. Balagurov A.M., Vakhrushev S.V., Naberezhnov A.A., Okuneva N.M., Savenko B.N., Sangaa D. Modulated Structure of the Crystal $Na_{1/2}Bi_{1/2}TiO_3$. JINR, P14-90-423, Dubna, 1990 (in Russian).

16. Balagurov A.M., Mironova G.M. Neutron Diffraction Study of the Synthesis of the $YBa_2Cu_3O_x$ Ceramics. Superconductivity, 1990, 3, p.545 (in Russian).

17. Balagurov A.M., Mironova G.M., Rudnickij L.A., Galkin V.Yu. Time Resolved Neutron Diffraction Investigation of Effect of Hydrogen on the High-T_c Superconductor $YBa_2Cu_3O_{7-\delta}$. Physica C, 1990, 172, p.331.

18. Balagurov A.M., Lyubutin I.S., Mironova G.M., Terziev V.G., Shapiro A.Ya. Neutron Diffraction Study of the System $YBa_2(Cu_{1-x}Fe_x)_3O_{6+\delta}$ for $0 \leq x \leq 0.27$ and $0.3 \leq \delta \leq 1.3$. Superconductivity, 1990, 3, p.615 (in Russian).

19. Balagurov A.M., Nikitin A.A., Novozhilov V.E., Ostrovnoj A.I., Savenko B.N., Sirotin A.P., Smirnov L.S., Taran Yu.V. Time-of-Flight Neutron Diffractometer at the Pulsed Booster IBR-30. JINR Comm., P14-91-529, Dubna, 1991 (in Russian).

20. Belushkin A.V. IBR-2 - the fast pulsed reactor at Dubna. Neutron News, 1991, v.2, p.14-18.

21. Belushkin A.V., Goremychkin E.A., Gundorina S.F., Muzychka A.Yu., Nazarov V.M., Natkaniec I., Sashin I.L., Fiderkevich A. Investigation of Possible Influence of Microadmixtures on the Dynamics of High Temperature Superconductors $La_{2-x-y}Re_ySr_xCuO_{4-\delta}$. JINR Comm., 14-90-190, Dubna, 1990 (in Russian).

22. Belushkin A.V., David W.I.F., Ibberson R.M., Shuvalov L.A. High-Resolution Neutron Powder Diffraction Studies of the Structure of $CsDSO_4$. Acta Cryst., 1991, v.B47, p.161-166.

23. Belushkin A.V., Carlile C.J., David W.I.F., Ibberson R.M., Shuvalov L.A., Zajac W. Neutron Scattering Study of Crystal Structure and Proton Diffusion in Protonic Conductors with Hydrogen Bonds. Physica B, 1991, v.174, p.268-271.

24. Belushkin A.V., Carlile C.J., Shuvalov L.A. The Diffusion of Protons in the Superionic Conductor $CsHSO_4$ by Quasielastic Neutron Scattering. JINR Preprint, E14-91-1, Dubna, 1991; J.Phys.: Condensed Matter (in press).

25. Belushkin A.V., Vagov A.V., Zemlyanov M.G., Parshin P.P. Lattice Dynamics of $Ba_{1-x}K_xBiO_3$ as Studied by Neutron Scattering and Computer Simulation. Preprint JINR, E14-91-519, Dubna, 1991; J.Phys.: Condensed Matter (submitted).

26. Beskrovnyi A.I., Dlouha M., Jirak Z., Vratislav S., Pollert E. Neutron Diffraction Study of the Modulated Structure of $Bi_2(Sr,Ca)_3Cu_2O_{8+\gamma}$. Physica C, 1990, 166, p.79.

27. Beskrovnyi A.I., Dlouha M., Jirak Z., Vratislav S. Study of the Modulated Structure of $Bi_2(Sr,Ca)_3Cu_2O_{8+\gamma}1$ in the Range 8-920 K. Physica C, 1990, 171, p.19.

28. Bezzabotnov V.Yu., Gross T., Ostanevich Yu.M., Cser L., Jancso G. Small Angle Scattering in Tetramethylurea Solutions. JINR Preprint, E14-90-586, Dubna, 1990. (Submitted to Journ.Phys.Chem.).

29. Borbely S., Smirnov L.S., Kouneristii Yu.K., Nartova T.T., Tarasova O.B., Bezzabotnov V.Yu., Ostanevich Yu.M. Thermal Stability of $Ti_{41}Zr_{41}Si_{18}$ Metallic Glass Studied by Small-Angle Neutron Scattering. phys.stat.sol.(b), 1991, v.164, p.343-350.

30. Chrusciel J., Zajac W. Quasielastic Neutron Scattering Study of Molecular Reorientation in the Nematic and Smectic Phases of 4-n-Pentylphenyl-4'-n-octyloxythobenzoate. Liquid Crystals, 1991, 10, p.419-424.

31 Chernenko L.P., Korneev D.A., Petrenko A.V., Babalykin N.I., Skripnik A.V. Measurement of Magnetic Field Penetration Depth in Niobium Polycrystalline Films by Polarized Neutron Reflection Method. JINR Preprint, E3-91-330, Dubna, 1991.

32. Dokukin E.B., Korneev D.A., Petrenko A.V. Relaxation of Magnetic Flux in High-T_c Superconducting Ceramics $YBa_2Cu_3O_7$ Studied by Neutron Polarization Analysis. Journal of Magnetism and Magnetic Materials, 1991, 90&91, p.637-639.

33. Gordeliy V.I., Ivkov V.G., Ostanevich Yu.M., Yaguzhinskiy L.S. Detection of Structural Defects in Phosphatidylcholine Membranes by Small-Angle Neutron Scattering. The Cluster Model of a Lipid Bilayer. Biochemica and Biophysica Acta, 1991, 1061, p.39.

34. Goremychkin E.A., Belushkin A.V., Mayer J., Muzychka A.Yu., Natkaniec I., Sashin I.L., Osborn R., Taylor A.D. Crystal Field Effects in $La_{1.9-x}Tm_{0.1}Sr_xCuO_4$ (x=0.0, 0.2) and $RE_{0.1}Y_{0.9}Ba_2Cu_3O_{6.9}$ (RE = Tm, Tb) Studied by Inelastic Neutron Scattering. In: Progress in High Temperature Superconductivity. World Scientific, 1990, v.21, p.324-331.

35. Gorski N., Ostanevich Yu.M. Inverted Micelles in a Ternary System AOT-Water-Benzene as Studied by Small-Angle Neutron Scattering. Ber.Bunsenges. Phys.Chem., 1990, 94, p.737-741.

36. Gorski N., Yu.M.Ostanevich. Critical Micelle Concentration in the AOT-Water-Benzene System as Determined by Small-Angle Neutron Scattering. Ber. Bunsenges. Phys. Chem., 1991, 95, No.8, p.871.

37. Habrylo S., Bragin S.I., Brankowski J., Iwanski W., Mayer J., Natkaniec I., Nawrocik W., Zawalski K. A Setup for Neutron Studies of Condensed Phases Under High Pressure at the Spectrometer of Inverted Geometry. High Pressure Research, 1990, 4, p.457-459.

38. Habrylo S., Janik J.M., Janik J.A., Mayer J., Natkaniec I., Stanek T., Zajac W. Phase Diagram of 4,4'-di-n-butyloxyazoxybenzene. Neutron Diffraction Measurements at Higher Pressures. IFJ Report No. 1529/PS, Krakow, 1991.

39. Haeussler F. et al. Monitoring of the Hydration Process of Hardening Cement Pastes by Small-Angle Neutron Scattering. Cement & Concrete Research, 1990, 20, 4, p.644-654.

40. Haeussler F., Baumbach H., Eichhorn F. Application of Small-Angle Neutron Scattering. VTT Symposium 115 (Microstructure and Properties of Concrete), Expert Meetings, Espoo, 6-11 November, 1988 and 3-10 November, 1989. Ed. by Heikki Kukko. Building Materials Lab., VTT Espoo 1990, p.102.

41. Helming K., Eschner Th. A New Approach to Texture Analysis of Multiphase Materials Using a Texture Component Model. Cryst.Res.Technol., 1990, 25, p.8.

42. Helming K., Voitus W., Walther K. Progress in Texture Investigations at the Pulsed Reactor IBR-2. Proc. ICNS'91, Oxford, 27-31 August, 1991.

43. Helming K. Minimal Pole Figure Ranges for Quantitative Texture Analysis. Textures and Microstructures, 1991, 13, p.6.

44 Holderna-Matuszkiewicz K., Natkaniec I., Habrylo S., Mayer J. Neutron Scattering Investigation of d-Camphor and dl-Borneole Under Hydrostatic Pressure. High Pressure Research, 1990, 4, p.453-456.

45. Ivanov A.N., Litvin D.F., Mikishova N.I., Savenko B.N., Smirnov L.S., Fykin L.E. High Pressure Cell for Neutron Diffraction Studies. Preprint ITEF, 40-91, Moscow, 1991.

46. Khavryutchenko V.D., Natkaniec I., Sheka E.F. Neutron Scattering Spectroscopy in Surface Chemistry: Computational and Real Experiments. Proc. VI Int.School. on Neutron Physics, Alushta, USSR, 1990. JINR, D3,14-91-154, Dubna, 1991, p.157.

47. Kolesnikov A.I., Natkaniec I., Antonov V.E., Belash I.T., Fedotov V.K., Krawczyk J., Mayer J., Ponyatovsky E.B. Neutron Spectroscopy of $MnH_{0.86}$, NiH_1 and $PdH_{0.99}$ and Harmonic Behaviour of Their Optical Phonons. Physica B, 1991, 174, p.257-261.

48. Korneev D.A., Pasyuk V.V., Petrenko A.V., Jankovski H. Antireflecting Sublayers and Their Influence on the Polarizing Efficiency of Magnetic Neutron Mirrors. JINR Preprint, E3-91-197, Dubna, 1991. Submitted to "Nucl. Instr. and Meth.".

49. Korneev D.A., Pasyuk V.V., Petrenko A.V., Jankovsky H. Absorbing Sublayers and Their Influence on the Polarizing Efficiency of Magnetic Neutron Mirrors. JINR Preprint, E3-91-197, Dubna, 1991; Nucl.Instr. and Meth.(In print).

50. Korneev D.A. A New Polarized Neutron Method for Studying Depth Inhomogeneously Magnetized Magnetic Films. JINR Preprint, E3-90-293, Dubna, 1990.

51. Korneev D.A., Chernenko L.P. Investigation of Magnetic Field Penetration into Oxide Superconductors by the Method of Polarized Neutrons Reflection. Poverkhnost, Fizika, Khimia, Mekhanika, 1990, v.9, p.71-70 (in Russian).

52. Mayer J., Chrusciel J., Habrylo S., Holderna K., Natkaniec I., Hartmann M., Wurflinger A., Urban S., Zajac W. Neutron Scattering Studies of the D-O and D-12 Cyklohexane Under High Pressure. High Pressure Research, 1990, 4, p.460-462.

53. Mayer J., Urban S., Habrylo S., Holderna K., Natkaniec I., Wurflinger A., Zajac W. Neutron Scattering Studies of C_6H_{12} and C_6D_{12} Cyklohexane Under High Pressure. phys.stat.sol., 1991, v.166b, p.381-394.

54. Muzychka A.Yu., Divis M., Goremychkin E.A., Natkaniec I., Sashin I.L. Crystal Field in Nd_2CuO_4. JINR, P3-91-450, Dubna, 1991.

55. Pasyuk V.V., Korneev D.A., Petrenko A.V., Dokukin E.B. Neutron Reflectivity Studies on Superconducting, Magnetic and Absorbing Thin Films on the Polarized Neutron Spectrometer at the Pulsed Reactor IBR-2. JINR Preprint, E3-91-276, Dubna, 1991; Proc. II Int.Conf. on Surface X-Ray and Neutron Scattering, Bad Honnef, Germany, 25-28 June, 1991.

56. Pasyuk V.V., Korneev D.A., Petrenko A.V., Jankovski H. A Neutron Reflectivity Study of Titanium Thin Film Aging. JINR Preprint, E3-91-275, Dubna, 1991; Proc. 7 Int.Conf. Surface and Colloid Science, Compiegne, France, 7-13 July, 1991.

57. Pasyuk V.V., Korneev D.A., Petrenko A.V., Jankovsky H. Neutron Specular Reflection for Thin Films, Surfaces and Interfaces Studies. Proc. of XXV Zakopane School on Phys. World Scientific, Singapore, 1990, v.1.

58. Pasyuk V.V., Korneev D.A., Petrenko A.V., Jankovsky H. Influence of an Absorbing Sublayer on Polarizing Property of Magnetic Neutron Mirrors. Proc. of XXVI Zakopane School on Phys. World Scientific, Singapore, 1991.

59. Pasyuk V.V., Nagy D.L. Calculation of Mossbauer Reflectometry Spectra. Hyperfine Interactions (in print).

60. Pavlov M.Yu., Rublevskaya I.N., Serdyuk I.M., Zaccai G., Leberman J. and Ostanevich Yu.M. Experimental Verification of the Triple Isotopic Subtraction Method in Small-Angle Neutron Scattering. J.Appl.Cryst., 1991, v.24, p.243-254.

61. Plestil J., Baldrian J., Ostanevich Yu.M., Bezzabotnov V.Yu. Small-Angle Neutron Study of Swollen Nylon-6. Journ. of Polymer Science. Part B: Polymer Physics, 1991, v.29, p.509-514.

62. Plestil J., Pospisil H., Ostanevich Yu.M., Degovics G. A Novel Small-Angle Scattering Procedure for Molecular Weight Determination. Advantages and Limitations. J.Appl. Cryst., in press.

63. Preuss E., Wuttig M., Sheka E.F., Natkaniec I., Nechitaylov P.B. Amplitude Weighted Density of Bulk and Surface Vibrations; Ultrafine Nickel Particles. J.Electron Spect. Related Phenomena, 1990, 54/55, p.425-443.

64 Prokert F., Sangaa D., Savenko B.N. Neutron Diffraction Studies of the Incommensurate Modulation Structure in $Sr_xBa_{1-x}Nb_2O_6$ Single Crystals of Various Compositions. JINR, E14-90-540, Dubna, 1990.

65. Prokert F., Balagurov A.M., Beskrovnyi A.I., Savenko B.N., Sangaa D. Investigation of Diffuse Phase Transition in the Crystal $Sr_xBa_{1-x}Nb_2O_6$ (x = 0.70, 0.75). JINR, 14-90-240, Dubna, 1990.

66. Prokert F., Balagurov A.M., Savenko B.N., Sangaa D. Neutron Diffraction Study of Electric Field Effect on the Crystal $Sr_xBa_{1-x}Nb_2O_6$ (x = 0.70, 0.75). JINR, 14-90-239, Dubna, 1990.

67. Savenko B.N., Keen D.A., Mroz B., Sangaa D., Wilson C.C. Neutron Diffraction Study of the Low Temperature Domain Structure in $LiKSO_4$. Physica B, 1991, (to be published).

68. Savenko B.N., Ivanov A.N., Mroz B., Sangaa D., Smirnov L.S. Hydrostatic Pressure Effect on the Phase Transition in $LiKSO_4$. Izv. AN SSSR, 1991 (to be published) (in Russian).

69. Savenko B.N., Sangaa D., Prokert F. Neutron Diffraction Studies on $Sr_xBa_{1-x}Nb_2O_6$ Single Crystals with x = 0.75, 0.70, 0.61, 0.50 and 0.45. Ferroelectrics, 1990, 107, p.207.

70. Sheka E.F., Natkaniec I., Khavrutchenko V.D., Nechitaylov P.B., Muzychka A.Yu., Ogenko V.M. Markichev I.V., Brankowski J., Krawczyk J. Vibrational Spectroscopy of Dispersed Silica: Inelastic Neutron Scattering. J.Electron Spect. Related Phenomena, 1990, 54/55, p.855-876.

71. Sheka E., Khavryutchenko V., Natkaniec I., Ogenko V., Markichev I., Muzychka A. Nechitailov P. Neutron Spectroscopy of Water Adsorbed on Silica. Physica B, 1991, 174 p.182-186.

72. Sheka E., Nikitina E., Khavryutchenko V., Zayetz V., Natkaniec I., Nechitailov P., Muzychka A. Neutron Scattering From Water Adsorbed on Ultrafine Nickel Particles. Physica B, 1991, 174, p.187-191.

73. Tylczynski Z., Savenko B.N., Sangaa D., Beskrovnyi A.I. Neutron Investigation of Ferroelastic Phase Transition in K_2ZnCl_4. Ferroelectrics, 1990, 107, 265.

74. Vuong N.V., Guy L.C., Tuong V.H. et al. Grain Surface Effect on the Oxygen Content in Y123 Ceramics. JINR, P17-91-342, Dubna, 1991 (in Russian).

75. Walther K., Nikitin A.N., Voitus W., Ivankina T. Neutron Diffraction Investigation of Quartz Rocks Textures. Izv. USSR Ac. of Sci. Inst. of the Earth, 1990, No.11 (in Russian).

76. Walther K., Ivankina T.I., Nikitin A.N., Voitus W. et al. Determination of Effective Elastic Modules of Quartz Rocks from Texture Analysis Data. Izv. USSR Ac. of Sci., 1991, No.2 (in Russian).

77. Zajezzhev M.V., Ivanovski I.M., Morozov V.A., Novikov A.G., Savostin V.V., Fomichev N.K., Shilisevich A.L., Morozov V.A. et al. Slow Neutron Scattering Study of the Microdynamics of Potassium-Oxygen Alloys. Preprint PhEI-2154, Obninsk, 1990.

APPLIED RESEARCH

1. Akinshin D.V., Astapov A.A. et al. Investigation of the Effect of ^{84}Kr and ^{16}O Ions Beams on Noise Characteristics of YBaCuO Microbolometers. Pis'ma ZHETF, 1991, v.17, issue 2, p.9-14 (in Russian).

2. Alfimenkov V.P., Luschikov V.I., Mareev Yu.D., Pikelner L.B. Investigation with Polarized Resonance Neutrons of Magnetic Structure of High Temperature Superconductors. JINR Preprint, P3-90-54, Dubna, 1990 (in Russian).

3. Astapov A.A., Barashenkov V.S. et al. Irradiation of HTSC Bolometers with Heavy Ions (1 MeV/Nucleon) and High Energy Particles. JINR Comm., P7-90-241, Dubna, 1990 (in Russian).

4. Astapov A.A., Klimov A.Yu. et al. Anomalous Behaviour of Current Noise in YBaCuO Microbolometers at Temperatures above T_c. Pis'ma ZhETF, 1991, v.17, issue 8, p.9-13 (in Russian).

5. Beskrovnyi A.I., Luschikov V.I. et al. Investigation of the Tetra-Ortho Transition Occuring on the Treatment of $YBa_2Cu_3O_6$ with Halogen (Br, I) Vapours. Report at the 3-rd Int.Conf. on Superconducting Materials and Mechanisms of Superconductivity, 22-26 July, 1991, Kanazawa, Japan.

6. Blokhin S.M., Vlasov A.A. X-Ray Determination of Films Thickness at Proton Excitation. JINR, P14-91-458, Dubna, 1991 (in Russian).

7. Buev A.R., Istomin N.L., Sermyagin A.V., Silaev E.A., Uchaikin S.V. Investigation of HTSC-Ceramic Screens with a Ferrosonde Teslameter. JINR Comm., P13-91-294, Dubna, 1991 (in Russian).

8. Frontasyeva M.V., Gundorina S.F., Gorbunov A.V., Onishenko T.L. Effect of the Production of Phosphorus Fertilizers on Environment. a) MTAA8, Vienna 16-20, September, 1991; b) JINR Preprint, E14-91-400, Dubna, 1991.

9. Gorbunov A.V., Maksjuta B.B., Onishenko T.L., Gundorina S.F., Frontasyeva M.V. Evaluation of the Effect of Agricultural Melioration with the Use of Phosphogypsum on Trace Elements Content in Soils and Vegetation. a) JINR Preprint, D14-91-389, Dubna, 1991; The Science of the Total Environment, 1991, 112.

10. Gorbunov A.V., Onischenko T.L., Gundorina S.F., Frontasyeva M.V. Peculiarities of the REE Distribution in Environmental Objects. The Science of the Total Environment, 1991, 111, p.28-41.

11 Herrera E., Nazarov V.M., Diaz O., Montero M.E. Neutron Activation Analysis Applied to the Study of the Composition of Cuban Geological Samples from Petroleum Ores. JINR Preprint, E14-91-397, Dubna, 1991.

12. Herrera E., Nazarov V.M., Diaz O., Montero M.E., Valdes L. Study of the Behaviour of Rare-Earth Elements and Other Elements in Rock from a Petroleum ore by N.A.A. a) MTAA8, Vienna, 16-20 September, 1991; b) JINR Preprint, E14-91-399, Dubna, 1991.

13. Ignatovich V.K., Luschikov V.I. Possibilities of Investigating Superconducting Gap with Neutrons. JINR, P4-91-142, Dubna, 1991 (in Russian).

14 Kobzev A.P., Shirokov D.M. Surface Analysis on the Van-de-Graaf Accelerator of LNP JINR. European Conf. on Applications of Surface and Interface Analysis. 14-18 October, 1991, Budapest, Hungary.

15. Kobzev A.P., Michaldik D. et al. Study of Y-Ba-Cu-O Films by the Method of Helium Neutrons Backward Scattering. JINR, P14-91-94, Dubna, 1991 (in Russian).

16. Kudryashev V.I., Gundorina S.F., Frontasyeva M.V. Chemical Composition of Filters Used for Air Probing. JINR, 18-91-443, Dubna, 1991 (in Russian).

7. Kuznetsov A.N. 8-Input ADC in CAMAC Standard JINR, P13-90-271, Dubna, 1990 (in Russian).

18. Likhachev A.G., Polushkin V.N., Uchaikin S.V., Vasiliev B.V. Gradiometer Based on Two Single-Hole SQUID's. IEEE Trans. on Instr. and Measur., 1990, v.39, No.6, p.1034-1037.

19 Litvinenko E.I., Likhachev A.G. Software for Computer-Aided Systems to Perform Experiments in the Field of High-T_c Superconductivity. Material Science Forum., 1990, v.62-64, p.207-210.

20 Matora I.M., Bogdzel A.A. et al. Energy Spectra and Photoelectronic Work Function of HTSC $YBa_2Cu_3O_7$. JINR, P13-91-158, Dubna, 1991 (in Russian).

21 Nazarov V.M., Chinaeva V.P., Frontasyeva M.V., Parry S., Bennet B.A. Fine-Powder AlO_2 and Si_2O_3 for Preparation of Multielement Standards for Rare-Earth Elements Analysis. a) MTAA8. Vienna, 16-20, September, 1991; b) JINR Preprint, E14-91-398, Dubna, 1991.

22. Nazarov V.M., Pavlov S.S., Herrera E., Frontasyeva M.V. Recent Developments of Radioanalytical Methods at IBR-2 Pulsed Fast Reactor of the JINR. a) 8th Intern.Conf. Modern Trends in Activation Analysis. MTAA8, Vienna, 16-20 September, 1991; b) JINR Preprint, D14-91-395, Dubna, 1991.

23. Obukhov Yu.V., Saveliev B.I., Khanin V.V. A Portable Quantum Magnetometer Operating in a Wide Temperature Range. PTE, 1991, No.5, p.166 (in Russian).

24 Obukhov Yu.V. On the Measurement of Long-Term Relaxation of the Magnetic Moment of Ceramics $YBa_2Cu_3O_{6+x}$. Materials Science Forum, 1990, v.62-64, p.199-202.

25. Polushkin V.N. Applications of High-T_c SQUIDs: On the Relationship between H_{c1} and J_c in Polycrystalline Ceramic. The Third Soviet-Germany Symposium on High-T_c Superconductivity, Sept. 6-13, 1991, St.Petersburg.

26. Polushkin V.N., Vasiliev B.V. High-T_c SQUIDs and Their Application. In Weak Superconductivity, 1990, New York, Nova Science Publishers, p.143-152.

27. Polushkin V.N. High-Temperature Radio-Frequency SQUIDs: Present State (review) Izmereniye, Kontrol, Avtomatizatsiya, 1990, No.3, p.14-24 (in Russian).

28. Polushkin V.N., Shtanko S.P., Uchaikin S.V., Vasiliev B.V. An Investigation of $Y_1Ba_2Cu_3O_{7-x}$ Josephson Junctions. Supercond. Sci.Technol., 1990, v.3, p.404-408.

29. Polushkin V.N., Likhachev A.G. The Thermal Noise in High-T_c RF SQUIDs. Experimental Technique. JINR Preprint, E13-91-193, Dubna, 1991.

30. Polushkin V.N., Likhachev A.G. The Thermal Noise in High-T_c RF SQUIDs. II. The Discussion of Experimental Results. JINR Preprint, 1991, E13-91-194, Dubna, 1991.

31 Polushkin V.N. The High-T_c rf-SQUIDs: Dynamics, Chaos and Noise. Proceedings of VII Symposium on Weak Superconductivity, 1991, Bratislava, p.20.

32. Rausch H., Sziklai I.L., Nazarov V.M., Bodon P., Erdelyvari I., Toth B. Determination of Impurities in High-Purity Sorbents by Neutron Activation Analysis. Journ. of Radioanal. and Nucl.Chem., 6, 1991, v.148, No.2, p.217-225.

33. Shnyrkov V.I., Tsoi G.M., Polushkin V.N., Glyantsev V.N., Kozyr A.G. High-T_c Superconductor rf-SQUIDs. In: Weak Superconductivity, 1990, New York, Nova Science Publishers, p.131-142.

34. Vasiliev B.V., Polushkin V.N. The Method of Manufacturing a Uni-induction Superconducting Quantum Interferometer. Invention Certificate No.1637615, 1990.

35 Vasiliev B.V., Polushkin V.N. Method of Manufacturing a Superconducting Quantum Interferometer. Invention Certificate No.1581158. 1990.

36. Vasiliev B.V., Polushkin V.N. Uni-induction High Temperature SQUID-Based Magnetometer. PTE, 1990, No.3, p.182-184. (in Russian).

37 Vasiliev B.V., Uchaikin S.V. On the Characteristic Voltage of High-T_c Superconductors Journ. of Supercond., 1991, v.4, No.3, p.243.

38 Vasiliev B.V. High-Temperature Ceramic SQUIDs. Journ. of Supercond., 1991, v.4, No.4, p.271.

39 Vasiliev B.V., Obukhov Yu.V. Critical Currents in YBaCuO Ceramics. Int. Conf. on Materials and Mechanisms of Superconductivity, High-Temperature Superconductors (M2S-HTSC), Kanazawa, Japan, 22-26 July, 1991.

40 Vasiliev B.V., Uchaikin S.V., Hiep H.L. Ceramic HTSC-SQUID Based Galvanometer. Journ. of Supercond., 1991 (submitted).

ELECTRONICS AND COMPUTING

1 Alfimenkov A.V. et al. Local Area Network "Micro-SONET". Proc. of the XIV Int Symp. on Nucl.Electronics. JINR, D13-90-600, Dubna, 1990.

2. Alfimenkov A.V. et al. Programming of Automatized Systems for Spectrometric Experiments on the Basis of Personal Computers in Local Area Network at LNP JINR. Proc. of the XIV Int. Symp. on Nucl.Electronics. JINR, D13-90-600, Dubna, 1990 (in Russian).

3. Balagurov A.M. et al. Registration and Automation Hardware for the Multidetector Neutron Time-of-Flight Diffractometer DN-2. Proc. of the XIV Int. Symp. on Nucl.Electronics. JINR, D13-90-600, Dubna, 1990 (in Russian).

4. Balagurov A.M. et al. A System for Experiments Automation on the Neutron Diffractometer DN-2 at the Pulsed Reactor IBR-2. JINR Comm., P10-91-155, Dubna, 1991 (in Russian).

5. Barabash I.P. et al. Measuring Module for Experiments with Ultracold Neutrons. JINR Comm., 13-91-274, Dubna, 1991.

6. Barabash I.P. et al. Hardware for Research of Transition Processes in Condensed Matters by Neutron Diffraction. JINR Comm., P10-90-88, Dubna, 1990 (in Russian).

7. Bogdzel A.A., Nguyen Trung Tuan. A PC/AT-Based Multiparameter Nuclear Data Acquisition System. Abstract to Eighth Int. Symp. on Modular Information Computer Systems and Networks. Dubna, 1991, p.122 (in Russian).

8. Bogdzel A.A. et al. Fast Multisection ^{239}Pu Fission Chamber. JINR Preprint, P3-90-385, Dubna, 1990 (in Russian).

9. Ermakov V.A. An On-Off Automated Unit for Measuring Storage Channels. JINR Comm., P10-90-36, Dubna, 1990 (in Russian).

10. Dien N.N. et al. Microprocessor Controller for Temperature Regulation in Experiments on the Neutron Diffractometer. Proc. of the XIV Int.Symp. on Nucl.Electronics. D13-90-600, Dubna, 1990 (in Russian).

11 Dien N.N. et al. Key-Driven Programmable Temperature Regulator. JINR Comm., 13-90-491, Dubna, 1990 (in Russian).

12. Dien N.N., Rodionov K.G. Microprocessor Controller in CAMAC Standard for Temperature Regulation and Stabilization. JINR Comm., P10-90-398, Dubna, 1990 (in Russian).

13. Dien N.N., Rodionov K.G. Commutator for Communication Between Terminal and Autonomous Microprocessor System. JINR Comm., P10-90-346, Dubna, 1990 (in Russian).

14. Novozhilov V.E. The Detector Number Coding Device for Investigations on Pulsed Reactors by the Time-of-Flight Method. JINR Comm., P10-91-147, Dubna, 1991 (in Russian).